INFORMATION TO USERS

This manuscript has been reproduced from the microfilm master. UMI films the text directly from the original or copy submitted. Thus, some thesis and dissertation copies are in typewriter face, while others may be from any type of computer printer.

The quality of this reproduction is dependent upon the quality of the copy submitted. Broken or indistinct print, colored or poor quality illustrations and photographs, print bleedthrough, substandard margins, and improper alignment can adversely affect reproduction.

In the unlikely event that the author did not send UMI a complete manuscript and there are missing pages, these will be noted. Also, if unauthorized copyright material had to be removed, a note will indicate the deletion.

Oversize materials (e.g., maps, drawings, charts) are reproduced by sectioning the original, beginning at the upper left-hand corner and continuing from left to right in equal sections with small overlaps.

Photographs included in the original manuscript have been reproduced xerographically in this copy. Higher quality 6" x 9" black and white photographic prints are available for any photographs or illustrations appearing in this copy for an additional charge. Contact UMI directly to order.

Bell & Howell Information and Learning
300 North Zeeb Road, Ann Arbor, MI 48106-1346 USA
800-521-0600

A Closed-Loop Driver/Vehicle Directional Dynamics Predictor

Xiaobo Yang

A thesis

In

The Department

of

Mechanical Engineering

Presented in Partial Fulfillment of the Requirements

for the Degree of Doctor of Philosophy at

Concordia University

Montreal, Quebec, Canada

April 1999

ABSTRACT

A Closed-Loop Driver/Vehicle Directional Dynamics Predictor

Xiaobo Yang
Concordia University, 1999

The highway safety related to vehicle operation on the road is a complex function of dynamic interactions between the vehicle, the driver and the environment. The safety dynamics of a heavy vehicle thus relates to not only its directional stability and control limits, but also the control performance limits of the driver. In view of their lower stability limits, the directional dynamics of articulated freight vehicles have been extensively investigated assuming either negligible contributions due to driver or perfect adaptability of the driver to the vehicle motion. In this dissertation, a number of analytical models of varying complexities are developed to study the lateral, yaw and roll directional performance of an articulated vehicle. Nonlinear analytical models to estimate the cornering properties of tire are derived using Magic Formula and neural networks. Neural network techniques are also applied to derive a nonlinear vehicle model. Based upon a comparative study of response characteristics of various models, it is concluded that a vehicle model based upon yaw-plane dynamics with limited roll degree-of-freedom of the sprung mass can effectively predict the directional response. Parameter sensitivity analyses are performed to identify design parameters that affect the directional dynamics of the combination most significantly. System identification techniques are applied to derive vehicle parameters known to be uncertain. Different analytical models of the human driver are formulated to identify the most effective feedback motion variables and to study the contributions due to driver's interactions with the vehicle. The reported data attained from different field and driving simulator studies are reviewed to identify a range of driver's control parameters, and the performance limits of the drivers. A comprehensive closed-loop driver-articulated vehicle model is formulated, incorporating driver's preview, prediction and compensation abilities, and various motion cues arising from the vehicle's directional motion. The analytical model is analyzed to study the control demands imposed on the driver as functions of selected operational and environmental factors. The control performance limits of three different drivers with varying skill levels are formulated and coupled with the vehicle model. The coupled model is analyzed to identify optimal vehicle design parameters, such that the resulting design can be best adapted to the driver's skill. The results show that the proposed vehicle design that can be adapted for the driver yields considerable performance benefits in view of directional dynamics performance and thus the associated highway safety.

Acknowledgements

The author wishes to thank sincerely the thesis supervisors, Dr. S. Rakheja and Dr. I. Stiharu for their guidance and efforts during the course of this investigation.

The author wishes to acknowledge Quebec government, Concordia University and CONCAVE Research Center for FCAR doctorate scholarship, Graduate Fellowship, and Research Assistantship, respectively.

The author also wishes to thank the colleagues, faculty and staff of CONCAVE Research Center for their contributions to this study.

Finally, the author would like to express a deep appreciation to his parents, wife and the other family members for their continuous concerns, encouragement and supports.

TABLE OF CONTENTS

LIST OF FIGURES

LIST OF TABLES

NOMENCLATURE

A	System matrix
A_{fix}	Characteristic area of unit i along the longitudinal direction (m^2)
A_{fiy}	Characteristic area of unit i along the lateral direction (m^2)
A_k	Derivative vehicle system matrix A with respect to parameter β_k
$\bar{a}_{mi}$	Acceleration vector of unit i (m/s^2)
$\bar{a}_{msi}$	Acceleration vector of the sprung mass of unit i (m/s^2)
a_{xi}	Longitudinal acceleration of the c.g. of unit i (m/s^2)
a_{yi}	Lateral acceleration of the c.g. of unit i (m/s^2)
a_{zi}	Vertical acceleration of the c.g. of unit i (m/s^2)
B	System input matrix
b_i	Bias vector of layer i of neural network
b_{ij}	Track width of axle j on unit i (m)
B_k	Derivative vehicle system input matrix B with respect to parameter β_k
C	System output matrix
C_{Dix}	Coefficients of aerodynamic resistance for longitudinal direction of unit i
C_{Diy}	Coefficients of aerodynamic resistance for lateral direction of unit i
c_i	Longitudinal distance between the c.g. of sprung mass of unit i and articulation point (m)
C_k	Derivative vehicle system output matrix C with respect to parameter β_k
C_m	Tire aligning moment coefficient (Nm/rad)
C_w	Equivalent torsional damping due to front wheels rotation about the axis of the kingpin (Nms/rad)

C_α Tire cornering stiffness (N/rad)

$C_{\phi s}$ Equivalent roll damping coefficient of suspension of trailing unit (Nms/rad)

$C_{\phi t}$ Equivalent roll damping coefficient of suspension of lead unit (Nms/rad)

$C_{\psi h}$ Yaw damping of the fifth wheel (Nms/rad)

D Time delay of recurrent neural network

$D_L(s)$ Driver's proprioceptive element associated with the limb motion

$D_M(s)$ Driver's proprioceptive element associated with the muscle tissue motion

$D_N(s)$ Driver's neuromuscular dynamics function

D_w Longitudinal distance between the kingpin projection and the tire-ground contact point (m)

e_i Longitudinal distance between the c.g. of unsprung mass of unit i and articulation point (m)

F_{bk} Braking force acting on tire-ground interface (N)

F_{dr} Driving force acting on tire-ground interface (N)

$F_e(s)$ Driver's prediction function for external loop signal

$F_i(s)$ Driver's prediction function for internal loop signal

F_{ij} Tire cornering force at axle j on unit i (N)

$F_{ij}(s)$ Driver's prediction function for internal loop signal j

F_{ijk} Tire cornering force at tire k of axle j on unit i (N)

F_{ix} Longitudinal inertial force acting on unit i (N)

F_{iy} Lateral inertial force acting on unit i (N)

F_{iz} Vertical inertial force acting on unit i (N)

FPE Akaike's final prediction error

$f(t)$ Path input function of time

F_{wix} Longitudinal wind resistant force acting on unit i (N)

F_{wiy} Lateral wind resistant force acting on unit i (N)

F_{xijk} Longitudinal force acting at tire k of axle j on unit i (N)

F_y Tire cornering force

F_{yijk} Lateral force acting at tire k of axle j on unit i (N)

F_{zijk} Vertical force acting at tire k of axle j on unit i (N)

F_{zij0} Static vertical force acting on axle j on unit i (N)

$H_C(s)$ Compensatory function used in the comprehensive driver model

$H_d(s)$ Driver's compensatory function

h_{gi} Height of the c.g. of unit i from the ground (m)

$H_H(s)$ Driver's compensatory function for high frequency signal

$H_L(s)$ Driver's compensatory function for low frequency signal

h_{rci} Vertical distance between the articulation point and the roll axis of sprung mass of unit i (m)

h_{si} Vertical distance between the c.g. of sprung mass of unit i and articulation point (m)

h_{ui} Vertical distance between the c.g. of unsprung mass of unit i and articulation point (m)

i_{st} Steering ratio

I_{sw} Effective mass moments of inertia due to steering wheel (kgm^2)

I_w Effective mass moments of inertia due to the front wheels including linkage about the axis of kingpin (kgm^2)

I_{wij} Axial moment of inertia of axle j on unit i (kgm^2)

I_{xs} Roll moment of inertia of sprung mass of trailing unit (kgm^2)

I_{xt} Roll moment of inertia of sprung mass of lead unit (kgm^2)

I_{zs} Yaw moment of inertia of sprung mass of trailing unit (kgm^2)

I_{zt} Yaw moment of inertia of sprung mass of lead unit (kgm^2)

J Performance index

J_{ayi} Normalized mean squared values of the lateral acceleration of the unit i

J_{ri} Normalized mean squared values of the yaw rate of the unit i

$J_{\dot{\delta}}$ Normalized mean squared values of the steering wheel rate

$J_{\phi i}$ Normalized mean squared values of the roll angle of sprung mass of the unit i

K_{at} Prediction gain of the lateral acceleration of tractor ($rad/m/s^2$)

K_C Driver's compensatory gain used in the comprehensive driver model (rad/m)

k_d Constant discrete time lag

K_d Driver's compensatory gain

k_{f12} Roll stiffness of the fifth wheel associated with lead and trailing units (Nm/rad)

K_H Compensatory gain for high frequency signal

K_L Compensatory gain for low frequency signal (rad/m)

K_p Driver's prediction gain

K_{pj} Driver's prediction gain for internal loop signal j

K_w Equivalent torsional stiffness due to front wheels rotation about the axis of the kingpin (Nm/rad)

$k_{\phi s}$ Equivalent roll stiffness of suspension of trailing unit (Nm/rad)

$k_{\phi t}$ Equivalent roll stiffness of suspension of lead unit (Nm/rad)

$K_{\phi s}$ Prediction gain of the roll angle of trailer sprung mass (rad/rad)

K_γ Prediction gain of the articulation rate of the combination (rad/rad/s)

k_1 Constant gain of proprioceptive elements associated with limb motion

k_2 Constant gain of proprioceptive elements associated with muscle tissue (1/s)

L_i Roll moment acting on unit i due to torsional compliance of the fifth wheel and vehicle structure (Nm)

L_t Tractor wheelbase defined as $x_{11}+x_{12}$

M_{bij} Braking torque applied to wheels on axle j of unit i (Nm)

M_{ij} Tire aligning moment at axle j on unit i (Nm)

M_{ijk} Tire aligning moment at tire k of axle j on unit i (Nm)

m_{si} Sprung mass of unit i (kg)

m_{uij} Unsprung mass of axle j on unit i (kg)

M_z Tire aligning moment (Nm)

MSSE Mean sum squared error

n_b System order of output error model

n_f System order of output error model

PRBS Pseudo-random binary sequence

$P(s)$ Previewed function filter

q_e External loop feedback signal

q_i Internal loop feedback signal

QI Quasi-impulse

R Number of neurons in the input layer

r_i Yaw rate of unit i (rad/s)

RS Ramp step

R_T Effective tire radius (m)

s Complex frequency

S_f Orientation of previewed path (rad)

S_i Number of neurons in the hidden layer i of neural network

S_{ijk} Longitudinal slip ratio of tire k of axle j on unit i (rad)

S_{Jayi} Sensitivity coefficient of normalized mean squared values of the lateral acceleration of the unit i

S_{Jdp} Sensitivity coefficient of performance index J

S_{Jri} Sensitivity coefficient of normalized mean squared values of the yaw rate of the unit i

$S_{J\phi i}$ Sensitivity coefficient of normalized mean squared values of the roll angle of the unit i

SNR Signal to noise ratio

S_{xk} System state sensitivity coefficient with respect to parameter β_k

S_y Orientation of predicted path (rad)

S_{yk} System output sensitivity coefficient with respect to parameter β_k

T Simulation time (s)

T_C Driver's reaction time used in the comprehensive driver model (s)

T_I Lag time constant (s)

T_L Lead time constant (s)

T_N Neuromuscular time constant (s)

T_p Driver's preview time (s)

T_1 Time constant for the proprioceptive elements associated with the limb motion (s)

T_2 Time constant for the proprioceptive elements associated with the muscle tissue (s)

u_i Longitudinal velocity of unit i (m/s)

u_{ijk} Absolute velocity developed at tire k on axle j of unit i (m/s)

u_{iwx} Wind speed relative to unit i along the longitudinal direction (m/s)

u_{iwy} Wind speed relative to unit i along the lateral direction (m/s)

u_{wijk} Longitudinal velocity of tire k of axle j of unit i (m/s)

v_i Lateral velocity of unit i (m/s)

$\bar{V}_{mi}$ Velocity vector of unit i (m/s)

$\bar{V}_{msi}$ Velocity vector of sprung mass of unit i (m/s)

w_{ai} Maximum absolute values of the bias for the error in lateral acceleration of unit i

w_{ay} Threshold value for lateral acceleration of tractor and trailer ($3.0 m/s^2$)

$\bar{W}_i$ Weight matrix of layer i of neural network

w_r Threshold value for yaw rate of tractor and trailer (10deg/s)

w_{ri} Maximum absolute values of the bias for the error in yaw rate of unit i

w_ϕ Threshold value for roll angle of sprung mass of tractor and trailer (15 degrees)

$w_{\phi i}$ Maximum absolute values of the bias for the error in roll angle of sprung mass of unit i

x_{iA} Longitudinal distance between the c.g. of unit i and articulation point (m)

x_{ij} Longitudinal distance between the c.g. of unit i and axle j (m)

x_1 Longitudinal coordinate of the c.g. of tractor (m)

y_d Dual tire spacing (m)

y_1 Lateral coordinate of the c.g. of tractor (m)

y_2 Lateral coordinate of the c.g. of trailer (m)

$\bar{z}_i$ Vertical distance between the c.g. of unit i and articulation point (m)

α Angle between the steering column and a vertical axis (deg)

α_{ij} Slip angle of axle j on unit i (rad)

α_{ijk} Slip angle of tire k of axle j on unit i (rad)

β Parameter vector

δ_{FW} Front wheel steer angle (deg)

δ_N Random-like disturbance steering angle

δ_{sw} Steering wheel angle (deg)

δ_V Sum of steering wheel angle and the random-like disturbance steering angle

$\dot{\delta}_{th}$ Threshold values of the steering wheel rate (deg/s)

Δy_{th} Threshold values of the lateral position error between the previewed and resulting paths (m)

$\Delta\psi_{th}$ Threshold values of the orientation error between the previewed and resulting paths (deg)

ε_{y1} Lateral displacement tracking error of the tractor (m)

λ Path-follower or orientation coefficient

Γ Articulation angle (deg)

θ Coefficient vector in output error model

ψ_i Yaw angle of unit i (deg)

ϕ_i Roll angle of sprung mass of unit i (deg)

ρ Mass density of air (kg/m^3)

τ Driver's reaction delay (s)

τ_{at} Prediction time of the lateral acceleration of the tractor (s)

τ_d Driver's reaction time used in the comprehensive driver model (s)

τ_H Driver's reaction delay for high frequency signal (s)

τ_L Driver's reaction delay for low frequency signal (s)

τ_p Driver's prediction time (s)

τ_{pj} Driver's prediction time delay for internal loop signal j (s)

$\tau_{\phi s}$ Prediction time of the roll angle of trailer sprung mass (s)

τ_γ Prediction time of the articulation rate of the combination (s)

ς Factor for orientation participation in external loop feedback signal

ζ Damping coefficient for driver's neuromuscular dynamics

ω_{ij} Rotation angular speed of axle j on unit i (rad/s)

ω_n Natural frequency for driver's neuromuscular dynamics (rad/s)

$\dot{}$ First derivative with respect to time

$\ddot{}$ Second derivative with respect to time

$\dddot{}$ Third derivative with respect to time

$\hat{}$ Estimation of parameter

CHAPTER 1 INTRODUCTION AND LITERATURE REVIEW

1.1 GENERAL

The highway safety related to vehicle operation on the road is a complex function of dynamic interactions between the vehicle, the driver and the environment. The safety dynamics of a heavy vehicle directly relates to its directional stability and control limits, which are known to be considerably lower than those of other road vehicles. The directional dynamics performance characteristics of such vehicles, have thus been extensively investigated on the basis of dynamics of vehicle alone in order to derive their performance limits and an array of safety performance measures [1-7]. The directional control and thus the safety performance characteristics of heavy vehicles, however, are strongly influenced by not only various vehicle design and operating factors, but also the driver's interactions with the vehicle. An analysis of the reported highway accidents involving articulated freight vehicles revealed that human factors form the primary causal factor and account for nearly 85% of the total accidents [8-13]. A study of driver-vehicle interactions is thus extremely vital to enhance an understanding of the driver's contributions to the performance of the vehicle system.

The directional control of a vehicle is realized by the driver based upon the previewed path information and the perception of the vehicle motion under the constraints of driver's abilities, including visibility, correction, reaction, and neuromuscular dynamics as illustrated in Figure 1.1 [14-18]. The vehicle motion on the road thus forms a closed-loop system, where the primary inputs to the vehicle are determined by the driver as a function of various environmental, vehicle, and driver

factors. A study of control and safety performance of a road vehicle thus necessitates the directional analysis of the closed-loop driver-vehicle system.

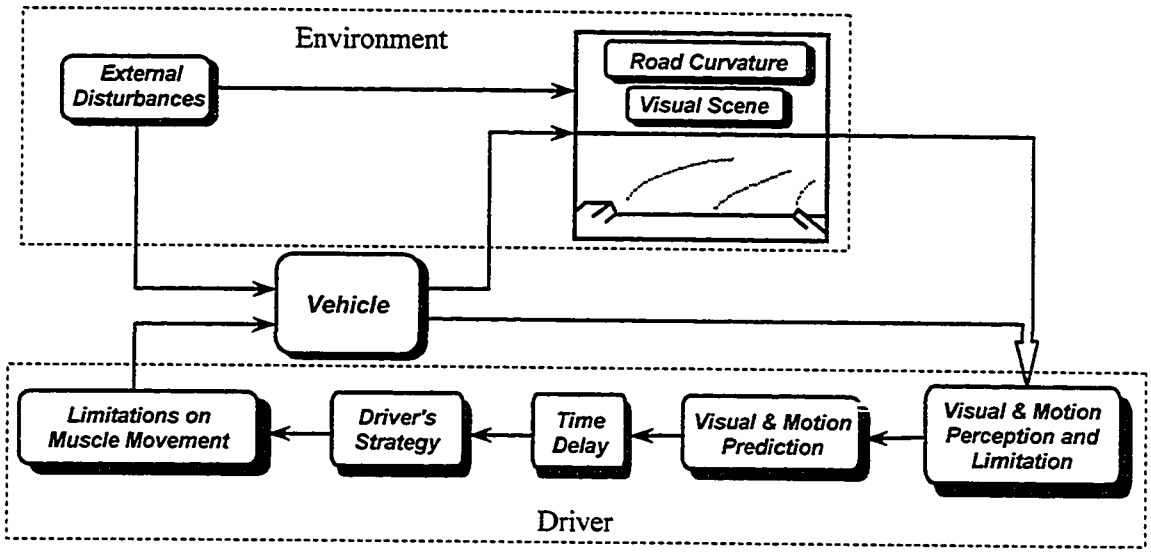

Figure 1.1: Interaction between the driver, the vehicle and the environment.

Articulated freight vehicles exhibit considerably lower directional performance limits than other road vehicles, due to their large dimension and inertia, high sprung mass center of gravity (c.g.) and interactions among various units of the combinations. The articulation forces and moments contribute considerably to the handling and directional control performance characteristics of such vehicles, which are known to be significantly complex than those of the single unit vehicles. Consequently, the control strategies employed by the drivers of articulated vehicles differ from those of the single unit vehicle drivers. Although a number of driver models based upon preview and compensatory tracking have been proposed for directional dynamics analysis of single vehicles [19-28], only a few studies have attempted to investigate the control behaviour of articulated vehicle drivers [29-32]. The studies on articulated vehicle dynamics, however, have evolved into highly complex analytical models incorporating nonlinear characterization of

tire-road interactions, suspension and brake components, and articulation dynamics, while the driver's contributions are assumed negligible. Furthermore, such models require estimation of a large number of vehicle parameters. The implementation of such models for the study of driver's contributions to the overall directional control performance poses considerable difficulties due to complexities of the models and uncertainties associated with various vehicle parameters.

The perception and control characteristics of the vehicle drivers are also known to vary with the individual's skill, perception and reaction abilities, environmental factors and dynamic response of the vehicle, in a highly complex manner. The stable directional performance behaviour of the vehicle is thus a function of control characteristics of both the vehicle and the driver. The driver, in general, contributes to the stable motion by: (*i*) selecting and maintaining the appropriate pathways, in the presence of various disturbances (crosswinds, roadway fluctuations, obstacles, etc.); and (*ii*) reducing the path deviations to certain threshold levels in a stable, well damped and rapidly responding manner. The vehicle, on the other hand, should be designed to achieve: (*i*) superior disturbance rejection abilities; (*ii*) adequate yaw and roll stability limits; and (*iii*) minimal driver's control effort [33].

In this dissertation, a number of analytical models are developed to study the directional performance of an articulated vehicle. Parameter sensitivity analyses are performed to identify design parameters that affect the directional dynamics of the combination most significantly. Different analytical models of the human driver are formulated to study the contributions due to driver's interactions to the directional performance of the coupled driver-vehicle system. The reported data attained from

different field and driving simulator studies are reviewed to identify a range of driver's control parameters, and the performance limits of the drivers. The control performance limits of three different drivers with varying skill levels are formulated and coupled with the vehicle model. The coupled model is analyzed to identify optimal vehicle design parameters, such that the resulting design can be best adapted to the driver's skill. The results show that the proposed vehicle design that can be adapted for the driver yields considerable performance benefits in view of directional dynamics performance and thus the associated highway safety.

1.2 REVIEW OF THE LITERATURE

The directional dynamics analyses of a closed-loop driver-vehicle system involve studies on directional behaviour of articulated vehicles, control characteristics of the human driver, static and dynamic characteristics of vehicle components and articulation mechanisms, characterization of tire-road interactions and identification of vehicle parameters. The relevant reported studies are reviewed and grouped under different subjects in the following subsections to develop the scope of the dissertation.

1.2.1 Directional Dynamics of Heavy Freight Vehicles

The weights and dimensions regulations on most heavy vehicle configurations have been relaxed considerably during the past two decades. The increased sizes and weights have adversely affected the handling, control and directional stability limits of these vehicles [2, 34-36]. Increased concerns towards highway safety of such vehicles have prompted extensive analytical and experimental studies on their directional response

properties [37-39]. A large number of analytical models of varying complexities have been developed for dynamic directional analysis of articulated freight vehicles [40-51]. Although majority of the models have been used to derive the directional performance of a wide range of vehicle configurations, the analyses of the results in conjunction with highway accidents data have evolved into an array of performance measures for heavy vehicle combinations [52-57].

The quality of a vehicle dynamics model, in general, relies upon the modeling methodology, characterization of properties of the vehicle and its components, and the validation of the model. The basic methodologies of modeling a vehicle include both analytical and experimental tasks. The analytical approach usually establishes the equations of motion of the vehicle and its components, which are considered valid under certain assumed conditions, while the experimental approach generally involves evaluations of the vehicle system or subsystem and estimation of vehicle parameters.

Among the major concerns related to the dynamics of articulated heavy vehicles, the handling performance characteristics directly relate to their operational safety. The handling performance of an articulated heavy vehicle involves the study of lateral, yaw and roll dynamics of the vehicle, which relate to three types of yaw instabilities: (*i*) Jackknifing or extensive truck yaw motion, which may occur during braking when the tractor's rear axle wheels experience lock-up; (*ii*) Trailer swing or trailer yaw motion, which may occur during braking when the trailer axle wheels experience lock-up; and (*iii*) Snaking or trailer yaw oscillation, which may occur at higher speeds [52, 58]. The latter two cases represent periodic instability and the first case may lead to severe traffic accidents. The heavy vehicles also exhibit poor roll stability, mostly due to high center of

gravity of the sprung masses. The lower limits of roll stability can lead to vehicle rollovers under transient steering maneuvers performed at high speeds [59-62].

The vehicle models, in general, are developed upon adequate integration of static and dynamic properties of various components, and considerations of the operating factors. The variations in the primary operating variables, such as speed and braking/acceleration, are mostly reflected in the tire models, while the contributions due to variations in road roughness are assumed negligible [63-72]. The static and dynamic properties of the suspension, steering and articulation components, however, are represented independent of the operating conditions. A large number of dynamic models of the heavy vehicle combinations have been developed to analyze their lateral, yaw and roll dynamic performance under varying operating conditions. The degrees of freedom associated with the models vary considerably, depending upon the number of axles and units of the combination, the analysis objectives, and simplifying assumptions [40, 73].

The yaw and lateral directional dynamic response characteristics of different heavy vehicle combinations have been extensively investigated through development and analysis of simplified yaw-plane models. While majority of the reported yaw-plane models assume linear cornering characteristics of the tires, some studies have incorporated nonlinear cornering properties of tires based upon regression functions and Magic Formula [63-65]. Vlk [74, 75] examined the yaw stability of articulated freight vehicles through analysis of a linear yaw plane model. From the steady and transient turning analyses, it was concluded that a tractor-semitrailer vehicle preserves yaw stability at speeds exceeding 70km/h, while a tractor-trailer combination becomes oscillatory unstable at speeds beyond 60km/h. Using the yaw plane model, Schmid [76]

concluded that the resultant tire side forces should be applied behind the center of gravity of the truck in order to ensure the yaw stability of the truck-trailer combination. The truck tends to deviate from its desired path above a certain speed, when this condition is not satisfied. Nalecz and Genin [77] also concluded that heavy vehicles, in general, begin to show unstable behaviour as the lateral acceleration approaches 0.3 to 0.4 g, depending upon the tire-road interactions.

The yaw plane models have been further used to study the influence of various geometric parameters and articulation damping on the lateral stability limits of the vehicles. An experimental study on the lateral stability of straight-running vehicle configurations with two-axle towbar trailers, equipped with either turntable or Ackerman steering, concluded that the trailer yaw oscillations can be effectively suppressed by introducing viscous damping within the turntable [3, 78]. Based upon the directional stability analysis of truck-trailer vehicles, Laurien [79] also concluded that the trailer yaw oscillations could be most effectively suppressed by introducing Coulomb damping at the hitch and at the trailer mechanism. The trailer with Ackerman steering was observed to be more prone to lateral oscillations than the trailer with turntable (dolly) steering. A nonlinear yaw plane model of an articulated vehicle, comprising nonlinear cornering properties of tires and two articulation dampers, was developed and investigated in a recent study [3]. The study concluded that the lateral and yaw stability limits of the vehicle could be enhanced with articulation dampers, while the cornering demand on tires can be reduced.

The yaw oscillations of a two-axle trailer with turntable steering was investigated theoretically by Paslay and Slibar [80], assuming two degree-of-freedom (DOF) model of

a two-axle trailer motion: yaw angle of drawbar and yaw angle of the trailer body. The experimental and analytical studies conducted by Zakin [81, 82] on one- and two-axle towbar trailers concluded that the lateral oscillations of the trailer may be reduced by increasing the wheelbase and the towbar length. Morozov et al. [83] developed a model of a two-axle turntable trailer incorporating turntable Coulomb friction in order to investigate the influence of friction moment and the position of the center of gravity on the lateral and yaw responses of the trailer. The influence of tire cornering forces, wheelbase of the trailer, and overall trailer length on the yaw oscillations was further investigated by Meyer [84], using a two DOF vehicle model.

The analysis of yaw plane model of a coupled truck-trailer, performed by Jindra [85] further concluded that the yaw oscillations of the trailer increase with an increase in the yaw moment of inertia of the trailer body. Increased viscous damping at the hitch or the turntable, drawbar length and trailer wheelbase resulted in reduced yaw oscillations. Gerlach [86] analyzed a similar mathematical model incorporating turntable offset, coulomb and/or viscous damping at the hitch and the turntable. The results of the study established that a truck-trailer combination with high cornering stiffness of the tires, either Coulomb or viscous damping at the hitch, long drawbar and the turntable center located ahead of the dolly axle, leads to good dynamic stability. While the viscous damping at the turntable resulted in lower yaw oscillations, the Coulomb damping resulted in continuous undamped yaw oscillations of the trailer.

A nonlinear yaw plane articulated vehicle dynamics model developed by Nordstrom et al. [87] was validated using several full-scale field tests with various numbers of axles of the trailer and the loads. The results of the simulation programs

correlated quite well with those derived from the tests. Mallikarjunarao and Fancher [5] developed a linear yaw plane analytical model to study the directional response and stability of tractor-semitrailer combinations with multi-axles and multi-articulated tanker trucks, while neglected the roll dynamics. An eigen-value analysis was performed to determine the natural modes of oscillation and the directional stability limits of the vehicle. The study concluded that the lateral acceleration of the pup-trailer of the Michigan double tanker is significantly larger when compared with that attained by the tractor, during an obstacle-avoidance maneuver performed at highway speeds. This rearward amplification of lateral acceleration was considerably reduced by increasing the rigidity of the pintle-hook connection.

The yaw plane models provide effective assessment of rearward amplification, dynamic off-tracking, and yaw and lateral stability limits of vehicle combinations, while the contributions due to pitch and roll motions and suspension dynamics can not be evaluated. Such models offer considerable advantages in which relatively fewer number of parameters are required to evaluate the directional performance with reasonably good accuracy. The major limitations of the model include its inability to evaluate the roll stability limits of the vehicles. Various reported studies on highway accidents have clearly established rollover as a common failure mode for heavy vehicles [34, 60, 73]. The static roll stability limit of a vehicle is frequently characterized by its rollover threshold, defined as the maximum lateral acceleration to which the vehicle can withstand without rolling over in a steady turning maneuver. The roll instability is attained whenever the overturning moment, generated by the centrifugal forces, exceeds the net stabilizing moment. For heavily laden vehicles, the rollover threshold is so low that rollover can

easily occur under severe maneuvers performed on paved surfaces. Typically laden heavy vehicles can roll over during turning maneuvers when the lateral acceleration approaches roughly 0.4g [73, 88].

The roll stability limits of heavy vehicles have been extremely investigated through development of single- and multi-axle roll plane models of varying complexities. These models, in general, incorporate vertical and roll stiffness characteristics of vehicle suspension, lateral stiffness properties of tires, and torsional compliance of the vehicle structure and the articulation mechanisms. While majority of the roll plane models have been developed to analyze the static rollover threshold under steady turning maneuvers, the dynamic roll characteristics of the vehicle under transient directional maneuvers have been addressed in only few studies [89, 90]. Isermann [88], and Miller and Barter [91] developed roll plane models of an articulated vehicle carrying rigid or liquid loads and investigated the sensitivity of the rollover threshold to variations in design and loading conditions. The lateral load shift due to movement of liquid cargo in a partially filled tank trailer, however, was neglected.

Although the suspension characteristics and torsional properties of the tractor frame and the fifth wheel arrangement were represented appropriately in the model, the representation of the lumped dual tires and the linear tire properties may introduce a certain error under evasive maneuvers. A comprehensive static roll model of the articulated vehicle, incorporating composite multi-axle representation, was developed by Mallikarjunarao et al. [92] to determine the rollover threshold of articulated vehicles during steady turning maneuvers. The static equilibrium of the vehicle in the roll plane is solved iteratively for small increments in roll angle of the semitrailer's sprung mass. The

multiple axle suspensions were modeled by grouping the axles in three composite axles. The static roll model is further validated using the tilt table test results. A kineto-static roll plane model of a tractor-semitrailer equipped with a partially filled tank of arbitrary cross-section was developed by Ranganathan et al. [89] to investigate the roll stability limits of partially filled tank vehicles under typical cornering maneuvers at a constant forward speed.

The tripped and maneuver-induced dynamic roll stability characteristics of heavy vehicles have also been investigated in few reported studies. Heavy vehicles, in general, exhibit maneuver-induced roll instability due to their poor rollover limits. The maneuver-induced roll dynamics and stability characteristics of heavy vehicles have thus been investigated in different experimental and analytical studies. Gillespie and Verma [93] developed a single-composite axle roll plane model to analyze the dynamic roll response of the vehicle. The study resulted in an overestimate of the rollover threshold due to single lumped axle representation. A comprehensive dynamic roll model of multi-axle and multi-unit vehicle has been recently proposed to study their maneuver-induced roll stability limits [90]. The study has evolved into a set of performance measures for such vehicles, such as load transfer ratio, rearward amplification and effective lateral acceleration [90, 94].

A number of three-dimensional vehicle models have been further developed to study the lateral, yaw and roll dynamic performances of heavy vehicles [40, 41, 95]. A constant forward speed model, referred to as Yaw/Roll model [95], has been extensively used to study the directional dynamics of various vehicle combinations. The model yields the yaw, roll and lateral response characteristics of the vehicles under constant speed

directional maneuvers. The steering maneuvers may be performed either in an open-loop maneuver by defining the time history of the front-wheel steer angle, or in a closed-loop maneuver by describing the path coordinates. The steer angle is generated using the path coordinates in conjunction with a simplified driver model. The simulation program can analyze vehicle combinations involving up to four units and eleven axles, and thus results in a maximum of 52 degrees-of-freedom.

The proposed model further incorporates nonlinear force-deflection and hysteresis properties of the suspension springs, and nonlinear cornering characteristics of the tires, while the suspension roll center is assumed to be located at a fixed distance from the sprung mass c.g. The vehicle model permits the dynamic analysis of vehicles with up to five steerable axles, in addition to the front axle, where the steering may be generated through self-steering or kinematic-controlled steering mechanisms. Flexibility in the specification of articulation-joint properties also enables the analyses of A-, B- and C-train combinations [2]. While the Yaw/Roll program has been extensively used to assess the directional dynamics performance measures of various heavy vehicle combinations under constant forward speed, the model is known to be complex due to its large number of DOF and requirement of large number of geometrical, inertial, suspension and tire parameters.

The directional dynamics of heavy vehicles under simultaneous applications of braking and steering have been investigated through development of variable speed three-dimensional models. The Phase IV program perhaps represents the most comprehensive vehicle dynamics model for analysis of yaw, roll and lateral stability of heavy vehicles subject to braking and steering [41]. The model integrates the properties of braking and

anti-lock brake system, nonlinear cornering properties of tires under braking and steering using lookup tables, nonlinear force-deflection properties of suspension springs, static properties of the articulation mechanism, and the combination of steering (open- and closed-loop), and driving/braking torque. The vehicle model is developed to analyze different vehicle combinations comprising up to three units and ten axles, with a maximum of 71-DOF. The Phase IV model is thus considered as a complex model, which requires extensive vehicle parameters.

The validity of different analytical models, of varying complexities, reported for directional dynamics of heavy vehicles, has been further examined by El-Gindy and Wong [96]. The study evaluated the performance of various models, including linear Yaw Plane, total braking and steering, Yaw/Roll and Phase IV models, for analysis of directional response characteristics. The study concluded that more sophisticated simulation models, such as the Phase IV model, do not necessarily yield more accurate predictions in quantitative terms than the simpler models, such as the linear yaw plane model. The transient steering response characteristics of a tractor-semitrailer in a lane-change maneuver, analyzed using the four simulation programs, were observed to be qualitatively similar for Phase IV, Yaw/Roll and Linear Yaw plane models. A comparison of the simulation results with the measured data further revealed that the more sophisticated Phase IV model does not necessarily yield more accurate transient response than the simpler linear yaw plane model.

1.2.2 Human Driver Models

The analysis and enhancement of highway safety associated with commercial vehicles not only involves the handling and stability analysis of the vehicles, but also the methods to evaluate driver's interactions with the vehicle. Many studies have established that the directional stability properties of a vehicle cannot be fully evaluated through measurement or analysis of the vehicle dynamics alone [97-113]. Analyses of reported highway accidents, invariably, reveal that the human factors form the primary causal factor and account for nearly 85% of the total accidents [8]. Upon recognizing the significant role of the driver's actions related to overall highway safety, a large number of studies have been performed in an attempt to characterize the driver-vehicle interactions. Majority of the efforts, however, have been directed towards characterization of the human driver behaviour, identification of performance limits of the driver under specified driving conditions and environmental factors, and development of analytical driver models [114-116]. The earlier analytical models were mostly developed for the human pilot in aircraft control applications [19, 21, 117]. The driver models for vehicular applications have been explored during the past two decades. These proposed models, with the exception of only a few [29, 31], however, have been applied for analysis of driver's interactions with two-axle single unit vehicles.

Tustin [118] proposed a quasi-linear function describing the human operator's tracking performance in a gunnery-type task. The proposed function was later used by McRuer and Krendel [21] to describe the characteristics of the human pilot for analysis of closed-loop pilot-aircraft pitch control system. Many driver models of varying complexities have evolved during the past three decades to study the dynamics of the

coupled single unit vehicle-driver systems. These driver models can be classified into two broad groups based upon their tracking objectives:

- *compensatory tracking models* utilize the instantaneous path error only and have been used to study the closed-loop pilot-aircraft system; and
- *preview tracking models*, where the path error is minimized by predicting the future path using the preview effect. The preview tracking models, incorporating the driver's prediction abilities and reaction time, are considered more appropriate for the study of closed-loop driver-vehicle systems [134, 140, 137, 149].

The vehicle driver, in general, may be understood as both the compensator and the estimator, with certain time delay, in a common closed-loop control system. The preview effect in conjunction with the perceived motion of the vehicle, enables a driver to follow a path within certain safety margin and to perceive the tracking error in relation with the perceived vehicle path. The tracking error is further applied as the input signal to the driver acting as a compensator to generate a control action in terms of steering, braking or acceleration. Certain time delay between the driver's perception and reaction, however, exist originating from brain reaction and neuromuscular delay, ranging from 0.1~0.5s [119-122]. The primary function of the compensator is to adjust the command signal to the vehicle in both gain and phase while the estimator is used to predict the motion of the vehicle, which depend upon the driver's experience and skill. The driver's preview strongly depends upon the driver's far-sight and identification abilities and vehicle speed.

Figure 1.2 illustrates the general structure of a compensatory tracking driver model, where $H(s)$ is the describing function of the driver, which operates on the perceived instantaneous path error of the vehicle, and $G(s)$ is the vehicle system function. The models proposed by Iguchi [123], Weir and McRuer [124], Legouis et al. [125-127], Hayashi [128], and Habib [129-131], can be grouped into the category of compensatory

tracking model. Iguchi [123] proposed a compensatory tracking model using a PID driver function, where the system gains were not related to the driver's physical behaviour due to the difficulties associated with distinguishing the physical mechanism of the driver's control corresponding to the PID driver function. Weir and McRuer [124] proposed a quasi-linear describing function characterizing the response reaction delay, neuromuscular lag, and compensation including gain, lag and lead time constants of the driver. The describing function was used to analyze a coupled two DOF vehicle-driver model behavior under cross wind gusts. The study concluded that the driver predominantly responds to the heading rate, and the steering angle is roughly proportional to the heading rate of the vehicle. McRuer et al. [132] further developed a crossover model to identify the model parameters based upon curve fitting of the measured data. The crossover model of human driver implies that the driver adopts a sufficient lead or lag equalization, such that the slope of the magnitude of the open loop transfer function of the driver-vehicle system is close to -20dB/decade in the region of crossover frequency. While the crossover model is neither appropriate nor accurate at frequencies much less than or much greater than the crossover frequency that depends strongly upon the maneuvers and tasks.

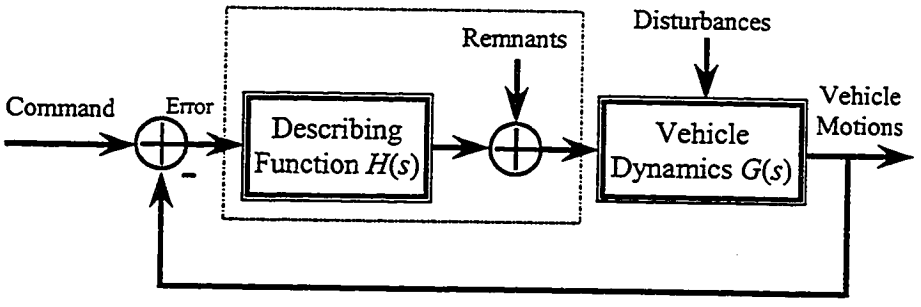

Figure 1.2: Structure of a compensatory tracking model.

Legouis et al. [125] and Hayashi [128] proposed optimization techniques to estimate the coefficients of the driver's describing function, where the cost function comprised lateral position error, yaw rate error and front-wheel steering angle. An optimal compensatory tracking model to derive an estimate of various uncertain parameters of the vehicle was also proposed and implemented by Habib [131], in which low and high frequency compensations are applied, and the driver compensator operates on perceived composite lateral position and heading errors of a car. A robust stability testing function was used for computing the robustness margin of the driver-vehicle system. Furthermore, three models of human driver were applied to characterize the driver-vehicle directional control by incorporating a two DOF model of a car [129]. The three models of driver behaviour considered in the study included: the lead compensator with time delay; the composite lateral and heading feedback compensator; and the so called "structural model" of the human driver [133]. The study concluded that the driver-vehicle system with the proposed "structural model" performs well at moderate and high frequency-gain region but becomes unstable in the low frequency-gain region. The system model incorporating a lead compensator performs well in the low and moderate frequency-gain regions, while that incorporating a composite lateral and heading feedback compensator performs well in the low, moderate and high frequency-gain regions with a bandwidth up to 11 rad/s.

Table 1.1 summarizes various compensatory tracking driver models reported in the literature together with the model structure, describing functions and range of model parameters, where reported. It is clearly shown that the parameter, referred to as compensatory gain, is assigned in all the compensatory driver models but the value of the

gain varies extensively, depending upon the assumed feedback signal, the parameter estimation methods and the operating conditions. The parameter estimation methods applied in the compensatory models include the regression methods using the crossover model with the available experimental data, and minimization of an assumed cost function comprising steering angle, lateral position error and/or yaw rate of vehicle [132]. Since the driver's preview function is entirely ignored in the compensatory models, such models are usually applied for stability analyses of the closed-loop driver-vehicle system.

The typical structure of a preview-tracking model is illustrated in Figure 1.3. The driver's control behavior is described by the function *H(s)*, while *P(s)* represents the preview effect. The feedback function *B(s)* relates to the path prediction ability of the driver and forms the most vital component of the model. Majority of the driver-vehicle models proposed in the literature utilize the preview tracking driver models in order to incorporate the essential preview and prediction effects of the driver [134-137]. These studies have established that the performance of the closed-loop driver-vehicle system is strongly related to the preview time or distance, which is a complex function of the driver physical behavior, maneuvers and tasks, vehicle speeds, road conditions, and vehicle dynamics. A number of measurement techniques based upon restricted and controlled preview distance under different road and speed conditions have been developed [99, 138-145]. These studies have reported a wide range of preview time ranging from 1.7 to 9.0s, and preview distance ranging from 6.1m to 128m, depending upon the test methods, test objectives, road conditions, speeds and maneuvers. Table 1.2 briefly summarizes different methods of measurements, test conditions and the results reported in these studies.

Table 1.1: A summary of reported compensatory tracking models.

Authors	Model	System Function and Parameter Values
Tustin [118]	Quasi-Linear Describing Function	$H(s)=Ke^{-\tau s}(1+T_L s)$, $\tau=0.3$ s, K and T_L determined from experimental data
Iguchi[123]	PID Compensatory	$H(s)=K_p+K_i/s+K_d s$
Weir and McRuer [124]	Quasi-Linear Describing Function	$H(s)=\frac{Ke^{-\tau s}(1+T_L s)}{(1+T_N s)(1+T_I s)}$, Response reaction delay $\tau=(0.15\pm0.05)s$, Neuromuscular lag $T_N=(0.1-0.5)s$, Lag time constant T_I=1 to 20 s, Lead time constant T_L=0.1 to 5 s, and Gain K=1.5-2.0 cps
McRuer, et al [132]	Cross-over	$H(s)G(s)=\frac{\omega_c e^{-\tau s}}{s}$; ω_c and τ dependent upon tracking tasks
Legouis et al [125-127]	Optimal Compensatory Control	$H(s)=Ke^{-\tau s}(1+T_L s)$, $\tau=0.2s$, K and T_L are estimated by minimizing the performance function: $J=0.5\int_0^T(w_1\Delta y^2+w_2\delta_{FW}^2)dt$
Hayashi [128]	Optimal Compensatory Control	$H(s)=\frac{Ke^{-\tau s}(1+T_L s)}{(1+T_I s)}$; K, T_L and T_I are estimated by minimizing: $J=\int_0^T(w_1\Delta y^2+w_2 r^2+w_3\delta_{FW}^2)dt$, where r is yaw rate
Habib [129]	Robust Steering Control	*H(s)* including low and high frequency compensation; Determination of uncertain vehicle parameters
Habib [131]	Lead compensator with time delay	$H(s)=Ke^{-\tau s}(1+T_L s)$, $\tau=0.15$ s, K=0.001~0.014 rad/m and T_L=0.5~10s, lateral position error as feedback, effective in low and moderate frequency-gain regions.
Habib [131]	Composite lateral and heading feedback compensator	$H(s)=\frac{K_y K_\psi e^{-\tau s}(1+T_L s)}{1+K_\psi e^{-\tau s}(1+T_L s)G_\psi(s)}$, $\tau=0.15$ s, K_y=0.001~0.12 rad/m, K_ψ=0.1~4.8rad/rad and T_L=0.5~10s, $G_\psi(s)$ is the vehicle transfer function of yaw angle against steering angle. Composite lateral position and yaw angle as feedback, effective in low, moderate and high frequency-gain regions.
Habib [131] and Hess [133]	Structural model of human driver	Incorporation with neuromuscular dynamics and effective in moderate and high frequency-gain region.

While considerable discrepancies among the reported results are evident, they can be attributed to varying test methods, conditions and objectives. An examination of the results, however, reveals some very important and significant trends. Under straight-line driving conditions, the preview distance increases nearly linearly with increase in vehicle

speed. The preview time thus increases, which yields decreased bandwidth of the closed-loop driver-vehicle system with increase in speed. At typical highway speeds, the preview time for single unit vehicles is observed to be in the vicinity of 3s, which tends to increase considerably with increase in the path curvature. The measurements performed by Mclean and Hoffmann [142], based upon restricted preview distances, concluded that the preview time can be approximated as half of the predominant period of the steering wheel motion, which ranges from 0.33s to 10s.

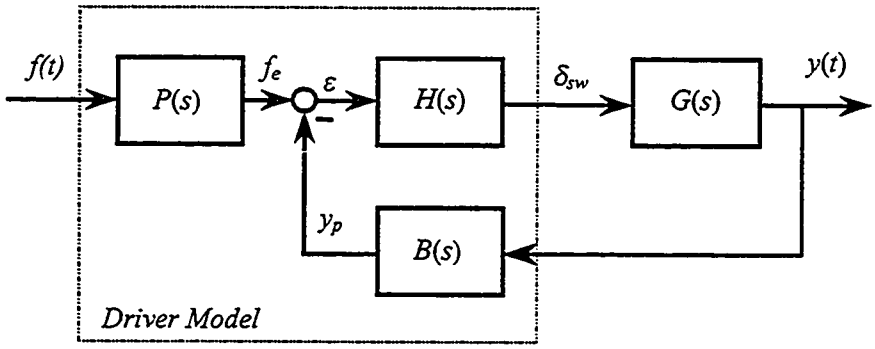

Figure 1.3: Structure of a preview-tracking model.

A large number of preview tracking driver models have been proposed and implemented to study the interactions of the driver and the single unit vehicles. These models, in general, incorporate three major components:

- previewed and anticipated vehicle paths based upon preview and prediction behavior of the driver;
- biological delays and control characteristics of the driver; and
- error compensation abilities of the driver.

The first component of the models comprising path preview and prediction behavior of the driver, also referred to as the anticipatory level, involves the consideration of road condition, speed and nature of the maneuver to estimate the preview distance and anticipated

path. The second component of the driver model constitutes the biological delays and gains arising from neuromuscular and proprioceptive behavior of the driver, related to the reaction time of the human muscles and tissues. In view of the extensive variations in the reaction times and complexities in characterizing the individual's delay, these delays are often grouped as a single overall reaction time of the driver [134, 135]. The last component of the model involves error compensation, and necessary control actions and gains of the driver, where the error may be expressed in terms of deviations in lateral position, orientation or yaw position, yaw rate, or a combination of these.

Table 1.2: Range of measured preview distance and time reported in the literature.

Authors	Measurement Method	Driving Condition	Speed (km/h)	Preview Distances (m)	Preview Time (s)
Gordon [138]	Monocular viewing through small aperture	Gentle meandering	22.0	Average: 42.7	7
Hoffmann and Joubert [139]	Variations in steering performance with restricted maximum preview distance	Difficult "slalom" course	27.4	15.2	2
Wierwille, et al. [99]	Driver transfer function obtained on a simulator	Simulated highway	110.0	91.4	3
Kondo and Ajimine [140]	Viewing through a narrow slit	Straight line	19.8-60.3	45.7-128. (Nearly proportional to speed)	9
Kondo and Ajimine [140]	Restricted maximum preview distance under different speeds	Straight line	11.0-49.4	9.1-36.6 (Nearly proportional to speed)	2-3
Kondo and Ajimine [140]	Sighting camera	Tight curves	11.0-27.4	6.1-21.3 (Roughly proportional to speed and curvature)	2-4
Mourant, et al [141]	Filming of eye position	Open highway	76.8-109.7	>91.4	>3
McLean & Hoffmann [142]	Restricted preview distance	Straight-lane at airport	32.2-48.3	21.3	1.7-5

In a recent study, Plöchl & Lugner [146] proposed a three decision level model similar to the above general structure:

- Compensatory level to eliminate the anticipated path deviations;
- Anticipatory level to track the previewed path curvature; and
- Local control to compensate the local path deviation.

Although the model was proposed to control the local path errors, the decision levels can be considered generally applicable to all coupled driver-vehicle system models. While majority of the driver models reported in the literature employ this general structure, the control and preview techniques used vary considerably. Sheridan [134] employed a dynamic programming technique to derive local optimal trajectory over the preview span, using an iterative algorithm. Three models were proposed to predict the driver response under a constrained preview of an input course. The first model, referred to as the extended convolution model, was a simple extension of linear convolution, while the second referred to as fast-time trials with dynamic model employed an iterative fast-time predictive computations simultaneously with continuous control in real-time. The final model involved a repetitively updated computation of optimal control strategy over the previewed span of input. The study concluded that the proposed three models characterize the constrained preview control better than the conventional describing function techniques. A linear first order path prediction model to derive an empirical estimate of the driver's control gain was proposed by Kondo [140], assuming negligible driver delays. The model can effectively predict the driver's directional control performance only when the lateral motion is relatively small since the lateral acceleration of vehicle was not considered in the model. Yoshimoto [136] proposed a second order

path prediction model incorporating driver's prediction and reaction time behavior, while the control gain was estimated empirically. This model provide a prediction of the driver's control behaviour better than the model proposed by Kondo [140].

An optimal estimator-predictor controller model was proposed by Tomizuka et al. [147] based upon a joystick experiment to follow a desired trajectory. The study concluded that the preview effect can significantly improve the tracking performance, and reported that a preview time, ranging from 0.3~0.7s, is sufficient to achieve considerable improvement. An optimal preview control model based upon minimizing the error between the previewed and actual path was developed by MacAdam [137] to determine the required front wheel steer angle. The technique was used to examine the straight-line regulatory driving task and the results were compared with the measured data at a vehicle speed of 80.28 km/h. The preview time of 3s and effective delay time of 0.26 s were selected to fit the experimental data. The method was further demonstrated by closed-loop simulation of an automobile driver/vehicle system during transient lane-change maneuvers where the vehicle was represented by the bicycle model and with speed of 96.5 km/h. It was suggested that automobile driver steering control strategy during path following can be viewed as a time-delay optimal preview control process.

All the above mentioned driver and driver-vehicle models are based upon compensation of lateral position error using single-point preview strategy, while the orientation errors are neglected. The directional performance of a heavy vehicle, however, is known to be influenced by not only its lateral position but also the yaw orientation. Guo [148, 149] proposed preview tracking models to minimize the error function based upon lateral position and orientation errors. A first order correction factor was identified

and integrated to the constant control gain of the driver using a 'preview-follower' control scheme to achieve optimal lateral acceleration behavior of the vehicle. The model was validated using extensive field test data.

Allen et al. [150] proposed a multi-loop quasi-linear driver model to determine the front wheel steer angle as a function of the previewed path curvature error. The study of driver-car performance over a range of maneuvers, including accident avoidance scenarios involving limiting handling performance of the vehicle. The car was represented as a three-DOF model including roll, lateral velocity and yaw rate, coupled with a driver control structure. The stability of the closed-loop system was analyzed at speeds of 48 and 96km/h based on the following assumptions: (1) the visual and motion feedback time delays are considered equal, and combined with the neuromuscular dynamics to yield an overall time delay for the driver; (2) the vehicle dynamics is simplified and represented by an equivalent gain and first order lag. Later, Xia and Law [23] applied the multi-loop quasi-linear driver model incorporating a nonlinear eight-DOF car model to investigate the handling behaviour of both conventional front-wheel and four-wheel steering automobiles under crosswind disturbances and collision avoidance maneuvers, resulting from combined steering and braking commands. The results revealed that the closed-loop system significantly improves the driver/vehicle performance under both excitations.

The concept of driver's adaptability to varying road conditions was introduced by Nagai and Mitschke [151]. In their study, an adaptive control model was developed to achieve variable driver control gains reflecting the driver's adaptation of the varying road conditions, and lateral acceleration response of both the reference and actual driver-

vehicle model. The biological neuromuscular and proprioceptive delays of the human driver were investigated using the "crossover" model [132]. Mitschke [152] proposed an anticipatory driver model based on the previewed road curvature and negligible driver's delay. Apetaur et al. [100] utilized the driver model, proposed by Mitschke [152], to derive a car-driver model assuming driver as an ideal controller capable of steering the vehicle to follow the previewed path. The car was modeled as a bicycle model with three-DOF, including longitudinal, yaw and lateral motions of the vehicle. The capabilities of the driver as an ideal controller were however limited by imposing constraints on the maximum attainable steering wheel angular movement (≤ 180 degrees), maximum angular velocity (≤ 400deg/s) and maximum angular acceleration (≤ 1000deg/s^2). The visibility varied from 10m under fog conditions to 300m under high speed highway driving.

The highlights of various preview tracking models, reported in the literature, are summarized in Table 1.3. The path decision process used in the above preview tracking models is primarily based upon geometry of the previewed path (curvature and lateral position deviations). The models, however, lack the flexibility in representing driver's decision-making behavior. The inherent uncertainty of the human driver thus can not be adequately represented. Alternatively, fuzzy control models have been proposed to account for subjective uncertainties associated with the path decision-making and tracking processes based upon the visual behavior of driver [153, 154]. The fuzzy logic controls employ a set of rules to direct the decision process and membership functions to convert the abstract linguistic variables, such as right- and left- steering maneuvers, and speed termed as 'slow' or 'fast' into precise numeric values required for the control. The

set of rules is frequently based upon anticipated driver's knowledge and experience, while the membership functions represent the driver's interpretation of the linguistic variables.

Table 1.3: A summary of preview tracking models reported in the literature.

Authors	Models	Highlights
Sheriden [134]	Dynamic Programming Optimal Trajectory (DPOTP)	Iterative optimal trajectory; computationally complex
Kondo [140]	Linear Prediction (LP)	Empirical driver's control gain, neglecting driver delays
Yoshimoto [136]	Second Order Predictable Correction (SOPC)	Empirical driver's control gain
Tomizuka [147]	Optimal Estimator-Predictor-Controller (OEPC)	Estimation of human tracking behavior
MacAdam [137]	Optimal Preview Control (OPC)	Optimal front wheel steering angle, lateral position error
Allen [150]	Multi-Loop Quasi-Linear (MLQL)	Lateral position and/or previewed curvature error
Nagai and Mitschke [151]	Adaptive Control (AC)	Identification of adaptive driver's gain as a function of road surface
Mitschke [152]	Anticipatory	Based upon previewed road curvature
Guo [148]	Feedback of Lateral Acceleration (FLA)	Based upon feedback of perceived lateral acceleration
Guo & Guan [149]	Optimal Preview Acceleration (OPA)	Identification of optimal vehicle lateral acceleration
Guo & Guan [149]	Position plus Orientation Preview Acceleration (POPA)	Identification of optimal vehicle lateral acceleration and jerk
Modjtahedzadeh and Hess [135]	Preview Compensatory Structure (PCS)	Identification of neuromuscular and proprioceptive dynamics
Plöchl and Lugner [146]	Three-Decision Levels (TDL)	Compensatory tracking of pre-viewed path curvature, anticipated path deviation, and local control
Hayhoe [155]	Cerebellum Articulation Controller	A look-up table cerebellum model
Kramer and Rohr [156]	Visual Pattern Processing	Pattern recognition for lane keeping
Willumeit et, al [157]	Eye-Movements	Simulator experiments on eye-movements and steering angle
Kageyama and Pacejka [153]	Risk Level Decision	Course decision and tracking based upon risk as a function of heart rate
Gu and Yu [154]	Fuzzy Control Model	Normally distributed membership function of fuzzy variables
Thakur and White [158]	Risk Time basis model	Risk time estimation by driver from trajectory and anticipation of hazards.
MacAdam and Johnson [159]	Neural Network model	Two-layer network with sigmoid, linear activation function and back-propagation

Hayhoe [155] proposed a closed-loop two-DOF car-driver model based upon the theory of neurophysiological processes occurring in the cerebellum. The model learns through experience and adapts to the driver's behavior, using the fuzzy logic. The model was further implemented on a simple bicycle model of a car and learning was accomplished through an explicit driver model formulated to operate from sampled inputs and discrete output. Despite extreme simplifying assumptions of the real processes occurring in the nervous and muscular systems, the model reproduced certain aspects of driver behavior not accountable by other driver models, specifically (*i*) the model learns through experience, thus providing possible means of studying learning and adaptive behavior; (*ii*) input data was accepted discontinuously and can be non-linear; (*iii*) output was in the form of discontinuous changes in steering wheel position; (*iv*) for simple path following, the output had a random dispersion about the mean; and (*v*) the model was applicable to all control situations, depending only on input cues and, possibly, other commands to the controller.

Conventional closed-loop driver-vehicle system models consider the driver's visual field in terms of path coordinates from a bird's-eye view (curvature, width, etc). The models based upon such geometric description of the path, however, exhibit poor correlation with the single-vehicle accident data. Kramer and Rohr [156] developed a model to emphasize the visual field and the visual behavior of the driver, and eye and hand movements using the measurements performed on a driving simulator. The simulation results derived from the fuzzy driver model, proposed by Willumeit et al [157], provided good correlation with the measured eye and steering movements during lane keeping tasks.

Kageyama and Pacejka [153] proposed a fuzzy control model, assuming that the risk level of driver can be related to the forward view, and the heart rate. The error between the desired path associated with minimum risk level and the previewed path is then used to perform the control task. The model included the mental influence as a risk from the environment, which is used by the driver to decide upon the course and inputs to the vehicle. A fuzzy control method was used to decide the different risk levels arising from right- and left-hand side of the road, distant views (such as curves), and obstacles, and the desired path was described by the minimum risk level. A closed-loop driver-car fuzzy control model, incorporating lateral displacement, yaw velocity and steering wheel angle as the fuzzy variables, was proposed by Gu and Yu [154], assuming normally distributed membership functions. A car model, incorporating DOF due to lateral displacement, yaw velocity and sprung mass roll angle, coupled with the driver fuzzy control model was analyzed to describe complex control tactics and behavior of drivers. A more comprehensive driver model, proposed by Thakur and White [158], incorporates the continuous cyclic process of driver's actions consisting of perception, decision, execution and response with certain time lag. The total cycle time was shown to depend upon a risk time, defined as the time of occurrence of a possible accident from the present state, as estimated by the driver.

The proposed driver models have been invariably used in conjunction with single unit vehicles, with the exception of the model proposed by MacAdam [137]. This model based upon lead vehicle lateral position error control was employed in an articulated vehicle model to determine the front wheel steer angle, while the contributions of the trailer dynamics were entirely neglected. It has been well known that the dynamic

characteristics of an articulated heavy vehicle differ significantly from those of a single unit vehicle and control of an articulated vehicle requires higher driving skills. Such differences primarily arise from the interactions between the tractor and the trailer, which may vary significantly due to variations in the operating conditions and maneuvers. Unlike the single unit vehicle driver, an articulated vehicle driver consciously controls the vehicle based upon certain perception of the motion of both the towing and trailing units. While the lateral position and the orientation of the vehicle serve as the primary error cues, the lateral acceleration and roll motions of both units subconsciously influence the driver's directional control strategies. Although the control strategies of articulated vehicle driver have not been reported in the literature, it is generally accepted that heavy vehicle drivers possess higher driving skills.

1.3 SCOPE AND OBJECTIVES OF THE DISSERTATION

From the review of reported studies, summarized in the previous section, it is apparent that the directional dynamics characteristics of articulated commercial vehicles have been extensively investigated in an open-loop manner. The driver's contributions to the vehicle stability and control limits have been mostly ignored. Furthermore, a large number of vehicle models have been proposed with varying degrees of complexities. While comprehensive three-dimensional models permit analyses under wide range of design and operating conditions, but they require more tedious characterization of a large number of vehicle parameters. Simplified yaw-plane models, on the other hand, yield lateral and yaw directional response in a reasonably accurate manner, assuming negligible contributions due to roll dynamics and braking of the vehicle. For the development of a

coupled articulated vehicle-driver model and identification of vehicle design that can be adapted to the driver, it is desirable to develop a simpler, yet credible vehicle model, which can be effectively interfaced with a more elaborate driver model. A yaw plane model with limited roll-DOF is thus addressed in this dissertation research, which can effectively predict the vehicle motion and contributions due to dynamics associated with vehicle roll.

From the review of literature relevant to driver-vehicle models, it is concluded that most of the reported models have been developed for single unit vehicles. Since the dynamics of single unit vehicles differ considerably from those of multiple unit vehicles, the articulated vehicle drivers employ significantly different control strategies. Furthermore, these drivers possess certain perception of the motions of the trailing unit. The limited number of driver models, proposed for applications in articulated vehicles, employ control strategies based on lateral position error of the lead unit alone. It has been recognized that the highway safety associated with articulated vehicle is further related to lateral position of the trailing unit and yaw position of both the units. The development of a driver model, based upon the motion of both units, is thus addressed in this dissertation research, to enhance an understanding of the driver's interaction with the articulated vehicle dynamics.

The weights and dimension limits on heavy vehicles have been invariably derived from the open-loop dynamic analyses. Furthermore, in the vehicle design process it is assumed that the driver can effectively control the transient directional response of the vehicle under emergency situations. The safety performance of such vehicles can be conveniently enhanced by considering the control performance limits of the driver in the

design process. The weights and dimensions, and design of articulated vehicles may thus be realized to adapt to drivers of varying skills.

1.3.1 Objectives of the Dissertation

The overall objective of this investigation is to contribute towards attainment of effective closed-loop driver/vehicle directional control model of an articulated vehicle-driver system, and to establish a methodology to design vehicles that can be adapted to drivers of different skills. The specific objectives of the study are summarized below:

a. Develop an effective directional dynamic model of the articulated vehicle to predict the yaw and roll dynamics response, while incorporating nonlinear tire model.
b. Perform sensitivity analyses to identify vehicle parameters that affect the directional performance most significantly.
c. Propose a methodology to identify important vehicle parameters, which are difficult to quantify with high levels of uncertainty.
d. Investigate different structures of closed-loop driver-vehicle models to identify various feedback variables required to minimize path tracking errors.
e. Identify various driver model parameters through formulation and minimization of a comprehensive performance index as a function of various safety performance measures of the vehicle combination.
f. Identify the range of driver model parameters, more specifically the parameters describing the control performance limits of drivers as a function of their skill and experience.

g. Propose a methodology to determine most desirable vehicle design parameters related to weights, dimensions, suspension, tires and articulation, such that the vehicle can be ideally adapted to the driver's skill.

h. Identify most desirable design parameters of an articulated vehicle that can be adapted to drivers with superior and inferior driving skills, and demonstrate the potential performance benefits of the proposed adaptive vehicle.

1.3.2 Organization of the Dissertation

In Chapter 2, analytical models of articulated heavy vehicle are developed to derive its dynamic behaviour to steady and transient steering maneuvers. The response characteristics of the simplified yaw plane model and yaw plane model with limited roll degree-of-freedom (DOF) are compared with those of a comprehensive three-dimensional model. The results are analyzed to select an appropriate vehicle model in view of its computational efficiency and requirement of vehicle parameters. In the modeling of the vehicle dynamics, the tire dynamics is represented by Magic Formula and neural network, respectively. The effectiveness of the proposed model is demonstrated by comparing its response with the available measured data.

In Chapter 3, the yaw-plane model with limited roll-DOF, is used to perform parameter sensitivity analyses. The results are analyzed to identify vehicle parameters that affect its directional response most significantly. A system identification methodology is formulated to identify vehicle parameters that are known to exhibit high degree of uncertainty in their estimation, from the measured response.

Different structures of closed-loop driver-articulated vehicle models are systematically formulated and analyzed in Chapter 4. A comprehensive performance index comprising various safety measures of heavy vehicles is formulated to identify the driver model parameters and to assess the performance characteristics of different model structures. The results are analyzed to identify appropriate feedback variables for the coupled model.

In Chapter 5, a comprehensive driver-articulated vehicle model is developed and validated to study the influence of maneuver severity, vehicle forward speed and external disturbances on the driver and vehicle performance, based upon minimization of the proposed composite performance index and integration of the yaw plane linear and nonlinear models with roll DOF.

In Chapter 6, the driver's directional control performance limits are discussed, including reaction time, preview distance, compensatory gain, and frequency range. Three sets of control parameters are formulated to describe varying skill levels of the drivers. Coupled driver-vehicle models, comprising yaw-plane with roll-DOF vehicle model and models of three drivers, are formulated to identify most desirable vehicle design parameters. A methodology, based upon sequential minimization of the performance index, is proposed to identify vehicle design that can be adapted to specific driving skill.

The highlights of the dissertation research, major conclusions drawn and recommendations for the future work are finally presented in Chapter 7.

CHAPTER 2 OPEN-LOOP DIRECTIONAL DYNAMICS OF ARTICULATED VEHICLES

2.1 INTRODUCTION

The increasing use of commercial articulated vehicles in road transportation have prompted increased concerns towards highway safety, which are mostly attributed to their large dimensions and weight, and poor stability limits. While the weight and dimension regulations were mostly relaxed in the interest of improving the transport economy, extensive efforts have been mounted to establish and enhance the directional stability and performance limits of heavy vehicles. Such efforts have evolved into an array of analytical models, which can be effectively applied to assess the performance limits of vehicle combinations and their subsystems. The computational methods, complexities and capabilities of various vehicle models, however, vary considerably depending upon the nature of component characteristics, excitations, and generality to analyze varying configurations of vehicles.

The proposed analytical models vary from simplified constant speed linear yaw-plane models to comprehensive three-dimensional variable speed models [1,40,41,95]. In the previous Chapter, it was indicated that a more complex model does not necessarily yield more accurate results [96]. The choice of vehicle model thus relies mostly on the analysis objectives. Although the simplified linear yaw-plane model can predict lateral and yaw directional response of the vehicle similar to that predicted by the sophisticated Phase IV program [41], the resulting directional response can be considered valid within the linear side-slip range of tires, and in the absence of roll and pitch motions arising from lateral and longitudinal load transfer, respectively.

In this dissertation research, a simple yet credible model of an articulated vehicle is attempted to facilitate its integration with an adequate heavy vehicle driver model. A yaw-plane model, incorporating nonlinear cornering characteristics of the tires and compliance of the steering column, is thus initially developed to study the open-loop directional response of the vehicle. A limited roll-DOF is then introduced to account for vehicle roll and lateral load transfer. The cornering properties of tires are evaluated using the Magic Formula, proposed by Pacejka et al. [65]. The response characteristics derived from the proposed model are compared with the available measured data to demonstrate its validity. A neural network method is further implemented to model the vehicle dynamics based upon the simulated data.

2.2 DEVELOPMENT OF ANALYTICAL MODELS

In this section, the formulations for four different models for analysis of open-loop directional response behaviour of an articulated vehicle are described. The models developed include the yaw plane model, yaw plane model with limited roll DOF, yaw/roll plane model, and neural network model. Various simplifying assumptions are associated with each model, while the common assumptions adopted in all these models are listed below:

- The steering angle developed at the left and right wheel is considered to be identical, assuming parallel steering;
- The vehicle is assumed to move on a horizontal surface with uniform friction characteristics;
- All joints are considered frictionless and articulation takes place about the vertical axis. The tractor and semi-trailer units are free to yaw relative to each other, while the motions of two units are constrained along the lateral and longitudinal directions at the articulation point;

- The force-displacement characteristics of the suspension springs are considered to be nonlinear with lash based upon the measured data;
- Each element or unit of the vehicle combination is considered as a rigid body;
- Gyroscopic moments due to rotating elements such as wheels and tires are assumed to be small and hence neglected;

2.2.1 Yaw Plane Model

The lateral and yaw directional response characteristics of an articulated vehicle can be conveniently evaluated through development of a simplified yaw plane model. Yaw plane models of articulated vehicle combinations have been extensively reported in the literature [1,44,45,50]. Majority of these models, however, assume linear cornering properties of tires and negligible compliance due to the steering system. The cornering properties of the tires are known to be nonlinearly related with the normal load and side-slip angle. Figure 2.1 illustrates the cornering force (F_y) and aligning moment (M_z) characteristics of a typical heavy vehicle tire as a function of side-slip angle and normal load. A linear cornering force model can be considered valid for only small slip angle and constant normal load. Furthermore, the consideration of compliant steering is vital to study the driver's interaction with the vehicle. A yaw plane model of an articulated vehicle is thus developed to incorporate nonlinear tire properties and compliant steering. The simplifying assumptions associated with the model formulation are summarized below:

- The roll and pitch motions of the units are assumed to be small and thus neglected;
- The nonlinearities arising from clearance between the joints and gears of the steering system are neglected;

- The contributions due to the suspension forces in the yaw plane are assumed negligible;

- The variations in longitudinal tire forces are considered negligible, assuming constant forward speed;

- The unsprung masses are assumed to be rigidly attached to their respective sprung masses;

- The lateral transfer of load on the tires is assumed to be small in the absence of roll motion and the slip angles experienced at the left and right sides of a given axle are approximately equal. The properties of left and right tires of an axle can thus be represented by a single composite tire, and the cornering stiffness of each axle is the sum of the cornering stiffness of the tires mounted on that axle.

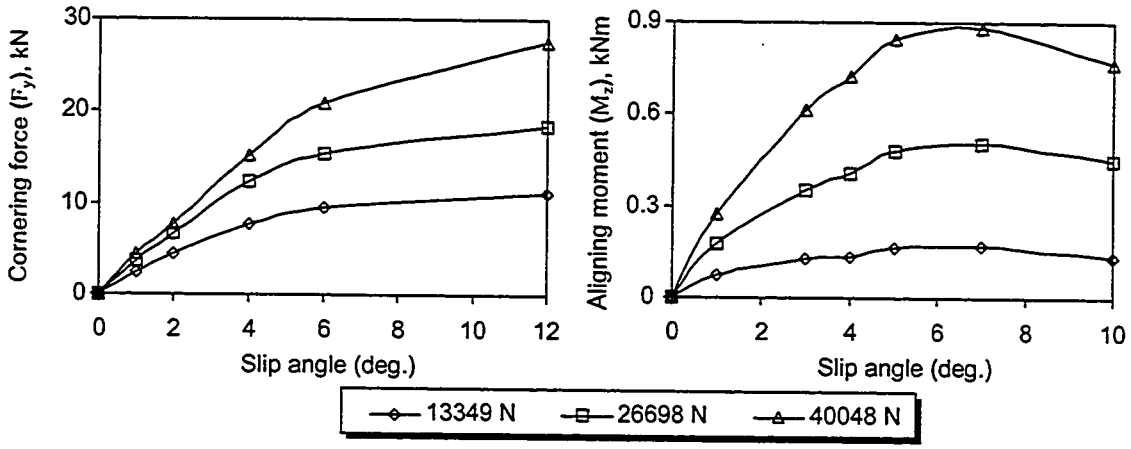

Figure 2.1: Cornering force and aligning moment characteristics of a heavy vehicle tire.

Figure 2.2 illustrates the yaw plane model of an articulated vehicle comprising a three-axle tractor and four-axle trailer. The model formulated is sufficiently general to include varying number of axles for each unit. The motion of each mass center is specified by its translational velocity components, u_i and v_i, and an angular velocity r_i about z axis passing through the mass center. Upon elimination of the constraint forces at the articulation joints, the following equations of motion are obtained [1,31,32]:

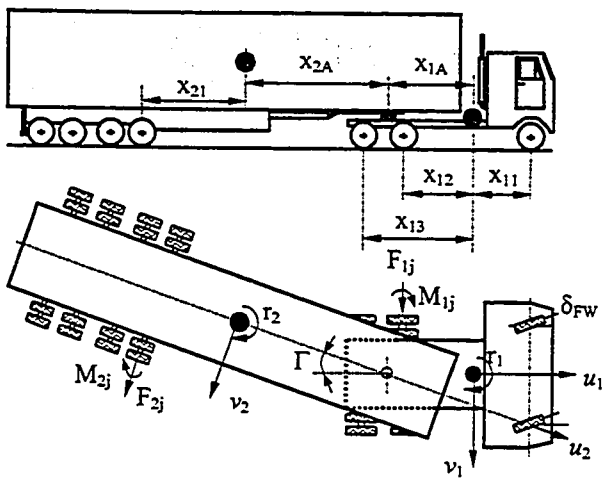

Figure 2.2: Yaw plane model of an articulated vehicle.

Lateral force equation of the coupled vehicle:

$$m_1(\dot{v}_1 + u_1 r_1) + m_2(\dot{v}_2 + u_2 r_2) = \sum_{j=1}^{3} F_{1j} + \sum_{j=1}^{4} F_{2j} \tag{2.1}$$

Yaw moment equation for the tractor:

$$I_1 \dot{r}_1 = x_{1A}\left[m_2(\dot{v}_2 + u_2 v_2) - \sum_{j=1}^{3} F_{2j} \right] + F_{11}x_{11} - F_{12}x_{12} - F_{13}x_{13} + \sum_{j=1}^{3} M_{1j} \tag{2.2}$$

Yaw moment equation for the semitrailer:

$$I_2 \dot{r}_2 = x_{2A}\left[m_2(\dot{v}_2 + u_2 v_2) - \sum_{j=1}^{4} F_{2j} \right] - \sum_{j=1}^{4} (F_{2j}x_{2j} - M_{2j}) \tag{2.3}$$

where, F_{ij} and M_{ij} are the lateral cornering force and aligning moment, respectively, developed at tire on axle j of unit i (j=1, 2, 3 for i=1; and j=1, 2, 3, 4 for i=2). F_{ij} and M_{ij} are expressed as nonlinear functions of side slip angle developed at the tires, α_{ij}, in the following manner:

$$F_{ij} = f_F(\alpha_{ij}) \quad \text{and} \quad M_{ij} = f_M(\alpha_{ij}) \tag{2.4}$$

where, (2.5)

$$\alpha_{11} = \frac{v_1 + x_{11} r_1}{u_1} - \delta_{FW} \text{ and } \alpha_{ij} = \frac{v_i - x_{ij} r_i}{u_i} \text{ (for } i\text{=2, } j\text{=2, 3; for } i\text{=2, } j\text{=1, 2, 3, 4)}$$

The constraints posed by the articulation yield following relationships for the lateral (v_1, v_2) and yaw velocities (r_1, r_2) of the two units:

$$v_2 = v_1 - u_1 \Gamma - x_{1A} r_1 - x_{2A} r_2 \text{ and } \dot{\Gamma} = r_2 - r_1 \tag{2.6}$$

where Γ is the articulation angle between the two units. The steering system model is schematically illustrated in Figure 2.3, where I_{sw} and I_w are effective mass moments of inertia due to steering wheel, and the front wheels including linkage, about the axis of the kingpin, respectively. K_w and C_w are the equivalent torsional stiffness and damping coefficients due to front wheels rotation about the axis of the kingpin, α is the angle between the steering column and a vertical axis, i_{st} is the steering ratio, T_{sw} is the driver's input torque to the steering wheel, and F_{11} is the lateral force developed by the front wheel tires. The equation of motion for the steering system can thus be expressed as:

$$I_{sw}(\ddot{\theta}_{sw} + \dot{r}_1 \cos\alpha + \ddot{\phi}_1 \sin\alpha) i_{st} + I_w \ddot{\delta}_{FW} + C_w \dot{\delta}_{FW} + K_w \delta_{FW} + F_{11} D_w = T_{sw} i_{st} \tag{2.7}$$

where $\theta_{sw} = i_{st} \delta_{FW}$ is the steering wheel angle and δ_{FW} is the front wheel steering angle, $\dot{r}_1$ and $\ddot{\phi}_1$ are the yaw and roll accelerations of tractor, respectively. The roll acceleration component in Equation (2.7) is suppressed for the yaw-plane model.

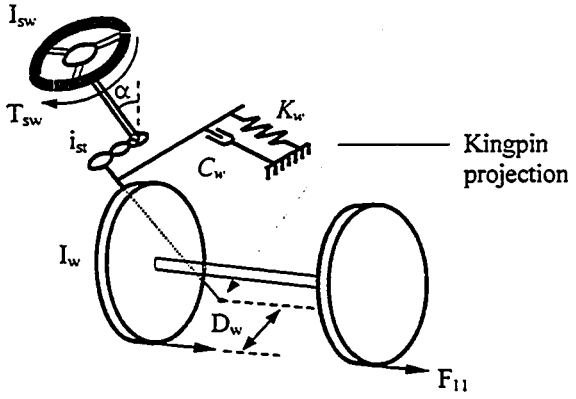

Figure 2.3: The steering system model [148].

Equations (2.1) through (2.6) fully describe the dynamic behaviour of the three-DOF articulated vehicle model in the yaw plane, while Equation (2.7) describes a relationship between the steering wheel and front wheel angles.

2.2.2 Yaw Plane Model With Limited Roll Degree-of-Freedom

The yaw plane model, formulated in the previous section, permits directional dynamics analysis of the vehicle combination, assuming negligible roll motion. Heavy vehicles, in general, experience certain roll motion due to centrifugal actions arising from a steering maneuver, and due to compliant suspension and tires. The roll motion of the vehicle and the resulting lateral load transfer affects the dynamic behaviour of the vehicle in a considerable manner. Contributions due to vehicle roll can be conveniently investigated by integrating sprung mass roll-DOF to the yaw plane model. A modified yaw plane model is thus developed to incorporate four-DOF for the tractor (forward speed, u_1; lateral velocity, v_1; yaw velocity, r_1; roll angle, ϕ_1), and two-DOF for the trailer (articulation angle, Γ; and roll angle, ϕ_2). The lateral (v_2) and yaw (r_2) velocities of the trailer mass are derived from the constraint imposed by the fifth wheel articulation. The analytical model is developed subject to following simplifying assumptions, in addition to those listed in Section 2.2:

- The roll motion of the sprung masses occur about their respective roll centers, which are located at fixed distances beneath the sprung masses;
- The contributions due to suspension lash are assumed to be small;
- The cornering force and aligning moment developed by the tire are considered to be nonlinear functions of longitudinal deformation slip, side-slip angles and vertical load. The influence of wheel camber on lateral force generation, however, is assumed negligible;

- The xz plane divides the body symmetrically and the axes are parallel to the principal axes of the body;
- The resultant wind resistances act at the c.g. of the tractor and semitrailer;
- The yaw damping resistance moment due to articulation mechanism is proportional to the relative yaw rate of the fifth wheel;
- The roll motions of the unsprung masses are assumed to be negligible due to the large vertical stiffness of tires, while the effective radii of all the tires are considered to be identical;
- The pitch and vertical motions of the vehicle traversing a perfectly smooth road are small and hence neglected.

The common origin of reference frames for the tractor and trailer is taken at the kinematic center of the connecting joint. In the straight-line driving and undisturbed state, the axis systems of the tractor and semitrailer are coincident and the xy planes are parallel to the ground. The tractor and trailer axes systems undergo longitudinal velocities (u_1, u_2) and lateral velocities (v_1, v_2) along the axes x_1, x_2 and y_1, y_2, respectively, as shown in Figure 2.4. The figure also illustrates the modified yaw plane model, where $\bar{z}_1$ and $\bar{z}_2$ denote the vertical distances between the c.g. of tractor and trailer, respectively, with respect to the fifth wheel, and h_{g1} and h_{g2} are the c.g. heights of tractor and trailer from the ground plane.

Figure 2.5 illustrates the coordinates of the centers of tractor and trailer and their sprung and unsprung masses, in the initial state. The sequence of rotations, yaw followed by roll, is adopted for formulation of the equations of motion. The coordinate vector $\{\bar{i}_1 \quad \bar{j}_1 \quad \bar{k}_1\}$ subject to yaw (ψ) and roll (ϕ) rotation can be transformed to $\{\bar{i}_2 \quad \bar{j}_2 \quad \bar{k}_2\}$ in the following manner:

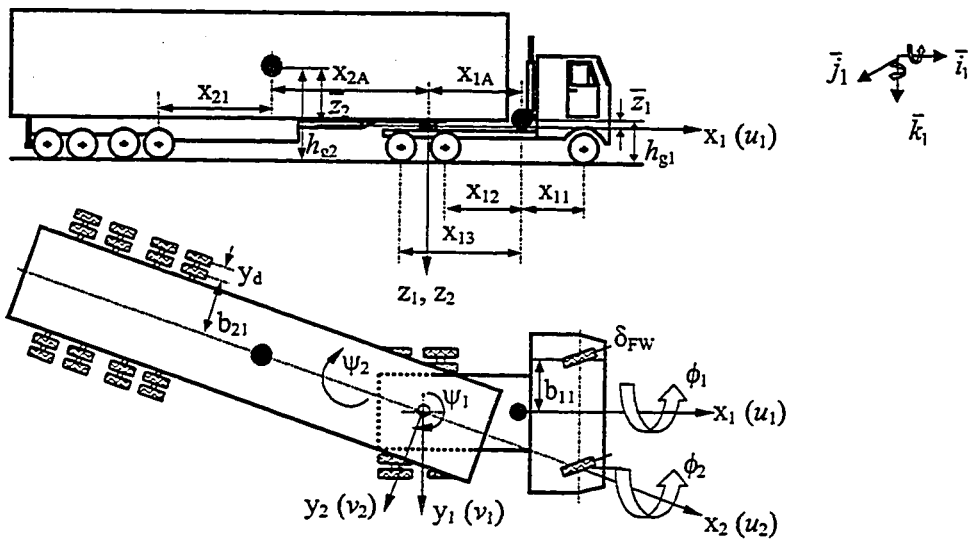

Figure 2.4: The axis systems for tractor and semitrailer with common origin at the kinematic center of coupling.

$$\begin{Bmatrix} \bar{i}_2 \\ \bar{j}_2 \\ \bar{k}_2 \end{Bmatrix} = \begin{bmatrix} \cos\psi & \sin\psi & 0 \\ -\sin\psi\cos\phi & \cos\psi\cos\phi & \sin\phi \\ \sin\psi\sin\phi & -\cos\psi\sin\phi & \cos\phi \end{bmatrix} \begin{Bmatrix} \bar{i}_1 \\ \bar{j}_1 \\ \bar{k}_1 \end{Bmatrix} \tag{2.8}$$

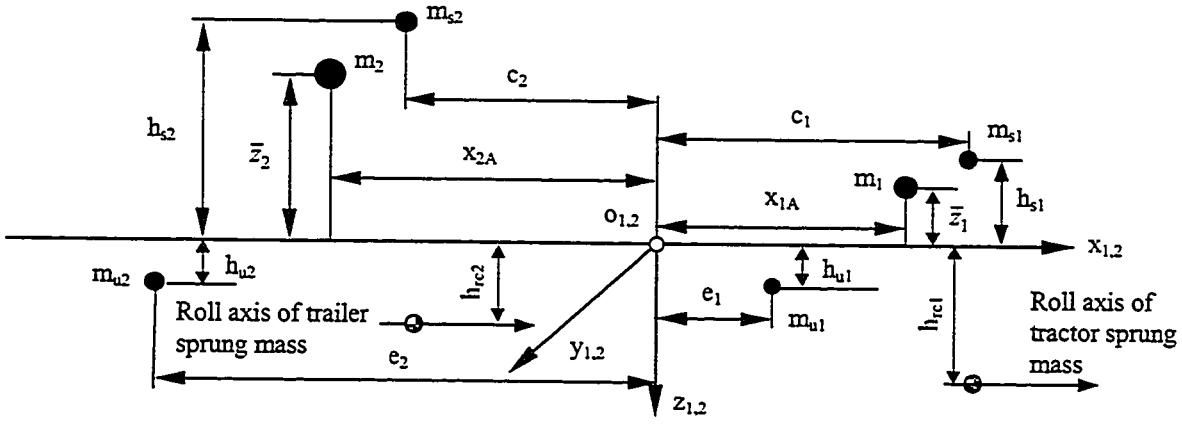

Figure 2.5: Coordinates of the mass centers.

The absolute velocities and accelerations of the tractor and trailer masses (m_1 and m_2) and their sprung masses (m_{s1} and m_{s2}) are then derived as:

$$\vec{V}_{m1} = u_1\bar{i}_1 + (v_1 + x_{1A}\dot{\psi}_1 + \bar{z}_1\dot{\phi}_1)\bar{j}_1$$

$$\vec{V}_{ms2} = u_2\vec{i}_2 + (v_2 - c_2\dot{\psi}_2 + h_{s2}\dot{\phi}_2)\vec{j}_2$$

$$\vec{V}_{ms1} = u_1\vec{i}_1 + (v_1 + c_1\dot{\psi}_1 + h_{s1}\dot{\phi}_1)\vec{j}_1$$

$$\vec{V}_{ms2} = u_2\vec{i}_2 + (v_2 - c_2\dot{\psi}_2 + h_{s2}\dot{\phi}_2)\vec{j}_2$$

$$\begin{aligned}\vec{a}_{m1} = &\left[\dot{u}_1 - \dot{\psi}_1(v_1 + x_{1A}\dot{\psi}_1 + \bar{z}_1\dot{\phi}_1)\right]\vec{i}_1 + (u_1\dot{\psi}_1 + \dot{v}_1 + x_{1A}\ddot{\psi}_1 + \bar{z}_1\ddot{\phi}_1)\vec{j}_1 + \\ &\dot{\phi}_1(v_1 + x_{1A}\dot{\psi}_1 + \bar{z}_1\dot{\phi}_1)\vec{k}_1 = a_{m1x}\vec{i}_1 + a_{m1y}\vec{j}_1 + a_{m1z}\vec{k}_1\end{aligned}$$

$$\begin{aligned}\vec{a}_{m2} = &\left[\dot{u}_2 - \dot{\psi}_2(v_2 - x_{2A}\dot{\psi}_2 + \bar{z}_2\dot{\phi}_2)\right]\vec{i}_2 + (u_2\dot{\psi}_2 + \dot{v}_2 - x_{2A}\ddot{\psi}_2 + \bar{z}_2\ddot{\phi}_2)\vec{j}_2 + \\ &\dot{\phi}_2(v_2 - x_{2A}\dot{\psi}_2 + \bar{z}_2\dot{\phi}_2)\vec{k}_2 = a_{m2x}\vec{i}_2 + a_{m2y}\vec{j}_2 + a_{m2z}\vec{k}_2\end{aligned}$$

$$\begin{aligned}\vec{a}_{ms1} = &\left[\dot{u}_1 - \dot{\psi}_1(v_1 + c_1\dot{\psi}_1 + h_{s1}\dot{\phi}_1)\right]\vec{i}_1 + (u_1\dot{\psi}_1 + \dot{v}_1 + c_1\ddot{\psi}_1 + h_{s1}\ddot{\phi}_1)\vec{j}_1 + \\ &\dot{\phi}_1(v_1 + c_1\dot{\psi}_1 + h_{s1}\dot{\phi}_1)\vec{k}_1\end{aligned}$$

$$\begin{aligned}\vec{a}_{ms2} = &\left[\dot{u}_2 - \dot{\psi}_2(v_2 - c_2\dot{\psi}_2 + h_{s2}\dot{\phi}_2)\right]\vec{i}_2 + (u_2\dot{\psi}_2 + \dot{v}_2 - c_2\ddot{\psi}_2 + h_{s2}\ddot{\phi}_2)\vec{j}_2 + \\ &\dot{\phi}_2(v_2 - c_2\dot{\psi}_2 + h_{s2}\dot{\phi}_2)\vec{k}_2\end{aligned} \qquad (2.9)$$

where $\vec{V}_{m1}$ and $\vec{V}_{m2}$ are the absolute velocities of tractor and trailer masses, respectively, and $\vec{V}_{ms1}$ and $\vec{V}_{ms2}$ are the velocities of their sprung masses. $\vec{a}_{m1}$, $\vec{a}_{m2}$, $\vec{a}_{ms1}$ and $\vec{a}_{ms2}$ are the absolute accelerations of tractor and trailer masses and their sprung masses, respectively. The other geometrical parameters are denoted in Figure 2.5.

Figure 2.6 illustrates the forces and moments acting on the vehicle, where F_{w1x} and F_{w1y} are the resultant wind resistances acting on the tractor along the longitudinal and lateral directions, respectively. F_{w2x} and F_{w2y} are the resultant wind resistances acting on the trailer. F_{xijk}, F_{yijk} and M_{ijk} are the longitudinal and lateral forces, and aligning moments developed at the tire k (k=1, 2 for j=1 and i=1; and k=1, 2, 3, 4 for the other j and i) on the axle j (j=1, 2, 3 for i=1; and j=1, 2, 3, 4 for i=2) of unit i (i=1 for tractor; and i=2 for trailer), respectively. L_1 and L_2 are the roll moments acting on tractor

and semitrailer due to torsional compliance of the fifth wheel and vehicle structure, respectively. M_h represents the yaw damping torque developed at the articulation joint.

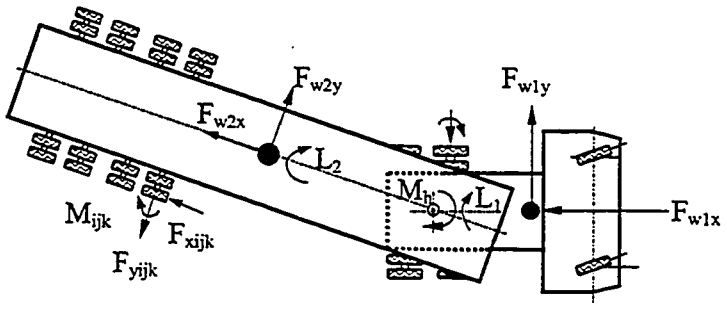

Figure 2.6: The forces system of tractor and semitrailer under breaking.

The fifth wheel articulation permits relative yaw rotations of the two units and limited relative roll rotation due to torsional compliance of the fifth wheel and trailer structure. The articulation points or the origins, o_1 and o_2, of the units are thus coincident. The velocities and accelerations developed at the articulation are constrained and yield:

$$u_2 = v_1 \sin(\Gamma) + u_1 \cos(\Gamma)$$
$$v_2 = \frac{v_1 \cos(\Gamma) - u_1 \sin(\Gamma)}{\cos(\phi_2 - \phi_1)} \tag{2.10}$$

$$\dot{u}_2 = (\dot{u}_1 - v_1\dot{\psi}_1)\cos(\Gamma) + (\dot{v}_1 + u_1\dot{\psi}_1)\sin(\Gamma) + v_2\dot{\psi}_2$$
$$\dot{v}_2 = \frac{(\dot{v}_1 + u_1\dot{\psi}_1)\cos(\Gamma) - (\dot{u}_1 - v_1\dot{\psi}_1)\sin(\Gamma) + v_2\dot{\phi}_2 \sin(\phi_2 - \phi_1)}{\cos(\phi_2 - \phi_1)} - u_2\dot{\psi}_2 \tag{2.11}$$

where $\Gamma = \psi_2 - \psi_1$. The force equilibrium for the tractor and trailer masses may be expressed as:

$$\bar{F}_I = m_1\bar{a}_{m1} + m_2\bar{a}_{m2} = F_{Ix}\bar{i}_1 + F_{Iy}\bar{j}_1 + F_{Iz}\bar{k}_1 \tag{2.12}$$

where,

$$F_{Ix} = m_1 a_{m1x} + m_2\left[a_{m2x}\cos(\Gamma) - a_{m2y}\cos(\phi_2 - \phi_1)\sin(\Gamma) + a_{m2z}\sin(\phi_2 - \phi_1)\sin(\Gamma)\right]$$
$$F_{Iy} = m_1 a_{m1y} + m_2\left[a_{m2x}\sin(\Gamma) + a_{m2y}\cos(\phi_2 - \phi_1)\cos(\Gamma) - a_{m2z}\sin(\phi_2 - \phi_1)\cos(\Gamma)\right]$$
$$F_{Iz} = m_1 a_{m1z} + m_2\left[a_{m2y}\sin(\phi_2 - \phi_1) + a_{m2z}\cos(\phi_2 - \phi_1)\right] \tag{2.13}$$

The equilibrium between the external forces and the inertia forces yields the following set of equations of motion:

Longitudinal motion of the tractor (x_1):

$$F_{Ix} = -\sum_{k=1}^{2} F_{x11k} - \sum_{j=2}^{3}\sum_{k=1}^{4} F_{x1jk} - F_{w1x} - F_{w2x}\cos(\Gamma) - F_{w2y}\sin(\Gamma)\cos(\phi_2 - \phi_1)$$
$$-\cos(\Gamma)\sum_{j=1}^{3}\sum_{k=1}^{4} F_{x2jk} - \sin(\Gamma)\cos(\phi_2 - \phi_1)\sum_{j=1}^{3}\sum_{k=1}^{4} F_{y2jk}$$

Lateral motion of the tractor (y_1):

$$F_{Iy} = \sum_{k=1}^{2} F_{y11k} + \sum_{j=2}^{3}\sum_{k=1}^{4} F_{y1jk} - F_{w1y} - F_{w2x}\sin(\Gamma) - F_{w2y}\cos(\Gamma)\cos(\phi_2 - \phi_1)$$
$$-\sin(\Gamma)\sum_{j=1}^{3}\sum_{k=1}^{4} F_{x2jk} + \cos(\Gamma)\cos(\phi_2 - \phi_1)\sum_{j=1}^{3}\sum_{k=1}^{4} F_{y2jk}$$

Roll motion of the tractor (ϕ_1):

$$I_{xt}\ddot{\phi}_1 + m_{s1}(h_{s1} + h_{rc1})[\dot{v}_1 + u_1 r_1 + c_1\ddot{\psi}_1] = m_{s1}g(h_{s1} + h_{rc1})\sin\phi_1 - C_{\phi t}\dot{\phi}_1 - K_{\phi t}\phi_1 -$$
$$F_{w1y}(\bar{z}_1 + h_{rc1}) - L_1$$

Yaw motion of the tractor (ψ_1):

$$m_1 x_{1A}(\dot{v}_1 + u_1 r_1 + \bar{z}_1\ddot{\phi}_1) + I_{zt}\dot{r}_1 = (x_{1A} + x_{11})\sum_{k=1}^{2} F_{y11k} + \sum_{j=2}^{3}(x_{1A} - x_{1j})\sum_{k=1}^{4} F_{y1jk} +$$
$$\sum_{k=1}^{2} M_{11k} + C_{\psi h}(r_2 - r_1) + \sum_{j=2}^{3}\sum_{k=1}^{4} M_{1jk} + b_{11}(F_{x111} - F_{x112}) -$$
$$\sum_{j=2}^{3}\left[(b_{1j} + y_d)(F_{x1j1} - F_{x1j4}) + b_{1j}(F_{x1j2} - F_{x1j3})\right] - F_{w1y}x_{1A} \qquad (2.14)$$

where I_{xt} and I_{zt} are the roll and yaw mass moments of inertia of the sprung mass of the tractor about the longitudinal axis passing through the roll center of the sprung mass and z_1 axis, respectively. $C_{\phi t}$ and $K_{\phi t}$ are the equivalent roll damping and stiffness coefficients of the tractor axles suspension, $C_{\psi h}$ is the yaw damping due to the fifth wheel, and y_d and h_{rc1} are the dual tire spacing and the vertical distance between the x_1 axis and the roll axis of the tractor sprung mass, respectively. The equations for the roll

and yaw-DOF for the trailer about the roll axis of trailer sprung mass and z_2 axes are derived as follows:

Roll motion of the trailer (ϕ_2):

$$m_{s2}(h_{s2}+h_{rc2})(\dot{v}_2 - c_2\ddot{\psi}_2 + u_2 r_2) + I_{xs}\ddot{\phi}_2 = m_{s2}g(h_{s2}+h_{rc2})\sin\phi_2 - C_{\phi s}\dot{\phi}_2 - K_{\phi s}\phi_2 - F_{w2y}(\bar{z}_2 + h_{rc2}) - L_2$$

Yaw motion of the trailer (ψ_2):

$$I_{zs}\dot{r}_2 - m_2 x_{2A}(\dot{v}_2 + u_2 r_2 + \bar{z}_2\ddot{\phi}_2) = -\sum_{j=1}^{4}\left[(x_{2A}+x_{2j})\sum_{k=1}^{4}F_{y2jk} - \sum_{k=1}^{4}M_{2jk}\right] + F_{w2y}x_{2A} + -C_{\psi h}(r_2 - r_1) - \sum_{j=1}^{4}\left[(b_{2j}+y_d)(F_{x2j1}-F_{x2j4}) + b_{2j}(F_{x2j2}-F_{x2j3})\right] \quad (2.15)$$

where I_{xs} and I_{zs} are the roll and yaw moments of inertia of the sprung mass of semitrailer about the roll axis of the trailer sprung mass and z_2 axis, respectively, $C_{\phi s}$ and $K_{\phi s}$ are the roll damping and stiffness coefficients of the semitrailer axle suspension. h_{rc2} is the vertical distance between the x_2 axis and the roll axis of the trailer sprung mass.

AERODYNAMICS FORCES

The aerodynamic resistances acting on the two units are expressed in the following form [160]:

$$F_{w1x} = \frac{\rho}{2}C_{D1x}A_{f1x}(u_1 - u_{1wx})^2,\ F_{w2x} = \frac{\rho}{2}C_{D2x}A_{f2x}(u_2 - u_{2wx})^2,$$
$$F_{w1y} = \frac{\rho}{2}C_{D1y}A_{f1y}(v_1 + x_{1A}r_1 - (\bar{z}_1 + h_{rc1})\dot{\phi}_1 - u_{1wy})^2, \text{ and}$$
$$F_{w2y} = \frac{\rho}{2}C_{D2y}A_{f2y}(v_2 - x_{2A}r_2 + (\bar{z}_2 + h_{rc2})\dot{\phi}_2 - u_{2wy})^2 \quad (2.16)$$

where ρ is mass density of air. $C_{D1x}, C_{D1y}, C_{D2x}$ and C_{D2y} are the coefficients of aerodynamic resistance, which range between 0.8 and 1.3 for heavy vehicles [160].

$A_{f1x}, A_{f1y}, A_{f2x}$ and A_{f2y} are the characteristic areas of the tractor and semitrailer along the longitudinal and lateral directions, respectively. u_{1wx}, u_{2wx}, u_{1wy} and u_{2wy} are the wind speeds along x_1, x_2, y_1, and y_2 directions, respectively.

BRAKING FORCES & MOMENTS

Under application of braking, the sum of braking forces developed at the tires of axle j of the unit i, can be related to the braking torque, in the following manner:

$$R_T \sum_k F_{xijk} - M_{bij} = I_{wij}\dot{\omega}_{ij}; \quad k = \begin{cases} 1,2 & i = j = 1 \\ 1,2,3,4 & otherwise \end{cases} \tag{2.17}$$

where ω_{ij} is the angular velocity of the wheels on axle j of unit i, I_{wij} is the moment of inertia of the wheels, R_T is the effective wheel radius, and M_{bij} is the braking torque applied to wheels on axle j of unit i. The longitudinal slip ratio developed at tire k of axle j of unit i is given by:

$$S_{ijk} = \frac{u_{wijk} - \omega_{ij} R_T}{u_{wijk}} \tag{2.18}$$

where u_{wijk} is the longitudinal velocity of tire k of axle j of unit i. The longitudinal velocity u_{wijk} is related to the absolute velocity of the tire u_{ijk} and side-slip angle α_{ijk} developed at the tire in the following manner:

$$u_{wijk} = u_{ijk} \cos\alpha_{ijk} \tag{2.19}$$

The absolute velocity u_{ijk} and side-slip angle α_{ijk}, developed at tire k on axle j of unit i, is derived from the following relationships:

Tractor Front Axle (i=1; j=1; k=1, 2)

$$u_{11k} = \sqrt{\left[v_1 + r_1(x_{1A} + x_{11}) - \dot{\phi}_1(\bar{z}_1 + h_{g1} - R_T)\right]^2 + \left[u_1 + (-1)^{k+1} r_1 b_{11}\right]^2}$$

$$\alpha_{11k} = \tan^{-1}\left[\frac{v_1 + r_1(x_{1A} + x_{11}) - \dot{\phi}_1(\bar{z}_1 + h_{g1} - R_T)}{u_1 + r_1 b_{11}(-1)^{k+1}}\right] - \delta_{FW} \tag{2.20}$$

Tractor Rear Axle (i=1; j=2, 3; k=1, 2, 3, 4)

$$u_{1jk} = \sqrt{\left[v_1 + r_1(x_{1A} - x_{1j}) - \dot{\phi}_1(\bar{z}_1 + h_{g1} - R_T)\right]^2 + (u_1 + t_k r_1 T_{1j})^2} \quad \text{and}$$

$$\alpha_{1jk} = \tan^{-1}\left[\frac{v_1 + r_1(x_{1A} - x_{1j}) - \dot{\phi}_1(\bar{z}_1 + h_{g1} - R_T)}{u_1 + t_k r_1 T_{1j}}\right] \tag{2.21}$$

Semitrailer Axle (i=2; j=1, 2, 3, 4, k=1, 2, 3, 4)

$$u_{2jk} = \sqrt{\left[v_2 - r_2(x_{2A} + x_{2j}) - \dot{\phi}_2(h_{g2} - \bar{z}_2 - R_T)\right]^2 + (u_2 + t_k r_2 T_{2j})^2} \quad \text{and}$$

$$\alpha_{2jk} = \tan^{-1}\left[\frac{v_2 - r_2(x_{2A} + x_{2i}) - \dot{\phi}_2(h_{g2} - \bar{z}_2 - R_T)}{u_2 + t_k r_2 T_{2j}}\right], \ (i = 1, 2, 3) \tag{2.22}$$

where t_k=1; for k=1, 2 and t_k=-1; for k=3, 4. T_{ij}=b_{1j}+y_d; for k=1, 4 and T_{ij}=b_{1j}; for k=2, 3 (i=1, 2). The lateral and longitudinal tire forces, however, are known to be strongly nonlinear functions of the side slip angle α_{ijk}, longitudinal slip S_{ijk} and the normal load. The Magic tire formula, proposed by Pacejka [65], is thus employed to derive the tire forces under simultaneous application of steering and braking. The tire model is described in Section 2.3.

ARTICULATION MOMENTS

The articulation imposes roll moments, L_1 and L_2, on the tractor and trailer units, respectively, due to torsional compliance of the fifth wheel articulation and vehicle

structure. The moments are evaluated from the relative angular displacement between the tractor and semitrailer in the following manner [35, 95]:

$$L_1 = \frac{k_{f1}k_{f2}\{\phi_2[1-\sin(\Gamma)]-\phi_1\cos(\Gamma)\}}{(k_{f1}+k_{f2})\cos(\Gamma)} \text{ and } L_2 = \frac{k_{f1}k_{f2}\{\phi_2[\sin(\Gamma)-1]+\phi_1\cos(\Gamma)\}}{k_{f1}+k_{f2}} \quad \text{for } 0 \le |\Gamma| < 90^\circ \tag{2.23}$$

where k_{f1} and k_{f2} are roll stiffness of fifth wheel associated with tractor and semitrailer structures, respectively.

VERTICAL TIRE FORCES

The sprung mass roll and lateral acceleration yield considerable shift of vertical load from the inside to outside tires, as illustrated in Figure 2.7. The vertical load acting on tires of the tractor and semitrailer axles can be derived from the equilibrium of moments about the roll center of the sprung masses in the roll plane:

Tractor:

$$m_1 a_{m1y}(\bar{z}_1 + h_{rc1}) + I_{xr}\ddot{\phi}_1 = m_{s1}g(h_{s1}+h_{rc1})\sin\phi_1 - L_1 - F_{w1y}(\bar{z}_1+h_{rc1}) - 2\sum_{j=2}^{3}\Delta F_{z1j2}b_{1j} - 2\left[\Delta F_{z111}b_{11} + \sum_{j=2}^{3}\Delta F_{z1j1}(b_{1j}+y_d)\right] - (h_{g1}-\bar{z}_1-h_{rc1})\left(\sum_{k=1}^{2}F_{y11k} + \sum_{j=2}^{3}\sum_{k=1}^{4}F_{y1jk}\right)$$

Trailer:

$$m_2 a_{m2y}(\bar{z}_2 + h_{rc2}) + I_{xs}\ddot{\phi}_2 = m_{s2}g(h_{s2}+h_{rc2})\sin\phi_2 - L_2 - F_{w2y}(\bar{z}_2+h_{rc2}) - 2\left[\sum_{j=1}^{4}\Delta F_{z2j1}(b_{2j}+y_d) + \sum_{j=1}^{4}\Delta F_{z2j2}b_{2j}\right] - (h_{g2}-\bar{z}_2-h_{rc2})\sum_{j=1}^{4}\sum_{k=1}^{4}F_{y2jk} \tag{2.24}$$

where, ΔF_{zijk} represents the variations in the vertical loads of the tire k on axle j of unit i, which is related to dynamic load transfer due to sprung mass roll. Assuming linear vertical stiffness due to tires, the variations in vertical loads acting on a dual tire set satisfy the following relationships:

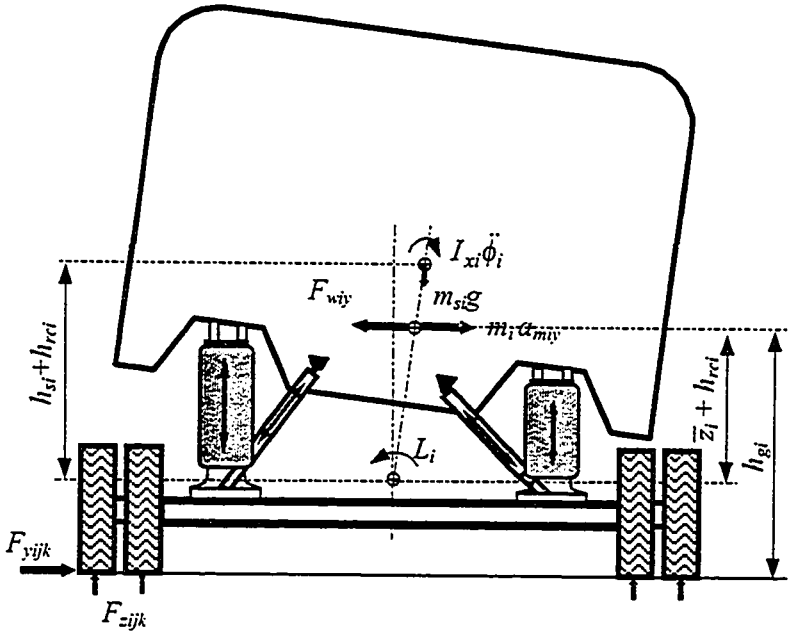

Figure 2.7: Forces and moments acting on the axle j of unit i in the roll plane.

$$\Delta F_{z111} = \frac{F_{z110}(h_{s1}+h_{rc1})\phi_1}{2b_{11}};\ \Delta F_{zij1} + \Delta F_{zij2} = \frac{F_{zij0}(h_{si}+h_{rci})\phi_i}{2(b_{ij}+0.5y_d)} \text{ and } \frac{\Delta F_{zij1}}{\Delta F_{zij2}} = \frac{b_{ij}+y_d}{b_{ij}};$$
$$i=1, j=2, 3 \text{ and } i=2, j=1, 2, 3, 4 \tag{2.25}$$

where F_{zij0} represents the static vertical force acting on axle j of unit i, h_{si} denotes the vertical distance between the c.g. of sprung mass of unit i and articulation point, and h_{rci} represents vertical distance between the articulation point and the roll axis of sprung mass of unit i. Equations (2.7) to (2.25), describe the dynamics of a 14-DOF articulated vehicle system model. The DOF include: (*i*) forward speed of tractor, u_1; (*ii*) lateral velocity of tractor, v_1; (*iii*) yaw angles of tractor and trailer, ψ_1 and ψ_2; (*iv*) roll angles of the sprung

masses of tractor and trailer, ϕ_1 and ϕ_2; (v) steering wheel angle, δ_{sw}; (vi) angular velocities of axle wheels, ω_{1j} (j=1, 2, 3) and ω_{2j} (j=1, 2, 3, 4).

2.2.3 Yaw/Roll Plane Model

A three-dimensional Yaw/Roll model, developed for analysis of directional response of single and multiple articulated vehicles, has been extensively used to evaluate the directional performance of heavy vehicles [95]. In the model, each sprung mass is treated as a rigid body with up to five degrees of freedom (dependent upon the constraints at the hitch), including motions along the lateral, vertical, yaw, roll and pitch directions. The axles are treated as beam axles which are free to roll and bounce with respect to the sprung mass to which they are attached. The relative roll motion between the unsprung and sprung masses are assumed to take place about roll centers, which are located at fixed distances beneath the sprung masses. The model permits the analysis of articulated vehicles which are equipped with any of the four coupling mechanisms, namely, conventional fifth wheel, inverted fifth wheel, pintle-hook, and kingpin. Both closed-loop (defined path input) and open-loop (defined steer angle input) modes of steering inputs can be accommodated, and the effects of the steering system compliance are taken into account. The detailed equations of motion for the model are given in [95].

2.2.4 Neural Network Model

The directional dynamics analyses of vehicle using analytical models involves estimation of large number of vehicle parameters, and highly complex and nonlinear characterization of the tire-road interactions, which pose unreasonable demands on the analysts. Furthermore, the uncertainties associated with some of the estimated parameters

can lead to considerable errors in the analysis. Alternatively, neural networks, relying on the training from available experimental data, can be implemented to model the dynamic behaviour of the vehicle and its components [161,162] in a highly efficient manner. For lateral, yaw and roll dynamics of heavy vehicles, the neural network approach only requires adequate samples of field measured data within the range of operating conditions of interest, including the maneuvers, and forward speed. The proposed neural network, when trained from the measured data, can be effectively used to predict the dynamic response of the vehicle system in a convenient manner.

A neural network (NN) is an information processing device that consists of a large number of simple nonlinear processing modules connected by elements that have information storage and programming functions. Neural networks have been extensively applied to emulate the behaviours of dynamic systems in recent years [159, 161-175], including pattern recognition, control classification, diagnostics, automation, and system dynamics. For dynamical systems, the particular interest is the ability of the neural network to deal with time-varying inputs or outputs through its own temporal operation. Thus recurrent NN is a good choice to model the behaviour of dynamical system, where the output of the network is a function of input and the network's output at the previous time step. In this section, the directional dynamics characteristics of a five-axle tractor semitrailer are predicted in terms of yaw rates of tractor and trailer, and lateral acceleration and roll angle response of the sprung masses over a wide range of forward speeds and front wheel steering inputs, using the Yaw/Roll plane model described in section 2.2.3. The results derived from the Yaw/Roll plane model are used to train a NN.

The trained NN is employed as an emulator for the vehicle undergoing maneuvers primarily within the range of training speeds and steering inputs.

The basic structure of the NN used in this section is proposed and illustrated in Figure 2.8. The input variables include the vehicle speed (u_1), the front wheel steer angle (δ_{FW}), and the feedback from the output of the NN with time delay D. The output variables of the NN contain the yaw rates, lateral accelerations and roll angles of the sprung masses of the tractor and the trailer. The size of the NN is denoted by the weight matrixes W_1 and W_2 of dimension ($S_1 \times R$) and ($S_2 \times S_1$), respectively. The vectors b_1 ($S_1 \times 1$) and b_2 ($S_2 \times 1$) denote the bias vectors. The activation functions in the first and second layer are the tansig and linear functions, respectively.

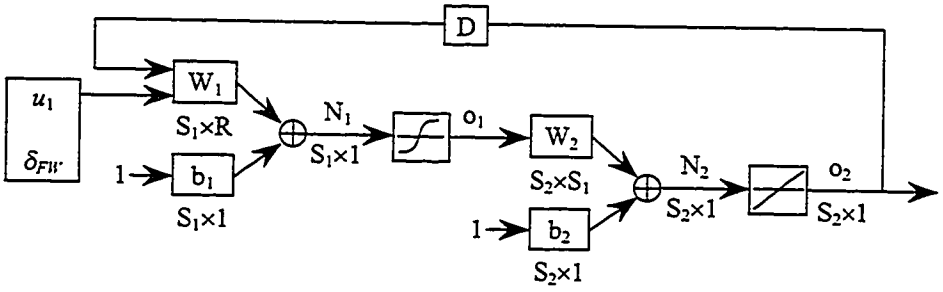

Figure 2.8: A recurrent neural network structure.

In designing an efficient and accurate NN vehicle model, the primary considerations are as follows [176]:

- the choice of the size of the NN, which will be used to map the input-output data;
- the determination of the number of time steps of delayed recurrent output sets fedback to the network; and
- an examination of the accuracy of network to predict the new input data.

The architecture of the NN, illustrated in Figure 2.8, is selected such that it has a fixed number of neurons equal to the number of output parameters (S_2=6; r_1, r_2, ϕ_1, ϕ_2, a_{y1}, a_{y2}). The number of neurons in the input layer (R), however, depends upon the number of input parameters and the feedback delay from the output of the NN. The number of neurons in the hidden layer (S_1) can vary depending upon the training accuracy and the speed. It has been established that the feedback delay from the output of the NN reflects the order of the system [161]. The delay from the output thus can be taken as two time steps for each output variable, since the differential equations of the vehicle model under consideration are of the second order. Each of the two time delays of the output set implies a time derivative. Therefore, the number of the neurons in the input layer is taken as $R=2+2S_2$, where the first constant 2 refers to two inputs.

The NN is taught using the data derived from the analysis of the Yaw/Roll vehicle model of an articulated vehicle, described in Section 2.2.3. The vehicle is assumed to perform an evasive maneuver under different speeds. A composite steer input is formulated to facilitate the directional analysis at various speeds, including 30, 60, 90, and 110 km/h. Figure 2.9 illustrates the directional response of the vehicle in terms of yaw rates (r_1, r_2), lateral accelerations (a_{y1}, a_{y2}) and roll angles (ϕ_1, ϕ_2) of the tractor and semitrailer units at different speeds, together with the front wheel steer angle, δ_{FW}. The training process is such that the weighting matrixes (W_1, W_2) and the bias vectors (b_1, b_2) are adjusted to minimize the mean sum squared error (MSSE) between the output of the NN and the training data:

$$MSSE = \frac{1}{6N}\sum_{l=1}^{N}\sum_{i=1}^{2}\left[\left(\frac{r_{il}-r_{inl}}{w_{ri}}\right)^2+\left(\frac{\phi_{il}-\phi_{inl}}{w_{\phi i}}\right)^2+\left(\frac{a_{yil}-a_{yinl}}{w_{ai}}\right)^2\right] \tag{2.26}$$

where N is the total number of the data points. w_{ri} (i=1, 2), $w_{\phi i}$ (i=1, 2) and w_{ai} (i=1, 2) are the maximum absolute values of the bias for the error in yaw rate, roll angle and lateral acceleration, respectively, of the sprung mass of the tractor and trailer. r_{il}, ϕ_{il} and a_{yil} are the training data used to describe the yaw rate, roll angle and lateral acceleration response, respectively, of the vehicle unit i. r_{inl}, ϕ_{inl} and a_{yinl} are the corresponding outputs of the NN model. It should be noted that the weighting factors, w_{ri}, $w_{\phi i}$ and w_{ai}, are chosen in such a way that the three response signals in yaw rate, roll angle and lateral acceleration of both units, contribute nearly equally to the training of network considering the differences in their numerical values.

The MSSE values are computed for varying different time delay recurrences for the training data, and results are summarized in Table 2.1. The delays of up to three time steps are applied to the set before being fedback to the NN input. For each of the four cases involving delays of different time steps, the learning process is carried out for 20000 epochs with the simulation data shown in Figure 2.9, and the number of neurons in the hidden layer (S_1) is taken as 15 by trial and error. The results revealed insignificant change in the MSSE after 20000 epochs. From the comparison of the MSSE, it can be seen that the NN with up to two time delayed recurrent output sets yields the least MSSE, while the NN without recurrence is trained most poorly. This investigation implies again that the time delay reflects the order of the differential equation of the vehicle model.

Table 2.1: MSSE of the NN model for the training data (S_1=15).

Number of delayed recurrent output sets	MSSE ($\times 10^{-1}$)
No recurrence	10.92
One step time delay recurrence	4.84
Two-step time delay recurrence	2.15
Three-step time delay recurrence	6.92

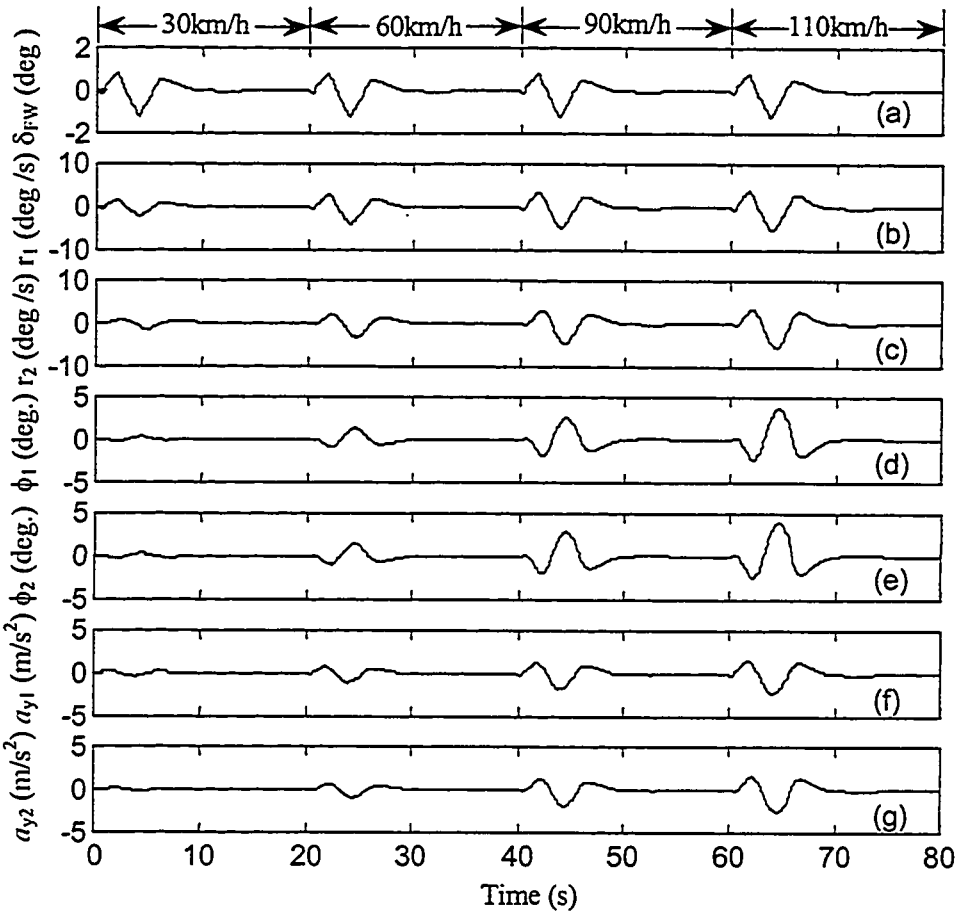

Figure 2.9: Time histories of vehicle response at different speeds used for training of the NN.

The influence of number of neurons in the hidden layer (S_1) on the training performance of the network is further investigated. The MSSE values for various values of S_1 are computed and presented in Table 2.2. The maximum training epoch is limited to 20000, for each value of S_1, and a two-step time delay of the recurrent network is adopted, using the training data shown in Figure 2.9. The results show that the NN model with 15 or greater neurons (S_1) in the hidden layer yields least value of MSSE. The value of MSSE for the NN model with the value of S_1 greater than 15, however, does not change significantly.

The effectiveness of the trained recurrent NN with two-step time delay, is examined by comparing the output of the NN with the results attained through analysis of

the Yaw/Roll model. The Yaw/Roll model is analyzed under an arbitrary steering input, shown in Figure 2.10, at a speed of 80km/h. Figure 2.11 illustrates the comparison of the dynamic behaviour of the vehicle derived from the analytical model with that attained from the NN model. The results clearly show reasonably good agreement between the two models in terms of their yaw rate, roll angle, and lateral acceleration response characteristics. The value of MSSE was obtained as 0.3672. It can thus be concluded that the trained NN model can predict the behaviour of the analytical vehicle model under the given steering input and vehicle speed.

Table 2.2: MSSE of the NN model for various values of S_1.

Number of neurons in the hidden layer (S_1)	MSSE ($\times 10^{-1}$)
5	7.11
10	3.23
12	2.94
14	2.60
15	2.15
16	2.15
18	2.15

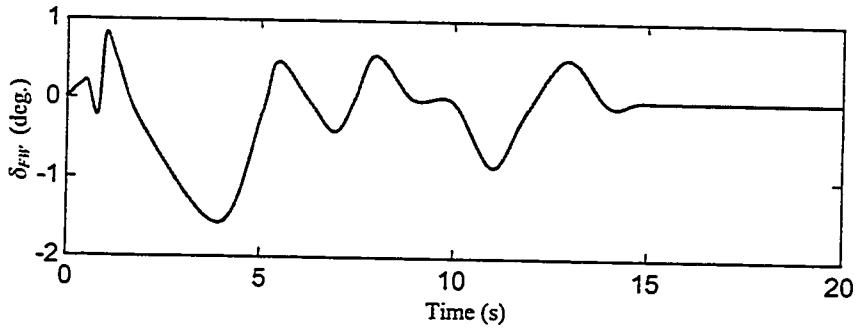

Figure 2.10: Time history of the front wheel steering angle.

The MSSE values representing the prediction accuracy of the dynamic behaviour of the analytical vehicle model under various vehicle speeds, are further evaluated and summarized in Table 2.3. The results clearly show that the NN model yields large values of MSSE at speeds, beyond the range of training speeds (30-110km/h). The NN model

yields higher values of MSSE at extremely low (20km/h) and high (120km/h) speeds, while the values vary only slightly in the training speed range of 40-100km/h.

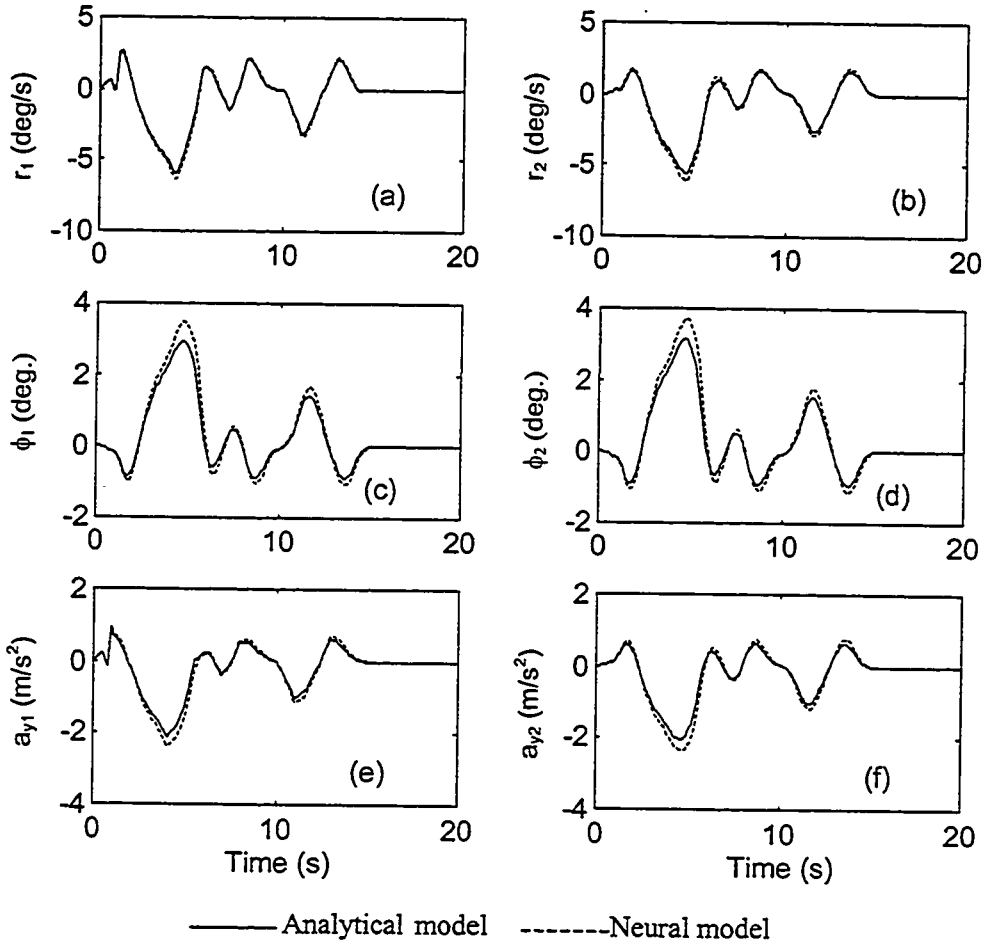

Figure 2.11: Comparison of response characteristics derived from the analytical and the NN models.

Table 2.3: MSSE of the NN model for various vehicle speeds (S_1=15).

Vehicle speeds (km/h)	MSSE
20	0.6721
40	0.3144
60	0.2095
80	0.3672
100	0.3914
120	0.6417

2.3 TIRE FORCES AND MOMENTS

The handling, stability and directional control performance of heavy vehicles are most significantly influenced by the tire properties. The longitudinal and lateral forces developed by the tires, however, are complex functions of many vehicle design and response variables, such as normal load, side-slip angles, longitudinal slip, braking and cornering force demands, tire-road adhesion, and speed. The yaw plane models, reported in the literature, invariably assume linear cornering properties of tires in the absence of braking. More comprehensive constant speed models consider cornering properties as a function of side slip angle and normal load, using either look-up tables or regression models [63,66,67]. While look-up tables require extensive measured data, the regression models are considered valid over a specified range. The look-up tables and regression models tend to become extremely complex, when simultaneous braking and steering of vehicle is considered.

Alternatively, considerable efforts have been made to develop black-box models that involve trigonometric or other transcendental functions. Of particular interest is the trigonometric model, which was first suggested by Bakker et al. [63]. In recent years, the model is referred to as the Magic Formula (MF), partly because of its complex and unusual structure, and its power to simulate many important tire performance functions with high degree of accuracy [65]. Neural network techniques can also be implemented to learn the tire dynamic behavior using the experimental data. In this dissertation, the tire models are derived on the basis of Magic Formula and neural networks for their applications under braking and steering.

2.3.1 Magic Formula for Tires

Bakker et al. [63] proposed the following Magic Formula (MF) to derive the forces and moments developed by tires under a wide range of operating conditions:

$$Y = S_y + D\sin\{C\arctan[B(X - S_x)(1-E) + E\arctan[B(X - S_x)]]\} \tag{2.27}$$

where the dependent variable Y represents any quantifiable tire response, such as a force or moment. The independent variable X is a tire service variable, such as the slip angle, inclination angle, or longitudinal slip. The six constants S_x, S_y, B, C, D, and E must be identified from the experimental data using nonlinear curve-fitting algorithms. Physical interpretations of these constants may be derived from Figure 2.12. The constants S_x and S_y, referred to as the coordinates of a Center Point, can be estimated with reasonable accuracy directly from the experimental data for a tire. The constants B and D can be considered as the size factors of x and y, respectively, with origin placed at the center point. The constant B relates approximately to the slope in the linear range, while the constant D describes the peak value of the force or moment (y), as illustrated in Figures 2.13. The other two parameters, C and E determine the shape of the normalized variable y/D, and thus are referred to as the shape factors. The value of C can be estimated from the experimental data corresponding to a large value of x. The constant k illustrated in the Figure is given as $k = 0.5\pi\, sign(E)$ for $E \neq 1$, and $k = \tan^{-1}(0.5\pi)$ for $E = 1$. The role of shape factors C and E on the output of the MF is also illustrated in Figure 2.14. The results show that the proposed model can generate varying forms of input-output relations depending upon the shape factors.

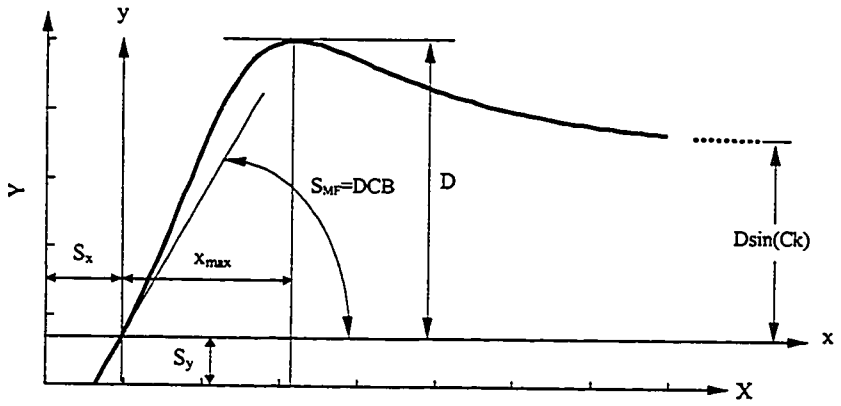

Figure 2.12: Parameter diagram in Magic Formula.

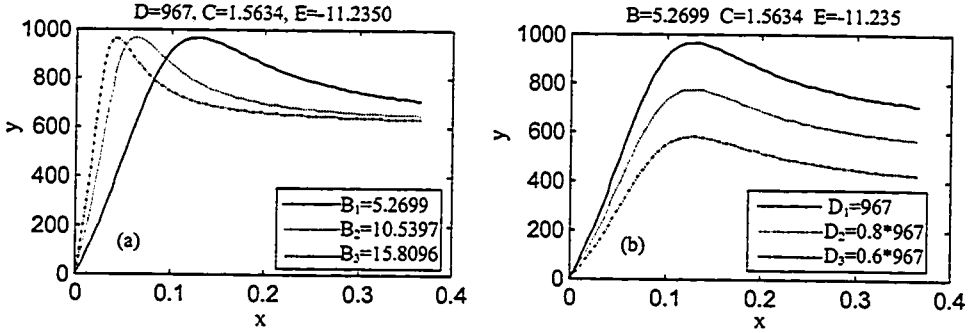

Figure 2.13: Influence of size factors on output of the Magic Formula.

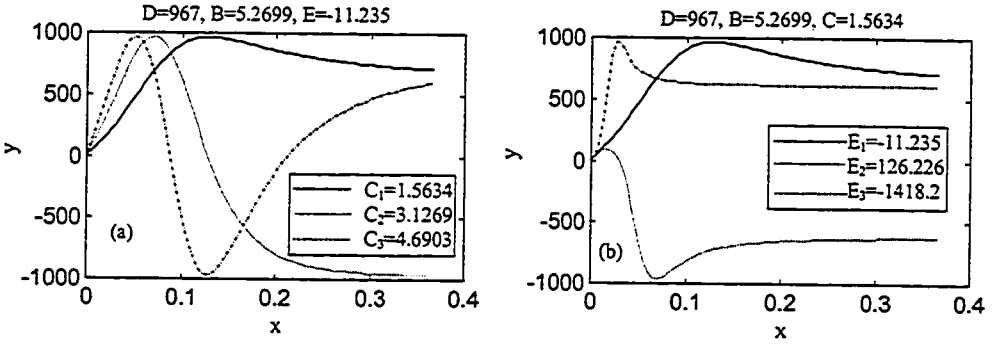

Figure 2.14: Influence of shape factors on output of the Magic Formula.

It should be noted that small values of $x=X-S_x$ yield the MF as, $y = Y - S_y = DCBx$. The initial slope of the curve S_{MF} is thus related to the constants, B, C and D, such that $S_{MF} = DCB$. These constants can thus be estimated from the peak values

and initial slope identified from the measured data. The Magic Formula further reveals that the first peak value of variable, $y = Y - S_y$, is equal to D, when

$$C \arctan\left\{B(X - S_x)(1 - E) + E \arctan\left[B(X - S_x)\right]\right\} = \frac{\pi}{2} \tag{2.28}$$

Upon identification of x=X-S_x, corresponding to the peak value, the above equation is solved to estimate the shape factor E. The initial estimates of the model are used to derive more precise values of the constants by minimizing the cost function:

$$J = \sum_{i=1}^{N} \left[Y_{MF}(X_i) - Y_{mea}(X_i)\right]^2 \tag{2.29}$$

where Y_{MF} is the output variable derived from Equation (2.27) and Y_{mea} is the measured quantity as a function of input variable X_i. N is the number of measured data points.

This methodology yields the individual tire characteristics as a function of a single variable in a highly efficient and convenient manner. The application of MF becomes more complex, while its significance also becomes more apparent, when the response characteristics are derived as a function of many variables, such as normal load, slip angles, and deformation slip. The six constants of the MF are then expressed by functions of all pertinent parameters. A given dependent tire variable (such as lateral force, aligning moment, or a force) can then be estimation as a function of many independent variables (slip angle, inclination angle, deformation slip and load).

Figure 2.15(a) illustrates the MF constants as function of the vertical load, derived from the measured lateral force characteristics of a Michelin XZA 11.5R22.5 radial tire [3]. The MF is then employed to generate the corresponding lateral force as the function of both the slip angle and the vertical load as shown in Figure 2.15(b). It can be seen that the size factor D increases and size factor B decreases nearly linearly with increase in the

vertical load. While both the shape factors, C and E, increase with the increase in the vertical load. Figure 2.16 illustrates the aligning moment characteristics derived from the MF and corresponding constants.

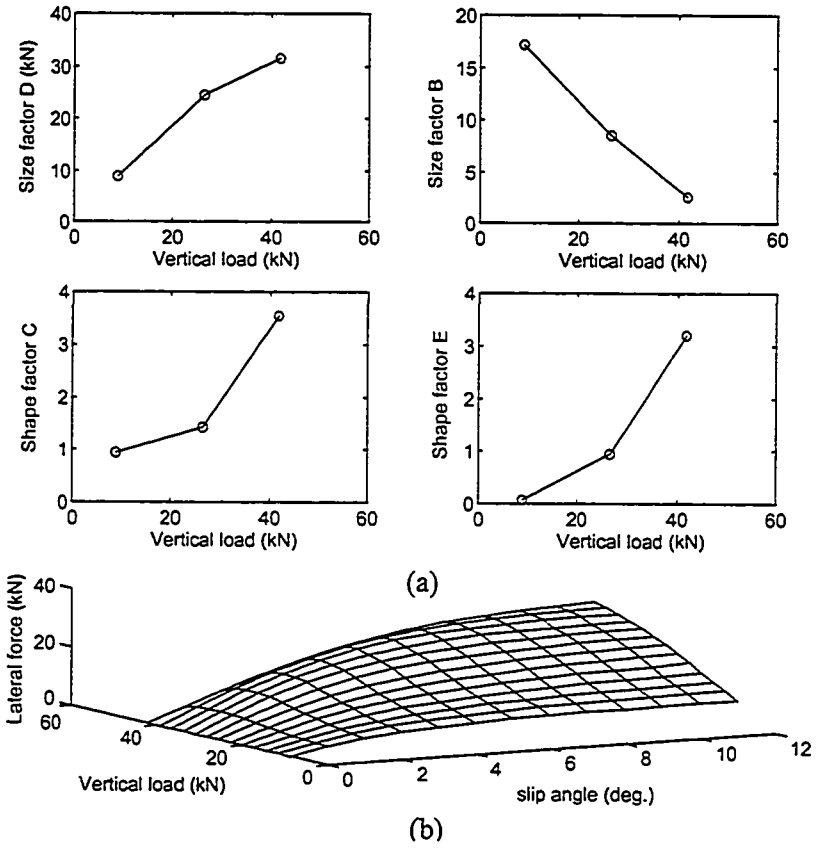

Figure 2.15: (a) MF constants as a function of the vertical load; and
(b) Lateral force as a function of the slip angle and vertical

The dependency of the MF constants on both the vertical load and forward velocity derived from the measured tire data is illustrated in Figure 2.17(a). The tire-road adhesion coefficient is also related to the road surface, normal load, forward speed and slip ratio, defined as the ratio of the tangential force developed at the tire-road interface to the normal load. For a given road surface, the variations in adhesion coefficient with variations in vertical load, speed and slip ratio, derived from the MF for the same tire, are illustrated in Figure 2.17(b). The results presented in Figures 2.15 to 2.17, clearly

illustrate that the cornering forces, aligning moments and braking forces developed by tires are coupled and strongly influenced by forward speed, normal load, side slip angle and longitudinal slip. The MF can be efficiently applied to describe the complex tire forces and moments by curve-fitting the measured data in an efficient manner. In this study, the measured data of an 11.5R22.5 radial tire is used to characterize its cornering and braking forces, and aligning moment properties, using the MF defined in Equation (2.27).

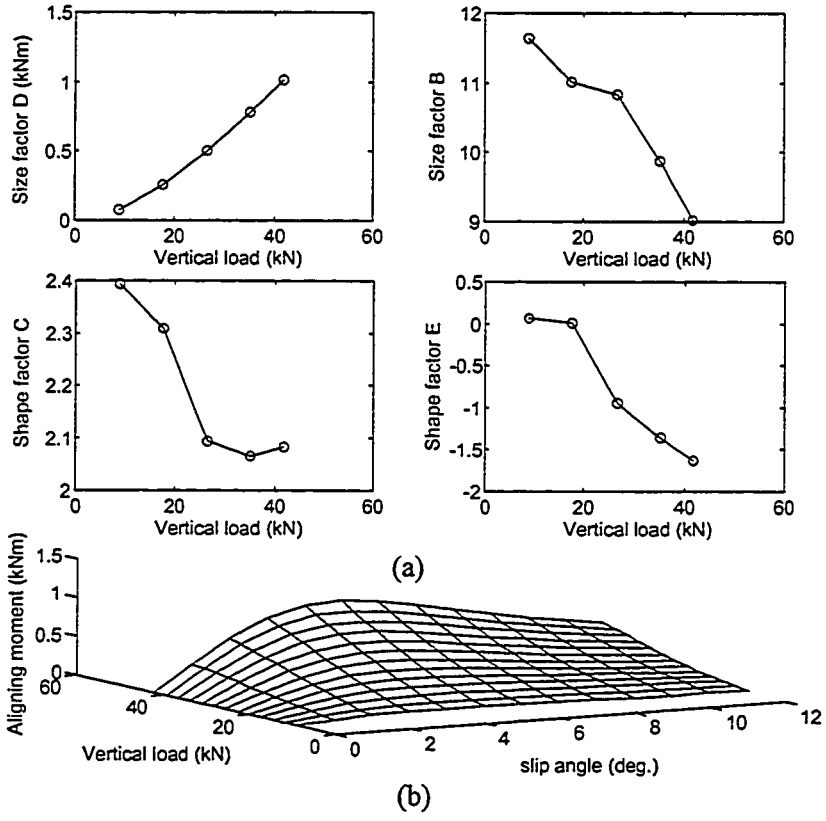

Figure 2.16: (a) MF constants as a function of vertical load (aligning moment).
(b) Aligning moment as a function of the slip angle and vertical load.

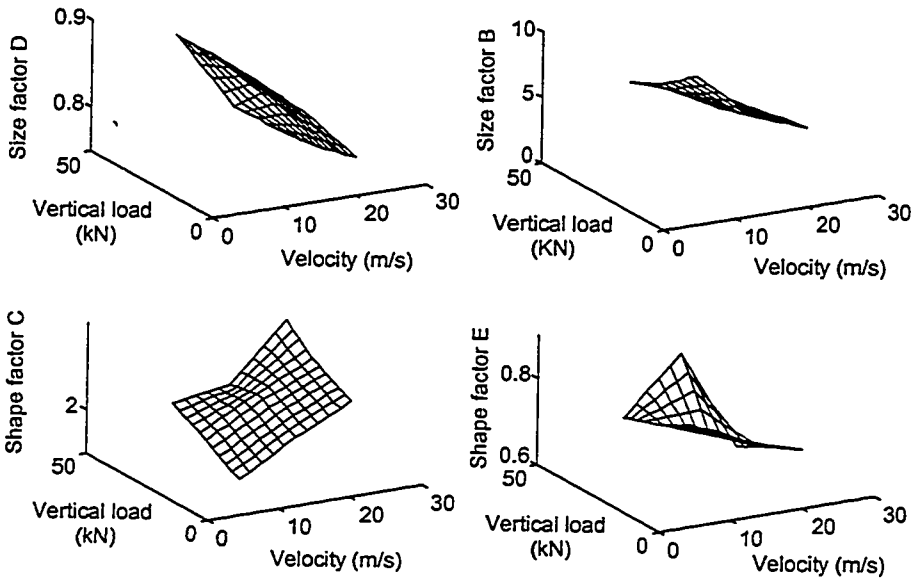

(a)

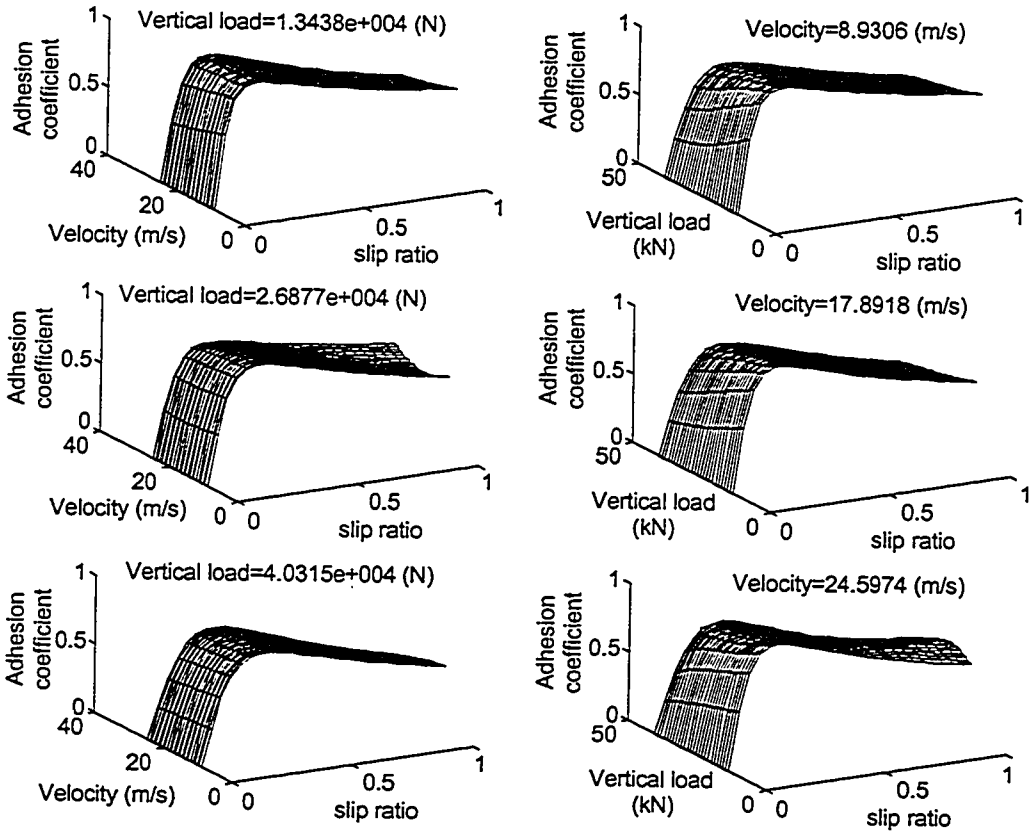

(b)

Figure 2.17: (a) MF constants as a function of velocity and vertical load (longitudinal adhesion coefficient). (b) Longitudinal adhesion coefficient as a function of the slip ratio, vertical load and velocity.

2.3.2 Tire Modeling by Neural Network

The lateral force, aligning moment, and the longitudinal adhesion coefficient of the tire are of paramount interest in predicting the directional dynamics of the vehicle. Such variables, however, are complex functions of the operating conditions, structure and the material of the tire, including the vehicle speed, slip ratio, vertical load, slip angle, air pressure, road condition, etc. In normal operation of a specific vehicle, only small variations may be expected in the structure, material and air pressure, while the variations in the vehicle speed, slip ratio, vertical load, slip angle may be significant. The vehicle speed, slip ratio, vertical load, and slip angle are thus considered as the most important independent variables, while the lateral force, aligning moment, and the longitudinal adhesion coefficient form the dependent variables from the tire model. In this section, a two-layer neural networks (NN) model is proposed to characterize the dependent variables, as illustrated in Figure 2.18.

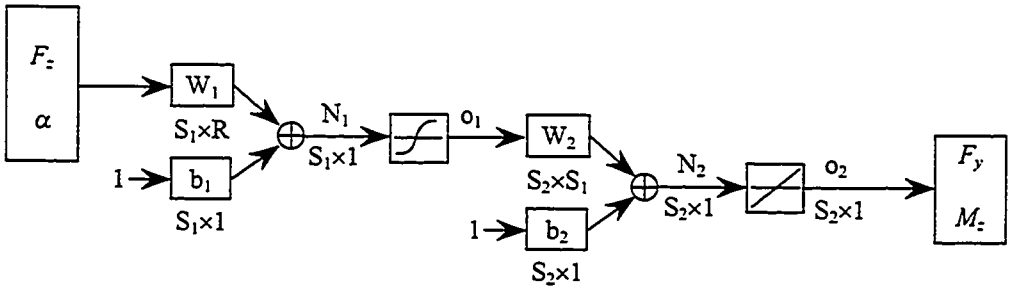

(a) Lateral force and aligning moment

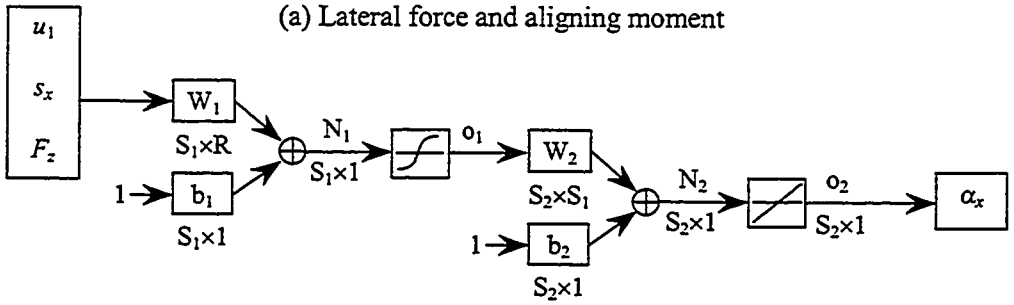

(b) Longitudinal adhesion coefficient

Figure 2.18: The structure of a feed forward neural network model for tires.

The normal load F_z and side slip angle α serve as the inputs, when only cornering force (F_y) and aligning moment (M_z) characteristics are desired in the absence of braking. The forward speed u_1, normal load F_z and slip ratio S_x are the desired inputs, for generation of longitudinal adhesion coefficient (α_x) under application of braking. The size of the NN developed for estimation of adhesion coefficient is denoted by the weight matrices (W_1 and W_2), and bias vectors (b_1 and b_2). The activation functions in the first and second layer are the tansig and linear functions, respectively. The number of neurons in the output layer is fixed as S_2=1, while the number of neurons in the input layer (R) is fixed as 3. The number of neurons in the hidden layer (S_1) can vary depending upon the training accuracy and the speed. The training process under braking is such that the weighting matrices (W_1, W_2) and the bias vectors (b_1, b_2) are adjusted to minimize the mean sum squared error (MSSE) between the output of the NN and the training data available:

$$MSSE = \frac{1}{N}\sum_{l=1}^{N}(\alpha_{xl} - \alpha_{xnl})^2 \tag{2.30}$$

where N is the total number of the training data available for the longitudinal adhesion coefficients, α_{xl} and α_{xnl} (l=1, ..., N) represent the longitudinal adhesion coefficients derived from the training data and the NN tire model, respectively. The training process for deriving the cornering force and aligning moment is carried out by minimizing the MSSE function, given by:

$$MSSE = \frac{1}{2N}\sum_{l=1}^{N}\left[\left(\frac{F_{yl} - F_{ynl}}{w_{Fy}}\right)^2 + \left(\frac{M_{zl} - M_{znl}}{w_{Mz}}\right)^2\right] \tag{2.31}$$

where F_{yl} and F_{ynl} (l=1, …, N) are the lateral forces derived from the training data and the NN tire model, respectively, while M_{zl} and M_{znl} are the corresponding aligning moments. w_{Fy} and w_{Mz} are the weighting functions of the bias between the lateral forces and aligning moment, respectively, derived from the NN and the training data. In this model, the number of neurons in the input and output layers are selected as S_2=R=2, while the number of neurons in the hidden layer (S_1) can vary depending upon the desired speed and accuracy of the training. The training data for the NN of tire models are taken as those illustrated in Figures 2.15 to 2.17. The NN model, developed to characterize α_x, resulted in minimal value of MSSE corresponding to S_1=25, as illustrated in Table 2.4. The maximum number of training epoch was limited to 15000. The NN model, derived for estimating of F_y and M_z, resulted in least MSSE for S_1=17, as summarized in the Table.

Table 2.4: Variations in MSSE as a function of S_1

NN Model			
α_x		F_y and M_z	
S_1	MSSE ($\times 10^{-6}$)	S_1	MSSE
10	2.0071	8	0.3547
20	1.4313	13	0.2101
22	1.1511	15	0.1981
24	0.9663	16	0.1629
25	0.9236	17	0.1457
26	0.9236	18	0.1457
28	0.9236	20	0.1457

The resulting NN model is analyzed to derive α_x characteristics of the tire as a function of normal load (F_z), slip ratio (S_x) and forward speed, and F_y and M_z characteristics of the tire as a function of the normal load (F_z), slip angle (α), respectively. The results are compared with those derived from the MF tire model. The

magnitudes of errors between the two models are expressed in terms of bias as functions of F_z, α, S_x and u_1. Figure 2.19 illustrates the tire characteristics derived from the NN model and the resulting bias. Although the bias varies considerably with variations in the independent variables, the peak values of bias in α_x, F_y and M_z are attained as 4%, 7% and 5%, respectively. It can thus be concluded that the proposed NN model can be effectively used to characterize the tire properties over a wide range of operating conditions. It should be noted that the proposed neural networks for longitudinal adhesion coefficient, cornering force and aligning moment in this study are best appropriate for predicting longitudinal force, cornering force and aligning moment under purely braking or steering, respectively. The application of combined braking and steering requires a neural network in which the dependent variables, including longitudinal adhesion coefficient (α_x), cornering force (F_y) and aligning moment (M_z), are a function of the independent variables, including vertical load, speed, slip angle and slip ratio. Due to the lack of training data, the proposed networks thus may be approximately applied for the application of the combined braking and steering.

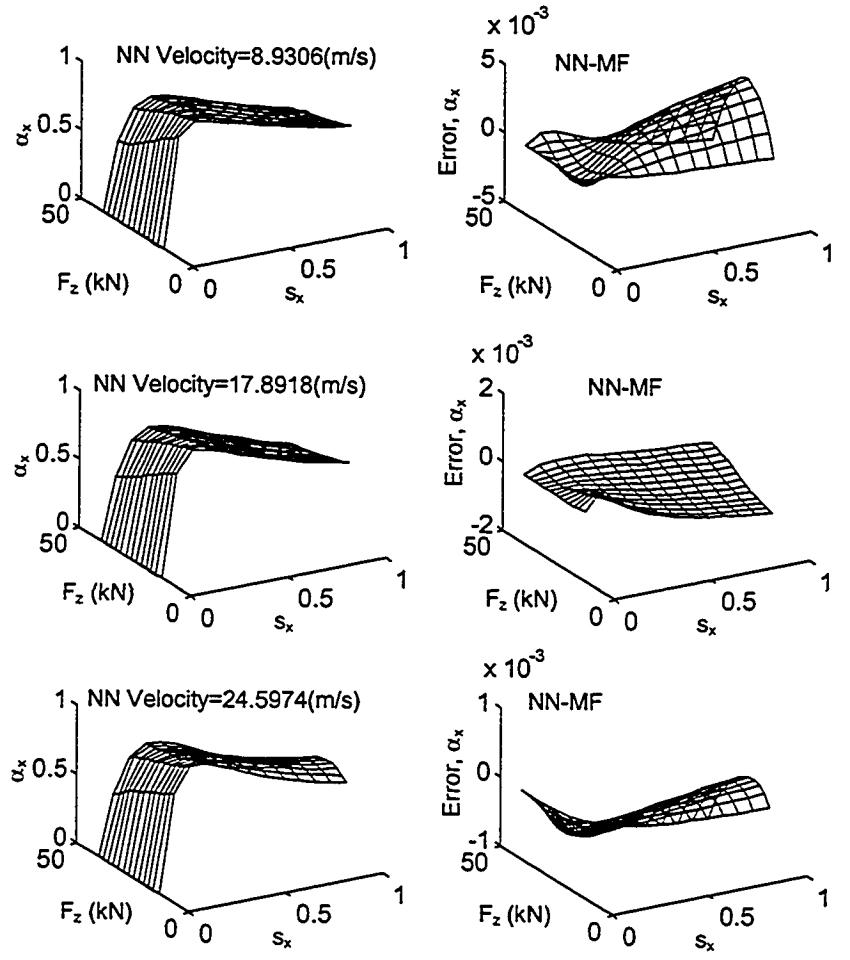

(a)

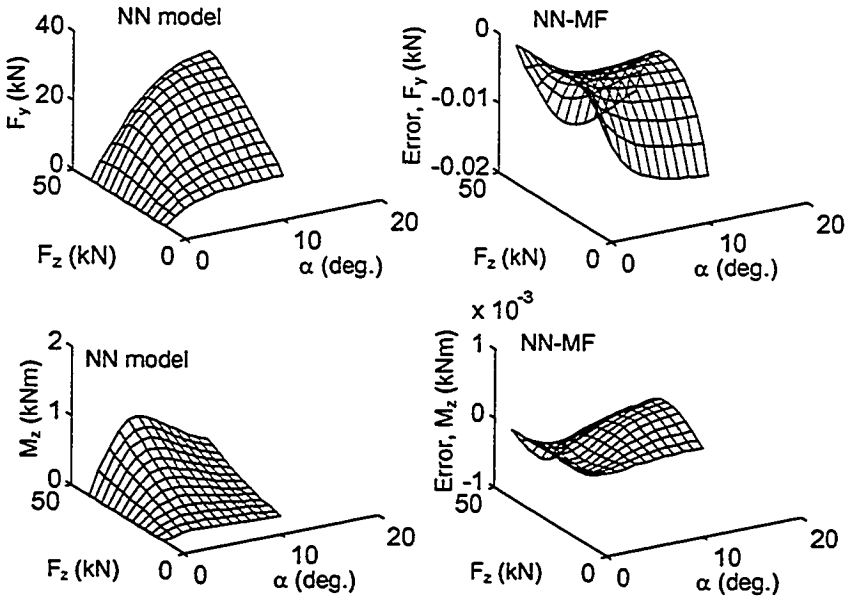

(b)

Figure 2.19: (a) Longitudinal adhesion coefficient of tire derived from the NN model and the error with respect to MF tire model; (b) Lateral force and aligning moment of tire derived from the NN model and the error with respect to MF tire model.

2.4 COMPARISON OF DYNAMICS MODELS OF HEAVY VEHICLE

The vehicle and tire models, developed in this study, are combined to yield seven different directional dynamics models of varying complexities. These include: (*i*) Linear yaw plane model (LYP) comprising linear cornering characteristics of tires; (*ii*) Nonlinear yaw plane model incorporating nonlinear cornering characteristics of tires derived from the MF (NYPMF); (*iii*) Nonlinear yaw plane model incorporating NN tire model (NYPNN); (*iv*) Linear yaw plane model with roll DOF (LYPR); (*v*) Nonlinear yaw plane model with roll DOF and MF tire model (NYPRMF); (*vi*) Nonlinear yaw plane model with roll DOF and NN tire model (NYPRNN); and (*vii*) Neural network vehicle model (NN). The prediction abilities of all the models are examined by comparing their directional response with those derived from the Yaw/Roll plane (YRP) model [95], and the reported measured data [96]. The proposed models are evaluated under ramp-step and lane change maneuvers, illustrated in Figure 2.20. The response characteristics of the models under ramp-steer input are compared with those derived from Yaw/Roll plane model, while the response characteristics under a lane change maneuver are compared with the measured data.

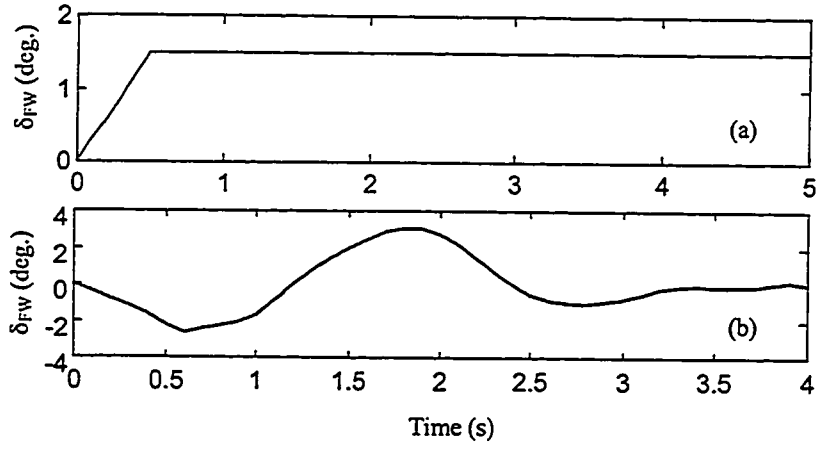

Figure 2.20: Front wheel steer input used for comparison of various vehicle models: (a) Ramp step; (b) Lane change.

2.4.1 Ramp Step Steer Maneuver

The directional response to a ramp step steer maneuver is investigated to analyze the steady-state response of a vehicle. The tractor semitrailer is assumed to travel on a dry, smooth asphalt surface with constant forward speed of 70 km/h. The response characteristics, evaluated in terms of lateral acceleration gains (a_{y1}/δ_{FW}, a_{y2}/δ_{FW}), and yaw rate gains (r_1/δ_{FW}, r_2/δ_{FW}), for all the models are summarized in Table 2.5. Figure 2.21 further illustrates the time histories of the lateral and yaw rate response derived from the models. The comparison clearly illustrates that all the yaw plane models (LYP, NYPMF and NYPNN) tend to underestimate the response, when compared with that of the YRP model. The nonlinear yaw plane models incorporating tire models based upon MF and NN yield response gains close to those obtain from the YRP model. The NN model of the vehicle also yields very similar response gain. While the NYPRMF and NYPRNN models tend to underestimate the response by 4-5%, the NN model overestimates the response by 1-2%. The results suggest that roll motion of the vehicle contributes considerably to the directional response of the vehicle. The nonlinear yaw plane models with limited roll DOF, and NN vehicle model can effectively predict the directional response of the vehicle under ramp step steering maneuver.

Table 2.5: Summary of response gains derived from different models.

Model	a_{y1}/δ_{FW} (m/s^2/degree)	a_{y2}/δ_{FW} (m/s^2/degree)	r_1/δ_{FW} (deg./s/degree)	r_2/δ_{FW} (deg./s/degree)
LYP	1.0107	1.0107	2.9787	2.9783
NYPMF	1.0876	1.0876	3.2048	3.2048
NYPNN	1.0984	1.0984	3.2366	3.2365
LYPR	1.1448	1.1444	3.3619	3.3609
NYPRMF	1.2347	1.2360	3.6344	3.6328
NYPRNN	1.2492	1.2483	3.6775	3.6778
NN	1.3304	1.3321	3.8601	3.8593
YRP	1.3015	1.3035	3.8334	3.8343

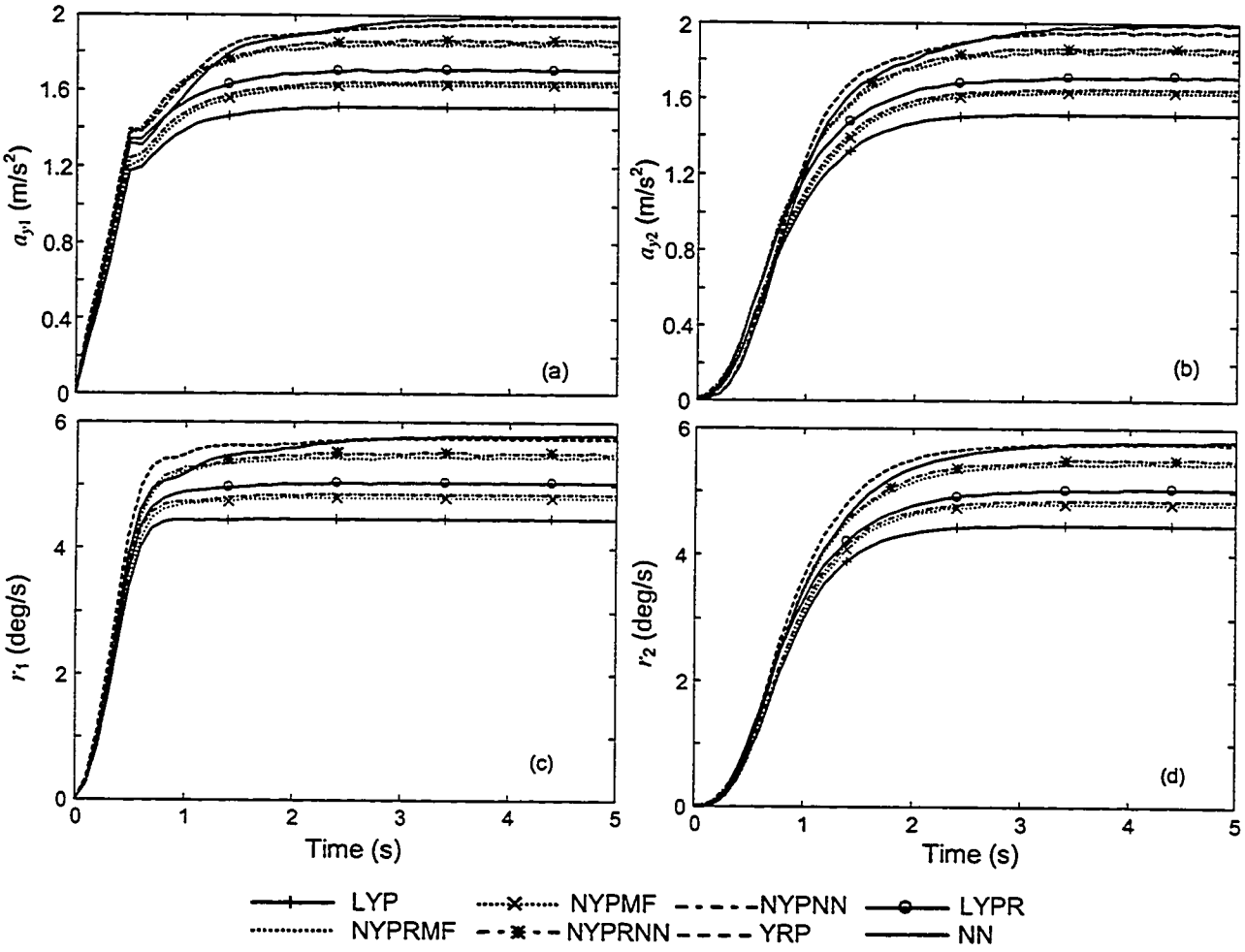

Figure 2.21: Comparison of ramp-step response of different vehicle models.

2.4.2 Lane Change Maneuver

Figure 2.22 illustrates the lateral acceleration (a_{y1}, a_{y2}) and yaw rate (r_1, r_2) response characteristics of the tractor and semitrailer units of the combination subject to a lane change maneuver at a speed of 70km/h. The response characteristics, derived from different models, are compared with the measured data reported in [96]. The deviations between the peak values of measured and model response are further evaluated for all the models, and expressed as the bias as shown in Table 2.6. The peak values of bias are

expressed in terms of maximum and minimum, which are derived on the basis of positive and negative peaks in the following manner:

$$\text{Max\%}= \frac{\text{Positive peak value of measured data-Positive peak value of the analytical response}}{\text{Positive peak value of measured data}} \times 100$$

$$\text{Min\%}= \frac{\text{Negative peak value of measured data-Negative peak value of the analytical response}}{\text{Negative peak value of measured data}} \times 100$$

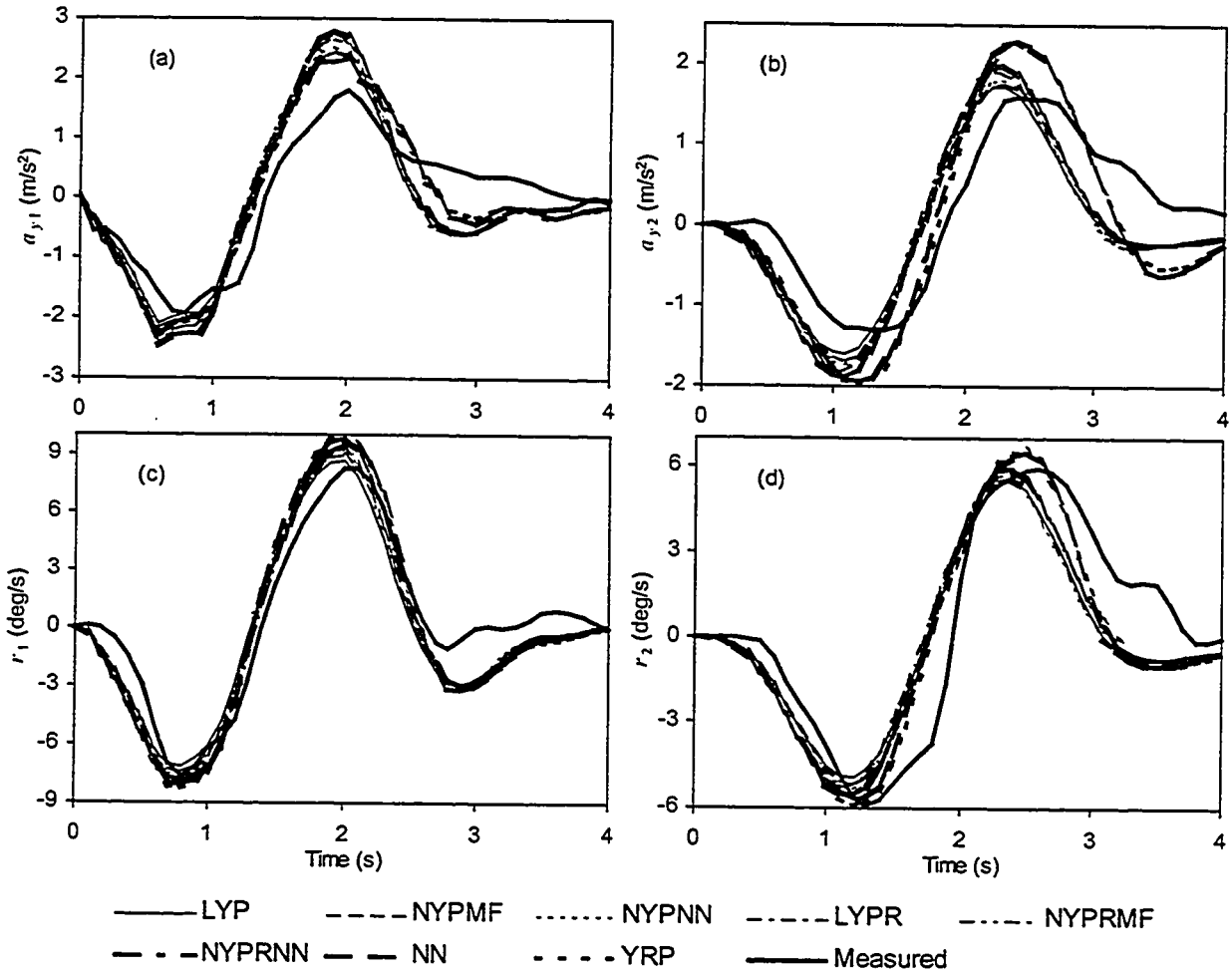

Figure 2.22: Comparison of transient directional response of the vehicle models, subject to a lane change maneuver, with the measured data.

The deviations in the response are also analyzed in terms of root mean square values (RMSV) of the bias between the analytical and measured data and summarized in

Table 2.7. The results presented in Figure 2.22 reveal that all vehicle models yield similar trends in the directional response, which are comparable with those observed from the measured data. While all the models yield similar response behaviour of the tractor mass (a_{y1}, r_1), the yaw plane models (with and without the roll DOF) tend to underestimate the peak response of the trailer mass (a_{y2}, r_2). The NN vehicle model correlates very well with the response behaviour of the Yaw/Roll model. All the models, however, reveal considerable deviations from the measured data. The yaw plane models (LYP, NYPMF and NYPNN), in general, exhibit largest deviations between the analytical and measured response. The addition of roll DOF results in considerably less deviation between the analytical and measured response. While the NN vehicle model predicts response close to the widely accepted and validated Yaw/Roll model, both the models reveal considerable deviations from the measured data. These differences can be partly attributed to the experimenter's abilities to control the test conditions, and the contributions due to road surface roughness, which is assumed as perfectly smooth in the model formulation. It should be noted that all the yaw plane models yield reasonably good estimate of the yaw velocities response, while a better estimate of lateral acceleration is achieved by the models incorporating the roll DOF.

From the comparison of the RMSV of the bias between the measured and the predicted response, it is apparent that the YRP model yields the least RMSV of the bias of the tractor lateral acceleration (0.4881) and the trailer yaw rate (1.5686). The YRP model, however, yields largest RMSV of bias in the tractor's yaw velocity response. The NYPRMF model yields the least RMSV of the bias in the trailer lateral acceleration and

the tractor yaw rate response. All the yaw plane models yield large RMSV of the bias in the response.

Table 2.6: Peak values of the relative bias.

Model	a_{y1}		a_{y2}		r_1		r_2	
	Max%	Min%	Max%	Min%	Max%	Min%	Max%	Min%
LYP	-47.9839	-24.3286	-19.6641	-36.9476	-11.8359	0.2684	5.8288	12.2415
NYPMF	-54.0577	-26.7347	-23.9288	-42.3948	-18.4256	-5.3762	0.6774	7.3908
NYPNN	-55.3881	-27.8965	-24.0533	-44.3162	-18.9510	-6.0894	-0.3534	6.7654
LYPR	-35.1224	-9.8265	-7.8068	-23.0429	-4.2771	7.3764	7.8781	16.9661
NYPRMF	-37.6897	-12.3854	-11.1432	-28.5429	-8.4160	3.3581	4.8853	13.2542
NYPRNN	-41.0593	-16.2064	-13.7322	-31.5343	-9.7584	1.7722	2.7411	11.2184
YRP	-29.4469	-20.5942	-41.1381	-50.7927	-18.7414	-8.2167	-9.7625	0.8962
NN	-29.1478	-19.8385	-42.5237	-49.3347	-14.2157	-2.5790	-8.8823	5.3278

Table 2.7: RMSV of the bias between the measured and analytical responses.

Model	a_{y1} (m/s^2)	a_{y2} (m/s^2)	r_1 (deg/s)	r_2 (deg/s)
LYP	0.6663	0.6531	1.4520	2.0200
NYPMF	0.6646	0.6186	1.4481	1.7913
NYPNN	0.6712	0.6216	1.4646	1.7854
LYPR	0.5790	0.5737	1.4008	1.8737
NYPRMF	0.5626	0.5386	1.3341	1.7065
NYPRNN	0.5976	0.5701	1.4666	1.7818
YRP	0.4881	0.5481	1.6154	1.5686
NN	0.5210	0.5936	1.5797	1.7098

It should be noted that the RMSV of the bias reflects the overall comparison between the analytical models and the experimental data, the model with least RMSV is thus considered as the most suitable one. From the results, summarized in Table 2.7, the NYPRMF model is considered to yield the least value of RMSV of the bias, including the lateral accelerations and yaw velocities of tractor and trailer. Therefore, the NYPRMF model is selected for further developments in integrating a driver model to study the dynamic vehicle-driver interactions.

2.5 SUMMARY

The directional dynamics models of a tractor-semitrailer vehicle are formulated based upon yaw plane, yaw plane with limited roll DOF, and neural networks. The steady state performance behavior of seven different models, realized upon integrating linear and nonlinear tire models, are compared with the response characteristics derived from the widely accepted Yaw/Roll plane model. The transient response characteristics of the analytical model are further compared with the field measured data to examine their relative prediction abilities. The comparison revealed that yaw plane models tend to underestimate the response, while NN vehicle model slightly overestimates the response under ramp-step steer input. The nonlinear yaw plane model with limited roll DOF yields reasonably good correlation with both the response behavior of the Yaw/Roll model and the measured data. Both the tire models, based upon Magic Formula and Neural networks, yield similar response behavior. Based upon the comparison of all the models with the measured response, it is concluded that the yaw plane model with limited roll DOF and nonlinear tire model based upon the Magic Formula (NYPRMF), yields reasonably good agreement with the measured data. The proposed NYPRMF model further allows the response analysis in a highly efficient manner. This model is therefore further used to develop coupled driver-vehicle models in the following Chapters.

CHAPTER 3 SENSITIVITY ANALYSIS OF THE OPEN LOOP DYNAMICS OF ARTICULATED HEAVY VEHICLES

3.1 INTRODUCTION

Directional dynamics analyses of heavy vehicles through analytical models require a large number of vehicle parameters. These include weights and dimensions, mass moments of inertia, structural, steering and articulation compliance, static and dynamic properties of tires and suspension components, brake system parameters, etc. The accuracy of the analytical results impinges upon accurate estimation of the vehicle parameters, which poses many complexities due to large sizes and nonlinear properties of various components. Accurate estimation of vehicle parameters, in general, requires comprehensive test and analysis facilities, while the time variations of the properties cannot be characterized. The significance of various vehicle parameters may be evaluated through sensitivity analyses of the vehicle response to variations in parameters. Such analyses would enable the analyst to identify a critical set of parameters to which vehicle response is more sensitive. The system identification efforts may thus be directed towards accurate estimation of such parameters, while an approximation may be accepted for remaining parameters to which vehicle response is less sensitive. Such analyses can further help in reducing the order of the analytical model by eliminating the parameters showing insignificant effects on the vehicle response.

In this Chapter, a performance index is formulated to describe the directional response and stability characteristics of an articulated tractor-semitrailer combination. Detailed parameter sensitivity analyses are performed using the yaw plane model with

roll DOF, as described in Chapter 2, to identify the most significant vehicle parameters. System identification methodology is further applied to attain an estimate of vehicle parameters, which are known to exhibit high degree of uncertainty.

3.2 PERFORMANCE INDEX

The safety and directional stability performance characteristics of heavy vehicles have been related to a number of measures derived from the directional response behaviour. A number of performance measures based upon lateral acceleration, load transfer ratio, rearward amplification and yaw response have been proposed [2-4]. The lateral acceleration response of the two units has been directly related to static rollover threshold of the combination, while the load transfer ratio relates to the dynamic rollover behaviour. The load transfer ratio can thus be expressed in terms of sprung mass roll angles. The rearward amplification describes the yaw velocity gain of the trailer with respect to yaw velocity of the tractor. A composite performance index may thus be formulated by integrating the above response parameters, which are directly related to most significant performance measures:

$$J_{dp} = J_{ay1} + J_{ay2} + J_{r1} + J_{r2} + J_{\phi 1} + J_{\phi 2} \tag{3.1}$$

where J_{ay1} and J_{ay2} are the normalized mean squared values (NMSV) of the lateral accelerations of the tractor and semitrailer, respectively, which relate to rollover threshold measure of the vehicle. J_{r1} and J_{r2} are the NMSV of the yaw rates of the two units, relating to the rearward amplification performance measure of the vehicle. $J_{\phi 1}$ and $J_{\phi 2}$ are the NMSV of the roll angles of the tractor and trailer, respectively, and relate to

the load transfer ratio performance measure of the vehicle. The NMSV of the individual performance indices are evaluated from:

$$J_{ayi}=\frac{1}{T}\int_0^T\left(\frac{a_{yi}}{w_{ay}}\right)^2 dt;\ J_{ri}=\frac{1}{T}\int_0^T\left(\frac{r_i}{w_r}\right)^2 dt;\ J_{\phi i}=\frac{1}{T}\int_0^T\left(\frac{\phi_i}{w_\phi}\right)^2 dt;\ i=1,2 \tag{3.2}$$

where w_{ay}, w_r, and w_ϕ are the weighting factors. w_{ay} is selected as 0.3g, known to be in the proximity of the static rollover threshold of the articulated heavy vehicle combinations. The yaw rate weighting factor is selected as 10 degrees/s, while w_ϕ is chosen as 15 degrees, which has been proposed as the threshold of the roll angle of the sprung mass [34, 37]. In Equation (3.2), a_{yi}, r_i and ϕ_i are the lateral acceleration, yaw rate and roll angle response of unit i of the combination, where i=1 and 2 refer to the tractor and trailer, respectively. T is the total simulation time.

3.3 SENSITIVITY ANALYSIS

The dynamic performances of an articulated heavy vehicle depend strongly upon the design and structure of the vehicle. While the design and choice of a vehicle structure can usually be characterized by various parameters. Thus a number of parameters of the vehicle and its components are involved in the modeling of the vehicle dynamics, while the contributions due to different parameters to the vehicle performance may differ considerably. It is thus significant to study the parameter sensitivity to vehicle performance in order to enhance the modeling efficiency and accuracy. Based upon the study in Chapter 2, a yaw plane model with roll DOF of articulated vehicle is considered as a time-invariant system, such that

$$\begin{cases} \dot{x}(t,\beta) = A(\beta)x(t,\beta) + B(\beta)u(t) \\ y(t,\beta) = C(\beta)x(t,\beta) \end{cases} \tag{3.3}$$

where $\beta \in R^r$ is the parameter vector with nominal value β. A, B and C are the state, input and output matrices of vehicle system as functions of vehicle parameter vector β, respectively. $u \in R^m$, $x \in R^n$ and $y \in R^p$ are the input, state and output vectors, respectively, given by:

$$x = \left\{ u_1, v_1, r_1, \psi_1, \phi_1, \dot{\phi}_1, r_2, \psi_2, \dot{\phi}_2, \omega_{11}, \omega_{12}, \omega_{13}, \omega_{21}, \omega_{22} \right\}^T;$$
$$y = \left\{ a_{y1}, a_{y2}, r_1, \phi_1, r_2, \phi_2 \right\}^T; \text{ and}$$
$$u = \left\{ \delta_{FW}, M_{b11}, M_{b12}, M_{b13}, M_{b21}, M_{b22} \right\}^T.$$

Under the assumption of differentiability at $\beta = \bar{\beta}$ of $A(\bullet)$, $B(\bullet)$ and $C(\bullet)$, the state and output sensitivity coefficients are defined as

$$S_{xk} = \left.\frac{\partial x(t,\beta)}{\partial \beta_k}\right|_{\beta=\bar{\beta}}, \quad S_{yk} = \left.\frac{\partial y(t,\beta)}{\partial \beta_k}\right|_{\beta=\bar{\beta}} \qquad k=1, 2, \ldots, r \tag{3.4}$$

where $\bar{\beta}$ is the parameter vector with some specific values for its components. Let $x(t) = x(t,\bar{\beta})$, and

$$w(t) = \left[x^T(t) \quad S_{x1}^T \quad \cdots \quad S_{xr}^T \right]^T, \quad \eta(t) = \left[S_{y1}^T \quad \cdots \quad S_{yr}^T \right]^T \tag{3.5}$$

then

$$\begin{cases} \dot{w}(t) = Fw(t) + Gu(t) \\ \eta(t) = Hw(t) \end{cases} \tag{3.6}$$

where

$$F = \begin{bmatrix} A & 0 & \cdots & 0 \\ A_1 & A & \cdots & 0 \\ \vdots & \vdots & \ddots & \vdots \\ A_r & 0 & \cdots & A \end{bmatrix}_{[n(r+1)]\times[n(r+1)]}; \quad A = A(\bar{\beta}); \text{ and } A_k = \left.\frac{\partial A(\beta)}{\partial \beta_k}\right|_{\beta=\bar{\beta}}; \; k=1, 2, \ldots, r$$

$$G=\begin{bmatrix} B \\ B_1 \\ \vdots \\ B_r \end{bmatrix}_{n(r+1)\times m}, \; B=B(\bar{\beta}); \text{ and } B_k=\left.\frac{\partial B(\beta)}{\partial \beta_k}\right|_{\beta=\bar{\beta}}; \; k=1, 2, \ldots, r$$

$$H=\begin{bmatrix} C_1 & C & \cdots & 0 \\ \vdots & \vdots & \vdots & \vdots \\ C_r & 0 & \cdots & C \end{bmatrix}_{pr\times n(r+1)}, \; C=C(\bar{\beta}), \; C_k=\left.\frac{\partial C(\beta)}{\partial \beta_k}\right|_{\beta=\bar{\beta}}, \text{ and } k=1, 2, \ldots, r.$$

Equation (3.6) describes the sensitivity of the vehicle system described by Equation 3.3, which is an enlarged system of order $n(r+1)$ [177]. Assuming that initial state of system does not depend upon β, such that $x(0,\beta)=x_0$, Equations (3.4) and (3.5) yield

$$w(0)=\begin{bmatrix} x_0^T & 0^T & \cdots & 0^T \end{bmatrix}^T \tag{3.7}$$

Equation (3.7) serves as the initial condition to solve Equation (3.6) under the input $u(t)$. The state sensitivity (S_{xk}) and output sensitivity (S_{yk}) coefficients can then be computed from the components of $w(t)$ and $\eta(t)$, respectively. Moreover, the parametric sensitivity with respect to any performance indices, which are related to the state and output variables, can be derived from the state and output sensitivity coefficients in conjunction with the performance index, defined in Equations (3.1) and (3.2) as follows:

$$S_{Jayik}=\frac{\partial J_{ayi}}{\partial \beta_k}=\frac{2}{Tw_{ay}^2}\int_0^T \frac{\partial a_{yi}}{\partial \beta_k}a_{yi}dt; \; S_{Jrik}=\frac{\partial J_{ri}}{\partial \beta_k}=\frac{2}{Tw_r^2}\int_0^T \frac{\partial r_i}{\partial \beta_k}r_i dt;$$

$$S_{J\phi ik}=\frac{\partial J_{\phi i}}{\partial \beta_k}=\frac{2}{Tw_\phi^2}\int_0^T \frac{\partial \phi_i}{\partial \beta_k}\phi_i dt; \text{ and } S_{Jdpk}=\frac{\partial J_{dp}}{\partial \beta_k}=\sum_{i=1}^{2}\left(\left|\frac{\partial J_{ayi}}{\partial \beta_k}\right|+\left|\frac{\partial J_{ri}}{\partial \beta_k}\right|+\left|\frac{\partial J_{\phi i}}{\partial \beta_k}\right|\right) \tag{3.8}$$

where i=1, 2 refers to the tractor and trailer, respectively.

3.3.1 Vehicle Response to Variations in Selected Parameters

The dynamic response characteristics of a heavy vehicle depends upon the static and dynamic properties of its components, and structure of the vehicle described by its weights and dimensions. The contributions of various vehicle parameters to the vehicle dynamic response, however, differ considerably. Parameter sensitivity analyses are performed to identify vital vehicle parameters, which affect the vehicle response most significantly. The analysis also yields parameters, whose contributions to the response may be considered relatively insignificant. From Equations (3.3), (3.4) and (3.6), it is evident that the state and output sensitivity functions depend upon the vehicle parameters and the input to the vehicle system. The sensitivity analyses thus necessitate description of realistic input signals, such as steering angle and braking/acceleration torque.

Figure 3.1 illustrates the time-histories of inputs, synthesized to perform various maneuvers, including: vehicle acceleration in the absence of steering (Stage 1); turning and braking (Stage 2); lane change and acceleration (Stage 3); and constant speed double lane change maneuver (Stage 4). In the figure, δ_{sw} represents the steering wheel angle, F_{bk} is the braking force applied at all the axle wheels, and F_{dr} is the driving force applied at the wheels of axles 2 and 3 of the tractor. The yaw plane model with roll-DOF of a five-axle tractor semitrailer is analyzes using the selected input signals and nominal vehicle parameters, summarized in Table 3.1. The response characteristics of the vehicle combination are illustrated in Figure 3.2. The peak values of the response, attained during four stages of maneuver, are further summarized in Table 3.2.

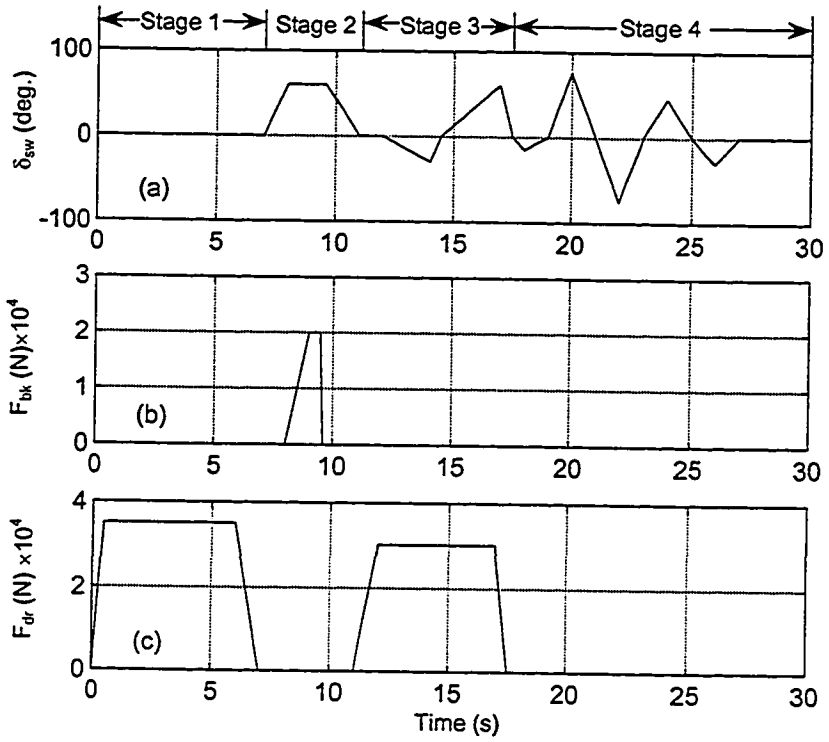

Figure 3.1: Input signals for simulation of yaw plane model with roll-DOF.

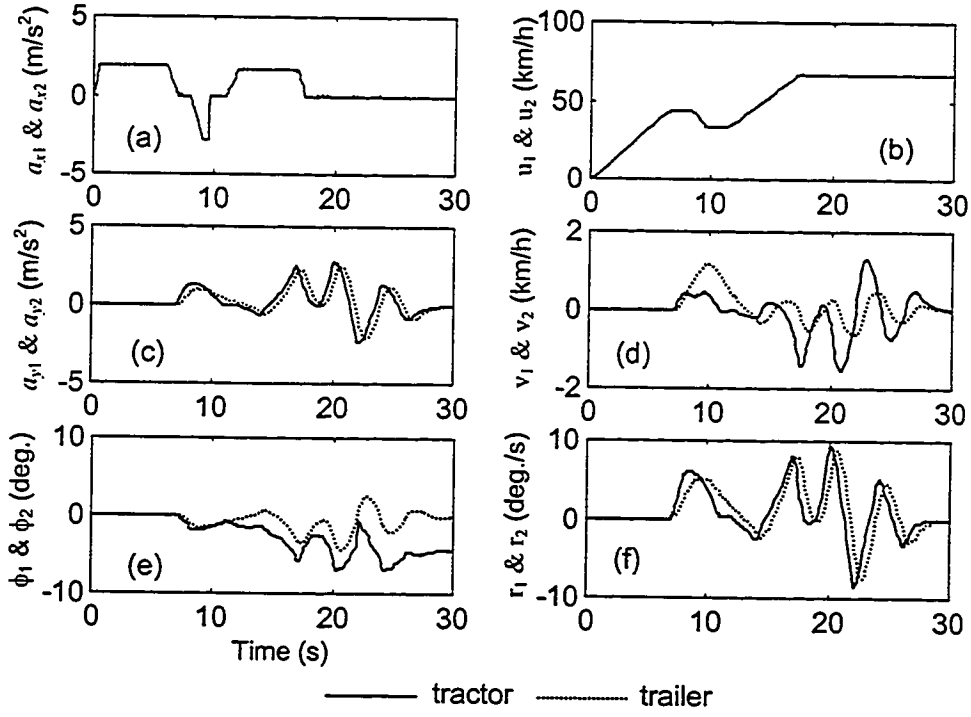

Figure 3.2: Vehicle response to the four-stage maneuver shown in Figure 3.1.

Table 3.1: Nominal parameters used for the yaw-plane model with roll-DOF of a five-axle tractor semitrailer.

Category	Parameter	Value	Parameter	Value
Geometrical	x_{11} (m)	0.856	x_{21} (m)	4.805
	x_{12} (m)	2.192	x_{22} (m)	5.770
	x_{13} (m)	3.411	x_{2A} (m)	5.558
	x_{1A} (m)	2.561	y_d (m)	0.330
	$\bar{z}_1$ (m)	-0.137	$\bar{z}_2$ (m)	0.838
	h_{g1} (m)	1.082	h_{g2} (m)	2.057
	h_{rc1} (m)	0.559	h_{rc2} (m)	0.483
	b_{11} (m)	1.016	b_{21} (m)	0.749
	b_{12} (m)	0.749	b_{22} (m)	0.749
	c_1 (m)	2.562	c_2 (m)	5.532
	h_{s1} (m)	-0.102	h_{s2} (m)	0.846
	h_{u1} (m)	0.724	h_{u2} (m)	0.724
	e_1 (m)	0.0	e_2 (m)	8.55
	R_T (m)	0.495		
Inertial	m_{s1} (kg)	4399.8	m_{s2} (kg)	27895.9
	m_{u11} (kg)	544.3	m_{u21} (kg)	680.4
	m_{u12}(kg)	1043.2	m_{u22}(kg)	680.4
	m_{u13}(kg)	1043.2	I_{xs} (kgm^2)	23105.6
	I_{xt} (kgm^2)	1695.3	I_{zs} (kg m^2)	439990.0
	I_{zt} (kgm^2)	11709.0	I_{w13} (kgm^2)	46.9
	I_{w11} (kgm^2)	24.5	I_{w21} (kgm^2)	30.6
	I_{w12} (kgm^2)	46.9	I_{w22} (kgm^2)	30.6
Suspension	$k_{\phi t}$ (kNm/rad)	811.3	$k_{\phi s}$ (kNm/rad)	2021.8
	$C_{\phi t}$ (kNms/rad)	35.5	$C_{\phi s}$ (kNms/rad)	77.7
Tire	C_α (N/rad)	141131.1	C_m (Nm/rad)	18043.2
Fifth wheel	C_{wh} (Nms/rad)	7994.4	$k_{f1,2}$ (kNm/rad)	14143.4
Steering system	I_{sw} (kgm^2)	0.108	K_w (Nm/rad)	735.0
	C_w (Nms/rad)	0.1	D_w (m)	0.217
	i_{st}	30	I_w (kg m^2)	9.8
	α (degree)	55		

Table 3.2: Peak values of vehicle response attained during four stages of maneuvers.

Parameter	Peak Value	Parameter	Peak Value	Parameter	Peak Value
a_{x1} (m/s^2)	2.7723	a_{y2} (m/s^2)	2.4620	r_1(deg/s)	9.9412
a_{x2} (m/s^2)	2.7988	v_1(km/h)	1.5311	r_2 (deg/s)	9.1124
u_1(km/h)	67.2557	v_2 (km/h)	1.1647	Γ(deg)	5.4750
u_2 (km/h)	67.2444	$\dot{r}_1$ (deg/s^2)	15.1332	ϕ_1(deg)	7.0258
a_{y1} (m/s^2)	2.8299	$\dot{r}_2$ (deg/s^2)	12.3218	ϕ_2 (deg)	4.3686

The results show the vehicle response in terms of longitudinal and lateral accelerations (a_{x1}, a_{x2} and a_{y1}, a_{y2}), forward and lateral velocities (u_1, u_2 and v_1, v_2), yaw rates (r_1, r_2) and roll angles (ϕ_1, ϕ_2) of the sprung masses of the tractor and the trailer. The vehicle combination exhibit peak response under evasive maneuver, which is performed at a high speed of 70km/h in Stage 4. It can be seen that the lateral accelerations of the c.g. of tractor and trailer approach their maximum values (2.8299 and 2.4620 m/s^2) during the evasive maneuver performed in stage 4 at t=20.0s and 20.6s, respectively, and the maximum values are smaller than the selected threshold value of 0.3g. The yaw rates of tractor and trailer approach their maximum values (9.9412 and 9.1124deg/s) during the same maneuver at t=20.1s and 20.8s, respectively. The roll angle response of sprung masses due to tractor and trailer approach peak values of 7.0258 and 4.3686 degrees, respectively. The results clearly show that the peak values of the response do not exceed the respective threshold values, and thus the vehicle response can be considered to be stable under specified maneuvers.

The sensitivity analyses are performed for variations in vehicle parameters, grouped in two classes: (*i*) parameters related to geometry; and (*ii*) parameters related to static and dynamic properties of components. In order to simplify the analysis, the parameters considered to be more certain are held fixed, which include tandem spread of the tractor drive axle and the trailer axle, and the dual tire spacing. The tire characteristics are assumed to be linear, while the aerodynamic resistances are considered negligible. Thus the geometrical parameters considered in this study are: (*i*) horizontal distance between the c.g. of tractor and trailer and the articulation point, x_{1A} and x_{2A}; (*ii*) c.g. heights of the tractor and trailer, h_{g1} and h_{g2}; (*iii*) horizontal distance between the front

and second axles and c.g. of the tractor, x_{11} and x_{12}; (*iv*) distance between the trailer first axle and its c.g., x_{21}; (*v*) tractor track width, b_{11} and trailer track width, b_{21}. The parameters related to static and dynamic properties of the vehicle and components, considered in this study are: (*i*) tractor and trailer sprung masses, m_{s1} and m_{s2}; (*ii*) tractor moments of inertia, I_{xt} and I_{zt}; (*iii*) trailer moments of inertia, I_{xs} and I_{zs}; (*iv*) cornering stiffness of tires, C_α and aligning moment coefficient of tires, C_m; (*v*) roll stiffness of tractor and trailer suspension, $k_{\phi t}$ and $k_{\phi s}$; (*vi*) roll damping of tractor and trailer suspension, $C_{\phi t}$ and $C_{\phi s}$; and (*vii*) yaw damping and roll stiffness of the fifth wheel, $C_{\psi h}$ and, k_{f12}.

The sensitivity of vehicle response to variations in selected parameters is analyzed using the performance index, formulated in Equations (3.1) and (3.2). The sensitivity coefficients of the performance indices are computed from the vehicle response, using Equation (3.6) and (3.8) and the inputs to the vehicle system shown in Figure 3.1. The front wheel steer angle (δ_{FW}) is attained from the steering wheel angle (δ_{sw}) and the steering ratio (i_{st}), assuming negligible compliance due to steering system.. The tire cornering stiffness, aligning moment and longitudinal adhesion coefficients are characterized as functions of vertical load, slip angle and slip ratio, using Magic Formula. The results of the sensitivity analyses are thus presented in terms of variations in the NMSV of the lateral accelerations (S_{Jay1}, S_{Jay2}), yaw rates (S_{Jr1}, S_{Jr2}) and sprung mass roll angles ($S_{J\phi1}$, $S_{J\phi2}$) response of tractor and trailer, respectively. It should be noted that the values of S_{Jayi}, S_{Jri} and $S_{J\phi i}$ (i=1, 2) reflect the overall rate of variations in the dynamic response of the vehicle with respect to the variation in the parameter, β_k. Higher absolute values of S_{Jayi}, S_{Jri} and $S_{J\phi i}$ (i=1, 2) indicate higher sensitivity of the dynamic performance

to the parameter, β_k. The results of the sensitivity analyses are discussed in the following subsections.

Horizontal distances between the c.g. and the articulation point, (x_{1A}, x_{2A})

Figure 3.3 illustrates the sensitivity of the vehicle response to variations in the horizontal distances between the c.g. of tractor and trailer and the hitch point (x_{1A} and x_{2A}). The figure further illustrates the variations in the NMSV of the total performance index, S_{Jdp}, due to the variations in x_{1A} and x_{2A}. The results show that the variations in x_{1A} primarily affect the lateral acceleration, and yaw rate response of both the tractor and the trailer. The variations in x_{2A}, however, influence the lateral acceleration, yaw rates and roll angles of both the units. An increase in x_{1A} or x_{2A} yields a decrease in the NMSV of the response (S_{Jayi}, S_{Jri}, and $S_{J\phi i}$, i=1, 2) and the performance index (S_{Jdp}) of the vehicle. It can be further seen that the roll response of the trailer (Figure 3.3 c) and the tractor (Figure 3.3 g) is not significantly sensitive to variations in x_{1A}, for x_{1A}>2.2m and x_{2A}, for 3<x_{2A}<8m, respectively. Since the signs of the values of S_{Jayi}, S_{Jri}, and $S_{J\phi i}$ (i=1, 2) indicate an increase (+) or decrease (-) in the vehicle response, Figure 3.3 (f) shows that the variations in x_{2A} yield an increase and decrease in the yaw rate response of trailer (J_{r2}) for x_{2A}>6.1m and x_{2A}<6.1m, respectively. Furthermore, Figure 3.3 (g) implies that the variations in x_{2A} yield an increase and decrease in the roll angle response of the trailer ($J_{\phi 2}$) for x_{2A}>4.3m and x_{2A}<4.3m, respectively. A comparison of response sensitivity to variations in x_{1A} and x_{2A} further reveals that the dynamic response of vehicle is relatively more sensitive to variations in x_{2A}.

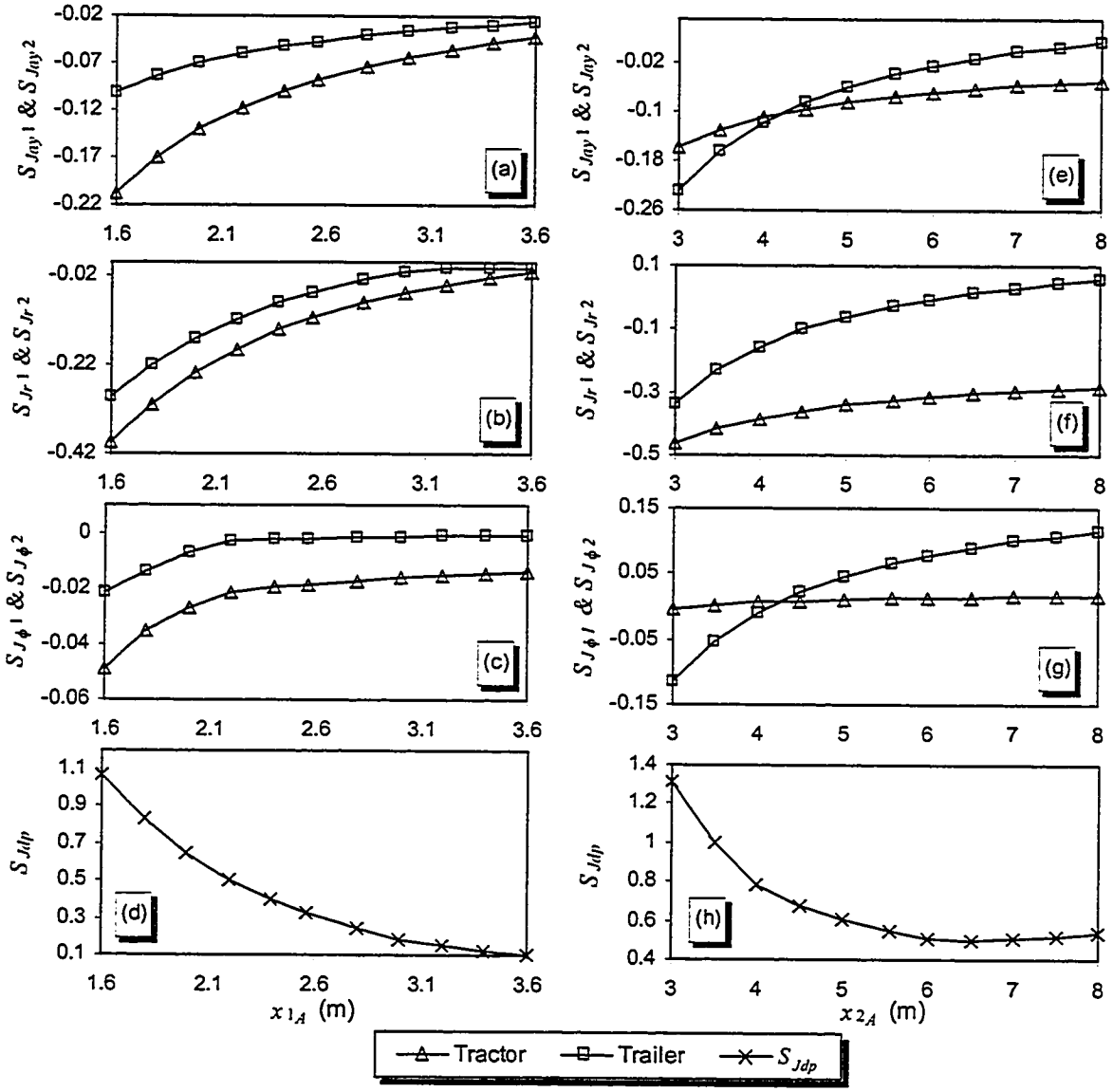

Figure 3.3: Sensitivity of vehicle performance to variations in x_{1A} and x_{2A}.

c.g. heights, (h_{g1} and h_{g2})

Figure 3.4 illustrates the sensitivity of the vehicle response to variations in c.g. heights of the tractor and trailer sprung masses (h_{g1} and h_{g2}). The results show that the variations in h_{g1} and h_{g2} primarily affect the response of tractor and trailer, respectively. An increase in h_{g1} or h_{g2}, however, yields an increase in the lateral acceleration, yaw rate and roll angle response (J_{ayi}, J_{ri} and $J_{\phi i}$) of both tractor and trailer units, since the signs of

all the values are positive. The results reveal that an increase in h_{g1} or h_{g2} yields an increase in the dynamic response of the vehicle, which may lead to a directional instability under high c.g. A comparison of the response sensitivity to variations in h_{g1} and h_{g2} further reveals that the dynamic response of vehicle is considerably more sensitive to increase in h_{g2}.

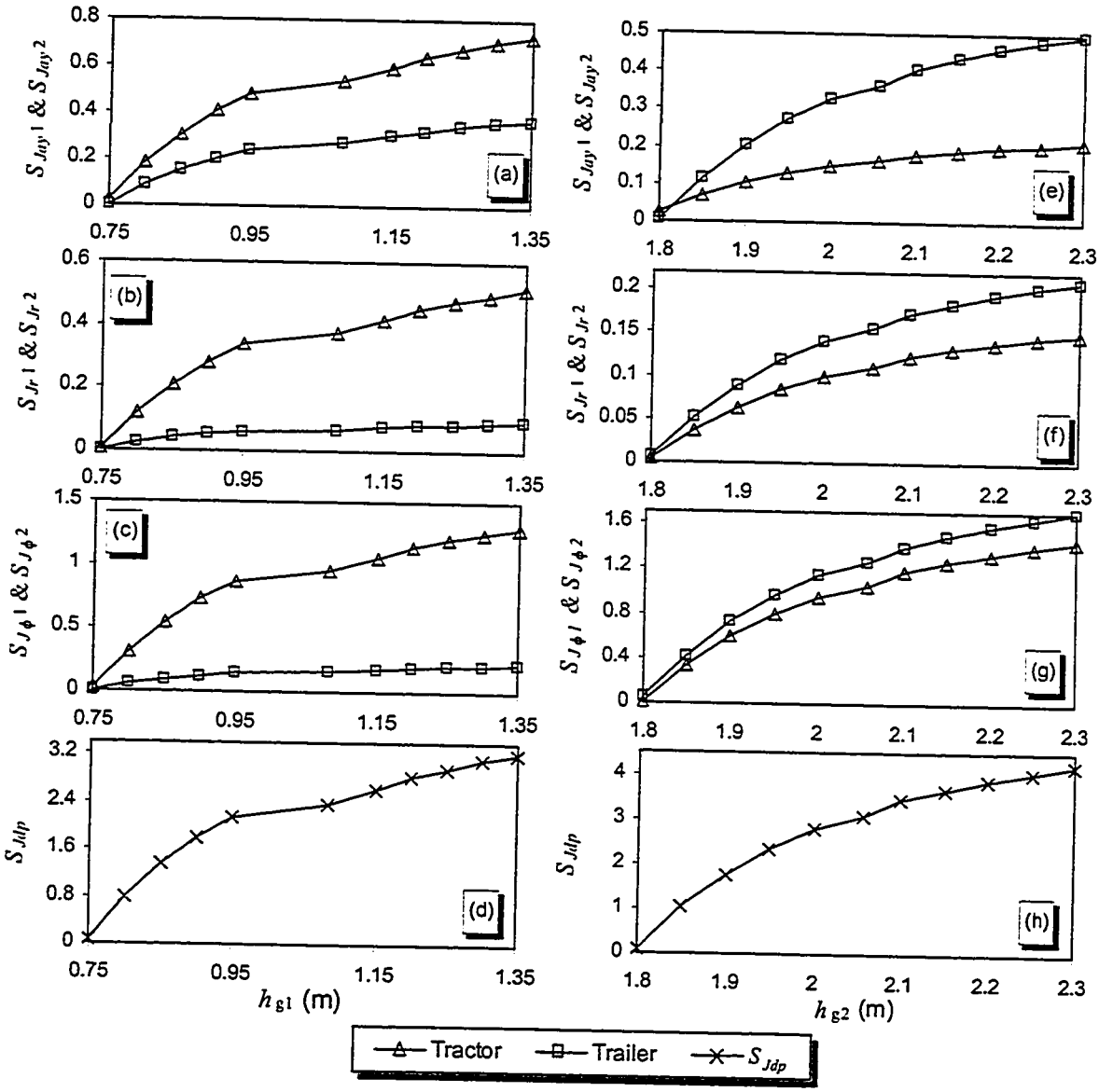

Figure 3.4: Sensitivity of vehicle performance to variations in h_{g1} and h_{g2}.

Horizontal distances between tractor axles and c.g., (x_{11} and x_{12})

The sensitivity of the vehicle response to variations in the horizontal distance between tractor axles and c.g. (x_{11} and x_{12}) is illustrated in Figure 3.5. The results show somewhat different trends in variations in the vehicle response with the variations in x_{11} and x_{12}, respectively. An increase in x_{11} yields a decrease in the NMSV of the lateral acceleration, yaw rate and roll angle response of trailer for x_{11}>0.6m and 0.7m, respectively. An increase in the NMSV of the lateral acceleration, yaw rate and roll angle response of tractor, however, is observed for x_{11}<0.7m. An increase in x_{12} also yields a decrease in the NMSV of the lateral acceleration, yaw rate and roll angle response of both units. The primary influence of variations in x_{12} is observed to be on the sensitivity coefficients of the response of the tractor. A comparison of response sensitivity to variations in x_{11} and x_{12} further reveals that the dynamic response of vehicle is more sensitive to variations in x_{12}.

Horizontal distances between trailer axle and c.g., (x_{21})

Figure 3.6 illustrates the sensitivity of the vehicle response to variations in the horizontal distance between trailer axle and c.g. (x_{21}). The results show that the variations in x_{21} primarily affect the response of the trailer unit. An increase in x_{21} yields a decrease in the NMSV of the variations in lateral acceleration of tractor and the roll angle response of both tractor and trailer units. While an increase in x_{21} yields an increase in the NMSV of the variations in lateral acceleration and yaw rate of the trailer for x_{21} <4m and 4.45m, respectively. The yaw rate response of the tractor, however, is observed to be least sensitive to variations in x_{21}. Figures 3.6(a), (b) and (c) further show positive values of

S_{Jayi} and S_{Jri} (i=1, 2) but negative values of $S_{J\phi 1}$ and $S_{J\phi 2}$. It can thus be derived that the roll stability of the tractor and trailer may be enhanced through increasing x_{21}, while the lateral and yaw stability limits may worsen.

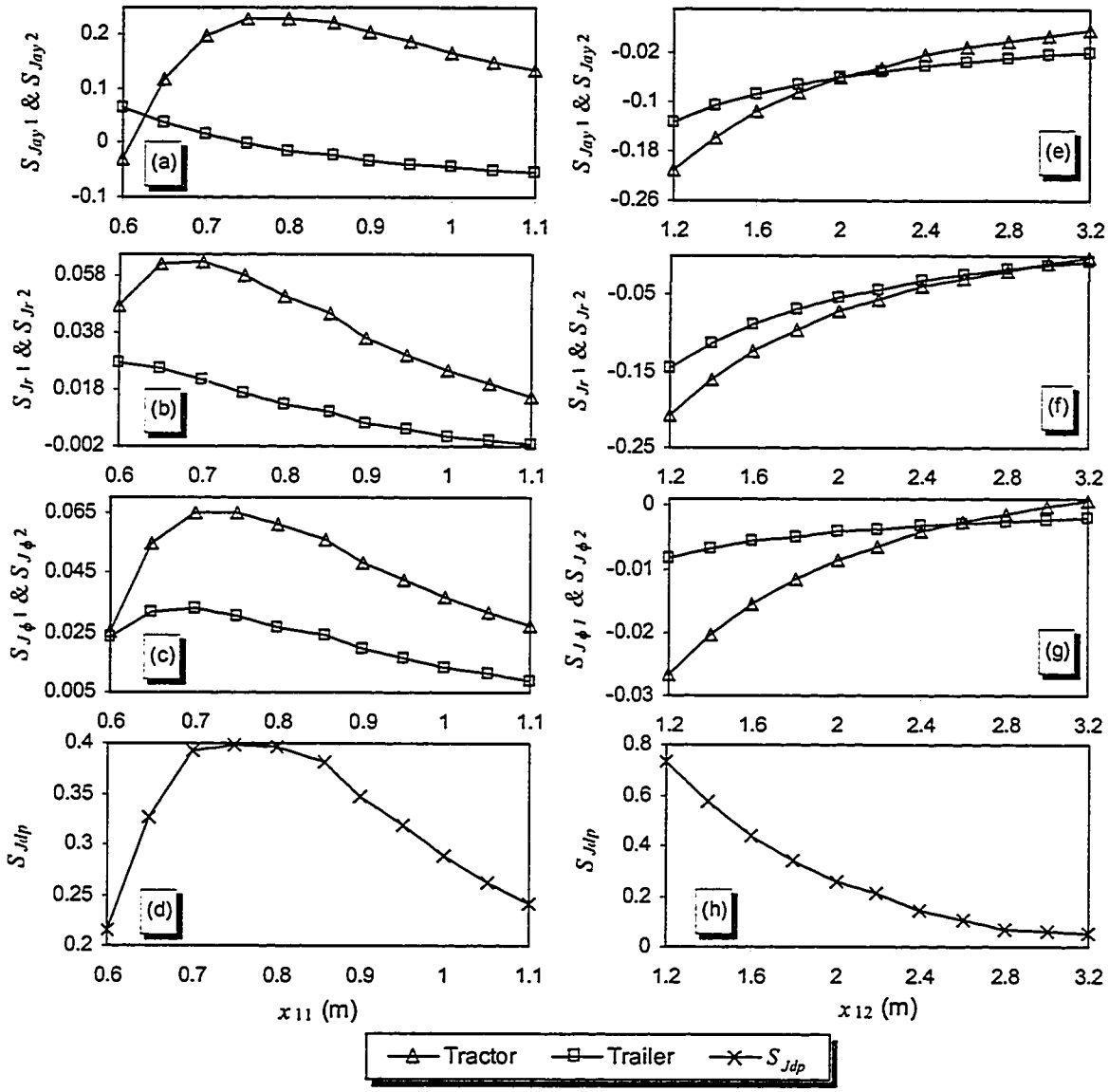

Figure 3.5: Sensitivity of vehicle performance to variation in x_{11} and x_{12}.

Track width, (b_{11} and b_{21})

The sensitivity of the vehicle response to variations in the track width of the tractor and the trailer (b_{11} and b_{21}) is illustrated in Figure 3.7. The results show that both

the parameters affect the vehicle response in a similar manner. An increase in b_{11} or b_{21} yields a decrease in the NMSV of the variations in the lateral acceleration, yaw rate and roll angle response of both tractor and trailer. The results further reveal that an increase in b_{11} and/or b_{21} yields enhanced lateral, yaw and roll stability limits, which is evident from the negative values of J_{ayi}, J_{ri} and $J_{\phi i}$. A comparison of response sensitivity to variations in b_{11} and b_{21} further reveals that the dynamic response of vehicle is almost equally sensitive to both, b_{11} and b_{21}.

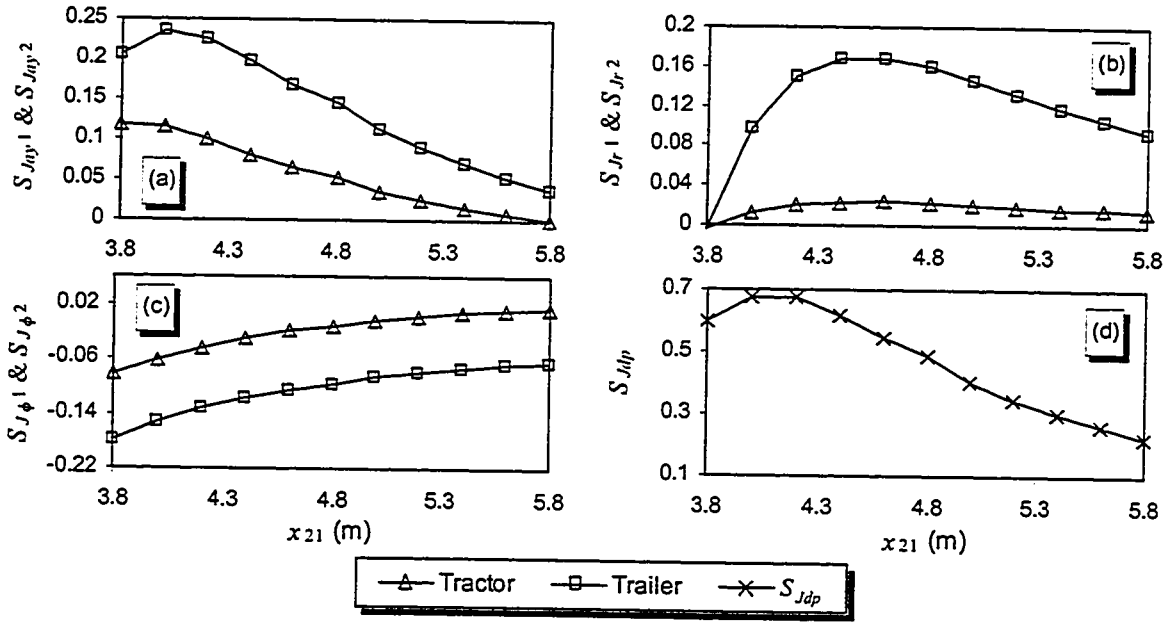

Figure 3.6: Sensitivity of vehicle performance to variations in x_{21}.

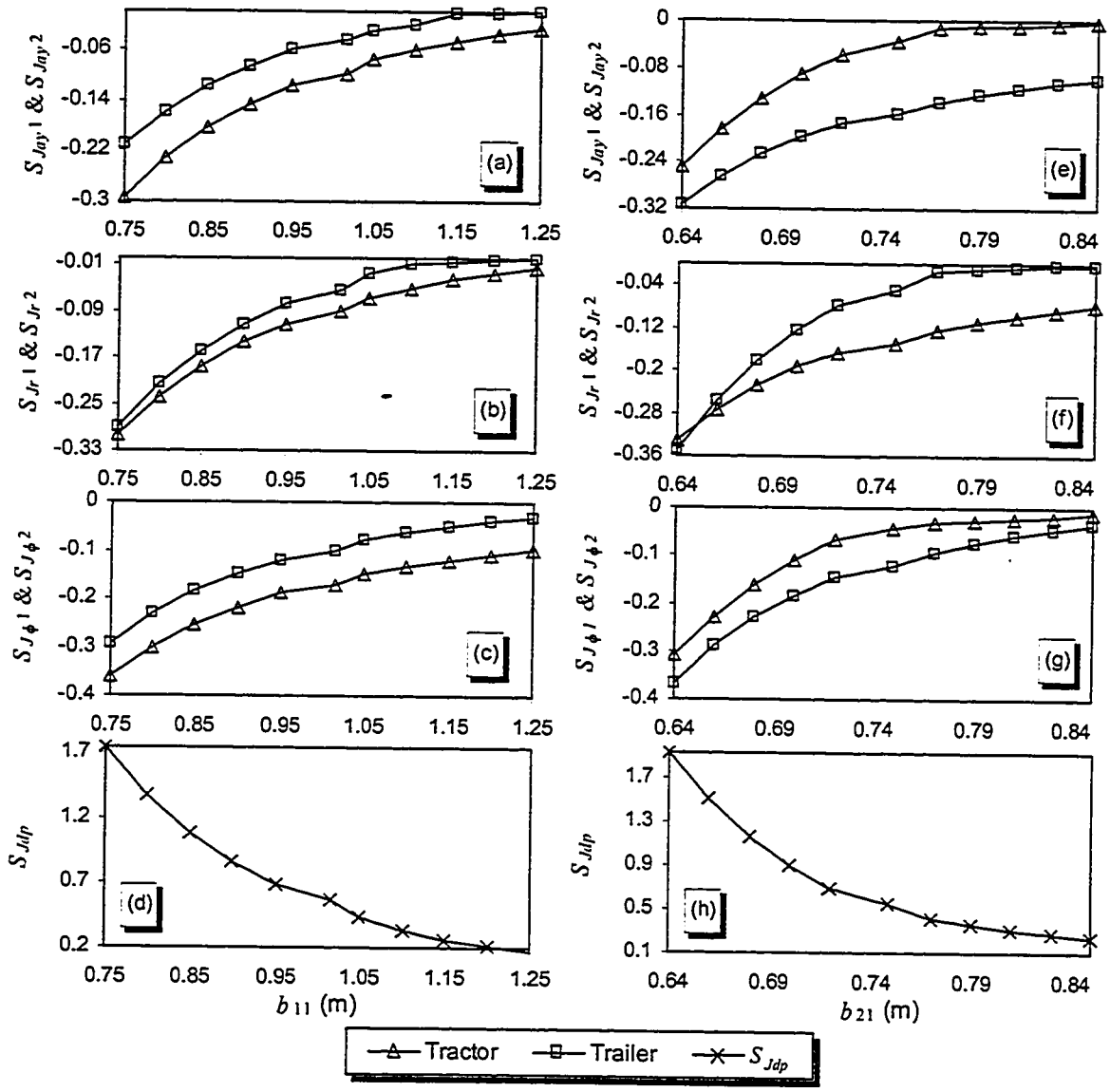

Figure 3.7: Sensitivity of vehicle performance to variations in b_{11} and b_{21}.

Sprung masses. (m_{s1} and m_{s2})

Figure 3.8 illustrates the sensitivity of the vehicle response to variations in sprung masses of tractor and trailer (m_{s1} and m_{s2}). The results show that the variations in m_{s1} and m_{s2} affect the lateral acceleration, yaw rate and roll angle response of tractor and trailer in a significant manner. An increase in m_{s1} yields increasing values of the variations in the NMSV of lateral acceleration, yaw rate and roll angle response of the tractor and the

trailer for m_{s1}<3800kg and 3600kg, respectively. For m_{s1} larger than 3800kg and 3600kg, respectively, the values of the variations in the NMSV of lateral accelerations, yaw rates and roll angles response of tractor and trailer decrease with an increase in m_{s1}. While the influence of m_{s2} on the vehicle response is similar to that observed for variations in m_{s1}, it yields positive values of the variations in the NMSV of lateral accelerations, yaw rates and roll angles response of tractor and trailer, indicating deterioration in the vehicle response with increase in the sprung masses. A comparison of the response sensitivity to variations in m_{s1} and m_{s2} further reveals that the dynamic response of vehicle is more sensitive to variations in m_{s1}.

Mass moments of inertia of the tractor and the trailer, (I_{xt}, I_{zt}, I_{xs} and I_{zs})

Figure 3.9 illustrates the sensitivity of the vehicle response to variations in mass moments of inertia of tractor (I_{xt} and I_{zt}). The results show that the variations in I_{xt} and I_{zt} primarily affect the lateral acceleration, yaw rate and roll angle response of the tractor, while those in I_{xs} and I_{zs} mostly affect the response of the trailer as shown in Figure 3.10. An increase in I_{xt} yields an increase in the variations of the NMSV of the lateral acceleration, yaw rate and roll angle response of the tractor for I_{xt}<2000kgm^2, I_{xt} <1500kgm^2 and I_{xt}<1300kgm^2, respectively. The trailer response sensitivity also increases with increase in I_{xt} in similar range. While an increase in I_{zt} yields an increase in the variations of the NMSV of the lateral acceleration, yaw rate and roll angle response of the tractor for I_{zt}<11200kgm^2, I_{zt}<12100kgm^2 and I_{zt}<11600kgm^2. The positive values of S_{Jayi}, S_{Jri}, and $S_{J\phi i}$ (i=1, 2) further indicate that the dynamic response of the vehicle due to a given steering angle and braking/acceleration inputs will increase with an increase in

I_{xt} and I_{zt}, which may be attributed to the increase in the roll and yaw moments of inertia of tractor. A comparison of response sensitivity to variations in I_{xt} and I_{zt} further reveals that the dynamic response of vehicle is more sensitive to variations in I_{zt}.

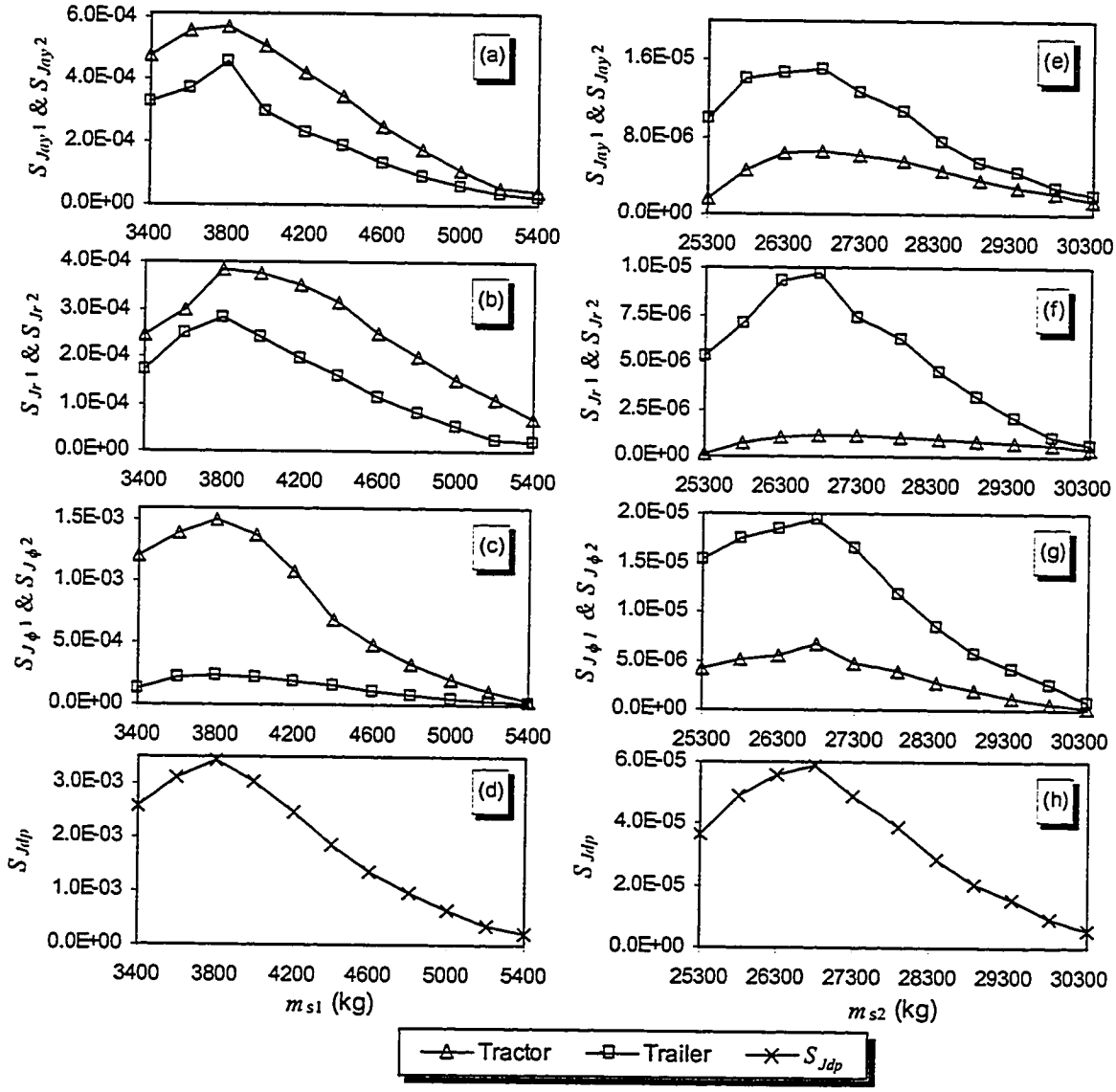

Figure 3.8: Sensitivity of vehicle performance to variations in m_{s1} and m_{s2}.

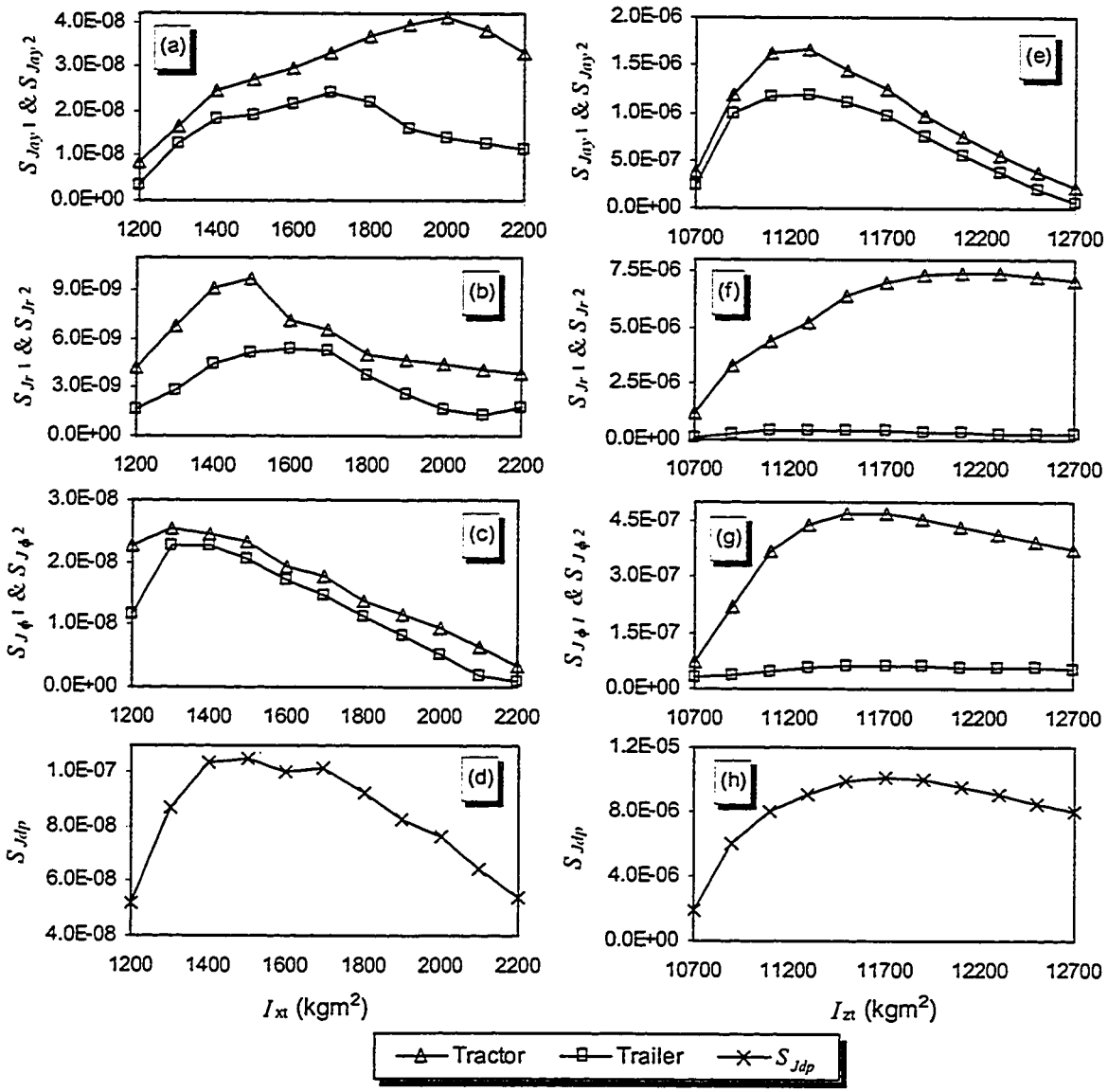

Figure 3.9: Sensitivity of vehicle performance to variations in I_{xt} and I_{zt}.

An increase in I_{xs} yields an increase in the variations of the NMSV of the lateral acceleration, yaw rate and roll angle response of the trailer for I_{xs}<23600kgm^2, I_{xs}<22600kgm^2, and I_{xs}<22600kgm^2 and I_{xs}<22100kgm^2, respectively. An increase in I_{zs} yields a decrease in the variations of the NMSV of the lateral acceleration, yaw rate and roll angle response for I_{zs}>420000kgm^2. It should be noted that the positive values of S_{Jayi}, S_{Jri}, and $S_{J\phi i}$ (i=1, 2) indicate that the dynamic response of the vehicle due to a given

steering angle and braking/acceleration inputs will increase with an increase in I_{xs} and I_{zs}, which may be attributed by the increase in the roll and yaw moments of inertia of trailer. A comparison of response sensitivity to variations in I_{xs} and I_{zs} further reveals that the dynamic response of vehicle is more sensitive to variations in I_{zs}.

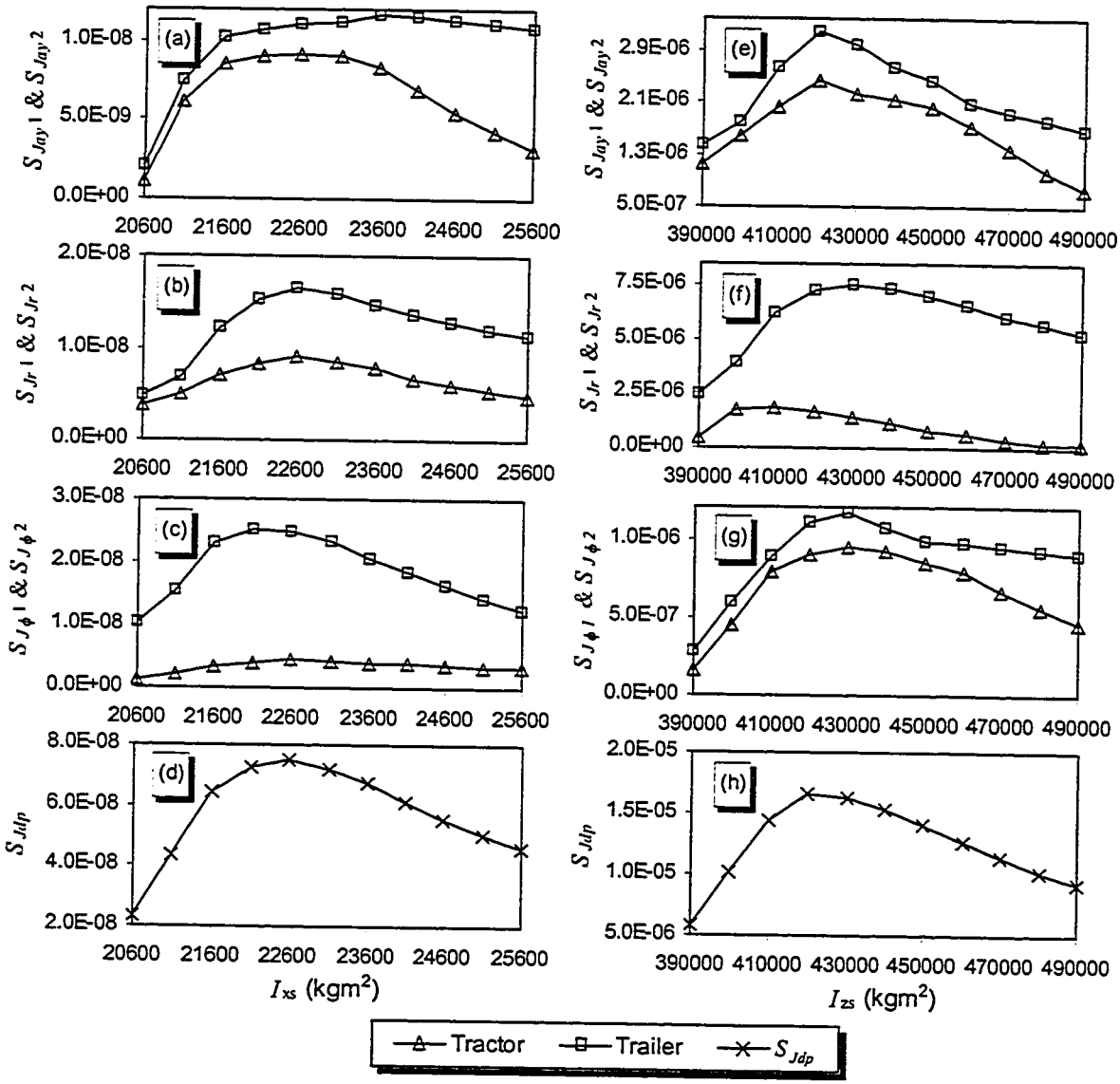

Figure 3.10: Sensitivity of vehicle performance to variations in I_{xs} and I_{zs}.

Cornering properties of tires, (C_α and C_m)

In this subsection, the tire cornering stiffness (C_α) and aligning moment coefficient (C_m) are assumed to be linear functions of the slip angle to investigate their influences on the dynamic performance of the vehicle. Figure 3.11 illustrates the sensitivity of the vehicle response to variations in cornering properties of tires (C_α and C_m). The results show that the variations in C_α primarily affect the lateral acceleration, yaw rate and roll angle response of the trailer, while the dominant influence of C_m is on the lateral acceleration and roll angle response of trailer and the yaw rate of tractor. An increase in C_α, in general, yields a decrease in the NMSV of the variations in lateral acceleration, yaw rate and roll angle response of both tractor and trailer. While an increase in C_m yields a decrease in the absolute NMSV of the variations in lateral acceleration, yaw rate and roll angle response of both tractor and trailer for C_m<14000Nm/rad. It should be noted that the positive and negative values of S_{Jayi}, S_{Jri}, and $S_{J\phi i}$, (i=1, 2) due to C_α and C_m, respectively, may indicate that an increase in the cornering stiffness and aligning moment of tires will increase and decrease the dynamic response of the vehicle, respectively, under selected steering angle and braking/acceleration force inputs.

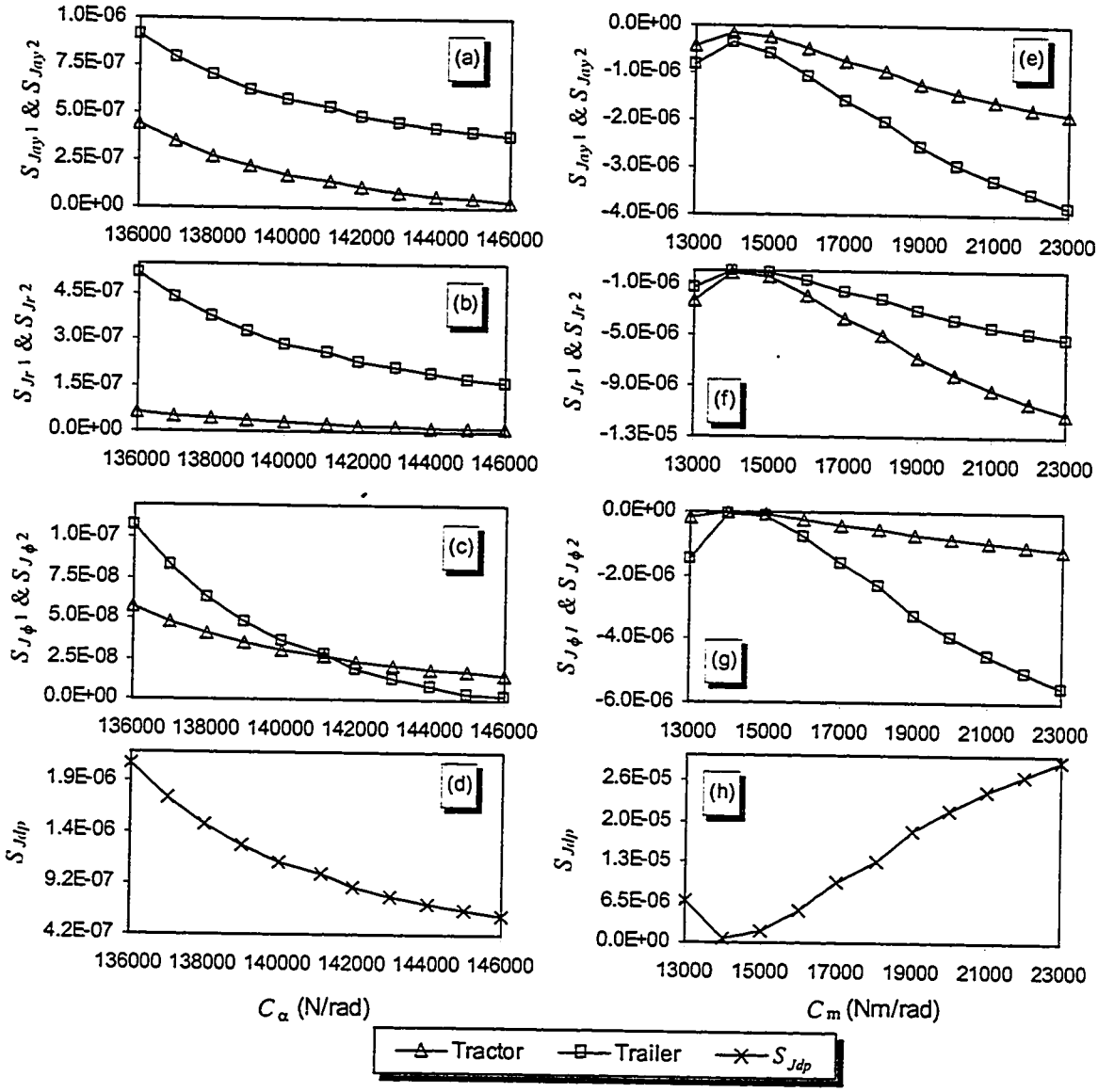

Figure 3.11: Sensitivity of vehicle performance to variations in C_α and C_m.

Suspension roll stiffness ($k_{\phi t}$ and $k_{\phi s}$) and damping ($C_{\phi t}$ and $C_{\phi s}$)

Figures 3.12 and 3.13 illustrate the sensitivity of the vehicle response to variations in suspension roll stiffness ($k_{\phi t}$ and $k_{\phi s}$) and damping properties ($C_{\phi t}$ and $C_{\phi s}$), respectively. The results show that the variations in these parameters affect the lateral acceleration, yaw rate and roll angle response of the tractor and trailer in a considerable manner. An increase in $k_{\phi t}$ or $k_{\phi s}$ yields a decrease in the variations of the absolute NMSV

of lateral acceleration, yaw rate and roll angle response of both tractor and trailer, for $k_{\phi t}$>770kNm/rad or $k_{\phi s}$ >1940kNm/rad. An increase in $C_{\phi t}$ or $C_{\phi s}$, in general, yields a decrease in the variations of the absolute NMSV of lateral acceleration, yaw rate and roll angle response of both tractor and trailer. It should be noted that the negative values of S_{Jayi}, S_{Jri}, and $S_{J\phi i}$, (i=1, 2) due to $k_{\phi t}$, $k_{\phi s}$, $C_{\phi t}$ and $C_{\phi s}$ may indicate that an increase the suspension stiffness and damping coefficient will decrease the dynamic response of the vehicle thus enhance the vehicle stability. A comparison of response sensitivity to variations in $k_{\phi t}$, $k_{\phi s}$, $C_{\phi t}$ and $C_{\phi s}$, further reveals that the dynamic response of the vehicle is more sensitive to variations in trailer suspension properties, $k_{\phi s}$ and $C_{\phi s}$.

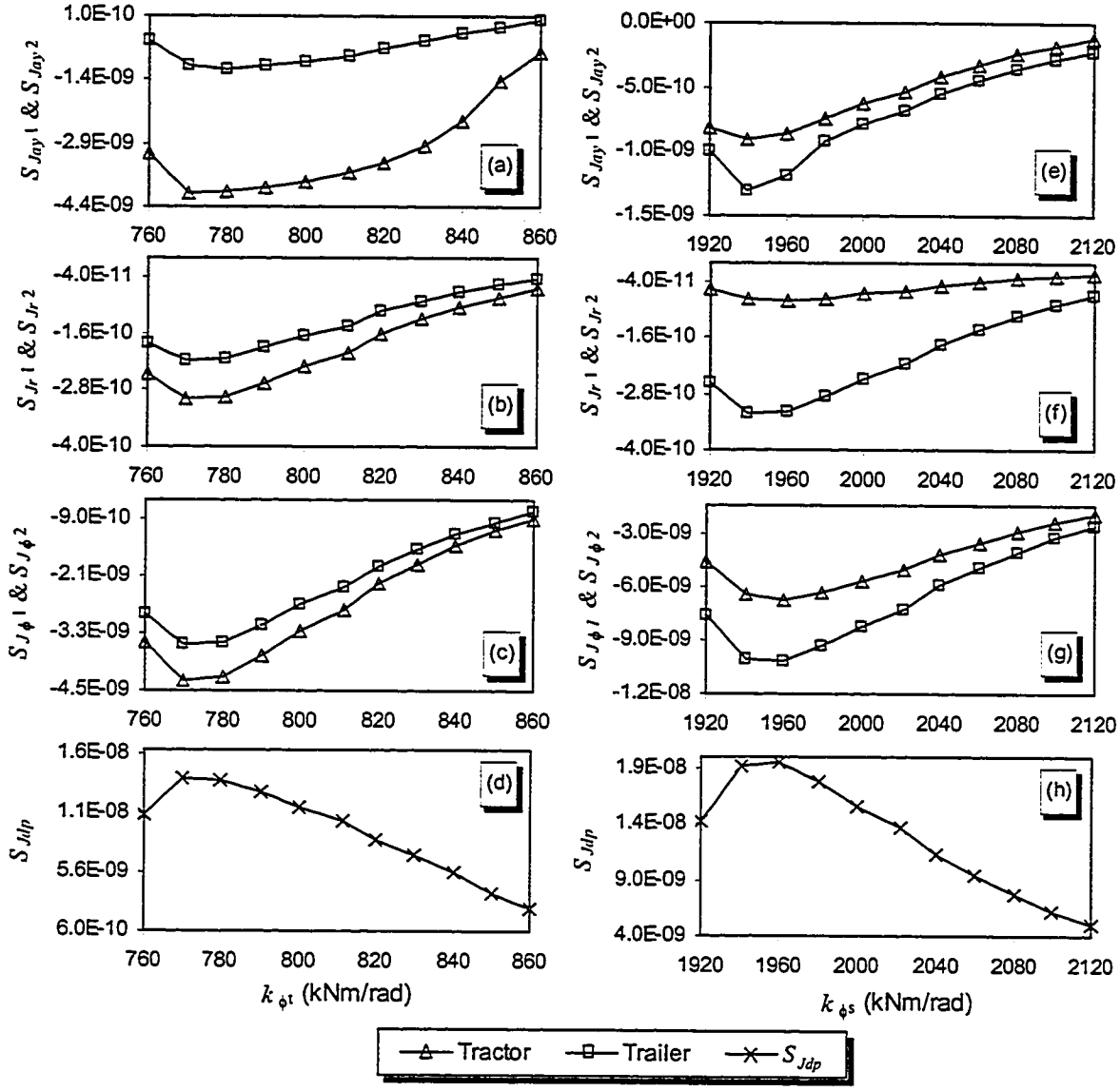

Figure 3.12: Sensitivity of vehicle performance to variations in $k_{\phi t}$ and $k_{\phi s}$.

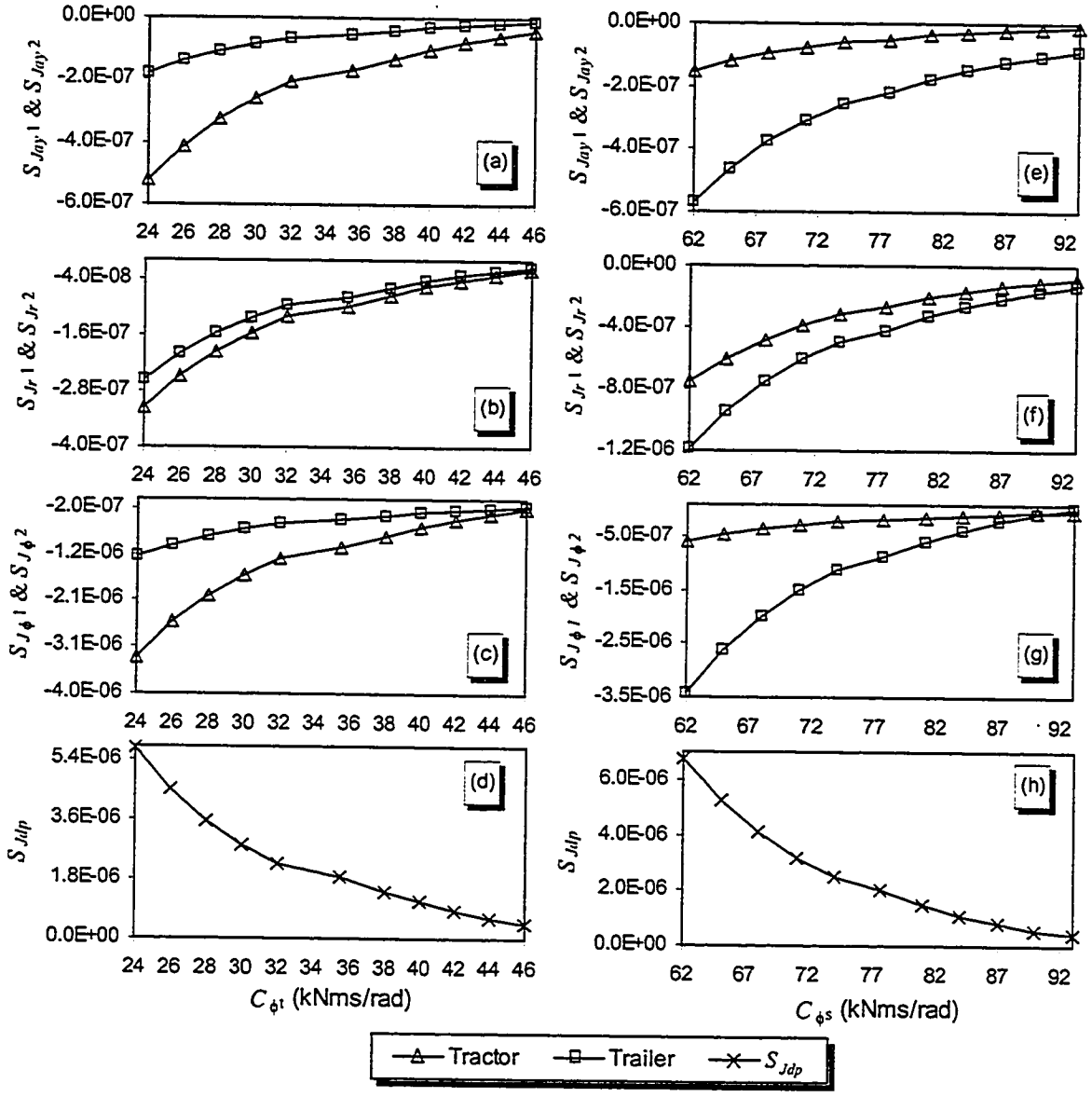

Figure 3.13: Sensitivity of vehicle performance to variations in $C_{\phi t}$ and $C_{\phi s}$.

Articulation damping, ($C_{\psi h}$) and roll stiffness (k_{f12})

Figure 3.14 illustrates the sensitivity of the vehicle response to variations in articulation damping ($C_{\psi h}$) and roll stiffness (k_{f12}) of the fifth wheel coupling. The results show that the variations in $C_{\psi h}$, in general, affect the lateral acceleration, yaw rate, and roll angle response of the tractor, while the variations in k_{f12}, primarily influence the

lateral acceleration response of the trailer and the yaw rate and roll angle response of the tractor. An increase in $C_{\psi h}$ and k_{f12}, in general, yields a decrease in the variations of the absolute values of NMSV of the dynamic response of the vehicle. It is evident that both $C_{\psi h}$ and k_{f12} yield negative values of S_{Jayi}, S_{Jri}, and $S_{J\phi i}$, (i=1, 2), which implies a decrease in the lateral acceleration, yaw rate and roll angle response under selected steering angle, and braking/acceleration inputs.

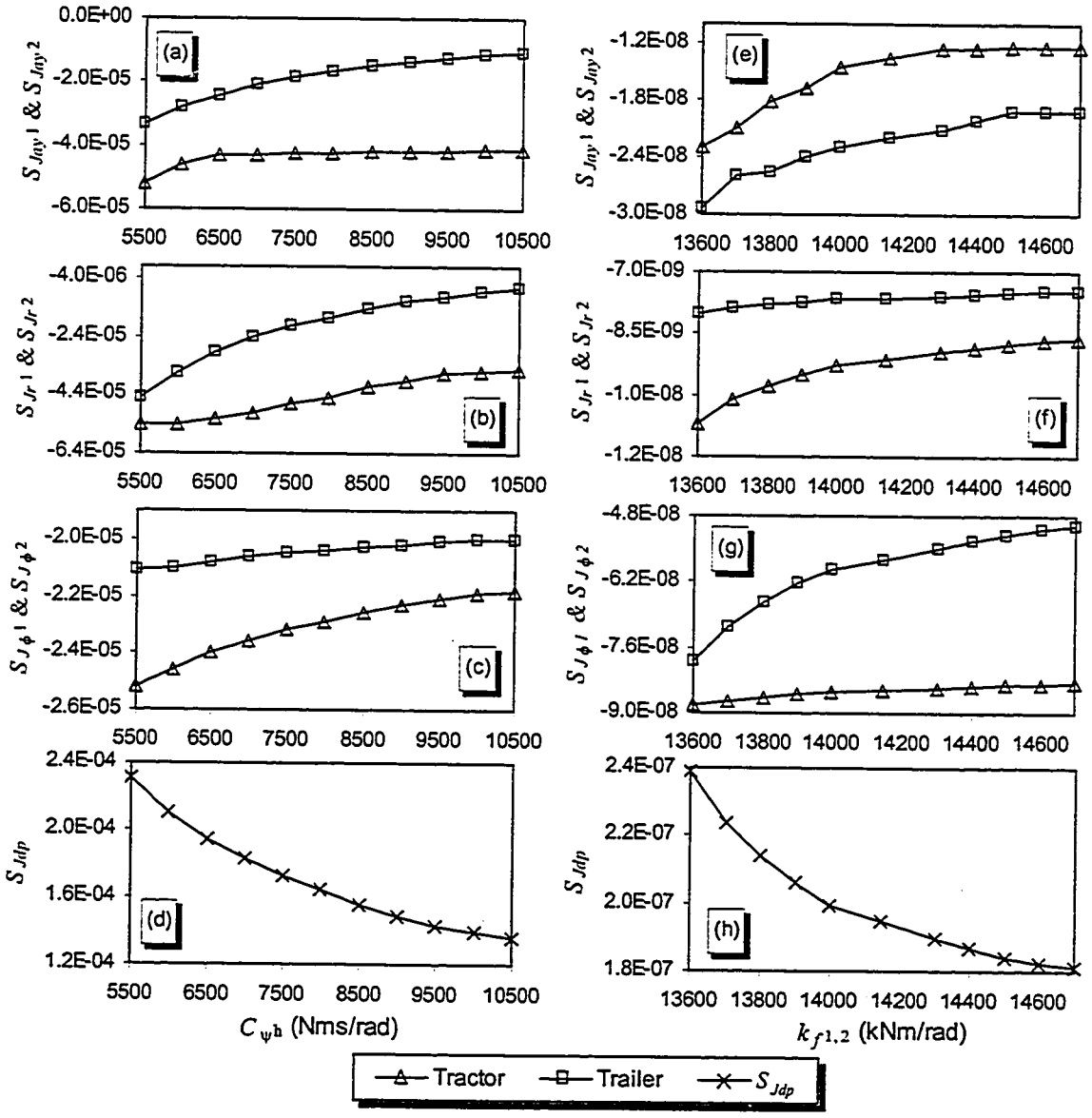

Figure 3.14: Sensitivity of vehicle performance to variations in $C_{\psi h}$ and k_{f12}.

3.3.2 Identification of Most Significant Vehicle Parameters

The results of the sensitivity analyses are examined to identify vehicle parameters that affect the vehicle response most significantly. The identification of such parameters is carried out by summarizing the peak values of sensitivity coefficients and corresponding geometry and dynamics parameters, as illustrated in Tables 3.3 and 3.4, respectively. The results show that the performance indices related to lateral accelerations (S_{Jay1} and S_{Jay2}), yaw rates (S_{Jr1} and S_{Jr2}) and roll angle ($S_{J\phi1}$ and $S_{J\phi2}$), approach their peak values corresponding to: x_{1A}=1.6m, x_{2A}=3.0m, h_{g1}=1.35m, h_{g2}=2.3m, x_{12}=1.2m, b_{11}=0.75m, and b_{21}=0.64m. The vehicle configuration, therefore, must be realized with x_{1A}, x_{2A}, x_{12}, b_{11}, and b_{21} values larger than the above values, while h_{g1} and h_{g2} must be selected below the above values, to ensure safe performance of the combination. The results also show that the c.g. heights yield the largest values of S_{Jayi}, S_{Jri} and $S_{J\phi i}$, (i=1, 2), therefore, they are considered to be the most significant parameters in view of the directional response of the vehicle. The performance indices related to lateral acceleration (S_{Jay1} and S_{Jay2}), yaw rates (S_{Jr1} and S_{Jr2}) and roll angle ($S_{J\phi1}$ and $S_{J\phi2}$), approach their peak values corresponding to x_{11}=0.8, 0.6, 0.7, 0.6, 0.75 and 0.7m, respectively, and x_{21}=3.8, 4.0, 4.6, 4.4, 3.8 and 3.8m, respectively. The vehicle geometry should thus be configured within above limiting values to enhance the directional stability of the vehicle.

The results related to dynamics parameters illustrated in Table 3.4 reveal that the performance indices related to lateral acceleration (S_{Jay1} and S_{Jay2}), yaw rates (S_{Jr1} and S_{Jr2}) and roll angle ($S_{J\phi1}$ and $S_{J\phi2}$), approach their peak values corresponding to m_{s1}=3800kg, m_{s2}=26800kg, C_{α}=136kN/rad, C_{m}=23kNm/rad, $C_{\phi t}$=24kNms/rad, $C_{\phi s}$=62kNms/rad, $C_{\psi h}$=5500Nms/rad and k_{f12}=13600kNm/rad. The vehicle configuration,

therefore, should avoid above dynamics parameters associated with the sprung masses, tire properties, suspension roll damping and the fifth wheel damping and stiffness to ensure the safe performance.

The performance indices related to lateral acceleration (S_{Jay1} and S_{Jay2}), yaw rates (S_{Jr1} and S_{Jr2}) and roll angle ($S_{J\phi1}$ and $S_{J\phi2}$), approach their peak values corresponding to I_{xt}=2000, 1700, 1500, 1600, 1300, 1400kgm^2, I_{zt}=11300, 12100, 11700kgm^2, I_{xs}=22600, 23600, 22100kgm^2, I_{zs}=420000, 410000, 430000kgm^2, respectively. For the suspension roll stiffness ($k_{\phi t}$ and $k_{\phi s}$), the performance indices approach their peak value corresponding to $k_{\phi t}$=760, 980, 770kNm/rad, and $k_{\phi s}$=1920, 1960, 1940kNm/rad, respectively. Therefore, the vehicle configuration should be selected to enhance the stability of the vehicle system through compromising the lateral, yaw and roll dynamic performance.

Table 3.3: Peak Sensitivity of response to variations in geometrical parameters and corresponding parameter value.

Parameter	Peak Sensitivity (*Corresponding Parameter Value*)						
	S_{Jay1}	S_{Jay2}	S_{Jr1}	S_{Jr2}	$S_{J\phi1}$	$S_{J\phi2}$	S_{Jdp}
x_{1A} (m)	-2.08E-01(*1.6*)	-1.01E-01(*1.6*)	-3.96E-01(*1.6*)	-2.94E-01(*1.6*)	-4.92E-02(*1.6*)	-2.19E-02(*1.6*)	1.07E+00(*1.6*)
x_{2A} (m)	-1.59E-01(*3.0*)	-2.29E-01(*3.0*)	-4.63E-01(*3.0*)	-3.39E-01(*3.0*)	-3.07E-03(*3.0*)	-1.16E-01(*3.0*)	1.31E+00(*3.0*)
h_{g1} (m)	7.27E-01(*1.35*)	3.70E-01(*1.35*)	5.15E-01(*1.35*)	9.22E-02(*1.35*)	1.30E+00(*1.35*)	2.17E-01(*1.35*)	3.22E+00(*1.35*)
h_{g2} (m)	2.11E-01(*2.3*)	4.97E-01(*2.3*)	1.49E-01(*2.3*)	0.208976(*2.3*)	1.44E+00(*2.3*)	1.692808(*2.3*)	4.19E+00(*2.3*)
x_{11} (m)	2.31E-01(*0.8*)	6.31E-02(*0.6*)	6.26E-02(*0.7*)	2.71E-02(*0.6*)	6.51E-02(*0.75*)	3.29E-02(*0.7*)	3.99E-01(*0.75*)
x_{12} (m)	-2.11E-01(*1.2*)	-1.33E-01(*1.2*)	-2.09E-01(*1.2*)	-1.47E-01(*1.2*)	-2.67E-02(*1.2*)	-8.23E-03(*1.2*)	7.35E-01(*1.2*)
x_{21} (m)	1.18E-01(*3.8*)	2.35E-01(*4.0*)	2.35E-02(*4.6*)	1.68E-01(*4.4*)	-8.40E-02(*3.8*)	-1.80E-01(*3.8*)	6.75E-01(*4.0*)
b_{11} (m)	-2.93E-01(*0.75*)	-2.11E-01(*0.75*)	-3.03E-01(*0.75*)	-2.90E-01(*0.75*)	-3.60E-01(*0.75*)	-2.93E-01(*0.75*)	1.75E+00(*0.75*)
b_{21} (m)	-2.49E-01(*0.64*)	-3.12E-01(*0.64*)	-3.31E-01(*0.64*)	-3.50E-01(*0.64*)	-3.08E-01(*0.64*)	-3.68E-01(*0.64*)	1.92E+00(*0.64*)

Table 3.4: Peak Sensitivity of response to variations in dynamics parameters and corresponding parameter value.

Parameter	Peak Sensitivity (*Corresponding Parameter Value*)						
	S_{Jay1}	S_{Jay2}	S_{Jr1}	S_{Jr2}	$S_{J\phi1}$	$S_{J\phi2}$	S_{Jdp}
m_{s1} (kg×*100*)	5.65E-04 (*38*)	4.58E-04 (*38*)	3.82E-04 (*38*)	2.83E-04 (*38*)	1.51E-03 (*38*)	2.43E-04 (*38*)	3.44E-03 (*38*)
m_{s2} (kg×*100*)	6.62E-06(*268*)	1.51E-05(*268*)	1.13E-06(*268*)	9.69E-06(*268*)	6.76E-06(*268*)	1.95E-05(*268*)	5.88E-05(*268*)
I_{xt} (kgm^2 ×*100*)	4.11E-08(*20*)	2.41E-08(*17*)	9.66E-09(*15*)	5.38E-09(*16*)	2.54E-08(*13*)	2.28E-08(*14*)	1.05E-07(*15*)
I_{zt} (kgm^2 ×*100*)	1.67E-06(*113*)	1.18E-06(*113*)	7.43E-06(*121*)	4.36E-07(*113*)	4.69E-07(*117*)	6.13E-08(*117*)	1.01E-05(*117*)
I_{xs} (kgm^2 ×*100*)	9.11E-09(*226*)	1.16E-08(*236*)	9.00E-09(*226*)	1.65E-08(*226*)	4.42E-09(*226*)	2.51E-08(*221*)	7.47E-08(*226*)
I_{zs} (kgm^2 ×*1000*)	2.42E-06(*420*)	3.20E-06(*420*)	1.83E-06(*410*)	7.51E-06(*430*)	9.42E-07(*430*)	1.16E-06(*430*)	1.65E-05(*420*)
C_α (N/rad ×1000)	4.39E-07(*136*)	9.06E-07(*136*)	6.45E-08(*136*)	5.18E-07(*136*)	5.71E-08(*136*)	1.07E-07(*136*)	2.09E-06(*136*)
C_m (Nm/rad)	-1.87E-06(*23000*)	-3.82E-06(*23000*)	-1.12E-05(*23000*)	-5.37E-06(*23000*)	-1.16E-06(*23000*)	-5.53E-06(*23000*)	2.90E-05(*23000*)
$k_{\phi t}$ (kNm/rad)	-4.12E-09(*760*)	-1.14E-09(*780*)	-3.01E-10(*770*)	-2.19E-10(*770*)	-4.29E-09(*770*)	-3.54E-09(*770*)	1.35E-08(*770*)
$k_{\phi s}$ (kNm/rad)	-8.20E-10(*1920*)	-1.43E-09(*1920*)	-8.11E-11(*1960*)	-3.21E-10(*1940*)	-6.78E-09(*1960*)	-1.02E-08(*1960*)	1.94E-08(*1960*)
$C_{\phi t}$ (kNms/rad)	-5.24E-07(*24*)	-1.78E-07(*24*)	-3.17E-07(*24*)	-2.57E-07(*24*)	-3.26E-06(*24*)	-1.20E-06(*24*)	5.74E-06(*24*)
$C_{\phi s}$ (kNms/rad)	-1.54E-07(*62*)	-5.72E-07(*62*)	-7.53E-07(*62*)	-1.19E-06(*62*)	-6.07E-07(*62*)	-3.43E-06(*62*)	6.70E-06(*62*)
$C_{\psi h}$ (Nms/rad)	-5.20E-05(*5500*)	-3.35E-05(*5500*)	-5.45E-05(*5500*)	-4.49E-05(*5500*)	-2.52E-05(*5500*)	-2.11E-05(*5500*)	2.31E-04(*5500*)
$k_{f1,2}$ (kNm/rad)	-2.31E-08(*13600*)	-2.94E-08(*13600*)	-1.07E-08(*13600*)	-8.00E-09(*13600*)	-8.84E-08(*13600*)	-7.90E-08(*13600*)	2.39E-07(*13600*)

3.4 IDENTIFICATION OF VEHICLE PARAMETERS

The directional dynamics analyses of heavy vehicles involve accurate estimation of various parameters, specifically those identified as the most significant ones in the previous section. An accurate estimation of a large number of parameters poses several complexities. A number of comprehensive linear and nonlinear directional dynamics models have been developed to study the lateral and roll stability of heavy vehicles, such as the YAW/ROLL and PHASE IV models [40-42, 95]. Such models, however, involve highly complex and nonlinear characterization of the tire-road interactions, and estimation of a large number of vehicle parameters, which pose unreasonable demands on the analysts. Freight vehicles operate with varying loading conditions and thus pose a tedious task of estimating various parameters, such as coordinates of the centers of the sprung masses, the mass moments of inertia and cornering properties of tires. The in-service tire tread condition, inflation pressure and the axle loads further complicate accurate descriptions of the cornering behaviour of tires. The uncertainties associated with the mass moments of inertia of the rigid sprung and unsprung weights, and cornering properties of tires, specifically, can lead to considerable errors in the analysis.

Alternatively, system identification techniques can be implemented to derive a reasonable estimate of the uncertain parameters and linear equivalent dynamic properties of the tire-road interface under the specified loading and operating conditions. The linear transfer function derived from the identification techniques can further serve as a simplified analytical model, which is considered valid in the vicinity of the specified operating conditions. The resulting linear transfer function can permit the directional dynamics analysis of the vehicle in a highly efficient manner. The parameter

identification from the system function, however, can be tedious, when large size models are considered. Although system identification techniques have been widely implemented to analyze vehicle structures and substructures, suspension and transmission systems [178, 179], the applications to estimate the lateral dynamics and associated parameters of articulated freight vehicles have not been reported.

The system identification is strongly related to the characteristics of the input signal. A wide range of input signals have been implemented in various system identification studies, ranging from single harmonic to impulse signals [180]. The selection of the input signal, in general, is dependent upon the qualitative system behaviour, and involves two important considerations. The first consideration concerns with the shape and frequency contents of the input signals, which must be selected to ensure stimulation of all the important modes. The cross correlation of the input signal and the noise in the measured signals forms another important consideration [181, 182]. The optimal input signal characteristics should have a wide frequency spectrum, so that the response yields all the important dynamic modes and a reasonably accurate estimate of the system parameters. Although an impulse function, which yields a flat power spectrum over a wide band of frequencies, is considered as an ideal input signal, a pseudo-random white noise signal is conveniently used due to difficulties associated with generation of an ideal impulse.

It may also be desirable to generate an input signal which is representative of the realistic excitation imposed on the system in order to perform an effective system identification. The lateral dynamics of vehicles are frequently investigated under open-loop ramp-step and trapezoidal steering maneuvers [183, 184]. While a ramp-step signal

can be easily generated, a trapezoidal input can be realized through a quasi-impulse. The magnitudes of such signals, however, need to be carefully selected to ensure high signal to noise ratio (SNR), and linear and stable behaviour in the vicinity of the specified operating conditions. It has been reported that the lateral dynamics of a road vehicle can be considered to be linear, when the tire-road adhesion coefficient is greater than 0.7 and the lateral acceleration is less than 0.3g [148].

In this section, a system identification technique is applied to derive the lateral dynamics transfer function of a heavy vehicle combination and to estimate a set of uncertain vehicle parameters under the specified load and maneuvers. The linear transfer function of an articulated freight vehicle is identified using Gauss-Newton algorithm under varying levels of SNR and three different steering inputs, including ramp-step, trapezoidal and a pseudo-random. The validity of the proposed methodology is demonstrated by comparing the coefficients of the identified function with those derived for the linear analytical model. The robustness of the identification technique in estimating vehicle parameters is further demonstrated using the data generated from the comprehensive YAW/ROLL model.

3.4.1 Vehicle System Identification Problem

The scope of the identification is to find a mathematical model of the vehicle system from the measured time history of the response $y(k)$ to a known steering input signal $u(k)$. The measured response may be expressed as the superposition of the undisturbed system response $w(k)$ to the identical steering input $u(k)$, and the measurement noise $e(k)$, which is assumed to be a white noise:

$$y(k) = w(k) + e(k) \tag{3.9}$$

The relationship between the input $u(k)$ and the undisturbed output $w(k)$ of the vehicle system can be expressed as a linear difference equation of the form:

$$w(k) + \sum_{i=1}^{nf} f_i w(k-i) = \sum_{j=0}^{n_b} b_j u(k-j) \tag{3.10}$$

where k refers to the integer discrete time, f_i and b_j are the constant coefficients, and n_f and n_b denote the order of the system.

With $F(q) = 1 + \sum_{i=1}^{nf} f_i q^{-i}$ and $B(q) = \sum_{j=0}^{n_b} b_j q^{-j}$, where q^{-1} denotes the backward shift operator with the property: $q^{-1}w(k)=w(k\text{-}1)$, an output error model of the system is formulated as:

$$y(k) = \frac{B(q)}{F(q)} u(k) + e(k) \tag{3.11}$$

From Equation (3.11), it is apparent that the measured system response is a function of unknown undisturbed output $w(k)$ and thus the constant coefficient vector $\theta = [b_j, f_i]^T$ and the known input function $u(k)$. The system response derived from the estimated coefficient vector $\hat{\theta}$ can be expressed as:

$$\hat{y}(k|\hat{\theta}) = \phi^T(k, \hat{\theta})\hat{\theta} \tag{3.12}$$

where

$$\phi(k, \hat{\theta}) = [u(k), u(k-1), \cdots, u(k-n_b), -w(k-1, \hat{\theta}), \cdots, -w(k-n_f, \hat{\theta})]^T \tag{3.13}$$

and $\hat{y}(k|\hat{\theta})$ is the predicted response, which is a pseudo-linear regression (PLR) due to the nonlinear effects of $\hat{\theta}$ in the vector $\phi(k,\hat{\theta})$ [185]. A loss function J is then formulated to minimize the output error:

$$J = \frac{1}{N}\sum_{k=1}^{N} 0.5\varepsilon^2(k,\hat{\theta}) \tag{3.14}$$

where N is the number of sampling points of the measured data and the error function $\varepsilon(k,\hat{\theta}) = y(k) - \hat{y}(k|\hat{\theta})$. The minimization problem is solved using Gauss-Newton method to derive the parameter vector $\hat{\theta}$. Since the vector $\hat{\theta}$ is identified for the discrete time system, the Tustin transformation can be applied to convert the discrete system into a continuous system in order to derive the coefficients of transfer function in the Laplace domain [181, 182, 185].

In such Gray-Box identification techniques, a good estimate of model structure (i.e. model order and time-lag) is vital for the accuracy of the identification [186, 187]. The magnitude of loss function *J*, in general, tends to decrease as the order of model increases. A considerably higher order model, however, may not yield further significant reduction in the loss function. The degree of fit tends to improve with increase in the order of the model until it approaches a true or optimal order. Alternatively, Akaike's Final Prediction Error criterion (FPE) can be applied to determine the structure of the model, where FPE is given by [181]:

$$FPE = \frac{1 + n/N}{1 - n/N} \times J \tag{3.15}$$

where $n=n_f+n_b+1$ is the total number of system coefficients to be estimated. Compared with the loss function J in Equation (3.14), the *FPE* considers the contributions from both

the error function $\varepsilon(k,\hat{\theta})$ and the model order. The *FPE* criterion imposes a weighting factor on the loss function, which is a function of the model structure and the total number of sampling points. Selection of a relatively large number of sampling points may lead to nearly unity value of the weighting factor. For a given length of measured data, the weighting factor is directly related to the model structure. It is thus proposed to select the order of the model that yields the lowest value of *FPE*.

A system with time lag, which may be originated from the hysteretic elements of the system, can be represented by the following difference equation:

$$w(k) = -\sum_{i=1}^{n_f} f_i w(k-i) + \sum_{j=0}^{n_b} b_j u(k-j-k_d) \tag{3.16}$$

where k_d is the constant discrete time lag that is constrained to being an integer. It has been shown that k_d can be successfully identified by repeatedly solving the least-squares parameter estimation problem for a given model order (n_f, n_b) and a sequence of k_d values (k_d=1, 2, ...) [181]. The best lag k_d estimate is the one that yields the smallest value of the loss function J in Equation (3.14) and *FPE* in Equation (3.15).

3.4.2 Application

The vehicle considered in the study comprises a three-axle tractor and a two-axle semitrailer, which represents one of the most commonly used configurations of articulated freight vehicles. Although the contributions due to the roll dynamics and the suspension forces are assumed negligible in a simplified yaw plane model, it has been established that such model yields reasonably accurate prediction of the lateral and yaw dynamics of the vehicle [96]. The yaw plane model is selected to limit the number of

transfer function coefficients and the uncertain parameters, which are computed upon manipulation of the coefficients. The yaw-plane model of articulated vehicle combination is described in Section 2.2.1. Assuming linear cornering properties of tires, the equations of motion can be analyzed to yield lateral acceleration gain of the leading unit in the following manner:

$$G(s) = \frac{a_{y1}(s)}{\delta_{FW}(s)} = \frac{A_4 s^4 + A_3 s^3 + A_2 s^2 + A_1 s + A_0}{s^4 + B_3 s^3 + B_2 s^2 + B_1 s + B_0} \tag{3.17}$$

where the coefficients A_0 to A_4 are functions of the vehicle parameters and speed, which relate to the numerator dynamics of the tractor unit. B_0 to B_3 are the coefficients of the characteristic equation of the combination and a_{y1} represents the lateral acceleration of the c.g. of the tractor with respect to the fixed axis system.

The lateral dynamic analysis of the vehicle necessitates various vehicle parameters, such as: geometry; mass, mass moments of inertia and weights, the coordinates of the c.g. of both units; and cornering and aligning moment properties of the tire. While the weights and dimensions parameters are easily identified, an accurate identification of mass moments of inertia of the tractor (I_{zt}) and trailer (I_{zs}), and aligning moment coefficient (C_m) and cornering stiffness of tires (C_α) of the tires pose certain difficulties. This may be attributed to varying loading patterns, speeds and road conditions, and nonlinear tire properties. The uncertainties associated with such parameters influence the directional behaviour of the vehicle considerably. Figure 3.15 illustrates the influence of variation in I_{zt}, I_{zs}, C_α, and C_m on the lateral acceleration gain response of the tractor, when the combination is subjected to a step steering input. The results show the response characteristics when each of the above parameters are varied

by +50%, -50% and +100%. The results clearly show that the variations in cornering stiffness affect the transient as well as steady state response most significantly, while variations in the aligning moment coefficient affect the steady state response. The variations in the mass moments of inertia (I_{zt} and I_{zs}) influence the transient directional response of the vehicle.

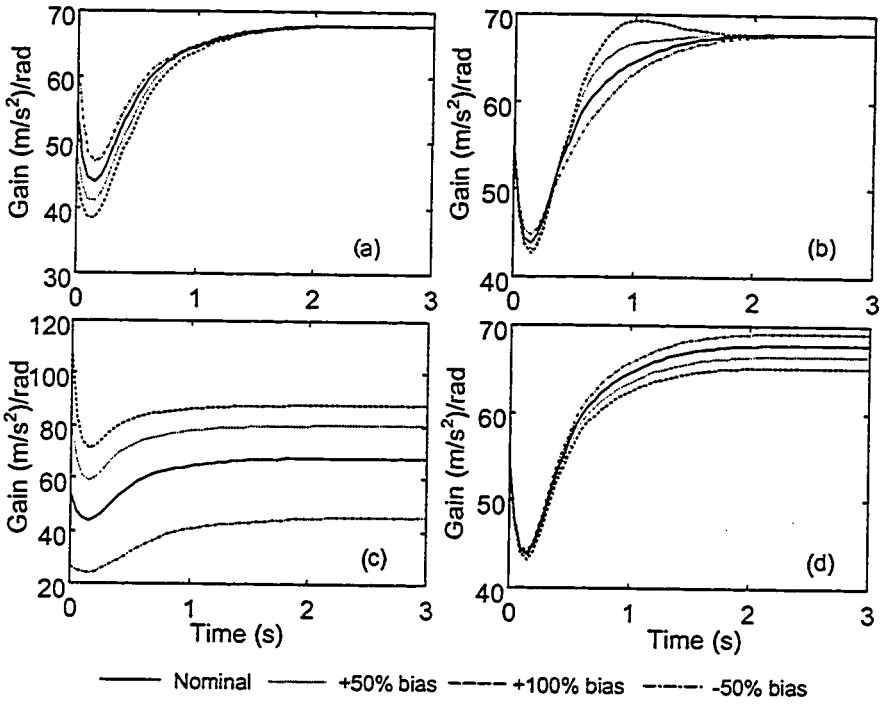

Figure 3.15: Influence of variations in the uncertain parameters on the lateral acceleration gain of the tractor: (a) I_{zt}; (b) I_{zs}; (c) C_α; (d) C_m

The influence of variations in the above parameters on the gain transfer function coefficients is also illustrated in Figure 3.16. The results are presented in terms of bias in the coefficients of the transfer function relative to those derived using nominal values. The results further show that the coefficients are mostly affected by the variations in C_α and least affected by the variation in C_m. While the influence of variations in I_{zs} is considerably larger than that in I_{zt}. It can be further seen that the variations in I_{zt} and C_α

mostly affect the coefficients A_0, A_1, and B_0 of the transfer function (Equation 3.17). While the variations in I_{zs} mostly contribute to the coefficients A_0, A_1, B_0, and B_1, the variations in C_m mostly affect B_0 and A_4. From the results, it can be concluded that the lower order coefficients of the transfer function are strongly dependent upon those parameters. The directional dynamics of the combination can thus be affected by the uncertainties associated with these parameters.

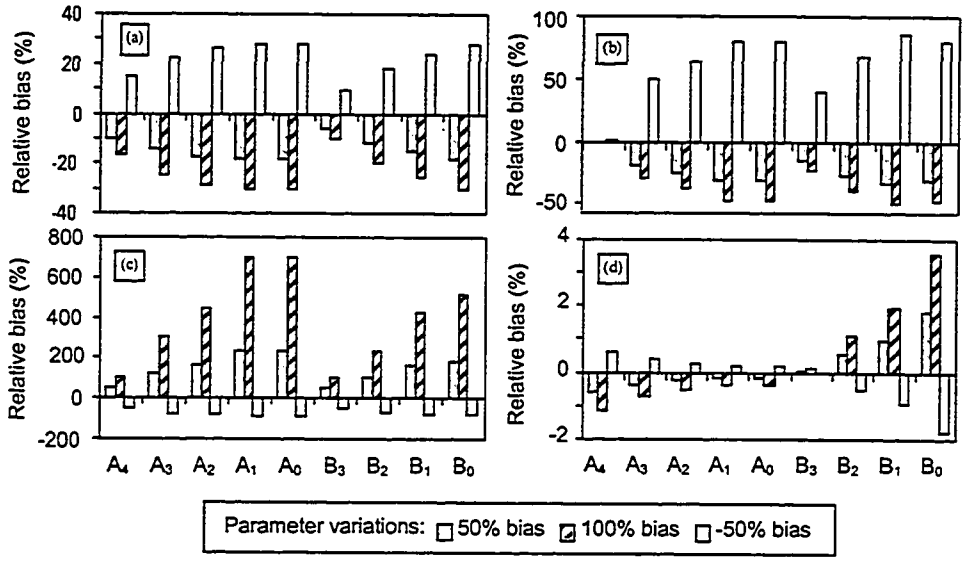

Figure 3.16: Influence of variations in uncertain vehicle parameters on the relative bias of the transfer function coefficients: (a) I_{zt}; (b) I_{zs}; (c) C_α; (d) C_m

The coefficients of the analytical transfer function $G(s)$, described in Equation (3.17), of the vehicle model considered in the study, are derived using a set of nominal parameters and u_1=80 km/h. The resulting coefficients of the transfer function are obtained as: A_4=54, A_3=653, A_2=5140, A_1=17080, A_0=27315, B_3=15.3, B_2=108.7, B_1=332.2, B_0=402.7.

The handling and directional dynamics of heavy vehicles are frequently evaluated under ramp step (RS) and trapezoidal steering inputs illustrated in Figure 3.17. In a ramp

step steer, the front wheel steer angle is initially increased at a constant rate until it approaches the desired value. The steer angle is then held constant. The trapezoidal input is similar to the ramp step input, except that the front wheel steer angle after certain period is reduced to zero value at a constant rate [148]. Although the steering inputs can be conveniently generated by the driver, the selection of these signals involves two primary considerations: (i) the essential modes associated with the lateral dynamics must be stimulated by the selected input signal; and (ii) the magnitude and shape must be carefully selected to ensure the stable operation of the vehicle. In this study, the RS and trapezoidal steering inputs, referred to as a quasi-impulse (QI), are generated to analyze the vehicle model and to perform the system identification. A pseudo-random binary sequence (PRBS) input is also proposed to ensure stimulation of all the important modes, as shown in Figure 3.17. The PRBS input is used to excite all the important modes in order to identify the system behaviour effectively. In this study, the magnitudes of RS and QI are selected as 2.3 degrees, while the amplitude of the PRBS input is limited to 1.0 degree.

Equation (3.17) is solved to derive the lateral acceleration response of the tractor c.g. under the three steering inputs. Although the system identification techniques are best applied on the available field measured data, the analytical response of the vehicle can serve as the undisturbed data for examining the effectiveness of the technique. Since the field measured data, invariably, comprises certain signal noise, a white noise signal (signal to noise ratio, SNR=20dB), $e(t)$, is superimposed to the undisturbed output. The resulting disturbed response, $y(t)$, is then taken to represent the field measured data under different steering inputs. Figure 3.18 illustrates the comparison of disturbed and

undisturbed lateral acceleration response of the tractor unit under RS, QI, and PRBS steering inputs.

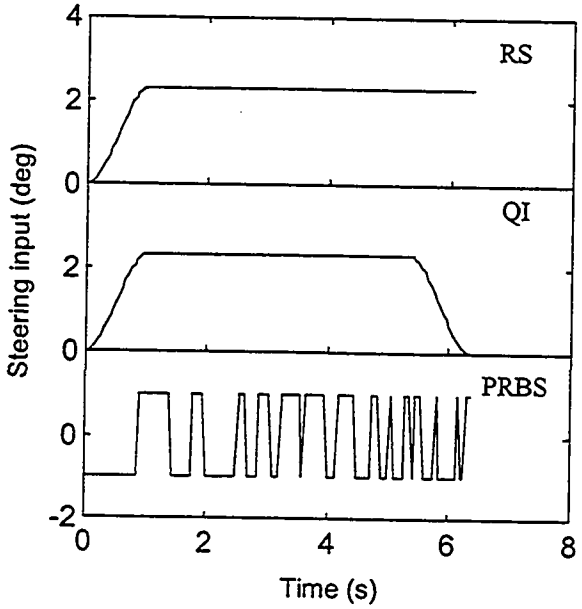

Figure 3.17: Steering input signals used for system identification.

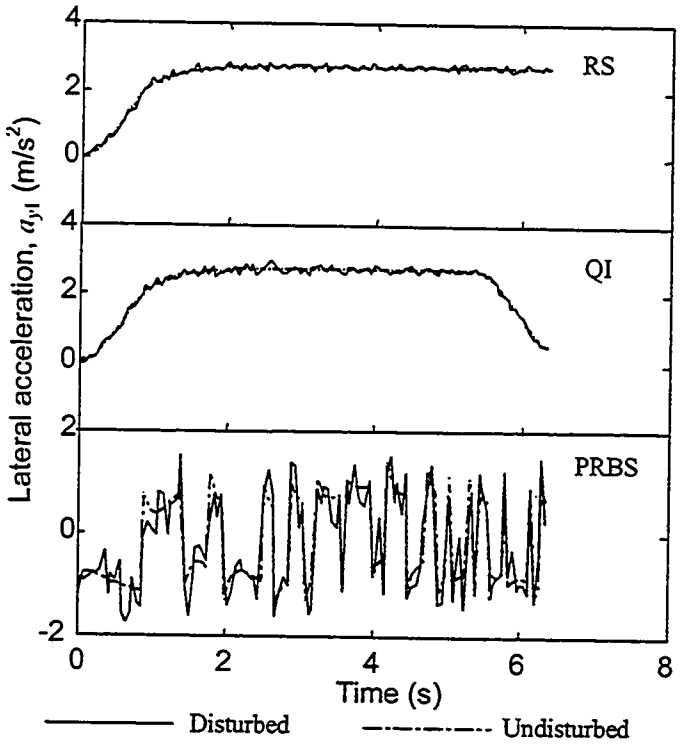

Figure 3.18: Comparison of disturbed and undisturbed lateral acceleration response of the tractor c.g. under different inputs.

The system identification problem, Equations (3.14) and (3.15), are solved using the above input data in conjunction with varying levels of SNR, in order to select an optimal order of the model. The minimization problem is solved for different orders of the model, ranging from 2 to 5, and an optimal order is derived corresponding to minimal value of loss function J and *FPE*, assuming k_d=0.

The results derived for different orders of the model and SNR are summarized in Table 3.5. The results clearly illustrate that the optimal order of the system model is 4, irrespective of the SNR and the steer input. The results further show that an increase in the measurement noises level yields higher values of loss function and *FPE*. While RS and QI inputs yield comparable values of the loss function, the proposed PRBS input yields the lowest values of the loss function and thus the *FPE*. It can be further observed that the system identification may converge to a lower order model under high levels of measurement noise, which may be attributed to significant excitation of the dominant modes. The results also show that an increase in the model order to 5 yields higher values of loss function and the *FPE*.

Table 3.5: Values of loss function and *FPE* (k_d=0) as a function of order of the model.

Function	$u(t)$	SNR (dB)	Order of model			
			2	3	4	5
J	RS	∝	0.2258	0.2199	2.0354E-11	9.8502E-10
		20	0.2264	0.2199	4.1213E-4	9.7024E-4
		10	0.4640	0.5446	0.4334	0.6883
	QI	∝	0.2190	0.2213	1.3495E-17	1.4072E-4
		20	0.2195	0.2221	5.9989E-4	4.8762E-3
		10	0.4282	0.4137	0.4007	0.5599
	PRBS	∝	8.8559E-4	3.7216E-5	2.7415E-26	4.353E-5
		20	0.0011	5.7081E-4	3.7822E-4	4.4439E-4
		10	0.1757	0.1612	0.1390	0.1698
FPE	PRBS	∝	9.5759E-4	4.1522E-5	3.1561E-26	5.1715E-5
		20	0.0012	6.3685E-4	4.3543E-4	5.2795E-4
		10	0.1899	0.1799	0.1600	0.1903

The influence of the time lag on the loss function is further investigated, while the model order is considered as the optimal one (n_f= n_b=4). The resulting values of the loss function derived under the PRBS input are summarized in Table 3.6, as a function of the SNR, and the time lag. The loss function tends to increase considerably, when time lag is incorporated. An increase in the time lag, however, yields only slightly change in the loss function. The results clearly show that the present application is a zero lag system, which is mostly attributed to the assumption associated with negligible hysteresis.

Table 3.6: Determination of model structure for PRBS input.

SNR (dB)	k_d =0	k_d =1	k_d =2	k_d =3
	Values of loss function (n_b=4, n_f=4)			
∝	2.7415E-26	2.3591	2.7354	2.9415
20	3.7822E-4	2.2737	2.6192	2.7673
10	0.1390	2.4261	2.8234	2.6163

The coefficients of the system function are further derived under different steering inputs and SNR values, while the model order is considered as 4. The resulting values of the coefficients are compared to demonstrate the effectiveness of the identification technique. The estimated coefficients under RS, QI and PRBS inputs are summarized in Table 3.7 for different values of SNR. A comparison with the true values of the coefficients, derived from the analytical transfer function, reveals reasonably accurate estimation of the coefficients when SNR is limited to 20dB. The table also summarizes the bias of the estimated coefficients relative to the true values. The results show that under SNR=20dB, the peak bias resulting from PRBS, QI and RS inputs are 1.07%, 1.66% and 2.56%, respectively. The higher order coefficients (B_2, B_3 and A_4) yield increased estimation errors. The PRBS input tends to yield the lowest estimation error.

Table 3.7: System function coefficients for different values of SNR and input signals.

Estimated Parameters		True values	SNR=20 dB				SNR=10dB			
			PRBS	QI	RS	Peak	PRBS	QI	RS	Peak
	Value	**54.3044**	54.8836	54.7714	54.9016	**Bias%**	55.5639	48.3757	56.0515	**Bias%**
A_4	Bias%		1.06654	8.60e-1	**1.0997**	**1.0997**	2.31943	**-1.1e+1**	3.21727	**-1.1e+1**
	Value	**653.400**	653.395	653.160	654.633		655.883	650.046	639.400	
A_3	Bias%		-6.4e-4	-3.7e-2	**1.888e-1**	**1.888e-1**	3.80e-1	-5.13e-1	**-2.1426**	**-2.1426**
	Value	**5140.59**	5140.31	5138.82	5141.02		5146.46	5136.26	5136.20	
A_2	Bias%		-5.4e-3	**-3.5e-2**	8.42e-3	**-3.5e-2**	**1.14e-1**	-8.43e-2	-8.53e-2	**1.14e-1**
	Value	**17080.3**	17081.0	17079.7	17080.0		17079.2	17076.3	17073.0	
A_1	Bias%		**4.04e-3**	-3.4e-3	-1.74e-3	**4.04e-3**	-6.40e-3	-2.38e-2	**-4.27e-2**	**-4.27-2**
	Value	**27315.7**	27315.8	27315.8	27315.8		27313.3	27318.1	27327.9	
A_0	Bias%		3.45e-4	2.90e-4	**3.92e-4**	**3.92e-4**	-8.9e-3	8.79e-3	**4.46e-2**	**4.46e-2**
	Value	**15.3416**	15.2413	15.1210	15.7346		12.7790	21.2878	27.3946	
B_3	Bias%		-6.5e-1	-1.43789	**2.56147**	**2.56147**	-1.67e+1	3.88e+1	**7.85e+1**	**7.85e+1**
	Value	**108.683**	108.684	110.486	108.682		110.489	107.867	110.351	
B_2	Bias%		8.62e-4	**1.65883**	-1.20e-3	**1.65883**	**1.66173**	-7.51e-1	1.53515	**1.66173**
	Value	**332.243**	332.349	332.717	332.377		319.575	334.335	340.397	
B_1	Bias%		3.20e-2	**1.43e-1**	4.03e-2	**1.43e-1**	**-3.813**	6.30e-1	2.45408	**-3.813**
	Value	**402.731**	402.621	403.785	400.714		414.054	420.063	404.297	
B_0	Bias%		-2.7e-2	2.62e-1	**-5.01e-1**	**-5.01e-1**	2.81165	**4.3037**	3.889e-1	**4.3037**
Peak Bias%			1.06654	1.65883	2.56147	**2.56147**	-1.67e+1	3.88e+1	**7.85e+1**	**7.85e+1**

The estimation errors, however, increase many folds, when the measurement noise level is increased (SNR=10dB). The peak biases are obtained as 16.7%, 38.8% and 78.5%, respectively, under PRBS, QI and RS steering inputs. The large estimation errors, however, continue to be associated with higher order coefficients (B_3 and A_4). Furthermore, the proposed PRBS input yields the lowest estimation error. From the results, it is evident that the system identification technique yields nearly consistent values of the coefficients, irrespective of the steering inputs, when the SNR is limited to 20 dB. Although an increase in the measurement noise yields poor estimation of the higher order coefficients, the peak error associated with lower order coefficients remains 4.30%. The

PRBS input yields reasonable estimation of all the coefficients, with the exception of B_3, within an error of 3.8%. This error is attributed to relatively low values of SNR at higher frequency modes.

The system identification technique is further applied to derive an estimate of uncertain vehicle parameters, such as moment of inertia (I_{zt}, I_{zs}), cornering stiffness (C_α) and aligning moment coefficients (C_m) of tires. It has already been established that the lateral dynamics of the vehicle is strongly dependent upon the accuracy of these parameters. The results of the system identification, described in the previous section, clearly show that a reasonably accurate estimate of system function coefficients can be achieved, provided a suitable input signal is adopted with reasonable levels of measurement noise. Since the function coefficients are related to the vehicle parameters, simultaneous solution of the coefficient equations can yield an estimation of the uncertain parameters. The coefficients of the system function of an articulated heavy vehicle, however, are quite complex functions of the weights, dimensions, inertia and tire parameters. The estimation of parameters thus poses many computational complexities. Alternatively, system identification approach can be applied to achieve the parameter estimates, by minimizing the error between the coefficients of the identified and analytical function. An error minimization problem is thus formulated as:

$$\varepsilon_p = \sum_{i=0}^{n_h} \left(\frac{A_i' - A_i}{A_i} \right)^2 + \sum_{j=0}^{n_f - 1} \left(\frac{B_j' - B_j}{B_j} \right)^2 \tag{3.18}$$

where ε_p is the error sum square. A_i, B_j and A_i', B_j' are the coefficients of the analytical and identified transfer functions. The minimization problem is solved using the algorithm illustrated in Figure 3.19. The algorithm considers an initial estimate of the uncertain set

of parameters to derive the coefficients A_i, B_j from the analytical transfer function. The system identification problem is then solved using field measured data and the corresponding steer input to obtain an estimate of the system function and thus the coefficients A_i', B_j'. The error minimization problem, expressed in Equation (3.18), is then solved until convergence is achieved.

The robustness of the proposed estimation algorithm is investigated by selecting the starting values of parameters with relatively high degree of bias with reference to the nominal parameters considered in Table 3.1. The minimization problem is solved using initial bias of 10%, 45% and 80% in I_{zl}, I_{zs}, C_α, and C_m, PRBS steer input, and SNR of 20dB. The accuracy of the resulting estimates of the parameters is computed in terms of bias relative to the nominal parameters, as shown in Figure 3.20. The results clearly show that the estimated parameters converge to the same values, irrespective of the bias in the starting values, which demonstrates high robustness of the proposed algorithm.

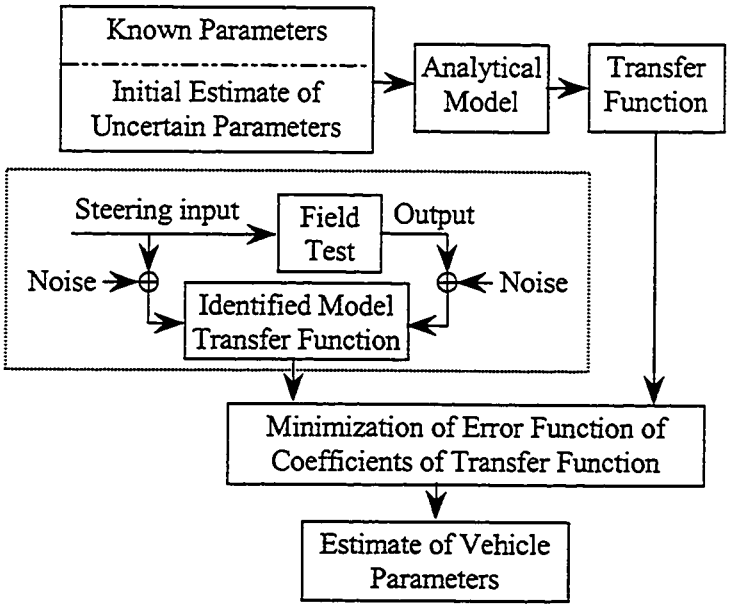

Figure 3.19: Algorithm for identification of vehicle parameters.

It can be further observed that the magnitudes of relative bias associated with the four estimated parameters are quite different, while the lowest bias appears to be for the cornering stiffness of the tires and the highest one occurs for the aligning moment coefficient of the tires. This observation conforms to the results presented in Figure 3.15, which illustrated that the lateral dynamics of vehicle is relatively less sensitive to the aligning moment properties and most sensitive to the cornering stiffness.

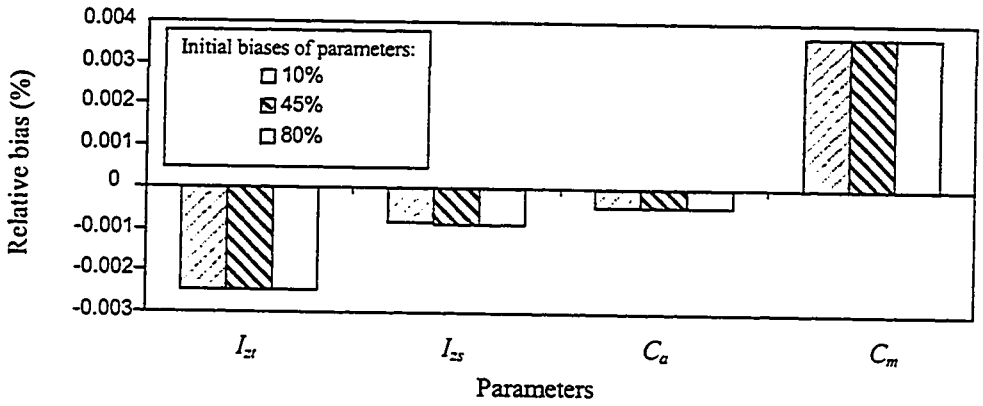

Figure 3.20: Relative bias in estimated parameters using different steering values.

The effectiveness of the parameter estimation technique is further investigated for different steering inputs, SNR of 20dB, and different starting values of the uncertain parameters. Figure 3.21 illustrates a comparison of the relative bias of the parameters estimated under different steering inputs, while the starting values are chosen with a bias of 45%. The results show high estimation error for the aligning moment coefficient and lowest estimation error in the cornering stiffness, irrespective of the steer input. This observation further verifies that the most sensitive parameter yields the least estimation error, while the least sensitive parameter generates the greatest estimation error. While the ramp step steer input yields highest error in all the parameters, the PRBS input provides the most accurate estimation of the uncertain parameters. The estimation errors

are well below 10% for all the parameters, when PRBS input is employed. The estimation error may be further reduced by increasing the SNR.

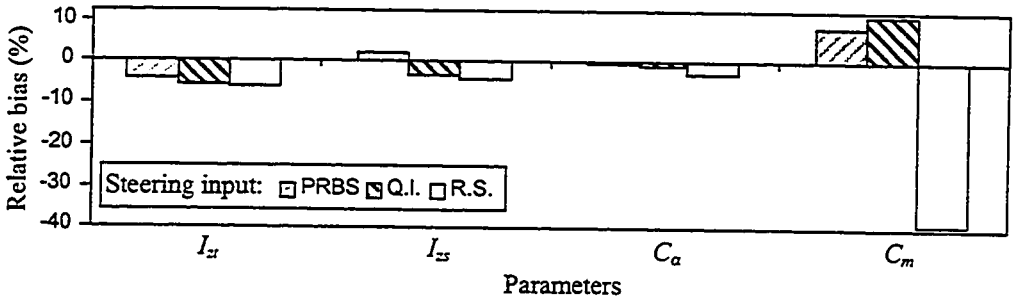

Figure 3.21: Comparison of estimation errors in system parameters under different steering inputs.

3.5 PARAMETER ESTIMATION USING VEHICLE RESPONSE DATA

The robustness of the system identification algorithm for estimating the stated uncertain parameters is further examined using the vehicle response data generated using the comprehensive YAW/ROLL model [95]. The YAW/ROLL vehicle model is analyzed using nonlinear cornering force and aligning moment characteristics, illustrated in Figure 2.1, and two different steer inputs: Trapezoidal (QI); and ramp-step (RS). The tire properties are incorporated in the model through a look-up table as a function of the vertical load and side-slip angle, while the suspension forces are also included as a nonlinear function of the relative deflection across the different springs. The system identification technique is applied based upon the lateral acceleration response characteristics derived from the YAW/ROLL model subject to RS and QI steering inputs, while the signal to noise ratio is taken as 20 dB. Equation (3.14) is solved to determine the order of the system function. The loss function summarized in Table 3.8, appear to be minimum when the order is selected as 4 or 5. It should be noted that the identification based upon data simulated using the yaw plane model revealed minimum loss function

corresponding to a system order of 4 (Table 3.6). The results presented in Table 3.8 reveal the possibility of a slightly higher order system, which may be attributed to the contribution due to roll dynamics of the vehicle. The minimum values of the loss function, however, are obtained for the 4th order system function, indicating only minimal contributions of the roll dynamics.

Table 3.8: Values of loss function J (k_d=0) (SNR=20dB, YAW/ROLL Model).

	$u(t)$	Order of model			
		2	3	4	5
J	RS	0.2513	0.2402	**7.0852E-4**	7.4135E-4
	QI	0.2487	0.2398	**7.0214E-4**	7.3921E-4

The vehicle parameters (I_{zt}, I_{zs}, C_α, and C_m) are estimated from the system function identified using the data derived from the YAW/ROLL model with SNR=20dB. The estimated parameters are compared with those obtained earlier based upon the yaw plane dynamics, as shown in Figure 3.22. For the sake of clarity, the values of I_{zt} and C_m are multiplied by 10. The results clearly show that estimations based upon the nonlinear simulation data are quite close to those derived from the linear yaw plane data. The estimations based upon the yaw plane and YAW/ROLL model data yield –5.99% and 6.99% error in I_{zt} under QI input, and –6.7% and 8.42% under RS input, respectively. The corresponding errors in I_{zs} are -3.50%, -3.81% for QI input, and -5.0% and 5.13% for the RS input, respectively. The estimated values of cornering stiffness of the tires correspond well with the linear cornering stiffness (side slip angle $\leq 4°$) corresponding to the median load of 26.698 kN. The estimation based upon the YAW/ROLL model data resulted in errors of 3.29% and 6.70% for QI and RS steering inputs, respectively. The corresponding errors based upon the yaw plane dynamics alone are obtained as –1.0%

and –4.0%. Both the models also yield comparable magnitudes of the error in C_m, and the errors under the RS input tend to be considerably high (-40% to 45%) irrespective of the data used for the identification purposes. It should, however, be noted that the aligning moment of tires is generally low and its contributions to lateral and yaw dynamics are relatively small. The results further show that the directional behaviour of the articulated vehicle is strongly related to the yaw plane dynamics, while the contributions due to roll dynamics are relatively negligible.

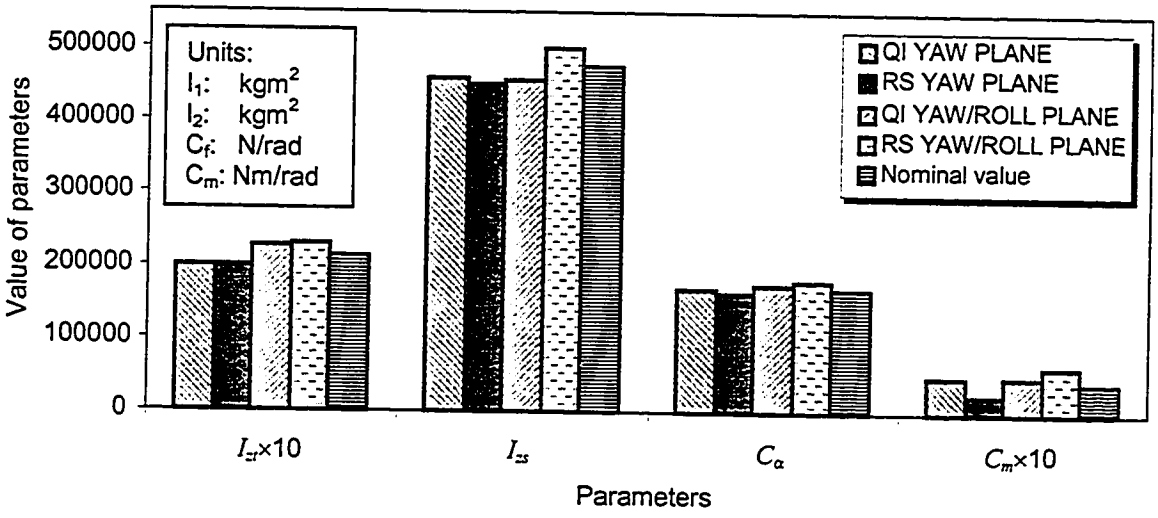

Figure 3.22: Comparison of the estimated parameters using YAW plane and YAW/ROLL models.

3.6 SUMMARY

In this Chapter, the parameter sensitivity analyses are performed to identify the vehicle parameters that affect the directional performance of the vehicle in most significant manner. Limiting values of various geometric, and static and dynamic parameters are identified in view of directional stability of the vehicle. The analysis of vehicle response to variations in geometry parameters revealed that the c.g. heights of the tractor and trailer units (h_{g1} and h_{g2}) are most significant, while the parameters describing

the horizontal distances between tractor front axle and its c.g. and between trailer axle and its c.g. (x_{11} and x_{21}) are relatively less significant. The analysis of vehicle response to variations in dynamic parameters further revealed that the inertial parameters of tractor, suspension properties of the trailer are more sensitive to the dynamic response of the combination than those of the trailer and those of the tractor, respectively. The tire properties and the fifth wheel yaw damping, in general, strongly affects the dynamic response of the trailer and the tractor, respectively. The roll stiffness of the fifth wheel mostly influences the lateral acceleration of trailer, the yaw rate and roll angle response of the tractor.

A system identification technique is further applied to determine the lateral dynamics of an articulated freight vehicle and to extract an estimate of significant vehicle parameters considered to be uncertain. It is concluded that the vehicle transfer function can be accurately characterized under PRBS and QI excitations, and SNR values superior to 20 dB. The proposed algorithm can provide the most effective estimates of the parameters to which lateral dynamics is most sensitive.

CHAPTER 4 CLOSED-LOOP DIRECTIONAL DYNAMICS OF HEAVY VEHICLES

4.1 INTRODUCTION

The results presented in Chapter 3 describe the performance limits of vehicles based upon their open-loop dynamics. The enhancement of highway safety associated with commercial vehicles, however, involves not only the study of handling and stability performance of the vehicle but also the driver-vehicle interactions. Many studies have established that the directional stability properties of a vehicle cannot be fully evaluated through measurement or analysis of the vehicle dynamics alone [21, 22, 140]. An analysis of the reported highway accidents involving articulated freight vehicles revealed that human factors form the primary causal factor and account for nearly 85% of the total accidents [13]. A study of driver-vehicle interactions is thus extremely vital to enhance an understanding of the driver's contributions to the performance of the vehicle system. Such study, however, necessitates the directional analysis of the closed-loop driver-vehicle system. While the directional stability dynamics of articulated vehicles have been extensively investigated assuming negligible contributions of the driver, only few studies have analyzed the closed-loop driver-articulated vehicle system [30, 137].

A number of driver models based upon preview and compensatory tracking, however, have been proposed for directional dynamics of single unit vehicles [131, 135, 137, 149]. Majority of these analytical studies, are conducted based upon the assumption that the driver always tries to minimize the lateral position and/or orientation tracking errors, and is constrained by the driver's physical limitations.

The safety performance of a road vehicle may be related to its ability to follow the desired trajectory, which is a complex function of the driver's behavior and the directional dynamics of the vehicle. The definition of the desired trajectory for an articulated vehicle, however, is quite complex unlike the case of a single vehicle, where the driver exhibits superior ability to predict the vehicle path. The driver's ability to predict the path of the trailer units in an articulated vehicle combination is most likely considerably lower. Under extreme dynamic maneuvers, the articulated vehicle may exhibit two forms of instabilities leading to jackknife and lateral oscillations of the trailer, which are partly attributed to the poor driver's perception of the trailer motion. The assessment of safety characteristics of such vehicles thus involves an understanding of the driver's control actions coupled with the directional dynamics of the vehicle, such that vehicle characteristics with enhanced safety and path following abilities can be identified.

While the studies on directional dynamics of heavy vehicles have evolved into a set of performance measures related to highway safety [2-4], the studies on driver's contributions have been limited, which is most likely attributed to lack of an effective driver-vehicle system model and characterization of the driver's behavior. The realization of an effective closed-loop system model involves integration of appropriate driver and vehicle models with lateral path control considerations, such as: path prediction abilities of the driver; reduction of path errors to an acceptable threshold level in a stable, well damped and rapid manner; and robust disturbance rejection while minimizing the driver's efforts. In this Chapter, the modeling considerations to study the driver's interaction with the vehicle are briefly reviewed. The single- and multi-loop structures of closed-loop

driver/articulated vehicle systems are systematically formulated and analyzed to study the influence of various prediction and feedback variables on the defined performance index.

4.2 MODELING CONSIDERATIONS FOR DRIVER'S INTERACTIONS

It has been established [149] that the directional control performance of a closed-loop driver/vehicle system depends directly upon the interactions between the driver and the vehicle under the input of the previewed path. During the directional control process, the driver acts as a sensor and the controller. The primary task associated with modeling of the closed-loop system involves the determination of the model structure and its parameters, such that the model can be considered representative of a real driver-vehicle system. The model structure, in general, is related to the feedback information of the driver, which is often quite complex to characterize. For a tractor-semitrailer vehicle driver, the possible motion feedback variables could include the path and orientation errors of the lead unit, and the lateral accelerations, yaw rates, roll angles and roll rates of both the units. These variables may be perceived by the driver directly and indirectly in formulating its directional control strategy. Based upon the dynamics of single unit trucks and cars, it has been reported that the path and orientation errors of the lead unit, and the lateral acceleration of the unit can serve as the primary feedback variables [14, 124]. For a tractor-semitrailer combination, the motion states of the trailer may further affect the directional control behaviour of the driver in a complex manner. A systematic study of the structure of driver-vehicle model should thus be performed to identify the significance of various feedback variables that the driver may perceive and utilize for the

control tasks. The outcome of the study may be further applied to design a vehicle that can be adapted to different drivers with varying skills.

The structure of driver/vehicle system model is related to the sensory feedback information used by the driver. Under various driving situations, the driver may use different motion variables of the vehicle as the sensory feedback to perform the path-tracking tasks. Different drivers may exhibit varying driving behaviour, such that the feedback sensors employed may differ considerably even under same driving conditions. The modeling approach for the driver directional control behaviour, therefore, should address the most common behaviour of the drivers. Although the mathematical treatment of the vehicle driver is quite complex, the control abilities of the driver to satisfy key guidance and control requirements for the vehicle system may be analyzed using certain sensory feedback variables. As stated earlier in Chapter 1, the guidance and control requirements for lateral path control can be summarized below:

- To select appropriate pathways and tolerances;
- To establish and maintain the vehicle on the specified pathway;
- To reduce path errors to threshold levels in a stable, well damped, and rapidly responding manner to ensure the safety of the vehicle;
- To maintain the established path in the presence of disturbances such as crosswinds, roadway fluctuations, and vehicle-centered disturbances.

These requirements primarily relate to the desired pathway decisions and to the relatively low-frequency directional modes of the driver-vehicle system. These requirements can further define the control loops that involve the feedback of vehicle motion quantities to attain the desired equilibrium state of motion. These feedback loops formed by the driver represent the perception and manipulation abilities of the driver. In

general, the motion cues to the driver are related to vehicle motion relative to the surroundings, and the driver's proprioceptive outputs, which can be visual, vestibular, kinesthetic, or auditory. Of these, the visual feedback is considered as the central and dominant, which must be sufficient to satisfy the guidance and control needs in the presence of possibly conflicting cues, such as lateral acceleration [25]. A wide range of possibilities for visual cues have been identified by considering guidance and control requirements, driver-centered requirements, availability of the cues in the visual field, and interpretations of such experimental evidences as driver eye movements [33]. The outer loop of the model structure is invariably based upon lateral position, which is vital to satisfy the basic guidance and control requirements for precision path following. While this feedback creates a path mode, it does not provide the path damping needed for a stable, well-behaved, closed-loop system. The path damping, in general, is achieved by the driver by generating low frequency lead on lateral position, or through the inner control loops based upon other feedback cues, such as path orientation angle, yaw rate, and lateral acceleration.

Widely used driver-vehicle system models involve three function blocks: (*i*) preview; (*ii*) prediction; and (*iii*) compensation, $H_d(s)$, as illustrated in Figure 4.1. The preview function is highly dependent upon the driver's visual cues and path decision process, where the preview time is the key parameter that affects the driver's steering strategy and thus the closed-loop driver-vehicle system performance. Extensive experimental studies on single unit vehicle have established that the driver's preview time varies between 0.5 and 9.0 s, depending upon the vehicle speed, maneuver severity, and driver's experience and habits [140, 142]. The prediction block reflects the driver's

biological activity in assessing and predicting the instantaneous vehicle motions, such as lateral position, orientation, and lateral acceleration. The prediction ability of the driver is a complex function of the driver's experience, skill and the vehicle dynamics. The third block, compensatory function, depends upon the driver's physical and biological conditions. The driver's reaction time and neuromuscular delay reflect the driver's physical limitations due to driver's brain and limb muscle, which are reported within the range of 0.1-0.5s [19]. The biological factors of the compensatory function are simply referred to as the compensatory gain and equalization function. The gain and equalization function differ widely from one task to another and may vary substantially with time due to the driver's experience accumulation and adaptation to the vehicle system. Many studies on single unit vehicles have reported the values of the compensatory gain, equalization lead and lag time constants, vary from 0.001 to 0.12rad/m, 0.01 to 5.0s and 0.01 to 20.0s, respectively [19, 131].

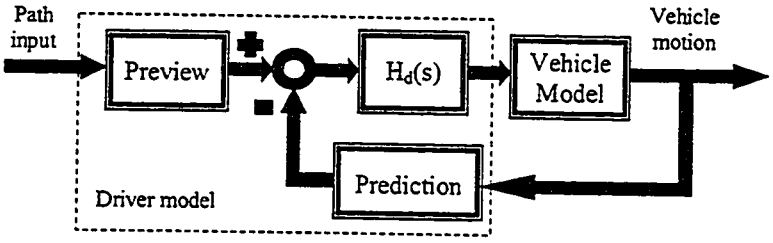

Figure 4.1: Single-loop structure of a driver/vehicle system.

The structure of the closed-loop driver-vehicle model may be derived using two general approaches: (*i*) experimental perceptual studies; and (*ii*) theoretical investigations. The experimental studies, usually performed in a driving simulator by constraining some channels of perceptions, can effectively identify most significant motion sensors under different constraints. Alternatively, the theoretical approach tends

to identify the vehicle motions that must be sensed, and commands required to achieve satisfactory path tracking. This modeling approach, however, does not lead to a unique solution. Further considerations thus must be given to the driver's ability to perceive or sense, the vehicle motion and input quantities, and to the nature of the operations required on the sensed quantities in closing the driver/vehicle system loop. Furthermore, the influence of the preview and prediction on the driver-articulated vehicle system performance can be studied using theoretical approach based upon a single loop structure. Under path tracking and evasive maneuvers, however, the driver control actions do not rely upon single feedback variable.

A heavy vehicle driver, with higher skill level and experience, specifically relies upon various motion cues arising from the dynamic response of the vehicle combination. Such motion cues may arise from the yaw rates, lateral accelerations and roll angles of the vehicle units. The significance of such motion cues, however, requires study of driver-vehicle models based upon multi-loop structure. From the results of single- and multi-loop structure, one can derive essential preview and prediction, and compensation blocks to formulate a comprehensive driver-vehicle model. It should be noted that the model structure is primarily derived to meet certain performance criterion for the closed-loop driver-vehicle system. It is thus vital to formulate a performance index in view of performance characteristics of an articulated vehicle, which differ considerably from that of a single unit vehicle.

4.3 PERFORMANCE INDEX

The directional control performance of a closed-loop driver-vehicle system strongly relies upon the nature of different perceived vehicle response variables. A systematic analysis of contributions of different motion variables necessitates the definition of a uniform performance index, which closely describes the safety performance of the vehicle, vehicle path and the driver's efforts. The methodology used for the study of the model structure in this Chapter is based upon the optimal control behaviour of the driver. It is assumed that the driver performs the directional control by minimizing the defined performance index, which may include the path and orientation errors of the tractor, steering wheel rate, and the lateral accelerations, yaw rates and roll angles of both the units. The demands posed on the driver effort and performance requirements for the driver are investigated by minimizing a weighted performance index comprising tracking error, lateral acceleration, yaw rate and roll angle response of the vehicle. The resulting model structure then represents a compromise among the performance variables within the constraints imposed by the driver's abilities.

The directional performance of an articulated vehicle is related to various safety measures, as discussed in Section 3.2. These include lateral accelerations (a_{y1} and a_{y2}), yaw rates (r_1 and r_2) and roll angles (ϕ_1 and ϕ_2) of the two units of the combination. The path errors in terms of lateral position and orientation errors must be further incorporated within the performance index to study the safety dynamics of the coupled driver-vehicle system. The overall vehicle performance, however, must be evaluated in appropriate consideration of the rate of steering effort required to achieve the desired performance. A

composite performance index is thus formulated upon integrating the weighted mean square values of the individual variables, in the following manner:

$$J = J_{y1} + J_{\psi 1} + J_{ay1} + J_{ay2} + J_{\phi 1} + J_{\phi 2} + J_{r1} + J_{r2} + J_{\dot{\delta}} \tag{4.1}$$

where J is the composite performance index. J_{y1} and $J_{\psi 1}$ are the weighted mean square values (WMSV) of lateral displacement and orientation errors, respectively, between the previewed path and the actual path followed by the c.g. of the tractor, given by:

$$J_{y1} = \frac{1}{T}\int_0^T \left[\frac{y_1(t) - f(t)}{\Delta y_{th}}\right]^2 dt \; ; \; J_{\psi 1} = \frac{1}{T}\int_0^T \left[\frac{\dot{y}_1(t) - \dot{f}(t)}{\Delta \psi_{th} \times u_1}\right]^2 dt \tag{4.2}$$

where $f(t)$ and $y_1(t)$ are the lateral coordinates of the previewed path and path followed by the tractor c.g., and $\dot{f}(t)$ and $\dot{y}_1(t)$ are the time derivatives of the path coordinates. Δy_{th} and $\Delta \psi_{th}$ define the threshold values of the lateral position and orientation errors between the previewed and resulting paths, respectively. In Equation (4.1), J_{ay1}, J_{ay2}, J_{r1}, J_{r2}, $J_{\phi 1}$ and $J_{\phi 2}$ are the weighted mean squared values of lateral accelerations (a_{y1} and a_{y2}), yaw rates (r_1 and r_2) and roll angle (ϕ_1 and ϕ_2) response of the two units, as described earlier in Equation (3.2). The term $J_{\dot{\delta}}$ describes the rate of steering wheel, $\dot{\delta}_{sw}$, and thus the required driver effort, and $\dot{\delta}_{th}$ is the corresponding threshold value. The performance measure $J_{\dot{\delta}}$ is computed from

$$J_{\dot{\delta}} = \frac{1}{T}\int_0^T \left[\frac{\dot{\delta}_{sw}}{\dot{\delta}_{th}}\right]^2 dt \tag{4.3}$$

where T is the simulation time. The threshold values of various performance variables are selected as Δy_{th}=0.5m, $\Delta \psi_{th}$=10 degrees, w_{ay} =0.3g, w_{ϕ}=15 degrees, w_r=10 degrees/s, and $\dot{\delta}_{th}$=360 degrees/s.

4.4 DRIVER MODELS BASED UPON SINGLE LOOP STRUCTURES

Although the driver's perception of the vehicle response may be conveniently represented by an appropriate sensor, the analysis of driver's control behaviour necessitates formulation of a control loop and its structure. In case of an articulated vehicle, the driver may perceive different motion variables arising from both the lead and trailing units in a qualitative manner. The control strategy of the driver and thus the performance characteristics of the vehicle system is strongly dependent upon the nature of perceived motion variables. The influence of different motion variables on the control performance of the driver-vehicle system can be perhaps best investigated using a single-loop structure, illustrated earlier in Figure 4.1. In this section, the contribution due to different motion variables are evaluated using the performance index defined in Equations (4.1) to (4.3) in conjunction with the yaw plane model with roll-DOF of a five-axle tractor-semitrailer combination, as described in Section 2.2.2. For the purpose of comparisons, the coordinates and orientation of a previewed path corresponding to an obstacle avoidance maneuver, performed at a speed of 80km/h, are selected as shown in Figure 4.2.

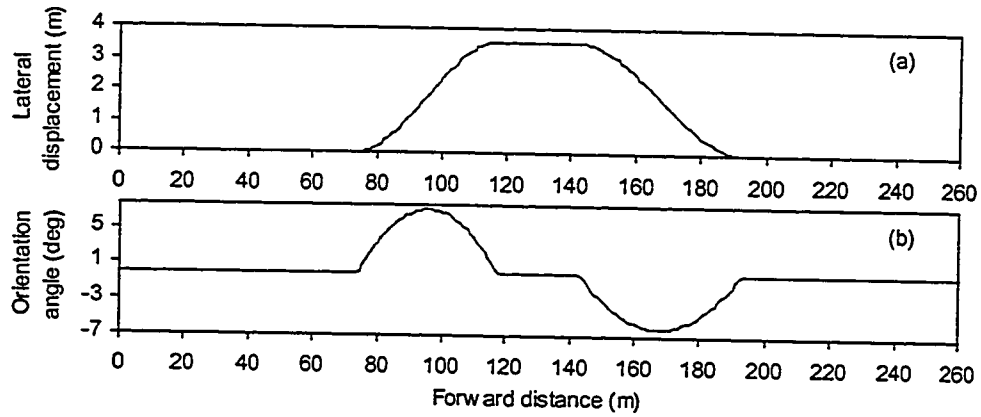

Figure 4.2: Path coordinates and orientation of the selected obstacle avoidance maneuver.

The driver is assumed to adopt a single point preview strategy to perform the path tracking task. The driver's control strategy is described by a describing function, $H_d(s)$, in the following manner [26]:

$$H_d(s) = K_d \frac{T_L s + 1}{T_I s + 1} e^{-(\tau + T_N)s} \tag{4.4}$$

where K_d is referred to as the control gain and $\frac{T_L s + 1}{T_I s + 1}$ is a simplified equalization characteristic function of driver's lag (T_I) and lead (T_L) time constants. τ is the driver's reaction delay and T_N is the neuromuscular time constant. The values of driver's reaction time τ and neuromuscular time constant T_N are identified from the reported data established from a wide range of experimental studies based upon field and driving simulator tests. The values reported in the published studies, however, vary considerably due to significant variations in the test conditions, test and analysis methods, and driver's skills. While a complete review of the published data is presented in Section 5.4 to identify the performance limits of the drivers, for the present analysis, these values are selected as τ=0.15s and T_N =0.1s. The lag and lead time constants (T_I and T_L), and control gain K_d, are derived upon minimizing the performance index J.

In the single loop model structure of the driver-vehicle system, shown in Figure 4.1, the path input is described by the coordinates of the lateral position and/or orientation of the path. The vehicle motion variables serve as the feedback to the driver, which may include: lateral positions of the c.g. of the sprung masses of lead unit and/or the trailing unit, and the yaw angle response of the lead and/or trailing units. The selection of the feedback variable from the vehicle response reflects the driver's preview strategy and prediction ability. The vehicle motion variables thus require appropriate considerations of

the prediction abilities of the driver, which is represented by a prediction function. The path preview ability of the driver is mostly described by a preview function. Assuming a single-point path preview, the preview function of the form $e^{T_p s}$ is widely used [110, 148, 149]. Although a wide range of driver's preview intervals T_p have been reported in the literature, as discussed later in Chapter 5, a value of 1.5s is considered in this relative analysis of various motion variables.

The primary considerations and assumptions associated with study of the driver's directional control behaviour include the following:

- The previewed path is expressed by a low-order polynomial function, since it primarily includes low frequency components;
- The vehicle path is previewed with respect to the body fixed coordinate system of the lead unit;
- The driver's control actions are always directed towards minimizing the performance index described in Equation (4.1).

The proposed single loop structures of driver-vehicle system are analyzed using four different preview and feedback strategies. These strategies are primarily based upon lateral position and orientations of the lead and trailing units, and include preview and feedback motion based upon: lateral position of c.g. of the lead unit (SLM1); orientation of the lead unit (SLM2); lateral position of c.g. of the trailing unit (SLM3); and orientation of the trailing unit (SLM4). The formulation of the prediction function for the single loop structures based upon above strategies are described as follows:

SLM1:

The drivers exhibit superior abilities to perceive the error between the lateral position of a reference point of the vehicle and a point on the previewed path. The

majority of the reported driver models are thus based upon the lateral position error [123, 131, 137, 149]. The path prediction based upon this error can be conveniently applied for articulated vehicles, since it does not require the driver's perception of the trailer motion. A driver model is thus formulated on the basis of position error between the lateral coordinates of the previewed and predicted paths, assuming single point preview and small variations in the heading angle as shown in Figure 4.3.

The function $f(t+T_p)$ represents the path previewed by the driver in the fixed X-Y coordinate system at the preview interval T_p, while $y_1(t+T_p)$ is the corresponding predicted path. The driver model attempts to minimize the position error, $\Delta y=[f(t+T_p)-y_1(t+T_p)]$ in order to improve the tracking performance. The predicted path is thus expressed by a second order function that implies $\ddot{y}_1 = \text{constant}$. The predicted path trajectory is expressed as a function of the preview interval, and velocity and acceleration along the lateral coordinate:

$$y_1(t+T_p) = y_1(t) + T_p \dot{y}_1(t) + T_p^2 \frac{\ddot{y}_1(t)}{2} \tag{4.5}$$

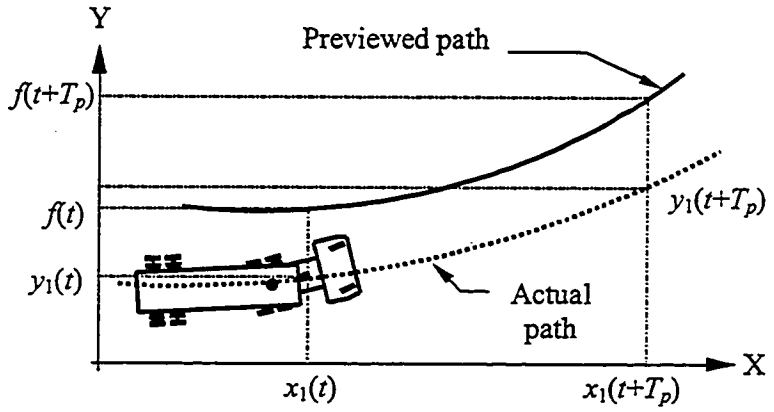

Figure 4.3: Single point preview strategy.

The primary objective of the closed-loop driver-vehicle model is to minimize the position error to enhance the tracking performance, which can be realized upon selecting appropriate values for the control variables, $\ddot{y}_1$. The desired path control parameter, $\ddot{y}_1$, is derived from solution of equation (4.5) using the known state vector, $\sigma(t) = \{y_1(t), \dot{y}_1(t)\}^T$. The lateral position error is ideally minimized by the driver by following the previewed path, such that

$$y_1(t + T_p) = f(t + T_p) \tag{4.6}$$

The minimization of lateral position error yields an ideal value of lateral acceleration of the lead unit ($\ddot{y}_1^*$), which can be derived from the solution of Equations (4.5) and (4.6):

$$\ddot{y}_1^*(t) = \frac{2\left[f(t + T_p) - y_1(t) - T_p \dot{y}_1(t)\right]}{T_p^2} \tag{4.7}$$

The above lateral acceleration is referred to as the ideal acceleration, since it can considerably reduce the position error. The lateral acceleration response of the lead unit, however, may differ considerably from the ideal value due to contributions arising from directional dynamics of the articulated vehicle, and the driver delays.

SLM2:

The path following properties of a vehicle rely strongly on its orientation, apart from the lateral position. The driver also exhibits superior abilities to sense the orientation error of the vehicle [131, 148, 149], specifically when driving on curved paths. A driver model is formulated based upon the orientation error between the previewed and the predicted paths of the c.g. of the lead unit alone to assess the

contributions of orientation error control on the overall driver-vehicle system. The predicted path orientation is expressed as a function of the preview interval, and velocity:

$$\psi_1(t+T_p) = \psi_1(t) + T_p\dot{\psi}_1(t) \tag{4.8}$$

The primary objective of the closed-loop driver-vehicle model is to minimize the orientation error to enhance the tracking performance, which can be realized upon selecting appropriate values for the control variable, $\dot{\psi}_1$. The orientation error is ideally minimized by the driver by following the previewed path orientation, such that

$$\psi_1(t+T_p) = \frac{\dot{f}(t+T_p)}{u_1} \tag{4.9}$$

Equations (4.8) and (4.9) yield an ideal value of yaw rate of the lead unit ($\dot{\psi}_1^*$):

$$\dot{\psi}_1^*(t) = \frac{\dot{f}(t+T_p) - \psi_1(t)u_1}{u_1 T_p} \tag{4.10}$$

The above yaw rate of the lead unit is referred to as the ideal yaw rate, since it can considerably reduce the orientation error. The yaw rate response of the lead unit, however, may differ considerably from the ideal value due to contributions arising from the driver delays and directional dynamics of the articulated vehicle.

SLM3:

The path tracking property of an articulated vehicle differs considerably from that of a single unit vehicle due to the dynamic coupling of the articulated units. The motion of the trailing unit, however, affects the path tracking performance in a complex manner. The articulated vehicle driver, to some extent, may perceive the lateral position of the trailing unit through the rear view mirror and from the knowledge of the vehicle motion. A driver model is formulated based upon the lateral position error between the previewed and the predicted paths of the c.g. of the trailing unit alone to assess the contributions of

lateral position error control from the trailing unit. The predicted path position of the trailing unit is expressed as a function of the preview interval, and velocity:

$$y_2(t+T_p) = y_2(t) + T_p\dot{y}_2(t) + T_p^2\frac{\ddot{y}_2(t)}{2} \tag{4.11}$$

The lateral position error of the trailing unit is ideally minimized by the driver by following the previewed path, such that

$$y_2(t+T_p) = f(t+T_p) \tag{4.12}$$

The minimization of lateral position error of the trailing unit yields an ideal value of lateral acceleration of the trailing unit ($\ddot{y}_2^*$), which can be derived from the solution of Equations (4.11) and (4.12):

$$\ddot{y}_2^*(t) = \frac{2\left[f(t+T_p) - y_2(t) - T_p\dot{y}_2(t)\right]}{T_p^2} \tag{4.13}$$

The above lateral acceleration is referred to as the ideal acceleration, since it can considerably reduce the position error of the trailing unit. The lateral acceleration response of the trailing unit, however, may differ considerably from the ideal value due to contributions arising from directional dynamics of the articulated vehicle, and the driver delays.

SLM4:

The orientation of the trailing unit to some extent affects the path tarcking performance of an articulated vehicle. The control strategy of an articulated vehicle driver may thus vary with the orientation of the trailing unit, specifically when driving on curved paths. A driver model is formulated based upon the orientation error between the previewed and the predicted paths of the c.g. of the trailing unit alone to assess the contributions of orientation error control of the trailing unit on the performance of closed-

loop driver-vehicle system. The predicted path orientation of the trailing unit is expressed as a function of the preview interval and velocity:

$$\psi_2(t+T_p) = \psi_2(t) + T_p\dot{\psi}_2(t) \tag{4.14}$$

The primary objective of the closed-loop driver-vehicle model is to minimize the orientation error to enhance the tracking performance, which can be realized upon selecting appropriate values for the control variable, $\dot{\psi}_2$. The orientation error is ideally minimized by the driver by following the previewed path orientation, such that

$$\psi_2(t+T_p) = \frac{\dot{f}(t+T_p)}{u_2} \tag{4.15}$$

Assuming small articulation angle and constant forward speeds of the lead and trailing units, Equations (4.14) and (4.15) yield an ideal value of yaw rate of the trailing unit ($\dot{\psi}_2^*$):

$$\dot{\psi}_2^*(t) = \frac{\dot{f}(t+T_p) - \psi_2(t)u_2}{u_2 T_p} \tag{4.16}$$

The above yaw rate of the trailing unit is referred to as the ideal yaw rate, since it can considerably reduce the orientation error. The yaw rate response of the trailing unit, however, may differ considerably from the ideal value due to contributions arising from the driver delays and directional dynamics of the articulated vehicle.

4.4.1 Identification of the Driver Model Parameters

While the vehicle parameters are considered to be either known or identifiable, the four driver models formulated on the basis of single-loop structures consist of three parameters: compensatory gain (K_d), lead time constant (T_L) and lag time constant (T_l). These parameters are known to depend upon the motion feedback variables, and

interactions among the driver, vehicle and the path in a highly complex manner. Although many studies have reported a range of some of these parameters derived from controlled experiments, a wide variation can be observed among the reported data [19]. The model parameters in this study are identified by minimizing the performance index defined in Equation (4.1) using damped Gauss Newton method [188]. In view of the difference in the steering gear ratio of single unit light vehicles and articulated heavy vehicles, the compensatory gain for lateral position error is considered within the range of 0.003 to 0.2 rad/m. The design variables (K_d, T_L and T_I) are thus subjected to the corresponding constraints based upon the range of reported data: $0.003<K_d<0.2$rad/m for lateral position error and $0.1<K_d<4.8$rad/rad for orientation error, $0.01<T_L<5.0$s and $0.01<T_I<20.0$s. It should be noted that the driver's compensatory gain, K_d, has different physical implications with the different motion feedback variables. For SLM1 and SLM3, based upon feedback from the lateral position of the c.g. of lead and trailing units respectively, the compensatory gain implies that the driver completes K_d radians of steering angle for one meter of lateral position error between the concerned unit c.g. and the previewed path. T_L and T_I affect the high frequency compensatory gain and phase. A higher value of T_L yields a higher value of the high frequency compensatory gain and lower value of the phase angle between the lateral position error and the steering angle. A higher value of T_I, however, yields a lower value of the high frequency gain and higher value of the phase angle between the lateral position error and the steering angle. For SLM2 and SLM4, based upon feedback from the orientation of the lead and trailing units respectively, the gain implies that the driver completes K_d radians of steering angle for one radian of the orientation error between the concerned unit and the previewed path.

4.4.2 Comparison of the Driver Performance for Different Preview & Prediction Methods

The four driver models with different feedback variables are analyzed to derive the driver performance in terms of the compensatory gain (K_d), lead (T_L) and lag (T_I) time constants, and the steering rate index, $J_{\dot{\delta}}$. The previewed path coordinates and orientation, illustrated in Figure 4.2, are applied as the inputs to the four driver-vehicle models, respectively. The performance index, J, expressed in Equation (4.1), is minimized to derive the driver model parameters, which are illustrated in Table 4.1. The steering rate response corresponding to four driver models are illustrated in Figure 4.4.

Table 4.1: Driver model parameters and steering rate index (Single loop structure).

Model	Driver model parameters and steering rate index			
	K_d	T_L (s)	T_I (s)	$J_{\dot{\delta}}$
SLM1	0.15 (rad/m)	0.10	2.1	0.0031
SLM2	1.8 (rad/rad)	0.25	5.0	0.0060
SLM3	0.18 (rad/m)	1.55	0.2	0.0257
SLM4	2.1 (rad/rad)	1.35	2.8	0.0068

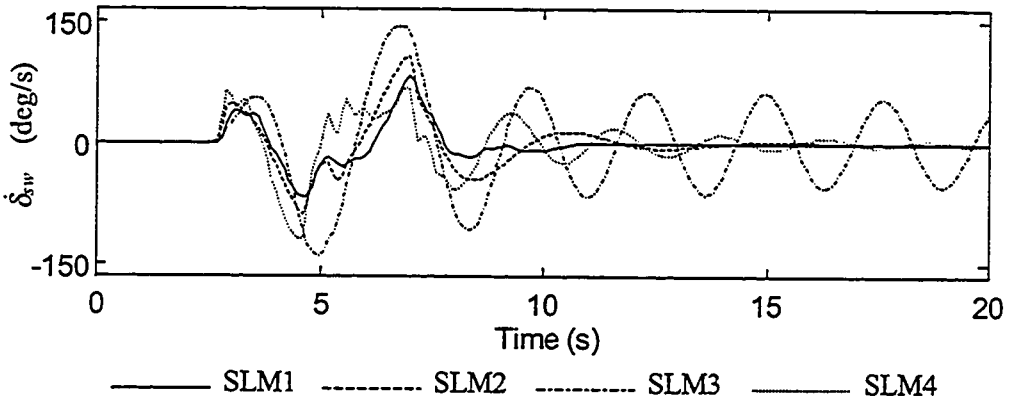

Figure 4.4: Steering rate response for various single loop model structures.

The results clearly show that the lateral position errors of the lead (SLM1) and the trailing (SLM3) units yield the least and largest values of the steering rate index and thus the required driver effort, respectively. A comparison of the steering effort response of

the vehicle model employing different structures reveals that the structures based upon lateral position and orientation errors of the lead unit yield smaller required steering effort, compensatory gain and lead time constant, and larger lag time constants. These results may be attributed to the interactions between the driver and the articulated vehicle, in which the driver tends to adapt different values of the vehicle steering gain in terms of the lateral position and orientation of the lead and trailing units. It is understood that the steering gains for the lateral position and orientation of the lead unit are higher than those corresponding to the trailing unit. Furthermore, the lead unit responds to the steering input more rapidly than the trailing unit. The driver is thus required to assume smaller compensatory gain, lead time constant and larger lag time constant to compensate and equalize the driver-vehicle interactions in order to perform the path tracking corresponding to the feedback variables from the lead unit. The steering rate response, illustrated in Figure 4.4, further shows that the driver performs the evasive maneuver rapidly when the control loop based upon lateral position of the lead unit, while the feedbacks from the orientation of the lead unit and lateral position and orientation of the trailing unit yield larger settling time. The driver model based upon feedback from the lateral position and orientation of the trailing unit yields more oscillatory steering rate response and thus poses larger steering effort demand on the driver.

4.4.3 Comparison of the Vehicle Performance Derived from Different Preview & Prediction Methods

The directional performance characteristics of the articulated vehicle are derived for different preview and prediction methods using the defined steering input illustrated in Figure 4.2. Figure 4.5 illustrates the time-histories of the directional response of the

vehicle employing four different single-loop model structures of the driver. The four driver models in conjunction with the articulated vehicle model yield considerably different path tracking performance and dynamic response as shown in Figure 4.5. The components of the performance index corresponding to the vehicle performance are further summarized in Table 4.2.

Table 4.2: Components of the performance index and total performance index of the vehicle response with various driver models (single-loop structure).

Model	Performance indices								
	J_{y1}	$J_{\psi 1}$	J_{ay1}	J_{ay2}	$J_{\phi 1}$	$J_{\phi 2}$	J_{r1}	J_{r2}	J
SLM1	0.4538	0.0162	0.0403	0.0495	0.0098	0.0103	0.0376	0.0329	0.6536
SLM 2	0.3201	0.0091	0.0618	0.0785	0.015	0.0164	0.0624	0.0534	0.6227
SLM 3	0.5691	0.0152	0.1501	0.2050	0.0403	0.0450	0.1801	0.1378	1.3681
SLM 4	0.5782	0.0135	0.0388	0.0538	0.0106	0.0117	0.0448	0.0356	0.7938

The results clearly show that the lateral position and orientation of the lead unit, when used as the feedback variable, yield fast and stable response. The feedbacks from the lateral position and orientation of the trailing unit yield oscillatory response. The best tracking performance in terms of J_{y1} and $J_{\psi 1}$, can be achieved using the orientation and lateral position of the lead unit as the feedback variables. The results thus imply that the orientation and the lateral position of the lead unit are the fundamental feedback variables used for path tracking, since they are relatively easy to be perceived by the driver. The driver may exhibit relatively poor perception and prediction abilities in terms of the orientation and lateral position of the trailing unit. Furthermore, the preview and prediction based upon lateral position of the trailing unit yields poor directional dynamic performance of the vehicle in terms of J_{ay1}, J_{ay2}, $J_{\phi 1}$, $J_{\phi 2}$, J_{r1} and J_{r2}. An examination of the composite performance index J, further reveals that preview and predictions based upon orientation and lateral position of the lead unit yields best directional performance

of the vehicle. These variables are thus recognized to be the essential feedback variables used for formulating the multi-loop structure of the driver model.

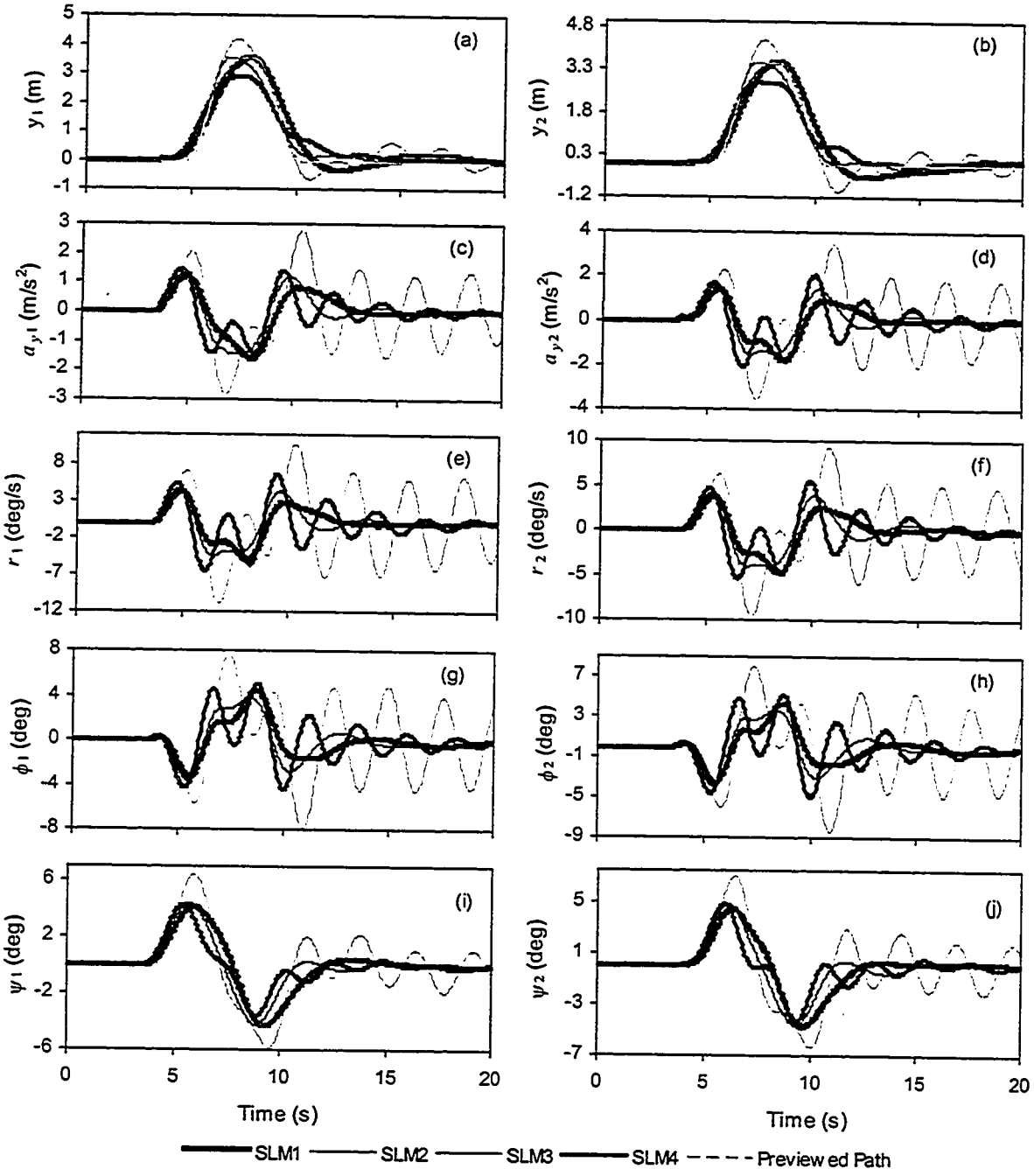

Figure 4.5: Tracking and directional response of the articulated vehicle subject to an obstacle avoidance maneuver and different single-loop preview and prediction strategies.

4.5 DRIVER MODELS BASED UPON MULTI-LOOP STRUCTURES

The single-loop structures of the driver model based upon orientation and lateral position of the lead unit provide good performance in terms of path tracking and directional response. A driver, however, controls the vehicle based upon not only the previewed path information but also the perception of the vehicle motion. It has been established that the driver's control behaviour is a complex function of the path input, vehicle motion and the driver's experience [139, 142]. Many studies have further established that the driver can sensitively perceive linear acceleration above 0.02g and the angular velocity above 0.001 rad/s through its vestibular system [16-18,189]. The linear acceleration and angular velocity of a heavy vehicle operating on a highway are frequently beyond the above threshold values. While the previewed path information comprises of the lateral displacement and the orientation error between the path input and the actual trajectory of the vehicle, the driver's perception of vehicle motion may be enhanced through lateral acceleration, yaw rate, and roll angle response of the vehicle.

A road vehicle, in general, is subjected to geometric constraints imposed by the highway in the form of stream line, shoulders and other obstacles. Under a specific vehicle speed, a severe vehicle response may occur as the driver performs the path tracking, such as the rollover and yaw oscillation of the articulated heavy vehicle. The occurrence of such a severe directional response is often controlled by the driver by decreasing the vehicle speed or by relaxing the requirements of path tracking task. The driver's compensatory abilities should thus depend upon the driver's perception of the vehicle motion and sensitivity to roll, yaw and lateral acceleration of both the tractor and trailer, in addition to the previewed path information. Such perception and sensitivity

could directly or indirectly arise from the instantaneous motion of the vehicle in a complex manner. The direct perception of the vehicle motion may be derived from the driver's subconsciousness and experiences, and knowledge of the vehicle's response, while an indirect perception of the motion may be generated from sensors installed to measure the important motion states of the vehicle. It should also be noted that driver's knowledge of rearward amplification properties of the vehicle enable him/her to perceive the motion state of the trailing unit.

A multi-loop structure of driver/vehicle system can thus be formulated to study the driver's directional control behaviour in a more realistic manner than the single-loop structure. From the studies on the single loop structure of the driver/vehicle system, it is apparent that the driver most likely, utilizes the tracking error information of the lateral displacement and orientation of the lead unit, rather than the trailer. The multi-loop structure of the driver-vehicle system is thus formulated on the basis of tracking information from the lateral displacement and orientation error between the previewed path and those of the lead unit. Figure 4.6 illustrates a proposed multi-loop structure of the driver/vehicle system, where the path input may be either lateral displacement or the orientation of the path. The functions $H_L(s)$ and $H_H(s)$ represent the low and high frequency components of the driver's compensatory characteristics. $F_e(s)$ and $F_i(s)$ represent the driver's prediction functions for the low (q_e) and high (q_i) frequency signals and also indicate the external and internal prediction loops. The low frequency signals may include the lateral displacement or orientation tracking errors, while the higher frequency signals comprise the roll angles, yaw rates and lateral accelerations for both the tractor and the trailer [22].

It has been established that the good multi-loop structure candidates are those that require little or no driver equalization, such that each loop is characterized by its gain and time delay [25, 28]. The components of the compensatory function of the driver, $H_L(s)$ and $H_H(s)$, can thus be defined as:

$$H_L(s) = K_L e^{-\tau_L s} \text{ and } H_H(s) = K_H e^{-\tau_H s} \tag{4.17}$$

where K_L and K_H are the compensatory gains, τ_L and τ_H are the time delays for the low and high frequency components, respectively.

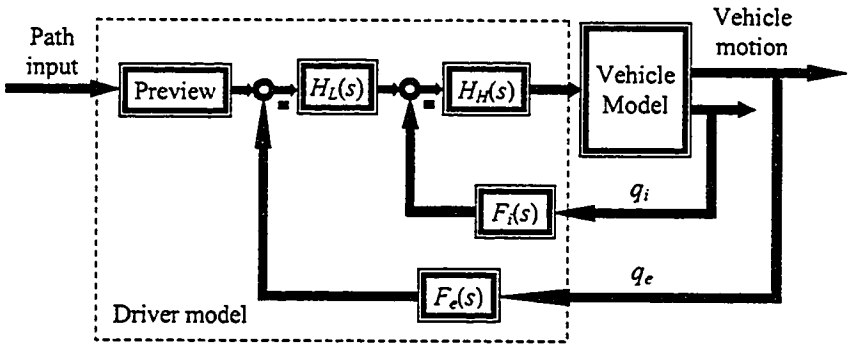

Figure 4.6: A multi-loop structure of driver/vehicle system.

The driver's prediction function in the external loop, $F_e(s)$, represents the driver's prediction ability of the vehicle motion on the preview time based upon the current states of the vehicle, including the lateral displacement and velocity. While the prediction function in the internal loop, $F_i(s)$, indicates the driver's perception of the vehicle motion, direct and indirect. In this study, the driver is assumed to be able to predict the lateral displacement of the vehicle by a second order function, and the orientation angle by a first order function, such that:

$$F_e(s) = 1 + T_p s + 0.5\zeta T_p^2 s^2 \text{ and } F_i(s) = K_p e^{\tau_p s} \tag{4.18}$$

where T_p is the driver's preview time, ς is the prediction factor (ς=1, for lateral displacement; and ς=0 for orientation). τ_p is the driver's prediction time, which could be positive or negative, depending upon the driver's motion perception channels. For the direct perception of motion by the driver arising from either experience or subconscious, knowledge of vehicle response, τ_p assumes a positive value. The indirect perception of motion realized through monitoring of the vehicle state yields a negative value of τ_p, since the delays associated with measurement, signal processing, display and detection are longer than the driver's prediction time. K_p is the prediction gain.

Different multi-loop structure models of the driver-vehicle system can be realized using different compositions of motion feedback variables. Eight different model structures are formulated using different motion perceptions of the driver to study their relative contributions to the performance characteristics of the driver-vehicle system. It should be noted that the proposed multi-loop structures employ the path preview information using the lateral position and orientation of the lead unit. Table 4.3 summarizes eight different multi-loop structures employing different motion perceptions of the driver, denoted by MLM1 through MLM8. The MLM1 model structure utilizes the tractor yaw rate as the internal motion feedback variable, while MLM2 model is formulated on the basis of driver's perception of the articulation rate. MLM3 and MLM4 models imply that the driver perceives the roll motions of the tractor and trailer sprung mass as the internal feedback signal, respectively. While MLM5 indicates that the driver focuses not only on the roll motion of the sprung mass of trailer but also the articulation rate, in addition to the lateral position and orientation of the lead unit, as shown in Figure 4.7. Since the articulation rate is related to the relative yaw velocities of the two units,

this compensatory model emphasizes the perception of the yaw response of two units and roll angle of the trailer sprung mass. The compensatory models MLM6 and MLM7 are formulated by replacing the roll motion in MLM5 by the lateral accelerations of the tractor and the trailer, respectively. The final compensatory model, MLM8, utilizes the lateral acceleration of tractor (a_{y1}), roll angle of trailer sprung mass (ϕ_2) and the articulation rate ($\dot{\Gamma}$) as the internal motion feedback variables, as illustrated in Figure 4.8.

It should be noted that the external signal (q_e) in the above models comprises the lateral displacement and orientation of the lead unit, while the internal signal varies with the corresponding motion feedback variables. The above models are analyzed to study the influence of various motion variables on the driver and vehicle performance in the following subsections.

Table 4.3: Feedback variables in the internal loop of various multi-loop structures.

Model	Feedback variables in the internal loop, q_i
MLM 1	Tractor yaw rate
MLM 2	Articulation rate
MLM 3	Roll angle of sprung mass of the tractor
MLM 4	Roll angle of sprung mass of the trailer
MLM 5	(i) Roll angle of sprung mass of the trailer (ii) Articulation rate
MLM 6	(i)Lateral acceleration of the c.g. of sprung mass of tractor (ii) Articulation rate
MLM 7	(i)Lateral acceleration of the c.g. of sprung mass of trailer (ii) Articulation rate
MLM 8	(i)Lateral acceleration of the c.g. of sprung mass of tractor (ii) Roll angle of sprung mass of the trailer, and (iii) Articulation rate

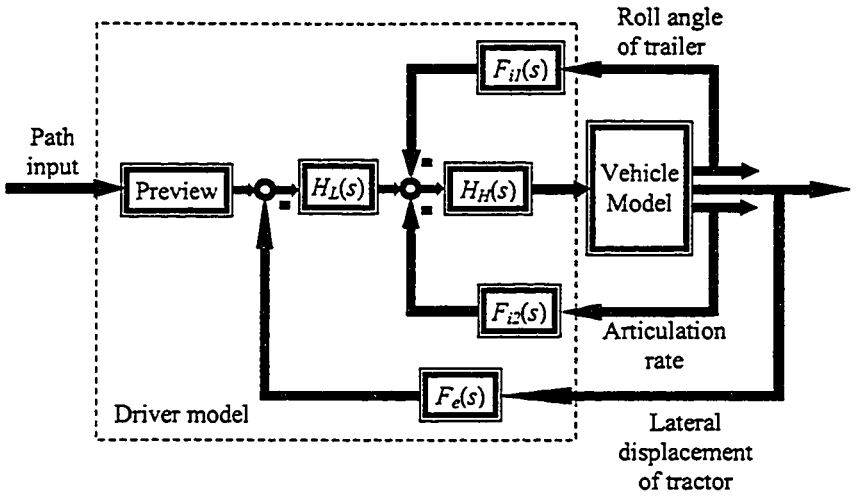

Figure 4.7: Multi-loop structure of the compensatory model employing driver's perception of the articulation rate and roll angle of the trailer sprung mass (MLM5).

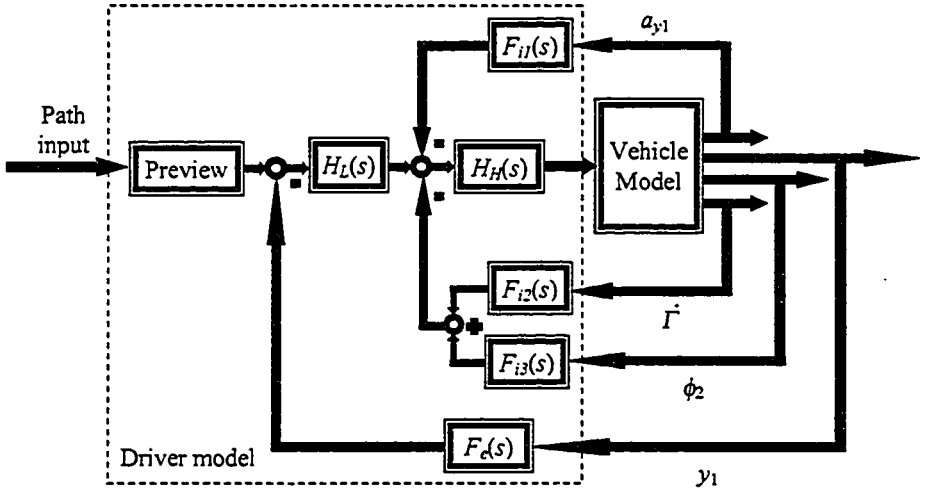

Figure 4.8: Multi-loop structure of the compensatory model employing driver's perception of the articulation rate, roll angle of the trailer sprung mass and lateral acceleration of tractor (MLM8).

4.5.1 Comparison of the Driver Performance Using Different Multi-loop Preview and Prediction Methods

The proposed multi-loop structure models are analyzed to identify the driver parameters and the steering effort index $J_{\dot{\delta}}$ using the obstacle avoidance maneuver, illustrated in Figure 4.2. The driver model parameters corresponding to each structure are estimated by minimizing the performance index in Equation (4.1). The simulations are

performed assuming driver's low frequency compensatory delay τ_L=0.15s and high frequency compensatory time delay τ_H=0.1s. The driver's prediction time is assumed as τ_p=-0.015s, indicating the indirect perception of motion. While the preview time is considered as 1.5s. The resulting parameters, including the compensatory and prediction gains, steering effort index $J_{\dot{\delta}}$ are illustrated in Table 4.4.

Table 4.4: Driver model parameters and steering rate index for different multi-loop structures.

Model	$J_{\dot{\delta}}$	Parameters				
		K_L (rad/m)	K_H (rad/rad)	K_{p1}	K_{p2} (rad/rad/s)	K_{p3} (rad/rad)
MLM1	0.0086	0.121	2.37	0.53 (rad/rad/s)	/	/
MLM2	0.0142	0.101	2.40	0.55 (rad/rad/s)	/	/
MLM3	0.0126	0.077	2.93	0.41 (rad/rad)	/	/
MLM4	0.0125	0.081	2.66	0.42 (rad/rad)	/	/
MLM5	0.0202	0.079	2.80	0.41 (rad/rad)	0.61	/
MLM6	0.0145	0.092	2.43	0.38 (rad/m/s^2)	0.66	/
MLM7	0.0170	0.087	2.62	0.34 (rad/m/s^2)	0.62	/
MLM8	0.0120	0.091	2.56	0.45 (rad/m/s^2)	0.60	0.4

The results show that the model based upon tractor yaw rate as the motion feedback variable (MLM1) yields the largest value of low and least value of high frequency compensation gains. The results may imply that the driver is required to undertake considerable compensation to minimize the lateral position and orientation errors, when the motion perception is dominated by the yaw rate of the tractor. The model structure based upon articulation rate as a feedback variable (MLM2) yields considerably higher prediction gain (K_{p1}). A comparison of the prediction gains, derived from MLM1 and MLM2, reveals that the driver is most likely required to be more sensitive to articulation rate than the yaw rate of tractor. The response characteristics of the models based upon roll motions of the trailer sprung mass (MLM4) and the tractor sprung mass (MLM3) as the feedback variable reveal that MLM3 yields lower value of

the prediction gain (K_{p1}) and the low frequency compensatory gain for lateral position and orientation errors (K_L) but larger value of the high frequency compensatory gain (K_H). These results may indicate that the driver is required to be more sensitive to the trailer roll angle feedback than the tractor roll angle. The combination of trailer roll angle and the articulation rate as the feedback variables (MLM5) yields relatively a smaller value of driver's prediction gain (K_{p1}), which is identical to that derived from MLM3. The models based upon articulation rate, and lateral accelerations of the tractor (MLM6) and the trailer (MLM7) yield relatively smaller values of the driver's prediction gains for lateral acceleration (K_{p1}), and the low frequency compensatory gain for the lateral position and orientation of the tractor (K_L). The MLM6 model, based upon lateral acceleration of the tractor, also yields lower value of the high frequency compensatory gain (K_H). These results imply that driver is more sensitive to the lateral acceleration of tractor than that of the trailer. Furthermore, the driver is required to be sensitive to the articulation rate, when the lateral acceleration of the tractor is considered as the feedback variable. Apart from the tractor lateral acceleration and articulation rate as feedback variables (MLM6), the use of roll angle of the trailer sprung mass as the other feedback variable (MLM8) yields a higher value of the driver's prediction gain (K_{p1}) of the lateral acceleration, but smaller value of the prediction gain (K_{p2}) for the articulation rate and low frequency compensatory gain (K_L) for the lateral position and orientation error of the tractor. These results further suggest that the driver is required to be more sensitive to the lateral acceleration of tractor and less sensitive to the articulation rate to achieve path tracking, when a perception of the trailer roll angle is considered to exist.

The steering rate index $J_{\dot{\delta}}$, which describes the steering effort demand posed on the driver, is observed to be the least for MLM1 model, based upon tractor yaw rate, and highest for MLM5, based upon trailer roll motion and articulation rate. These results imply that a good perception of tractor yaw rate minimizes the steering effort demand on the driver. The path tracking based upon the perception of trailer roll motion and articulation rate poses more steering demand on the driver. Figure 4.9 illustrates the time history of the steering rate, derived from the driver-vehicle models based upon MLM5, MLM6, MLM7 and MLM8. The results clearly show that the model structure, based upon tractor lateral acceleration, trailer roll angle and articulation rate (MLM8), yields minimum required steering effort. The driver model structure, based upon trailer roll angle and articulation rate alone, yields maximum required steering effort. The results thus imply that addition of motion perception based on lateral acceleration of the lead unit allows the path tracking with reduced steering effort and lower prediction gain for the articulation rate.

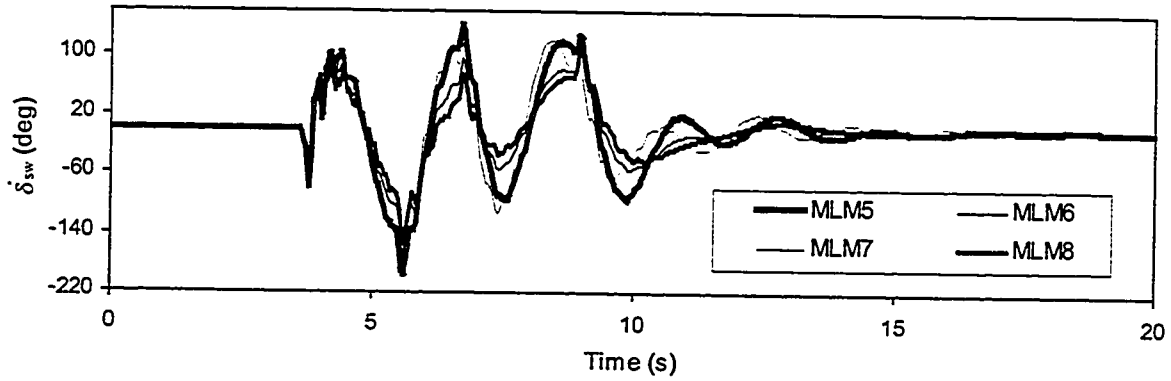

Figure 4.9: Steering rate response for various multi-loop driver model structures.

4.5.2 Comparison of the Vehicle Performance Derived from Different Multi-loop Preview and Prediction Methods

The various driver models with different motion feedback variables are further analyzed to derive the directional performance of the vehicle in terms of the components of the performance index, defined in Equation (4.1), and the peak values of the vehicle response variables. The components of the performance index and the corresponding peak values of the vehicle response variables, derived under an obstacle avoidance maneuver, are summarized in Tables 4.5 and 4.6, respectively.

Table 4.5: Performance indices for various multi-loop driver model structures.

Model	Performance indices								
	J_{y1}	$J_{\psi 1}$	J_{ay1}	J_{ay2}	$J_{\phi 1}$	$J_{\phi 2}$	J_{r1}	J_{r2}	J
MLM1	0.2095	0.0086	0.0904	0.1137	0.0239	0.0148	0.0708	0.0804	0.6207
MLM2	0.0635	0.0052	0.1036	0.1390	0.0269	0.0297	0.1115	0.0929	0.5865
MLM3	0.0686	0.0057	0.1044	0.1354	0.0213	0.0284	0.1088	0.0917	0.5769
MLM4	0.0686	0.0057	0.1035	0.1342	0.0256	0.0147	0.1078	0.0908	0.5634
MLM5	0.0429	0.004	0.0968	0.1429	0.0284	0.0218	0.1151	0.0925	0.5646
MLM6	0.0714	0.0051	0.0841	0.1191	0.0234	0.0259	0.0955	0.0782	0.5172
MLM7	0.0605	0.0045	0.0871	0.1057	0.0249	0.0277	0.1017	0.0819	0.5110
MLM8	0.0644	0.0055	0.0851	0.1127	0.0219	0.0241	0.091	0.0752	0.4919

Table 4.6: Peak values of vehicle responses of various multiple-loop structures.

Model	Peak values of response									
	ε_{y1} (m)	ε_{y2} (m)	$\varepsilon_{\psi 1}$ (deg.)	$\varepsilon_{\psi 2}$ (deg.)	a_{y1} (m/s^2)	a_{y2} (m/s^2)	r_1 (deg/s)	r_2 (deg/s)	ϕ_1 (deg)	ϕ_2 (deg)
MLM1	0.7746	0.8977	4.6212	5.0605	2.8939	3.1744	8.1978	8.8114	7.6561	7.8300
MLM2	0.3658	0.5064	2.9642	2.4315	3.0022	2.9428	8.9963	8.3190	7.6591	7.8016
MLM3	0.3504	0.5543	3.2392	2.5624	3.0329	3.2436	9.6113	9.0008	7.3257	7.8909
MLM4	0.3555	0.5461	3.2051	2.5763	3.0169	3.2275	9.5608	8.9566	7.6980	7.3622
MLM5	0.3349	0.3720	3.0243	2.1212	2.7610	3.3195	10.038	8.6106	7.9531	7.4497
MLM6	0.5645	0.6426	2.2471	2.9026	2.6449	2.8482	8.4554	8.0103	7.8844	7.7481
MLM7	0.5686	0.6225	2.2347	2.0525	2.6671	2.7707	9.8169	9.2146	8.1371	8.3846
MLM8	0.4982	0.5020	3.1554	3.7945	2.6522	3.0284	9.0717	8.5343	8.4226	7.4046

The results illustrated in Tables 4.5 and 4.6 clearly show that MLM8, incorporating lateral acceleration of tractor, trailer roll angle and articulation rate as the

motion feedback variables, yields the least value of the composite performance index J (0.4919). It is found that when a motion variable is served as the feedback signal, the corresponding dynamic response in terms of the performance indices and peak values is improved considerably. The MLM1, for example, based upon tractor yaw rate as the feedback variable, yields the least value of yaw rate of the tractor, J_{r1}=0.0708 and r_{1peak}=8.1978deg/s. The results therefore suggest that the motion feedback variable involved in the driver's directional control strategy enable the driver to effectively control that particular response variable, while tracking a desired trajectory. Since highway safety performance of a driver-vehicle system is directly related to its path tracking ability with acceptable levels of directional dynamic response, the selection of motion perception or feedback variables should be based upon the relative significance of the response variables and the required steering effort. A comparison of the results illustrated in Table 4.5 with those derived from the single loop structures of driver models (Table 4.2), further illustrates that the driver's perception of vehicle motion in the multi-loop structures tends to reduce the composite performance index J, irrespective of the structure used. It can thus be concluded that the driver's directional control strategies are function of both the path tracking and the vehicle motion, and the motion variables are the essential factors affecting the driver's behaviour.

4.6 SUMMARY

The single- and multi-loop structures of the driver-vehicle system models are formulated to study the contributions of various preview and prediction strategies to the path tracking and dynamic performance of the articulated vehicle. The driver model

parameters in the single loop structure are derived to analyze the driver performance. The results show that the preview and prediction based upon lateral position and orientation of the trailing unit yields oscillatory vehicle response and pose unacceptable steering demand on the driver. Eight different multi-loop structures of the driver-vehicle system are formulated to represent driver's perception of different vehicle motion variables. The results derived from the multi-loop structure further show that the lateral position and orientation of the lead unit are the fundamental feedback variables forming the external loop in the multi-loop driver models, while the lateral acceleration of the lead unit, articulation rate and the roll angle of the trailing unit form the efficient motion feedback cues affecting the driver's directional control behaviour. Such a model structure yields the best composite performance. It should be noted, however, the driver's neuromuscular dynamics are neglected in the study. A coupled driver-vehicle model, incorporating the driver's neuromuscular dynamics, is formulated in the following Chapter.

CHAPTER 5 A COMPREHENSIVE CLOSED-LOOP DRIVER-ARTICULATED VEHICLE MODEL

5.1 INTRODUCTION

From the review of past investigations on the driver-vehicle interactions, it is evident that vast majority of studies, with the exception of only few, focus on the single unit vehicles. Only few studies have investigated the influence of the coupling effects of articulated vehicle on the path tracking and dynamic performance of the vehicles. The results derived from the multi-loop preview and prediction models, presented in Chapter 4, further show that the directional control behaviour of the driver is a complex function of the path input and the perception of motion of the articulated vehicle units, including the lateral acceleration of the lead unit, articulation rate and the roll angle of the trailing unit. A comprehensive articulated vehicle-driver model is thus needed to study the directional control characteristics of the vehicle and to identify vehicle design factors that can be well suited to the driver. The analysis presented in Chapter 4, however, neglected the contributions due to the driver's proprioceptive elements and neuromuscular dynamics, which describe the physical limitations of the driver [121, 135]. In this Chapter, the proposed multi-loop structure model of the driver is modified to incorporate physical limitations of the driver, which is integrated with the articulated vehicle model to derive a comprehensive closed-loop driver-articulated vehicle model (CCDAVM).

5.2 MODEL STRUCTURE AND FORMULATION

The directional performance behavior of the coupled articulated vehicle and driver system is dependent upon the path preview, and driver's perception of directional

response of the lead and the trailing units. The driver-vehicle models reported in the literature, however, are based upon the feedback from the predicted motion behavior of a single unit. A driver model incorporating the feedback from the predicted motion of the trailer is developed to study its influence on the directional dynamics of the coupled articulated vehicle-driver system. The driver model is developed upon following primary considerations and assumptions:

- The driver's control actions are always directed towards minimizing the tracking error, lateral accelerations of the two units, articulation rate, and the roll responses of two units, subjected to constraints posed by the maximum rate of steering;

- The vehicle path is previewed with respect to the coordinate system fixed to the vehicle and the variations in the heading angle of the lead unit are assumed to be small when traveling on a highway;

- The previewed path primarily includes low frequency components, and can thus be expressed by a low-order polynomial function;

- The driver is assumed to have some fundamental knowledge or some measurement of the directional performance of the articulated vehicle in terms of lateral acceleration, articulation rate and the roll angle response of vehicle.

Assuming small variation in the heading angle of the lead unit, the single point path preview strategy can be schematically formulated, as shown earlier in Figure 4.3. The path previewed by the drivers at an interval of T_p is expressed by $f(t+T_p)$ in the fixed X-Y coordinate system. The corresponding estimated vehicle path, at the preview interval T_p is shown as $y_1(t+T_p)$. A number of driver models have attempted to minimize both position $[f(t+T_p)-y_1(t+T_p)]$ and orientation $[\dot{f}(t+T_p)-\dot{y}_1(t+T_p)]$ errors in order to improve the tracking performance, assuming that the predicted vehicle trajectory can be expressed by a second order function, such that $\ddot{y}_1 = \text{constant}$. Such models, however,

have demonstrated little success, since the position and orientation errors can not be controlled independently. Guo and Guan [149] have proposed a position and orientation preview acceleration model (POPA), by considering the predicted path trajectory as a third-order curve, such that $\dddot{y}_1 = \text{constant}$. The predicted path trajectory can thus be expressed as:

$$y_1(t+T_p) = y_1(t) + T_p\dot{y}_1(t) + \frac{T_p^2\ddot{y}_1(t)}{2} + \frac{\lambda T_p^3\dddot{y}_1(t)}{6} \tag{5.1}$$

where λ $(0 \le \lambda \le 1)$, a path-follower or orientation coefficient, is introduced to enhance the stability of the system, and to account for driver's path prediction skill. $\lambda = 1$ yields a third-order model of the predicted trajectory and reflects a higher degree of skill of the driver, $\lambda = 0$ yields a second-order model of the trajectory, based upon $\ddot{y}_1 = \text{constant}$. The orientation of the predicted trajectory can then be expressed as:

$$\dot{y}_1(t+T_p) = \dot{y}_1(t) + T_p\ddot{y}_1(t) + \frac{T_p^2\dddot{y}_1(t)}{2} \tag{5.2}$$

Equations (5.1) and (5.2) can be solved to determine the desired path control parameters, $\ddot{y}_1$ and $\dddot{y}_1$, using the known state vector, $\sigma(t) = \{y_1(t), \dot{y}_1(t)\}^T$. The tracking performance of the vehicle can be enhanced by minimizing the position and orientation errors, which can be realized upon selecting appropriate values for the control variables, $\ddot{y}_1$ and $\dddot{y}_1$. The position error is ideally minimized by the driver by following the previewed path, such that:

$$y_1(t+T_p) = f(t+T_p) \tag{5.3}$$

The orientation of the predicted (S_y) and previewed (S_f) trajectories can be derived from:

$$S_y = \frac{dy_1(x)}{dx} = \frac{1}{u_1}\dot{y}_1(t);\ S_f = \frac{df(x)}{dx} = \frac{1}{u_1}\dot{f}(t) \tag{5.4}$$

where u_1 is the constant forward speed of vehicle. The condition for eliminating the path orientation error can thus be expressed as:

$$S_y(t+T_p) = S_f(t+T_p);\ \text{or}\quad \dot{y}_1(t+T_p) = \dot{f}(t+T_p) \tag{5.5}$$

Equations (5.1) to (5.5) yield an ideal value of lateral acceleration of the lead unit ($\ddot{y}_1^*$), which can reduce both the position and orientation errors:

$$\ddot{y}_1^*(t) = \frac{6[f(t+T_p) - \frac{\lambda T_p \dot{f}(t+T_p)}{3} - y_1(t) + (1-\frac{\lambda}{3})T_p\dot{y}_1(t)]}{(3-2\lambda)T_p^2} \tag{5.6}$$

The actual lateral acceleration response of the lead unit, however, may differ from $\ddot{y}_1^*$ due to directional dynamics of the articulated vehicle, driver delays and the motion feedback from the vehicle dynamic response. It has been reported that the position, velocity, acceleration and acceleration rate serve as the primary sensory motion cues for the driver to undertake the desired control actions [14]. As discussed earlier in Chapter 4, the driver may also perform a maneuver based upon the prediction of the vehicle motion in terms of the sprung mass roll angle response and the articulation rate. The driver can thus perceive the difference of lateral acceleration and adjust the steering angle to minimize the error. The closed-loop driver-tractor-semitrailer model, comprising a driver model with preview, prediction and compensation models based upon optimal lateral acceleration of the tractor, and a vehicle model describing the lateral and roll dynamics of the vehicle, is formulated as illustrated in Figure 5.1.

In Figure 5.1, the preview block $P(s)$ represents the preview function, which is assumed to be an effective single point preview strategy, such that

$$P(s) = e^{T_p s}\left(1 - \frac{\lambda T_p s}{3}\right) \tag{5.7}$$

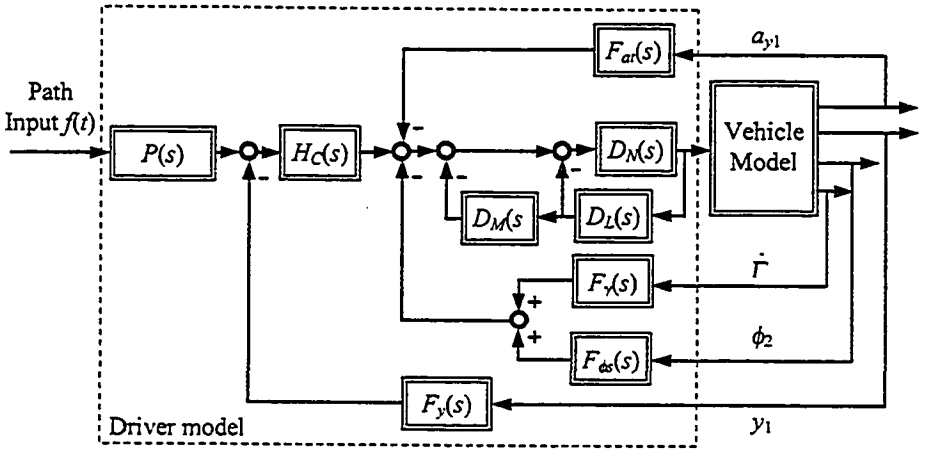

Figure 5.1: A comprehensive driver/articulated vehicle control model (CCDAVM).

The low frequency compensatory function, $H_C(s)$, is of the form:

$$H_C(s) = K_C(1 + T_C s)e^{-\tau_d s} \tag{5.8}$$

where K_C is the driver's compensatory gain, T_C is the driver's correction time constant and τ_d is the driver's reaction time. The functions $D_N(s)$, $D_L(s)$ and $D_M(s)$ represent the driver's neuromuscular dynamics, and the proprioceptive feedback elements derived from the motion of the human limbs and muscle tissues, respectively. While the neuromuscular dynamics of the driver is expressed by a second order system function, the dynamics due to proprioceptive feedback elements are described by first order system functions [135]:

$$D_N(s) = \frac{\omega_n^2}{s^2 + 2\zeta\omega_n s + \omega_n^2},\ D_L(s) = \frac{k_1 s}{s + \frac{1}{T_1}} \text{ and } D_M(s) = \frac{k_2}{s + \frac{1}{T_2}} \tag{5.9}$$

The study performed by Modjtahedzadeh and Hess has reported the value of natural frequency and damping ratio of the neuromuscular model as, $\omega_n = 10 rad/s$, $\zeta = 0.707$. T_1 and T_2 are the time constants, and k_1 and k_2 are constant gains, associated

with the feedback activity of the muscle spindles in the limbs driving the steering wheel, and the muscle tissue dynamics, respectively. It should be noted that the neuromuscular dynamics and the proprioceptive elements function as the high frequency compensation, which refers to frequencies within an approximate one decade range around the crossover frequency of the closed-loop driver-vehicle system [135].

The function $F_y(s)$, representing the driver's path prediction, is given by

$$F_y(s) = 1 + T_p s + \frac{T_p^2 s^2}{2} + \frac{\lambda T_p^3 s^3}{6} \tag{5.10}$$

The functions $F_{\phi s}(s)$, $F_\gamma(s)$, and $F_{at}(s)$ are the same as the blocks, $F_{i3}(s)$, $F_{i2}(s)$ and $F_{i1}(s)$ presented in Figure 4.8, which represent the motion feedback from the roll angle of the sprung mass of trailer, articulation rate between the two units, and the lateral acceleration of the c.g. of the tractor, respectively. These three functions are expressed as:

$$F_{\phi s}(s) = K_{\phi s} e^{\tau_{\phi s} s},\ F_\gamma(s) = K_\gamma e^{\tau_\gamma s} \text{ and } F_{at}(s) = K_{at} e^{\tau_{at} s} \tag{5.11}$$

where $K_{\phi s}$ and $\tau_{\phi s}$ are the driver's gain and time delay corresponding to prediction of the roll angle response of the trailer sprung mass. K_γ and τ_γ are the gain and delay time corresponding to prediction of the articulation rate response of the combination. K_{at} and τ_{at} represent the driver's prediction gain and delay time for the lateral acceleration of the tractor sprung mass c.g., respectively. It should be noted that the values of $\tau_{\phi s}$, τ_γ and τ_{at} could be positive or negative depending upon the driver's motion perception strategy.

5.3 ESTIMATION OF MODEL PARAMETERS

The driver-vehicle model, presented in Figure 5.1, consists of many driver model parameters, which are frequently derived from controlled experiments with varying objectives. The parameters include: the preview time (T_p); path-follower coefficient (λ); compensatory gain (K_C) and correction time constant (T_C); limb motion gain and time constant (k_1 and T_1), and muscle motion gain and time constant (k_2 and T_2) of the proprioceptive feedback components; trailer roll angle prediction gain and time ($K_{\phi s}$ and $\tau_{\phi s}$); articulation rate prediction gain and time (K_γ and τ_γ), and tractor lateral acceleration prediction gain and time (K_{at} and τ_{at}). The values of these parameters strongly depend upon the interactions among the driver, vehicle and the path in a highly complex manner. While a range of some of these parameters may be estimated from the reported analytical and experimental studies, number of driver model parameters need to be identified from the directional response of the driver-vehicle system under controlled steering maneuvers. Furthermore, the values of the model parameters reported in different studies differ considerably depending upon the test objectives, test conditions and the driver model. An objective function comprising the error function in lateral path, trailer and tractor lateral acceleration, steering wheel rate, orientation angle of tractor, roll angle of both sprung masses of tractor and trailer and the yaw rate of tractor and trailer, formulated in Equation (4.1), is thus applied subject to various constraints to derive a set of acceptable model parameters. The limit constraints on various model parameters are formulated using the range of reported data under similar test conditions as listed in Table 5.1. The constrained minimization problem, expressed in Equation (4.1), is then solved using damped Gauss Newton method to derive the model parameters.

Table 5.1: Range of driver model parameters.

No.	Parameters	Notation	Range
1	Preview time (s)	T_p(s)	$0.5<T_p<9.0$
2	Path-follower coefficient	λ	$0.0<\lambda<1.0$
3	Compensatory gain (rad/s)	K_C	$0.003<K_C<0.2$
4	Correction time constant (s)	T_C	$0.1<T_C<20$
5	Limb motion gain	k_1	$0.1<k_1<5.0$
6	Limb motion time constant (s)	T_1	$0.1<T_1<5.0$
7	Muscle motion gain (1/s)	k_2	$0.1<k_2<15.0$
8	Muscle motion time constant (s)	T_2	$0.1<T_2<2.0$
9	Trailer roll angle prediction gain	$K_{\phi s}$	$0.0<K_{\phi s}<100.0$
10	Trailer roll angle prediction time (s)	$\tau_{\phi s}$	$-2.0<\tau_{\phi s}<2.0$
11	Articulation rate prediction gain (rad/rad/s)	K_γ	$0<K_\gamma<100$
12	Articulation rate prediction time (s)	τ_γ	$-2.0<\tau_\gamma<2.0$
13	Tractor lateral acceleration prediction gain (rad/m/s^2)	K_{at}	$0<K_{at}<100$
14	Tractor lateral acceleration prediction time (s)	τ_{at}	$-2.0<\tau_{at}<2.0$

5.4 MODEL VALIDATION

The Equations (5.1) to (5.11) in conjunction with the equations of motion for linear (LYPR) and nonlinear (NYPRMF) yaw plane with roll-DOF, presented in Chapter 2, are solved under the directional maneuvers shown in Figure 5.2. The figure illustrates the coordinates of different paths followed by the vehicle during an obstacle avoidance maneuver. The maneuver '3' refers to highest degree of severity while the maneuver '1' corresponds to a least severe maneuver. The model validation in this study is attempted under a less severe maneuver '1'. The minimization function, Equation (4.1), is then solved to identify the driver model parameters. The minimization of the performance index was performed with different starting values of the model parameters, and the solutions were examined for convergence to a global optimum. The different runs converged to a single set of model parameters, which are presented in Table 5.2 for the linear and nonlinear vehicle models. The resulting directional response characteristics of the driver-vehicle model are compared with the field measured data, reported by Billing

and Mercer [190], to demonstrate the validity of the model and the identified parameters, where the vehicle speed is held constant at 58km/h. Figure 5.3 illustrates the comparison of front wheel steer and articulation angle response characteristics of the driver-vehicle model. The analytical and experimental results exhibit very similar patterns, and a very good agreement can be observed between the measured data and both the nonlinear and linear models. The good agreement is also observed between the lateral acceleration response characteristics derived from the analytical models and the field measured data, as shown in Figure 5.4.

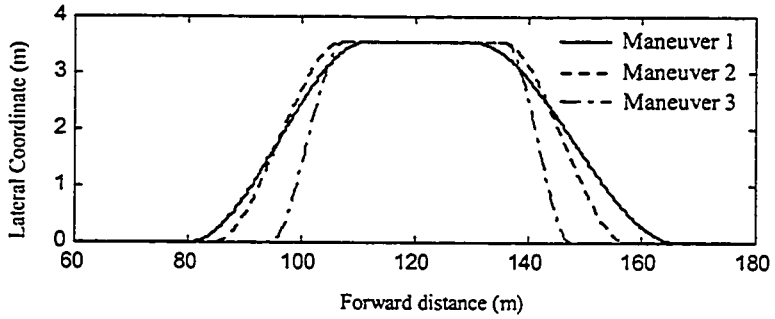

Figure 5.2: Lateral position coordinates of the selected evasive maneuvers.

Table 5.2: Driver parameters of the CCDAVM derived using maneuver '1' (u_1=58km/h).

No.	Parameters	Value (nonlinear vehicle model)	Value (linearized vehicle model)
1	T_p (s)	1.51	1.45
2	λ	0.47	0.43
3	K_C (rad/m)	0.116	0.112
4	T_C (s)	6.51	6.06
5	k_1	1.37	1.21
6	T_1 (s)	2.62	2.58
7	k_2 (1/s)	9.73	9.31
8	T_2 (s)	0.73	0.75
9	K_{ds}	0.71	0.64
10	τ_{ds} (s)	0.041	0.043
11	K_γ (rad/rad/s)	0.97	0.91
12	τ_γ (s)	0.055	0.057
13	K_{at} (rad/m/s^2)	0.59	0.51
14	τ_{at} (s)	0.038	0.042

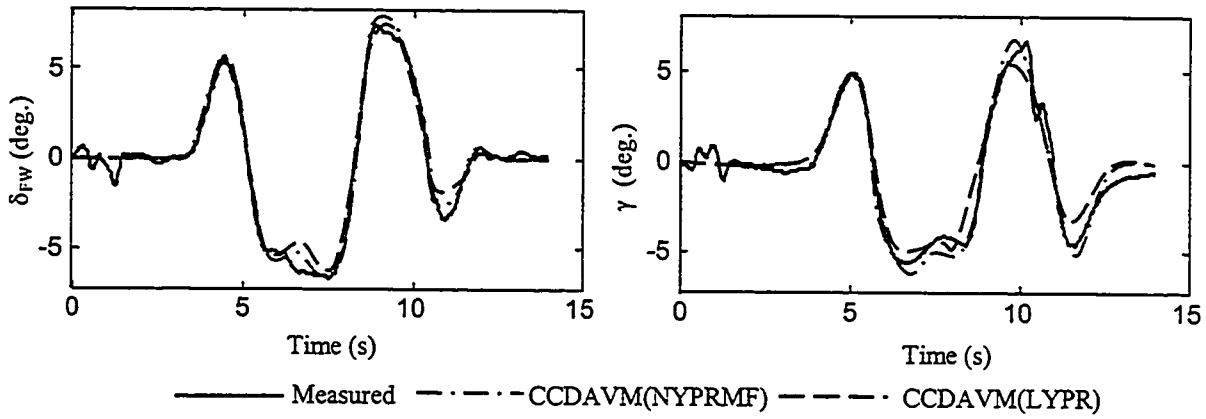

Figure 5.3: Comparison of front wheel steer angle and articulation angle response with the measured data.

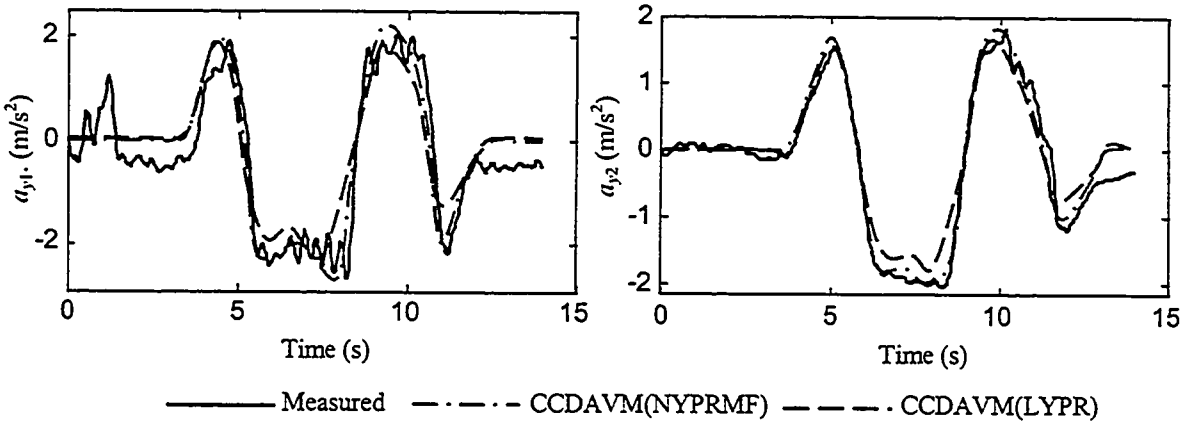

Figure 5.4: Comparison of lateral acceleration response of the tractor and trailer with the measured data.

The driver model parameters identified under the selected maneuver are further examined in relation to the range of values reported in the literature under similar maneuvers. The preview time of 1.51s for nonlinear vehicle model (denoted as NYPRMF) and 1.45s for linearized vehicle model (denoted as LYPR) are observed to be lower than those reported from the experimental studies on two-axle vehicles subjected to a slalom course or turning on tight curves, which range from 2-4s [139, 140]. The identified values of 1.51s and 1.45s, however, are closer to 1.7-2.0s range proposed by

Mclean and Hoffmann [142] through measurements under restricted maximum preview distance.

The path following coefficient identified from the study (λ=0.47 for NYPRMF and 0.43 for LYPR), lie within the range of reported values, $0.3 \leq \lambda \leq 0.5$ [148]. The proprioceptive gain and time constant associated with muscle spindle response, (k_1=1.37 and T_1=2.62 for NYPRMF; and k_1=1.21 and T_1=2.58 for LYPR) also correlate reasonably well with the reported values of k_1=1.0 and T_1=2.5s. The corresponding gain of muscle tissues movement, k_2=9.73 for NYPRMF and k_2=9.31 for LYPR, also correlate well with the reported value of 10. It should be noted that the reported value for proprioceptive time constant associated with muscle tissues movements (T_2) is chosen to cancel the lowest frequency nonzero pole in the vehicle dynamics, while the value of T_2=0.73 for NYPRMF and 0.75 for LYPR identified in this study corresponds closely with the lowest pole (s=1.34) of the characteristic polynomial of the linearized vehicle system. The values of path correction gain, K_C=0.116 rad/m for NYPRMF and 0.112 rad/m for LYPR, and the compensation time constant, T_C=6.51 for NYPRMF and 6.06 for LYPR, also correlate well with the respective reported values of 0.108 (rad/m) and 10s, respectively [148, 135].

It should be noted that parameters $K_{\phi s}$, $\tau_{\phi s}$, K_γ, τ_γ, K_{at}, and τ_{at}, have not been reported in literature thus far, due to lack of studies on heavy vehicle-driver interactions. The values of these parameters obtained in this study thus need further experimental validations. The results show some interesting trends in prediction times of various motion cues. The prediction time for the trailer sprung mass roll motion ($\tau_{\phi s}$) is slightly longer than that for the tractor lateral acceleration (τ_{at}), but considerably shorter than that for the articulation rate (τ_γ). These results imply that the driver is required to predict the

roll angle and lateral acceleration much quicker than the articulation rate, in order to perform the maneuver in a highly efficient manner. It can be further seen that the model parameters derived from NYPRMF and LYPR models are quite comparable, which implies relatively smaller contributions due to nonlinear cornering properties of tires under the maneuver considered.

5.5 DYNAMIC RESPONSE OF COUPLED DRIVER/VEHICLE SYSTEM

The control performance limits of the driver and thus the directional response of the vehicle are strongly influenced by the dynamic behaviour of the vehicle, severity of maneuver, vehicle speed, and external disturbances. The various vehicle maneuver and environmental factors further pose varying control demands on the driver. The articulated vehicle driver model, proposed in the previous section, can be effectively used to study the influence of vehicle speed, maneuver and some of the environmental factors on the control demands posed on the driver and the directional response of the vehicle. In this section, the coupled driver-vehicle system model comprising linear yaw plane model of vehicle with roll-DOF is analyzed to enhance knowledge of the driver behaviour as functions of vehicle speed, maneuver severity and steering disturbance. The results of the analyses are discussed below.

Influence of Evasive Maneuver Severity

The response characteristics of the driver-vehicle model subject to evasive maneuvers of varying severity are analyzed to study the influence of the maneuver on the driver behavior. The analyses are performed for three different maneuvers, while the

severity of the maneuver is increased by reducing the gate width, as shown in Figure 5.2. Maneuver 3 is considered most severe, while maneuver 1 can be considered as the least severe one. An examination of the resulting driver model parameters, presented in Table 5.3, can provide significant insight into the effects of the severity of the maneuver on the driver behavior. The preview time T_p tends to decrease with increasing severity of the maneuver, while the path-following coefficient λ increases, indicating that an increase in the maneuver severity poses increased demands on the driver's path prediction and following abilities. This behavior can also be observed from the lateral position error response of the tractor, which increases considerably with increase in the maneuver severity, as shown in Figure 5.5. The corresponding lateral coordinates of the trailer path are also illustrated in the Figure.

Table 5.3: Driver model parameters identified for various evasive maneuvers (u_1=58km/h).

No.	Parameters	Maneuver 1	Maneuver 2	Maneuver 3
1	T_p	1.45	1.40	1.21
2	λ	0.43	0.45	0.53
3	K_C	0.112	0.114	0.118
4	T_C	6.06	6.11	6.39
5	k_1	1.21	1.25	1.30
6	T_1	2.58	2.41	2.32
7	k_2	9.31	9.10	8.74
8	T_2	0.75	0.74	0.73
9	$K_{\phi s}$	0.64	0.67	0.69
10	$\tau_{\phi s}$	0.043	0.045	0.048
11	K_γ	0.91	0.94	0.98
12	τ_γ	0.057	0.058	0.060
13	K_{at}	0.51	0.48	0.43
14	τ_{at}	0.042	0.043	0.045

The gain K_{at} associated with the driver's prediction of the lateral acceleration of the c.g. of the tractor tends to decrease with the increase in maneuver severity, while the

corresponding prediction time τ_{at} tends to increase. This behaviour can be related to the increase in tractor's lateral acceleration response under a severe maneuver, as shown in Figure 5.6, which facilitates its perception by the driver. The variations in the rearward amplification, however, may pose increasing demands on the driver in predicting the trailer's lateral acceleration thus decreasing the prediction gain of the tractor's lateral acceleration. The proprioceptive gain k_1 associated with the activity of the muscle spindle and limb motion increases with the increasing maneuver severity, while the corresponding time constant T_1 decreases, which represent increasing demand on the muscle activity and its rate. This behavior can be related to rapid increase in the steering action required to undertake a severe maneuver, as shown in Figure 5.7.

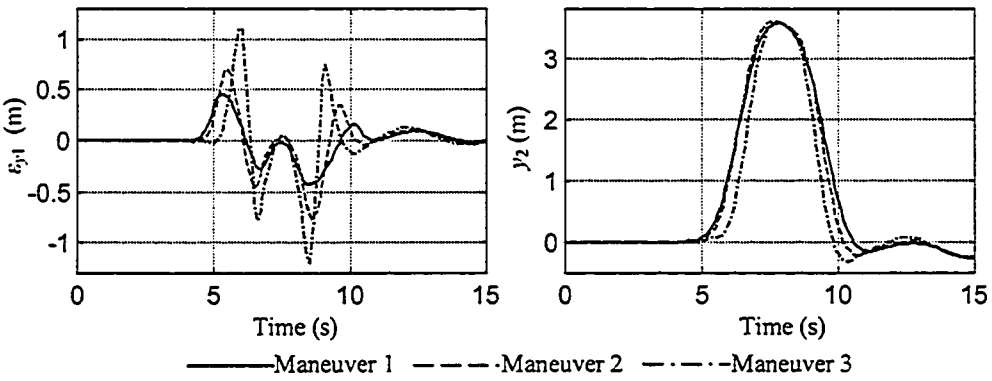

Figure 5.5: Influence of maneuver severity on the lateral position error.

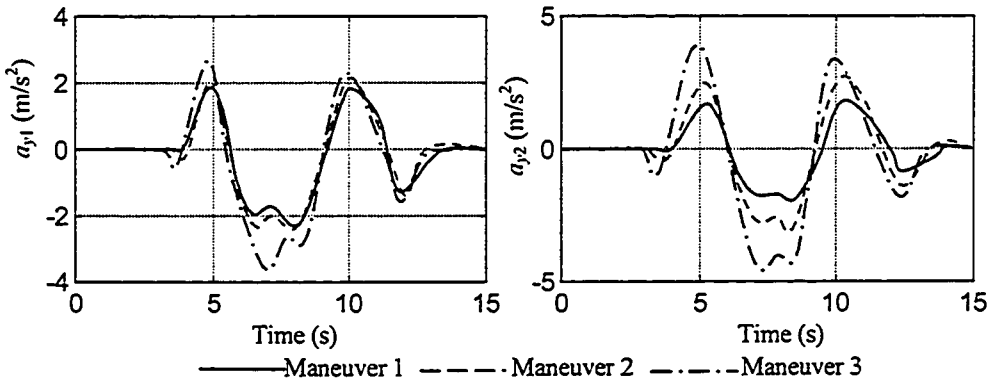

Figure 5.6: Influence of maneuver severity on the lateral acceleration response of the tractor and the trailer.

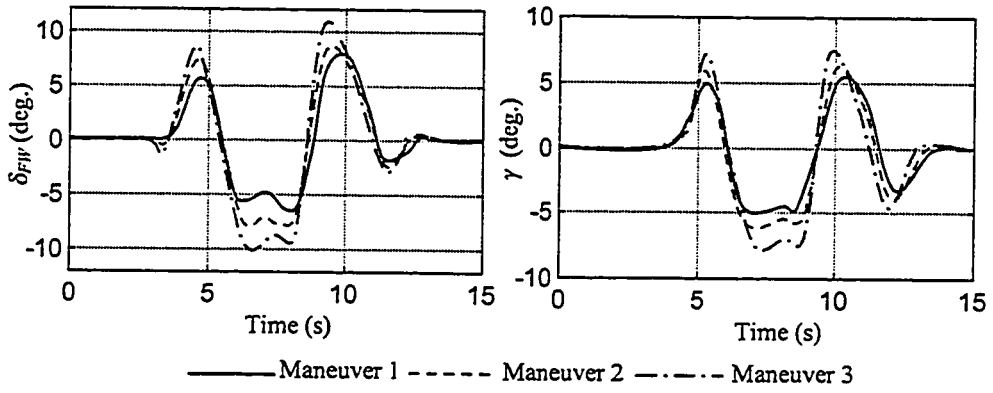

Figure 5.7: Influence of maneuver severity on the steer angle and articulation angle response.

The gain K_γ and prediction time τ_γ associated with the driver's prediction of articulation rate tends to increase with increase in the maneuver severity. This behaviour can be related to the driver's attention to the increase in the articulation angle (γ) response with the increase in maneuver severity, as shown in Figure 5.7. The gain k_2 associated with muscle tissue dynamics tends to decrease, while the decrease is only 2.26% for maneuver 2, and approximate 6.12% for maneuver 3. The time constant T_2 associated with the muscle tissues tends to decrease, while the decrease is only 1.33% for maneuver 2, and 2.67% for maneuver 3. The increase in K_C and T_C with increasing maneuver severity represent higher and rapid path correction abilities of the driver. The gain $K_{\phi s}$ and time $\tau_{\phi s}$ associated with the driver's prediction of the roll angle of the sprung mass of the trailer tend to increase with increase in maneuver severity, which can be related to the driver's attention to the rapid roll angle response of the sprung mass of the trailer with increase in the maneuver severity, as shown in Figure 5.8.

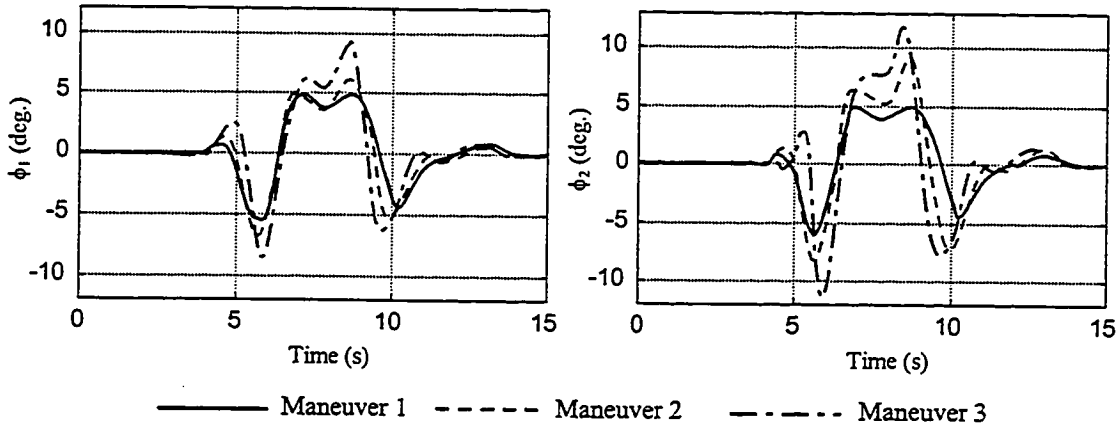

Figure 5.8: Influence of maneuver severity on the roll angle response of the tractor and the trailer.

Influence of Vehicle Speed

Many reported studies have clearly demonstrated that the preview time is strongly related to the vehicle speed [31,32,142]. The driver model parameters, associated with driver perception, reaction and correction abilities, are also known to be related to vehicle speed. The performance index, formulated in Equation (4.1), is thus solved under maneuver 1 performed at varying forward speeds, in order to study the influence of vehicle speed on the various driver model variables. The preview time tends to increase with increase in vehicle speed in a more or less linear manner at speeds below 90 km/h, as shown in Figure 5.9(a). The approximately linear relationship between vehicle speed and the preview time has also been reported by Kondo and Ajimine [140] under straight line driving and tight curve maneuvers. The result further shows a rapid change in preview time at speeds exceeding 100 km/h, which has also been observed in the study reported by McLean and Hoffmann [142]. It is speculated that a reduced preview for a typical driver increases his level of anxiety, whereas a larger visual field helps the driver to undertake necessary path correction more comfortably, thereby decreasing the degree

of steering effort. The driver's level of anxiety increases with the increase in vehicle speed, larger preview time and smaller correction gain are thus needed.

Figure 5.9(b) illustrates the influence of vehicle speed on the path following coefficient, λ. The results show that the coefficient decreases nearly linearly with increasing vehicle speed. It should be noted that an increase in λ yields a higher contribution of the path orientation error. A decrease in λ value at higher speeds thus poses more emphasis on the prediction and control of the lateral position error. It further implies that the effective preview time increases with vehicle speed. The driver pays much more attention to the lateral path position error than the change in path curvature at higher speeds. These observations are further supported by the range of values ($\lambda \leq 0.5$) and trends reported by Guo and Guan [149].

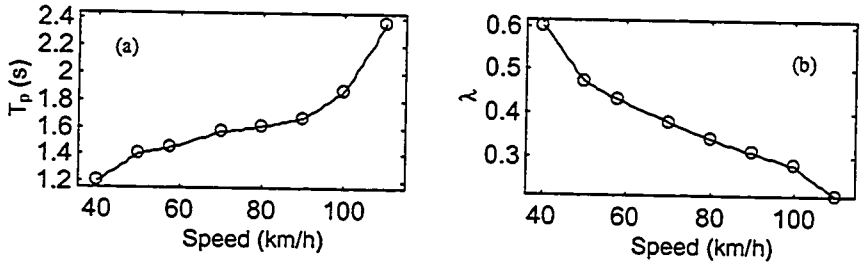

Figure 5.9: Influence of speed on: (a) preview time; and (b) path following coefficient.

The corresponding path correction gain (K_C) decreases, while the first-order path compensation time constant (T_C) increases with vehicle speed, as shown in Figure 5.10. The results indicate relaxed requirements on the path correction abilities of the driver at higher speeds. The variations in K_C and T_C are also approximately linear with the vehicle speed.

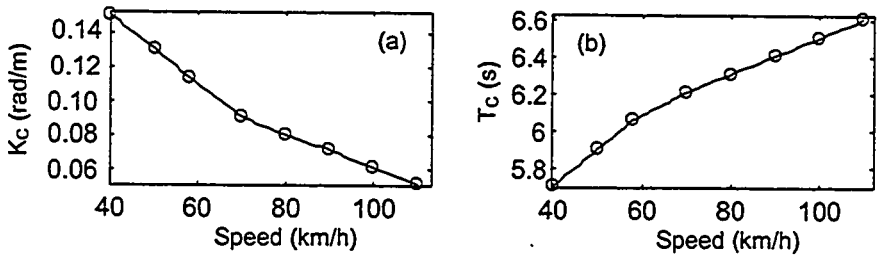

Figure 5.10: Influence of speed on compensatory gain and time constant.

From Equation (5.9), it can be seen that the rate of proprioceptive feedback derived from the motion of the human limbs increases with increase in the time constant T_1. The proprioceptive feedback rate derived from the motion of muscle tissues, however, increases with the increase in time constant T_2. The intensities of proprioceptive feedback derived from the motion of human limbs and the muscle tissues are directly related to the gains k_1 and k_2, respectively. The increase in vehicle speed, however, affects the feedback variables arising from the motion of limbs and muscle tissues, in a contradictory manner, as shown in Figure 5.11. The limb motion feedback gain k_1 and time constant T_1 increase with increase in vehicle speed, while the gain k_2 and time constant T_2, associated with the muscle tissues motion, decrease. It is speculated that variations in proprioceptive feedback are related to the tension state of the driver. An increase in the tension at higher speeds can cause fatigue and thus slower reaction time. The results presented in Figure 5.11 reveal that the path compensation at higher speeds necessitates rapid limb movements, while the demands on the efforts from the muscle tissues can be relaxed.

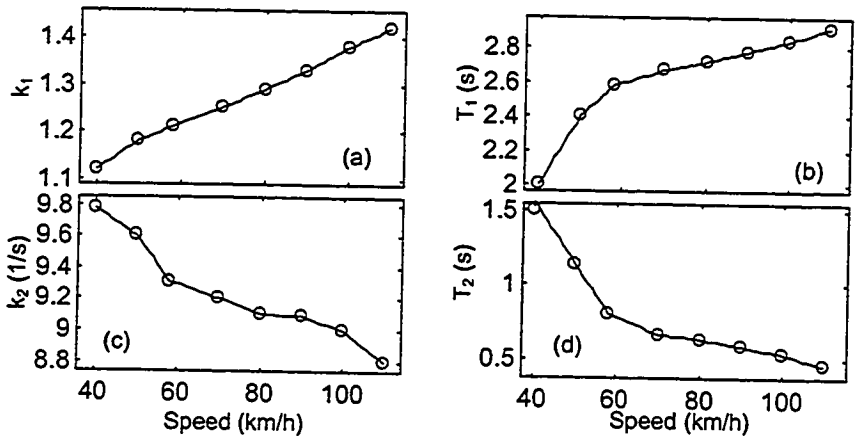

Figure 5.11: Influence of vehicle speed on the proprioceptive element parameters.

Figure 5.12 shows the influence of vehicle speed on the driver's prediction gain ($k_{\phi s}$) and time ($\tau_{\phi s}$) of the roll angle of the sprung mass of the trailer. It can be seen that both the gain and the time decrease with the increase in vehicle speed, which indicates a shorter time is needed to predict the roll angle response of trailer but smaller gain is required to make the whole system stable. Similarly, the influence of vehicle speed on the driver's prediction gain (k_γ) and time (τ_γ) of the articulation rate is illustrated in Figure 5.13. Both the gain and the time decrease with increase in vehicle speed, which means that a shorter time is required for the driver to predict the articulation rate but smaller gain is needed to make the whole system stable. Figure 5.14 illustrates the influence of vehicle speed on the driver's prediction gain (k_{at}) and time (τ_{at}) of the lateral acceleration of c.g. of tractor. Both the gain and time tend to decrease with increase in vehicle speed, which also indicates a shorter time is needed for the driver to predict the lateral acceleration and smaller gain is required to make the system stable. It can be further derived that the increase in vehicle speed leads to the increase in the dynamic response of the vehicle, thus

the roll angle of the trailer, articulation rate and the lateral acceleration of the tractor increase. Such an increase can improve the driver's prediction to these signals.

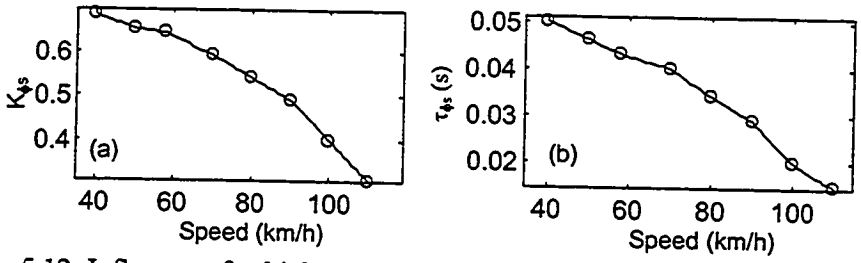

Figure 5.12: Influence of vehicle speed on the trailer roll angle prediction gain and time.

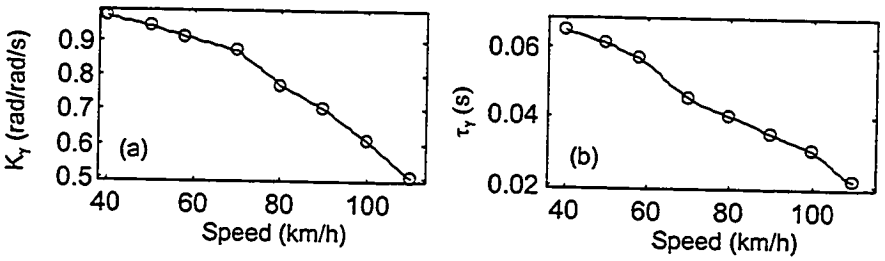

Figure 5.13: Influence of vehicle speed on the articulation rate prediction gain and time.

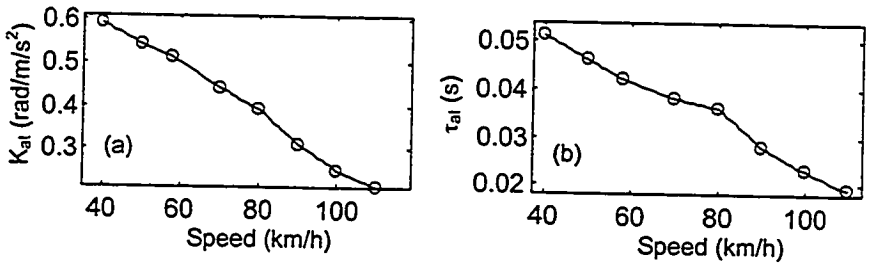

Figure 5.14: Influence of vehicle speed on the tractor lateral acceleration prediction gain and time.

Influence of External Disturbances

The dynamic response of a vehicle, in general, is influenced by various inputs, including the driver's steering angle, road excitation and cross wind. The driver's steering angle is primarily derived from the previewed path, the presence of road obstacles and the driver's remnant, which is defined as part of the driver's steering response that is not deterministically related to the closed-loop driver/vehicle system input, i.e., the previewed

path. It has been established that such definition of remnant can qualitatively account for the truly random component of the driver's output [26]. In this study, the remnant is considered to present random disturbances arising from either the driver's actions or the external sources, which are not included in the vehicle and the driver models. The analyses are performed to investigate the influence of the external disturbances on the driver's directional control behaviour. The external disturbance is represented by a normally distributed white noise signal with limited bandwidth. The peak value of the random signal is considered as 0.1 degree added to the front wheel steer angle, while the frequency bandwidth is considered to range from 0 to 30 Hz. The power spectral density of a typical normally distributed white noise signal, with limited bandwidth of 30 Hz, representing the disturbance of the front wheel steer angle, is illustrated in Figure 5.15.

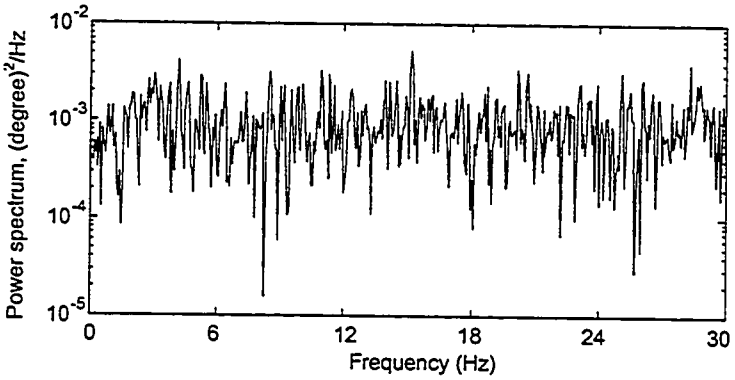

Figure 5.15: A typical normally distributed white noise signal with limited bandwidth.

Figure 5.16(a) illustrates the influence of the noise frequency bandwidth (NFB) on the preview time. It can be seen that the preview time tends to increase with the increase in the NFB until 10 Hz. This result indicates that the driver is sensitive to the contributions of the external noise under 10Hz, and a longer preview time is needed to stabilize the driver/vehicle system under higher frequency disturbances. The external disturbances occurring at frequencies above 10 Hz, however, do not influence on the

preview time. The influence of the NFB on the path following coefficient is illustrated in Figure 5.16(b). It can be seen that the influence is similar to that for preview time. The increase in NFB leads to an increase in path following coefficient for NFB lower than 10 Hz, which means that the driver is needed to concentrate more on the orientation of the previewed path, while the NFB higher than 10 Hz has no influence on path following coefficient.

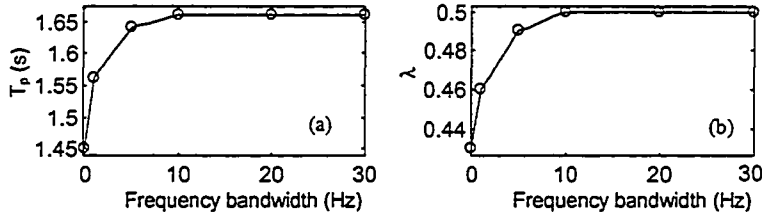

Figure 5.16: Influence of NFB on: (a) the preview time; and (b) path following coefficient.

Figure 5.17 illustrates the influence of the NFB on the driver's compensatory gain and time constant. It can be seen that the gain tends to decrease and the time constant tends to increase, with an increase in the NFB until it approaches 10 Hz. The results further show that the noise with NFB lower than 1 Hz affects the compensation abilities of the driver more significantly. These results indicate that the driver is more sensitive to lower frequency disturbances than the higher frequency disturbances.

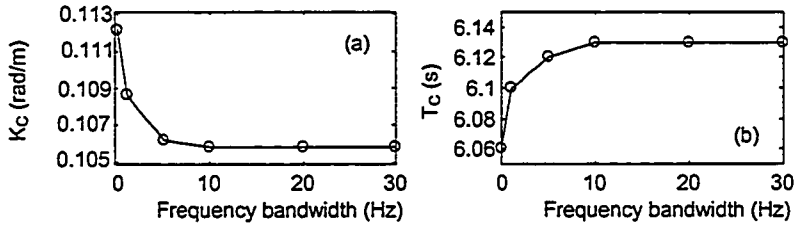

Figure 5.17: Influence of NFB on the compensatory gain and time constant.

The influence of NFB on the proprioceptive elements is shown in Figure 5.18. It can be seen that the increase in NFB leads to an increase of the limb motion feedback gain k_1 and time constant T_1. The time constant T_2 and gain k_2 associated with the muscle tissues motion, however, decreases with increase in NFB, when NFB is lower than 10 Hz. As stated in the previous section, the variations in proprioceptive feedback are related to the tension state of the driver. An increase in the tension under the disturbance of higher frequency noise can cause fatigue and thus slower reaction time. The results presented in Figure 5.18 reveal that the path compensation at higher NFB necessitates rapid limb movements, while the demands on the efforts from the muscle tissues can be relaxed. The driver's proprioceptive elements, however, are not affected significantly under disturbances with NFB greater than 10 Hz.

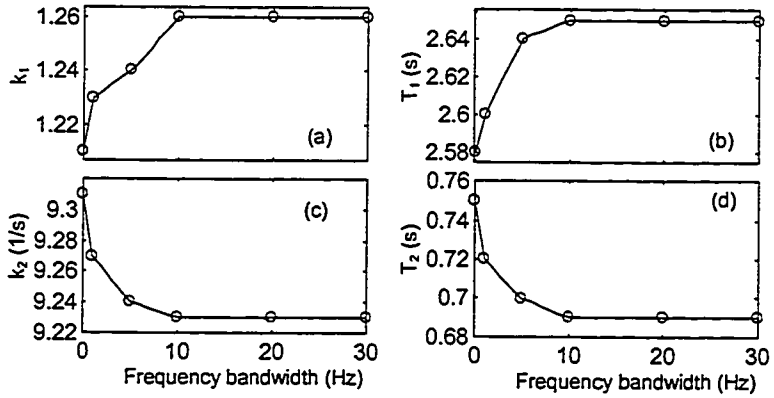

Figure 5.18: Influence of NFB on the proprioceptive element parameters.

Figure 5.19 illustrates the influence of NFB on the driver's prediction gain and time on the roll angle of the sprung mass of trailer. It is shown that the gain and the time tend to decrease with increase in NFB for NFB lower than 10 Hz. This result indicates that the disturbances with higher frequency components (up to 10 Hz) yields faster

response, and thus the driver is required to predict the roll angle of the trailer within a shorter time. The required gain, however, is small, such that the driver/vehicle system remains stable. The results presented in Figure 5.20 and 5.21 reveal similar influence of the NFB on the driver's prediction gain and time of the articulation rate and the lateral acceleration of c.g. of the tractor, respectively. It can thus be concluded that steering disturbances with frequency bandwidth lower than 10 Hz yield considerable influence on the driver's prediction abilities. The prediction gain for the trailer roll angle under disturbances at 10 Hz decreases by 9.38%, when compared with that obtained at 0 Hz. The corresponding decreases in articulation rate and lateral acceleration are obtained as 9.89% and 19.61%, respectively. Similarly, an examination of prediction times at 0 Hz and 10 Hz, reveals that the $\tau_{\phi s}$, τ_{γ} and τ_{at} decrease by 13.59%, 12.28% and 16.67%, respectively, when NFB is increased to 10 Hz.

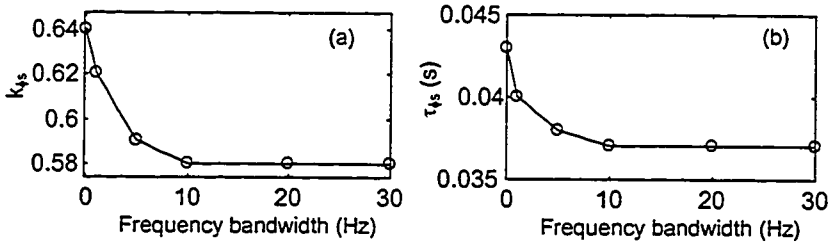

Figure 5.19: Influence of NFB on the trailer roll angle prediction gain and time.

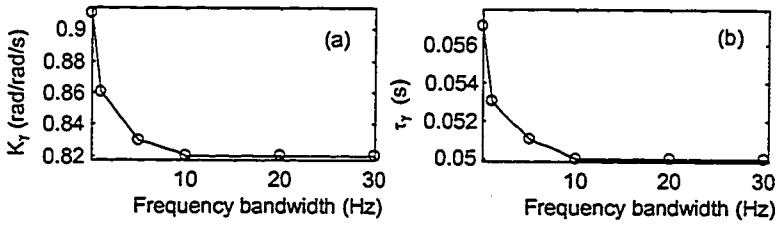

Figure 5.20: Influence of NFB on the articulation rate prediction gain and time.

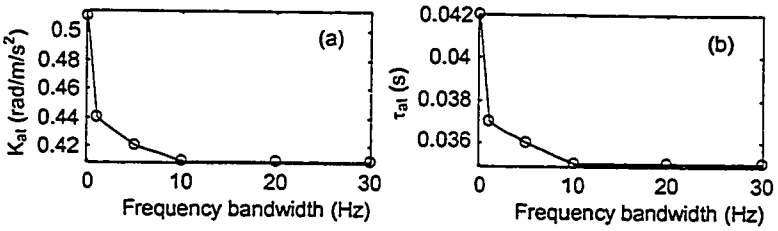

Figure 5.21: Influence of NFB on the tractor lateral acceleration prediction gain and time.

5.6 SUMMARY

A comprehensive driver-articulated vehicle model, incorporating linear and nonlinear yaw plane vehicle models with limited roll-DOF, is proposed to analyze the dynamic response under three evasive maneuvers with different severity. The proposed driver model is validated by comparing the analytical response with the field measured data. The comparison revealed reasonably good agreement between the analytical response and the measured data. Both the linear and nonlinear vehicle models results in good correlation with the measured data. The proposed driver model is further applied to study the influence of the vehicle speed, maneuver severity and external steering disturbance on the driver model parameters and the vehicle response. The results show that articulated vehicle drivers are required to adapt themselves to different maneuvers, speed and external disturbances to maintain optimal path tracking performance and safe dynamic response. The results suggest that the dynamic safety performance of such vehicles can be significantly enhanced when the driver parameters representing the control demands are incorporated into the vehicle design process. The coupled driver-articulated vehicle model is thus further applied in the following chapter to explore the adaptation of the vehicles to different drivers.

CHAPTER 6 ADAPTING VEHICLE TO THE DRIVER

6.1 INTRODUCTION

The safety dynamics and performance characteristics of a heavy vehicle are strongly influenced by its various design and operating parameters. While the weights and dimensional regulations limit the variations in axle loads and some of the geometry parameters of the vehicles, various other design parameters tend to vary considerably. These may include loading practices, coordinates of the sprung mass c.g., tire sizes and properties, suspension properties, articulation properties, etc. The directional response characteristics of the vehicle vary considerably with variations in many design parameters, as demonstrated in the results of the sensitivity analyses presented in Section 3.2. The drivers, in general, adapt to the vehicle directional response behaviour through their prediction and correction abilities. The driver's control actions are generally limited to braking and steering, which are undertaken with certain perception and reaction delays. The direction control performance characteristics of the drivers are limited by their reaction delays, neuromuscular delays, compensatory gains, visibility, preview and prediction abilities, etc.

The safety performance of such vehicles may be considerably enhanced by integrating the driver performance limits in the vehicle design process. The vehicle design may be realized to attain adequate path tracking and stable directional response under the constraints posed by the control performance limits of the driver. The coupled driver-vehicle model, developed and validated in Chapter 4, can be used in conjunction with the performance limits of the driver to derive most desirable design parameters for

the articulated vehicle. The resulting vehicle design can thus be considered to adapt to the driver and its performance limits.

In this Chapter, a concept of adapting an articulated vehicle to the driver's performance skills is explored. The limitations of the driver's directional control performance are discussed, in view of the reaction time, visibility, compensatory gain, and frequency range of driver's directional control. The performance limits are discussed for different drivers with varying skill levels. The closed-loop driver-vehicle model is then analyzed to derive most desirable vehicle parameters, including the geometrical and dynamic parameters.

6.2 DRIVER'S DIRECTIONAL CONTROL AND PERCEPTION LIMITATIONS

The dynamic behaviour of a human driver as the controller and sensor in a closed-loop driver/vehicle directional control system is subjected to extensive variations due to the differences in the operating conditions, gender, age, experience, etc. The directional performance of the vehicle is thus strongly influenced by the variations in the driver behaviour, which may be enhanced by integrating the driver into the design process. The design of a vehicle should thus include such variations in the driver's dynamic behaviour, since drivers with varying skills may drive the vehicle. It is thus vital to enhance an understanding of the driver's directional control behaviour and limitations in order to attain safer vehicle design. The significance of various driver control characteristics in view of vehicle control is thus discussed in the following sections. The data reported in various studies are further reviewed in an attempt to quantify the range of control characteristics of the driver population.

6.2.1 Reaction Time

The reaction time of a driver relates to the time taken by the driver to perceive and respond to an emergency situation or an emerging directional instability. The reaction time represents the time delay between the instant at which an emergency is perceived and the instant when a correction action is performed by the driver. The driver reaction time thus forms an important design parameter not only for the vehicle designer but also for the roadway designer. The response reaction time of a driver, however, is related to various information processing stages, which occur from the presence of a stimulus until the individual responds. Based upon the study performed by Perchonok and Pollack [144], the reaction time can be divided into four stages, as shown in Figure 6.1. The initial stage involves detection, during which the driver develops a conscious awareness of a possible event. The event may include an obstacle on the road, onset of a possible instability, or considerable path deviation. It should be noted that an obstacle may lie within the driver's field of view for certain time prior to its detection. Furthermore, the roll directional instabilities mostly initiate at the trailer wheel-road contact and driver tends to detect the onset of possible roll instability with certain delay [191]. The detection of trailer yaw oscillation and path deviations also involve certain delays in their detection by the driver. A significant time delay may thus exist between the presence of a stimulus and its detection. The detection of an event, in general, involves the eye movement and focus on the central portion of the retina, before subsequent action is undertaken.

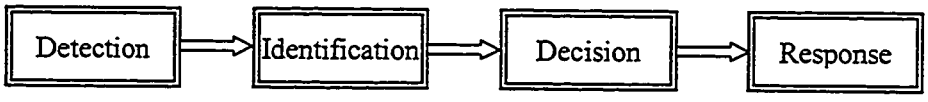

Figure 6.1: Four stages of response reaction.

In the second stage, referred to as the identification stage, the driver acquires sufficient information to identify the nature of the event. An adequate information, however, is necessary for the driver to undertake a decision for action, which involves certain time lapse. For example, the presence of an obstacle on the road is identified as a stationary or moving object with an estimate of its speed. A path deviation may be identified in terms of its magnitude and direction. An emerging vehicle instability or oscillation may be identified by its nature and severity. Following the detection and identification of an event, the driver undergoes the decision stage, which involves information processing and the choice of most desirable control action, such as steering, braking or acceleration. In the final stage, referred to as the response stage, the commands are issued by the motor center of the brain to the appropriate muscle groups to carry out the required actions.

The overall response reaction time of a driver is related to the drivers perception, processing and decision making abilities. The response reaction time is thus known to vary considerably among the drivers with varying skill and experience levels. Many other studies have concluded that major factors affecting the response time include:

- Driver's expectancy, which indicates the anticipation of an event [192];
- Use of drugs and driver fatigue, which affect the response time in an adverse manner [193];
- Driver age, it has been reported that perception-response time increases with age. The response reaction time, ranging from 0.44s to 0.52s, has been reported for different age groups [120].

It has also been reported that driver's reaction time is considerably smaller during normal control tasks, since the driver is able to make effective use of the preview effect

during the detection and identification stages [120]. The time delay associated with these two stages is thus considered negligible. Based upon the reported data, the range of driver response reaction time is considered to vary in the 0.1-0.5s, which represents the variations in the nature of event, driver skill, fatigue and age.

6.2.2 Visibility and Preview Distance

Visibility affects the detection and identification of an event and thus the preview distance. A quantifiable description of visibility, however, is extremely complex due to extreme variations in various environmental factors, and individual's perception of the visual field. Many studies have been attempted to quantify the affect of visibility on the directional and safety performance of vehicles, and to identify the threshold of visibility [120, 145]. Based upon analyses related to vehicle safety performance, Sivak et al. [145] suggested that a reasonable criterion for sufficiency of visibility distance is the distance needed to bring the vehicle to full stop, the stopping distance of the vehicle. The proposed visibility requirement is thus strongly dependent upon the vehicle speed, the road condition, braking performance of vehicle, the weather and light conditions (day or night).

The driver's preview distance is mostly governed by the visibility and maneuver difficulty (curvature, road adhesion, speed). Many studies performed primarily on control behaviour of single unit vehicles have identified the preview distance as one of the most critical factors related to the control performance. The results on directional dynamics of multiple unit vehicles, presented in Chapters 4 and 5, further emphasize the important significance of the preview distance. It shows that the preview distance (time) strongly depends upon the maneuver severity, speed and the driver's skill level in terms of

compensatory gain, reaction time and prediction strategies. Many experimental studies have been performed either in the field or on the driving simulator to identify a range of preview distance under varying constraints imposed on the field of vision [139-141]. These studies have reported a wide range of driver's preview distance, ranging from 15.2 m to 128m, depending upon the test conditions. Apetaur [100] suggested that the driver's visibility ranges from 10 m (during driving in fog conditions) to 300 m (high speed highway driving). A definite relationship exists between the visibility and the preview distance. As the preview distance required under specific speed and driving conditions exceeds the visibility, the directional control abilities of the driver are seriously deteriorated. Under such conditions, the drivers are required to reduce the vehicle speed in order to decrease the required preview distance such that it does not exceed the visibility. In the present study, the preview distance of the driver is thus limited by the visibility.

6.2.3 Compensatory Gain

The compensatory gain, in general, reflects the driver's ability to correct the perceived path tracking error. While the path deviations are strongly related to coupled driver-vehicle system dynamics, the path tracking performance of the vehicle are closely related to driver's perception and compensation ability. A compensation gain can be interpreted as a driver's primary adjustment coefficient, which is almost inversely proportional to the bandwidth of the input spectrum when the driver tries to track a randomly varying signal. It has been reported that the limiting values of product of bandwidth and the gain range from 1.5Hz to 2.0 Hz for low-frequency input spectra [19]. The compensatory gain is chosen by the driver, such that the tracking error is minimum

while the closed-loop driver-vehicle system remains stable. Different drivers, however, reveal varying compensation abilities or gains in terms of steering correction, while controlling similar path tracking errors. Such variations are attributed to variations in individual driver's judgment and/or psychological preparation to face the path tracking error and thus to control their vehicles along the expected path. Such judgments involve individual's perception of the difference between the previewed path and the predicted path, and are affected by the vehicle speed, preview distance, visibility, etc. Although a clear knowledge of the internal mechanism of this phenomenon does not yet exist, it has been established that the path tracking error compensatory gain is related to the driver's subjective attitude and experience [21, 22]. While an experienced driver assumes relatively smaller gain to compensate for the path error, an inexperienced driver requires higher compensatory gain. Wierwille et al. [99] investigated relative compensation abilities of drivers by considering an experienced male driver and an inexperienced female driver. They concluded that the inexperienced driver resulted in smaller lateral position error and larger closed-loop system bandwidth than the experienced driver. The inexperienced female driver, however, utilized more abrupt steering wheel motions than the male driver, which indicates relatively higher compensatory gain of the inexperienced driver.

McRuer et al. [22] performed a series of tests to identify the driver compensatory gains in terms of the path position and orientation tracking errors. The study involved six car drivers with varying driving skills. A total of 44 test runs were conducted to study the driver's compensation abilities under wind gusts and curved path following at a vehicle speed of 80km/h. The study reported mean values of the compensatory gains together

with the range of variations corresponding to different tracking/regulation tasks. The compensatory gains for position error tracking under gusts and curved path following tasks were reported as 0.0722±0.0256 rad/m and 0.1270±0.0951 rad/m, respectively. The corresponding gains for orientation tracking errors were reported as 0.195±0.045 rad/rad and 0.174±0.057 rad/rad, respectively.

Reid et al [106] conducted a series of tests involving drivers performing a double-lane change task in a fixed-base driving simulator. The study involved six different drivers, where each driver performed the maneuver eight different times on a simulated full-size car at a forward speed of 50km/h. The resulting compensatory gain, which is derived from front wheel angle, for lateral position and orientation errors for the six drivers are illustrated in Figure 6.2. The test data revealed considerably larger variations in the position error gain, when compared to those observed for the orientation error gains. The mean values of the compensatory gains were obtained as 0.0662 rad/m and 3.4717 rad/rad for position and orientation error tracking, respectively. The results of the above studies clearly illustrate that the compensatory gain varies considerably among the individual drivers and with the tracking task. Furthermore, it can be found that the lateral position gains in McRuer's study and Reid's study are close to each other, while the reported orientation gains differ considerably.

An analytical study of a driver-car system, performed by Habib [131], revealed that the lateral position and orientation error compensatory gains range from 0.001 to 0.12rad/m and 0.1 to 4.8rad/rad, respectively. The study of a driver-articulated vehicle system performed in previous Chapters 4 and 5 further illustrates that the driver's compensatory gain depends strongly upon the vehicle speed, maneuver severity, and the

prediction strategies. The highest value of compensatory gain for lateral position error was obtained as 0.18 rad/m (Table 4.1), when the lateral position error of the trailing unit was employed as the feedback variable. The lowest value of the compensatory gain for lateral position error was obtained as 0.06 rad/m (Figure 5.16) as the vehicle speed approached 110km/h and when the driver's compensation is derived from various vehicle motion variables, including the lateral acceleration of the lead unit, articulation rate and roll angle of the trailing unit, and the lateral position and orientation of the lead unit. The compensatory gain for the orientation error control was further observed to be in the range of 1.8 rad/rad to 2.1 rad/rad depending upon the driver's prediction strategy (Table 4.1).

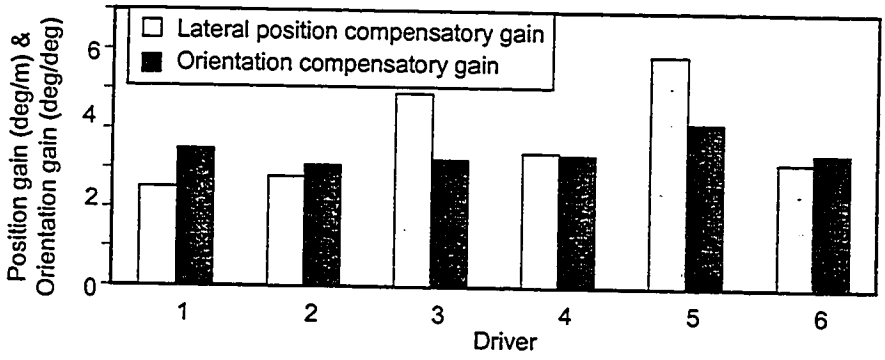

Figure 6.2: Lateral position and orientation gains of different drivers [106].

6.2.4 Driver's Steering Input

The frequency bandwidth of a driver/vehicle directional control system is strongly affected by the path input, while it is mostly determined by the driver's steering input. It is thus vital to enhance an understanding of the driver's steering spectrum in order to investigate the vehicle designs that can easily adapt to the driver under extreme situations, such as the obstacle avoidance. Although extensive studies on driver/vehicle

directional control systems have shown that the bandwidth of the driver's steering angle response is less than 1.0 Hz, an exact mean value of the bandwidth representing various drivers has not yet been identified [168,194]. Based upon experimental studies conducted by Furukawa and Nakaya [107], it has been reported that the power spectral density of the driver's steering wheel angle approaches its peak value in the vicinity of 0.75 Hz during a course-tracking task performed with a car operating at a constant speed of 80km/h. Such peak level presumably represents the driver's action for correcting a steering error. Lin et al. [194], in their recently published study, have proposed a range of predominant frequencies of driver's directional control inputs. The proposed level of steering input, however, can be considered as a "worst case scenario" for system design purposes. The power spectral density of steering wheel angle attained under such conditions is expressed as follows:

$$S_\delta(\omega) \approx \frac{0.00014}{\omega^2 + 16} \text{ rad}^2/(\text{rad/s}) \tag{6.1}$$

where $S_\delta(\omega)$ is the power spectral density of the steering wheel angle at frequency ω (rad/s), as illustrated in Figure 6.3. The spectral density of the steering wheel angle reveals that its bandwidth is approximately 2.6 rad/s.

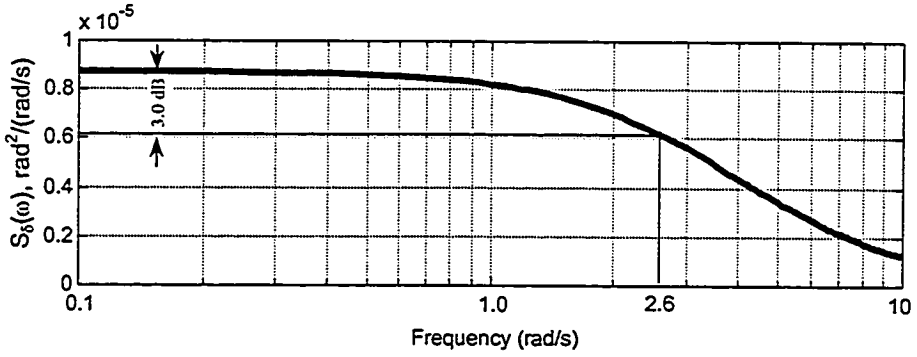

Figure 6.3: Maximum driver's steering input [194].

6.2.5 Summary of Control Performance Limits of Drivers

The driver's control limits in terms of the reaction time, preview distance, compensatory gain and steering input tend to vary considerably with individual skills, test conditions and environmental factors. From the various reported studies, it may be concluded that the reaction time for road vehicle driver ranges from 0.1 to 0.5s, depending upon the driver's age and skill. The preview distance is governed by the vehicle's speed, maneuver severity, visibility and driver's prediction strategies, which may range from 15.2m to 128m [139-141]. Higher vehicle speeds, in general, require longer preview distance. The compensatory gain is a key factor related to driver's skill and experience, which is also a function of the driver's preview and prediction strategies. The reported compensatory gain for single unit vehicle driver ranges from 0.0466 to 0.0978 rad/m for lateral position error and from 0.117 to 3.4717 rad/rad for orientation error [22, 106]. While the compensatory gain for articulated vehicle driver has not been reported in the literature. The results of the analytical study, presented in Chapters 4 and 5, reveal that the compensatory gain may range from 0.06 to 0.18rad/m, depending upon the driver's prediction strategies, maneuver severity and vehicle speed. It should be noted that the value of the compensatory gain further depends upon the steering gear ratio. The study performed by Lin et al. [194] further indicates that the driver's steering input frequency bandwidth is around 2.6 rad/s, which shows that the driver-vehicle directional control system is a low frequency system. The driver's control performance limits, considered in this study, are summarized in Table 6.1.

Table 6.1: Driver's control performance limits.

Parameters	Control limits
Reaction time (s)	0.1-0.5
Preview distance (m)	15.2-128
Compensatory gain for lateral position (rad/m)	0.001-0.18
Compensatory gain for orientation (rad/rad)	0.1-4.8
Steering frequency bandwidth (rad/s)	≈2.6

6.3 ADAPTIVITY OF VEHICLE TO THE DRIVER

Articulated freight vehicles with their excessive weight and large dimensions exhibit dynamic stability limits, which are considerably lower than those of the other road vehicles. Considerable design efforts have thus been mounted to develop active safety enhancement mechanisms and driver-friendly vehicle design. Such design efforts may be grouped into two broad classes: (i) human factors related developments; and (ii) directional dynamics related developments. The developments related to human factors include ergonomic designs of cab, driver work-station, enhanced ride comfort, etc. [10, 100]. The developments related to directional dynamics performance of vehicles have been primarily prompted by the concerns on their low stability limits. These include: developments in anti-lock brake system (ABS) to minimize the occurrence of potential yaw instability and jackknife; high roll stiffness suspension design to improve roll stability limits of vehicles; design of tires with improved adhesion performance on dry and wet surface, etc. [12, 13, 41]. Such developments, however, have evolved from the results attained from open-loop directional dynamics response of the vehicles. The contributions due to control performance characteristics or limits of driver are mostly ignored in the design process. Furthermore, the weights and dimension regulations for such vehicles have primarily evolved from the open-loop dynamic analyses of the vehicles, roadway designs and bridge formula [44, 49]. The vehicles are traditionally

designed with an assumption that the driver mostly adapts to its dynamic directional behaviour. In view of the reduced dynamic stability limits of articulated freight vehicles, and control performance limits of the drivers, it is vital to incorporate the driver's performance abilities in the design process. The directional and safety performance of such vehicles may be considerably enhanced, when control performance limits of the drivers under extreme operating conditions are appropriately taken into account. The essential vehicle design parameters may be selected such that the control requirements to minimize the peak path deviations in the vehicle response under extreme operating conditions lie within the performance limits of the driver. The resulting vehicle design may thus be considered to adapt to the driver in view of its directional performance. Such a design methodology would improve the driver's efficiency by reducing the control demands and stress on the driver.

6.3.1 Method of Analysis

The directional dynamics performance of an articulated vehicle is influenced by many design parameters, as illustrated earlier in Sections 2.3 and 3.3. A design sensitivity analysis of the coupled driver-vehicle system, involving variations in all the design parameters, may impose certain difficulties in analyses and interpretations. In this study, vehicle design parameters are lumped in five different groups to carry out design sensitivity analyses more effectively. The vehicle parameters are grouped as: (*i*) the geometry parameters; (*ii*) the weight/inertial parameters; (*iii*) the suspension parameters; (*iv*) the tire parameters; and (*v*) the fifth wheel parameters. The yaw plane model with roll DOF is analyzed in conjunction with the driver model formulated in Section 4.5. It should be noted that the widely known driver parameters are the compensatory gain,

reaction time and the preview distance. The other driver parameters mentioned in Chapters 4 and 5 have not been well recognized in the literature. The analyses are thus performed with three different drivers with varying driving abilities expressed in terms of their preview distance, compensation gain and reaction time, as described in Table 6.2. The driver 'A' exhibits superior driving skill, as demonstrated by least reaction time and compensatory gain, while driver C reveals least driving experience or skill. All the other parameters of the driver model are held fixed.

Table 6.2: Three drivers representing different driving behaviours.

Driver	Parameters			
	Reaction Time (s)	Compensatory Gain K_L (rad/m)	Maximum Steer Rate (degree/s)	Preview Distance (m)
A	0.1	0.09	360	80
B	0.25	0.15	300	60
C	0.35	0.2	250	40

The equations of motion for the yaw plane vehicle model with roll DOF coupled with the driver model employing multi-loop structure with feedback from the lateral acceleration of the lead unit, articulation rate of the combination and the roll angle of the trailing unit (MLM8) are solved for an obstacle avoidance maneuver, described in Figure 6.4. The solutions are performed using the drivers performance limits, presented in Table 6.2, together with K_H=2.56 rad/rad, K_{p1}=0.45 rad/m/s^2, K_{p2}=0.60 rad/rad/s, and K_{p3}=0.4 rad/rad. The obstacle avoidance maneuver, configured with gate length of 50m and road width of 5m at a forward speed of 100km/h, is considered to be sufficiently severe. The directional response characteristics of the vehicle are used to derive the different elements and total of the performance index, described in Equation 4.1. The total performance index, derived for each of the three drivers, is minimized to determine the most desirable values of vehicle parameters within the five groups of design parameters. The vehicle

design realized upon combining the optimal groups of parameters are then considered to adapt to the varying skill levels of the selected three drivers.

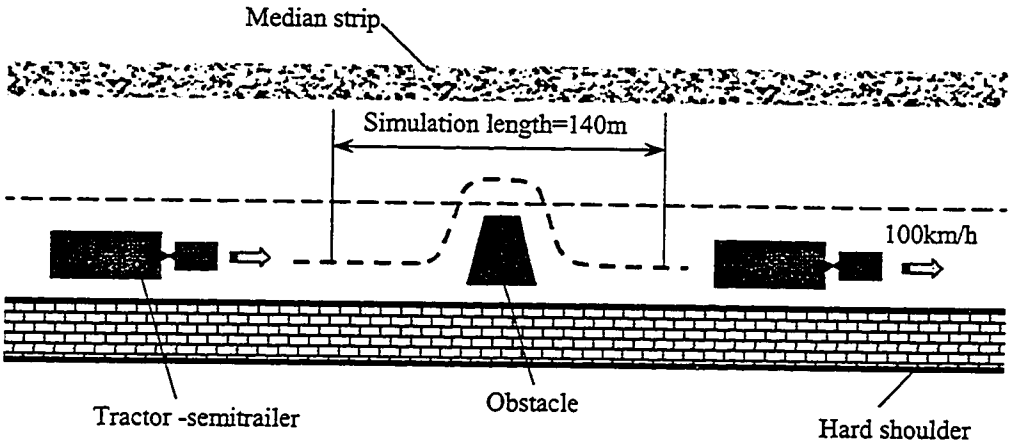

Figure 6.4: Description of the vehicle path corresponding to an obstacle avoidance maneuver.

6.4 RESULTS AND DISCUSSIONS

The performance index, described in Equation (4.1), is minimized subject to limit constraints for the concerned group of parameters, while the parameters within the remaining groups are held fixed. The resulting values of most desirable parameters and the corresponding values of components of the performance index, obtained for the three drivers, are discussed in the following subsections.

6.4.1 Identification of Desirable Range of Geometric Parameters

The results derived from the open-loop directional dynamics of articulated vehicle, presented in Section 3.3, clearly illustrate significant influence of various geometrical parameters on the dynamic characteristics of the vehicle. The most significant geometric parameters, as identified from the results of open-loop dynamics, are permitted to vary within a specified range. These include: (*i*) horizontal distance

between the tractor c.g. and the articulation point, x_{1A}; (*ii*) horizontal distance between the trailer c.g. and the articulation point, x_{2A}; (*iii*) c.g. height of the tractor, h_{g1}; (*iv*) c.g. height of the trailer, h_{g2}; (*v*) tractor wheelbase, L_t (L_t=x_{11}+x_{12}); (*vi*) distance between the first axle of trailer and its c.g., x_{21}; and (*vii*) track width of the tractor, b_{11}.

The vehicle model coupled with the driver model representing three different drivers is analyzed to derive the performance index. The most desirable values of identified geometric parameters are derived by minimizing the performance index, subject to limit constraints, which are summarized in Table 6.3 and represent possible extreme variations in the selected geometric parameters. The resulting values of optimal geometric parameters for the three different drivers are compared with the nominal values in Figure 6.5. The relative bias of the resulting geometric parameters with respect to their nominal values is illustrated in Table 6.4.

Table 6.3: Constraints of the range of geometrical parameters considered.

Name of parameters	**Range (minimum, maximum)**
h_{g1} (m)	0.8, 1.5
h_{g2} (m)	1.5, 3.5
x_{1A} (m)	0.0, 4.5
x_{2A} (m)	1.0, 8.0
L_t (m)	1.5, 6.0
b_{11} (m)	1.0, 2.0
x_{21} (m)	1.0, 6.0

Table 6.4: Relative bias of resulting geometrical parameters relative to their nominal values.

Driver	Relative bias (%)						
	h_{g1}	h_{g2}	x_{1A}	x_{2A}	b_{11}	L_t	x_{21}
A	-21.4	-22.703	-3.55	-2.84	13.19	-3.22	-2.601
B	-24.2	-25.134	-12.1	-12.7	23.03	-6.5	-5.723
C	-26.1	-27.078	-21.5	-22.3	32.87	-7.81	-12.59

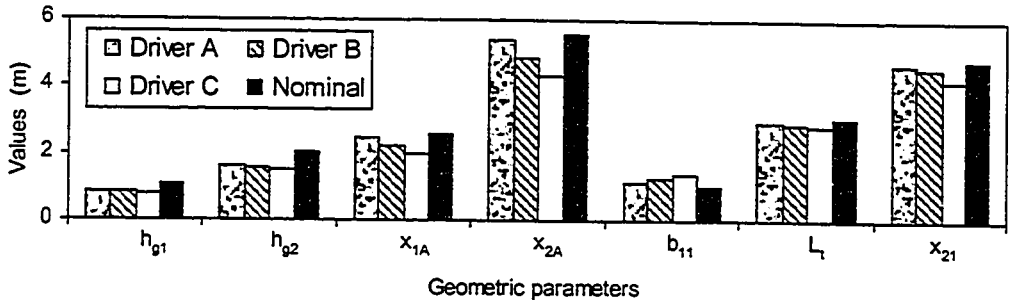

Figure 6.5: Comparison between optimal geometric parameters for the three different drivers and the nominal parameters.

The results show that different drivers adapt vehicles with different geometric parameters to achieve best control performance. The driver A, with highest skill level, exhibits better adaptability for a vehicle with relatively higher c.g. (h_{g1} and h_{g2}), shorter effective track width (b_{11}), and relatively longer tractor and trailer wheelbase (L_t, x_{21}, x_{1A}, and x_{2A}). The driver C, with lowest skill level, adapts to a vehicle with lower c.g. heights, wider track width and relatively shorter wheelbase. It should be noted that driver C exhibits slower reaction time, higher compensation gain, and shorter preview distance, and thus appears to be more suited for a more stable vehicle (lower c.g. heights, smaller length and wider track width). The optimal values obtained for the most skilled driver 'A' may thus be considered to represent the limiting values of the vehicle dimensions in view of the safety performance measures. These limiting values are summarized as: h_{g1}<0.85m; h_{g2}<1.59m; x_{1A}<2.47m; x_{2A}<5.4m; b_{11}>1.15m; L_t<2.95m; x_{21}<4.68m. A comparison between the optimal geometrical parameters and their nominal values shows that the geometric parameters adapted to driver 'A' are relatively close to their corresponding nominal values, which may indicate that the nominal geometric parameters of the articulated vehicle is more desirable for the skillful driver. The nominal

values of geometric parameters, however, are higher than those adapted to driver 'A', except for the track width (b_{11}) that is less than 1.15m.

The values of performance indices for the three drivers driving vehicles with optimal geometrical parameters are compared with those attained from nominal vehicle parameters as shown in Figure 6.6. The total performance index J is multiplied by 0.2 for clarity of illustration. The performance improvement ratio (PIR), defined as the ratio of the difference between the performance index derived from the nominal vehicle parameter and that adapted to a driver to the performance index derived from the nominal vehicle parameter, is illustrated in Table 6.5.

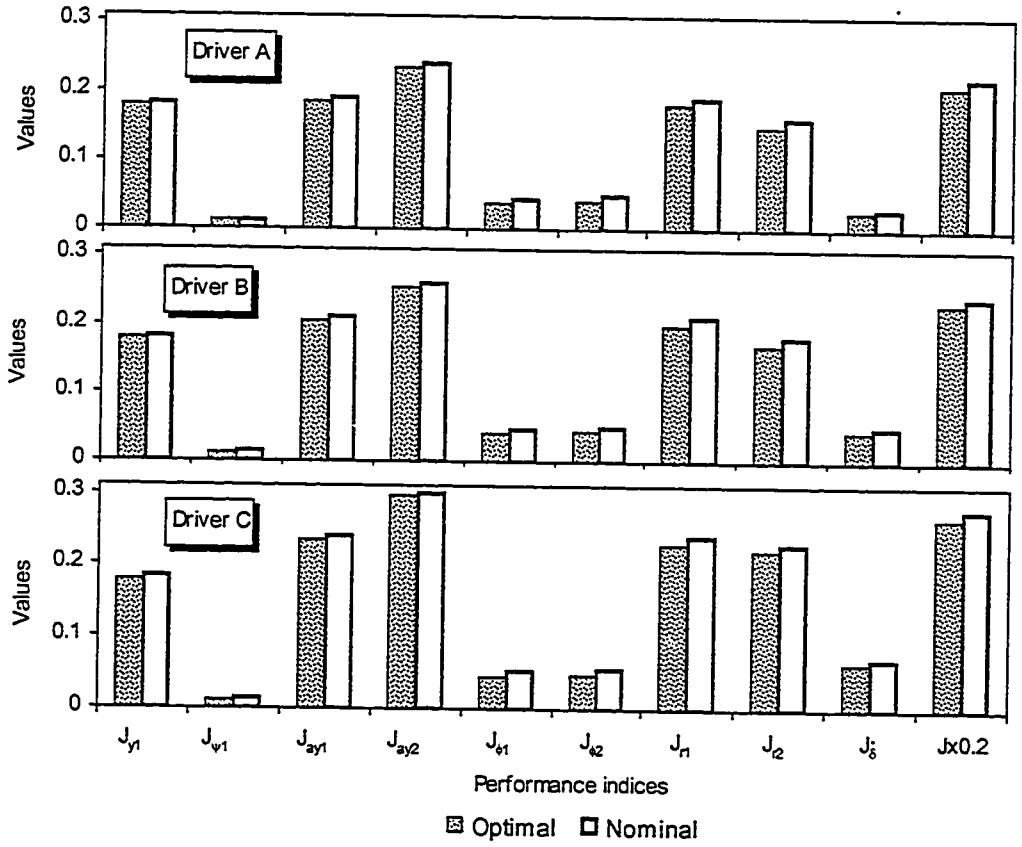

Figure 6.6: Comparison between the values of performance indices attained for the three drivers with optimal geometrical parameters and those with nominal parameters.

Table 6.5: Performance improvement due to optimal geometrical parameters.

Driver	Performance Indices Improvement (%)									
	J_{y1}	$J_{\psi 1}$	J_{ay1}	J_{ay2}	$J_{\phi 1}$	$J_{\phi 2}$	J_{r1}	J_{r2}	$J_{\dot{\delta}}$	J
A	0.56	3.85	2.63	2.083	17.78	18.37	5.263	6.25	16.67	4.88
B	1.1	5.3	2.38	1.923	14.89	15.69	4.762	5.556	10	4.38
C	2.19	6.72	2.08	1.667	13.46	14.29	4.167	4.348	7.143	3.97

The results clearly show that the dynamic performance of the vehicle and the steering effort of the driver can be improved by realizing the vehicle design with proposed geometric parameters alone. The driver 'A' yields exhibits better improvement in terms of lateral acceleration, yaw rates and roll angle response of both units, while driver 'C' exhibits better improvement in terms of the performance indices of the lateral position and orientation error of tractor. The results further show that the optimal geometrical parameters yield considerable improvement in the roll angle response of both units and steering effort index $J_{\dot{\delta}}$, but relatively small improvement in the path tracking performance (lateral position and orientation), lateral acceleration and yaw rates of both units, irrespective of the drivers. From the results, it may be concluded that the steering effort demands on the driver may be reduced considerably by the optimal geometric parameters, while maintaining similar dynamic performance of the vehicle. It should be noted that the driver 'C' with higher compensatory gain may pay more attention to the path tracking and thus yield better improvement in the lateral position and orientation tracking errors, while relatively smaller improvement in the steering effort is realized.

6.4.2 Identification of Desirable Range of Inertial Parameters

The driver-vehicle model with optimal geometrical parameters derived from the previous subsection is further analyzed to obtain the desirable range of the inertial

parameters corresponding to each driver. The inertial parameters considered in the study, include: (*i*) sprung masses of the tractor and trailer, m_{s1} and m_{s2}; (*ii*) yaw and roll mass moments of inertia of the tractor, I_{zt} and I_{xt}; (*iii*) yaw and roll mass moments of inertia of the trailer, I_{zs} and I_{xs}. The most desirable values of the inertial parameters are derived by minimizing the performance index, subject to limit constraints, which are summarized in Table 6.6 and represent possible variations in the selected inertial parameters. The resulting values of optimal inertial parameters for the three different drivers are compared with the nominal values in Figure 6.7, where m_{s2}, I_{zt}, I_{zs} and I_{xs} are multiplied by 0.2, 0.4, 0.01 and 0.1, respectively, for clarity of illustration. The relative bias of the resulting inertial parameters with respect to their nominal values is illustrated in Table 6.7.

Table 6.6: Constraints of the range of inertial parameters considered.

Name of parameters	Range (minimum, maximum)
m_{s1} (kg)	3000, 5500
m_{s2} (kg)	12000, 35000
I_{zt} (kgm^2)	8000, 16000
I_{xt} (kgm^2)	1000, 3000
I_{zs} (kgm^2)	200000, 600000
I_{xs} (kgm^2)	15000, 35000

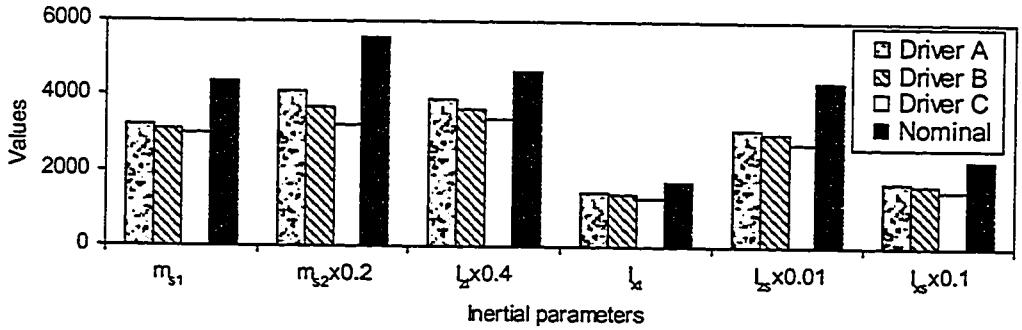

Figure 6.7: Comparison between optimal inertial parameters for the three different drivers and the nominal parameters.

Table 6.7: Relative bias of resulting inertial parameters relative to their nominal values.

Driver	Relative bias (%)					
	m_{s1}	m_{s2}	I_{zt}	I_{xt}	I_{zs}	I_{xs}
A	-27.1	-25.6	-16	-13.9	-29.3	-26.1
B	-29.5	-33.5	-22	-19	-32.3	-28.6
C	-31.7	-42.3	-28	-23.6	-38.2	-34.7

The results show that driver 'A' can adapt to vehicle with relatively larger values of the inertial parameters than the other two drivers. It may thus be concluded that a skilled driver with faster reaction can effectively adapt to heavier vehicles, while a driver with relatively poor skill and slower reaction time can be best adapted to lighter vehicles. The optimal values obtained for the most skilled driver 'A' may further be considered to represent the limiting values of the inertial parameters of the vehicle in view of its safety performance measures. These limiting values are derived as: m_{s1}<3209kg; m_{s2}<20755kg; I_{zt}<9800kgm^2; I_{xt}< 1460kgm^2; I_{zs}< 310967kgm^2; I_{xs}<17065kgm^2.

The values of performance indices for the three drivers with optimal inertial parameters are compared with those attained from analysis of the nominal parameters of the vehicle, as shown in Figure 6.8. The total performance index J is multiplied by 0.2 for clarity of illustration. The performance improvement ratio is illustrated in Table 6.8.

The results clearly show that the roll angles and yaw rates of both units and the steering effort posed on the driver improve considerably when optimal inertial parameters are used. It should be noted that the performance improvement ratios, illustrated in Table 6.8, also include the contributions due to optimal geometrical parameters. The differences between the performance improvement ratios presented in Tables 6.8 and 6.5 may thus be recognized as the contributions due to optimal inertial parameters alone. It can be further noticed that the optimal inertial and geometric parameters yield considerable

improvements in the yaw and roll dynamic response indices and the steering effort index, specifically for driver 'A' with higher driving skill level.

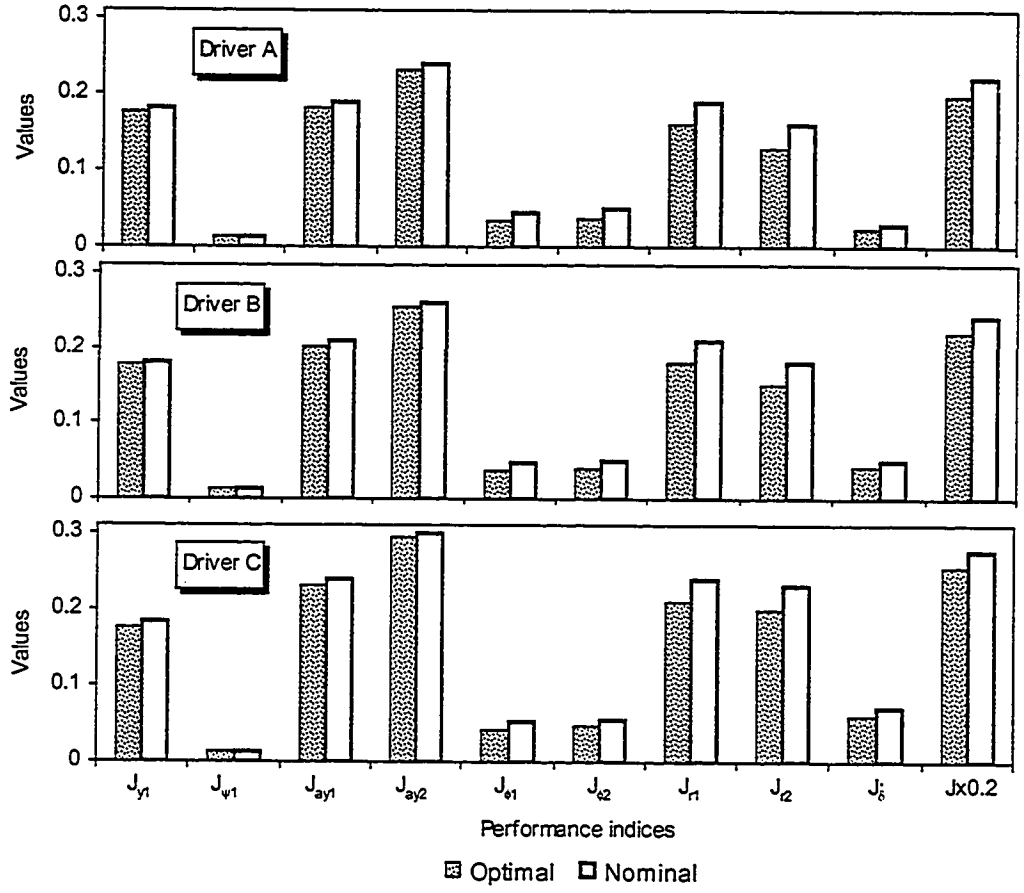

Figure 6.8: Comparison between the values of performance indices attained for the three drivers with optimal inertial parameters and those with nominal parameters.

Table 6.8: Performance improvement due to optimal inertial parameters and optimal geometric parameters.

Driver	Performance Indices Improvement (%)									
	J_{y1}	$J_{\psi 1}$	J_{ay1}	J_{ay2}	$J_{\phi 1}$	$J_{\phi 2}$	J_{r1}	J_{r2}	$J_{\dot{\delta}}$	J
A	1.67	6	4.21	3.33	24.44	26.53	15.79	18.75	23.33	10.1
B	2.21	6.06	3.81	2.31	19.15	19.61	14.29	16.67	16	8.8
C	4.37	7.46	3.75	2	17.31	17.86	12.5	13.04	14.29	8.16

6.4.3 Identification of Desirable Range of Suspension Parameters

The roll dynamics of a vehicle is strongly influenced by its suspension roll stiffness. The effective roll stiffness of the axle suspensions, however, is realized in order

to achieve a compromise between the ride and handling performance characteristics of the vehicle. The closed-loop driver-vehicle model is analyzed to identify the desirable range of suspension roll stiffness parameters as a function of the driver's skills. The analyses are performed to identify the effective roll stiffness and roll damping properties of the tractor ($k_{\phi t}$, $C_{\phi t}$) and trailer ($k_{\phi s}$, $C_{\phi s}$) axle suspensions.

The most desirable values of suspension parameters are derived by minimizing the performance index, subject to limit constraints, summarized in Table 6.9, which are considered to represent a wide range of variations. The analysis, however, is performed with the vehicle model with optimal geometric and inertial parameters, in conjunction with the driver model. The resulting values of optimal suspension parameters for the three different drivers are compared with the nominal values in Figure 6.9, where $k_{\phi t}$ and $k_{\phi s}$ are multiplied by 0.1 and 0.04, respectively, for clarity of illustration. The relative bias of the resulting suspension parameters with respect to their nominal values are illustrated in Table 6.10.

Table 6.9: Constraints of the range of suspension parameters considered.

Name of parameters	Range (minimum, maximum)
$k_{\phi t}$ (kNm/rad)	200, 1500
$k_{\phi s}$ (kNm/rad)	1000, 5000
$C_{\phi t}$ (kNms/rad)	20, 70
$C_{\phi s}$ (kNms/rad)	40, 110

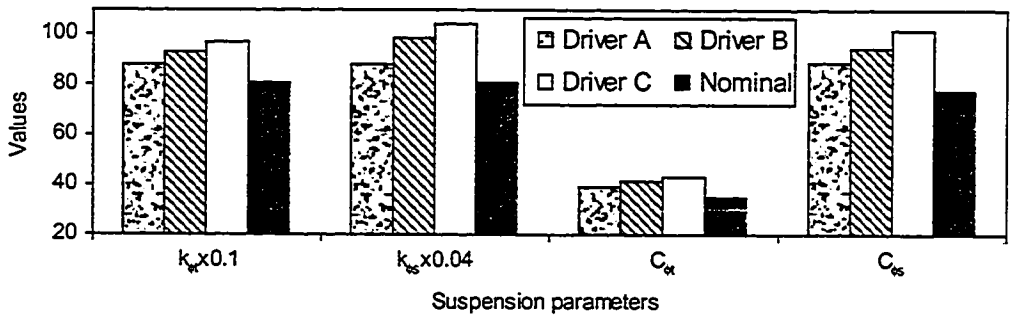

Figure 6.9: Comparison between optimal suspension parameters derived for the three different drivers and the nominal parameters.

Table 6.10: Relative bias of resulting suspension parameters relative to their nominal values.

Driver	Relative bias (%)			
	$k_{\phi t}$	$k_{\phi s}$	$C_{\phi t}$	$C_{\phi s}$
A	8.84	8.81	11.5	15.2
B	14.5	22.1	18	21.8
C	19.8	29	23.1	30.9

The results indicate that the skilled driver 'A' can better adapt to a vehicle with smaller values of suspension roll stiffness and damping coefficients than the other two drivers. It may thus imply that a driver with better skill and faster reaction can effectively adapt to soft suspension vehicles, while the drivers with poor skills and slower reaction require vehicle design with relatively hard suspensions. The optimal values obtained for the most skilled driver 'A' may further be considered to represent the limiting values of the vehicle suspension parameters in view of the safety performance measures. These limiting values are summarized as: $k_{\phi f}$>883kNm/rad; $k_{\phi s}$>2200kNm/rad; $C_{\phi f}$>39.6kNms/rad; $C_{\phi f}$>89.5kNms/rad. The nominal values of the suspensions thus should be increased to enhance the directional dynamics performance of the vehicle.

The values of performance indices obtained for the three drivers with optimal suspension parameters are compared with those attained from the analyses of the nominal vehicle, as shown in Figure 6.10. The corresponding performance improvement ratios are computed and illustrated in Table 6.11. The results clearly show that the optimal suspension parameters yield most significant reduction in the roll angle response of both the units. It should be noted that the performance improvement ratios, illustrated in Table 6.11, also include the contribution due to optimal geometrical and inertial parameters. The differences between the performance improvement ratios presented in Tables 6.11 and 6.8 may thus be considered to represent the contributions due to optimal suspension

parameters alone. It can be further noticed that the optimal suspension parameters together with the optimal geometrical and inertial parameters yield considerable improvements in the roll angle and yaw rate response of both the units, and the steering effort index, specifically for driver 'A'.

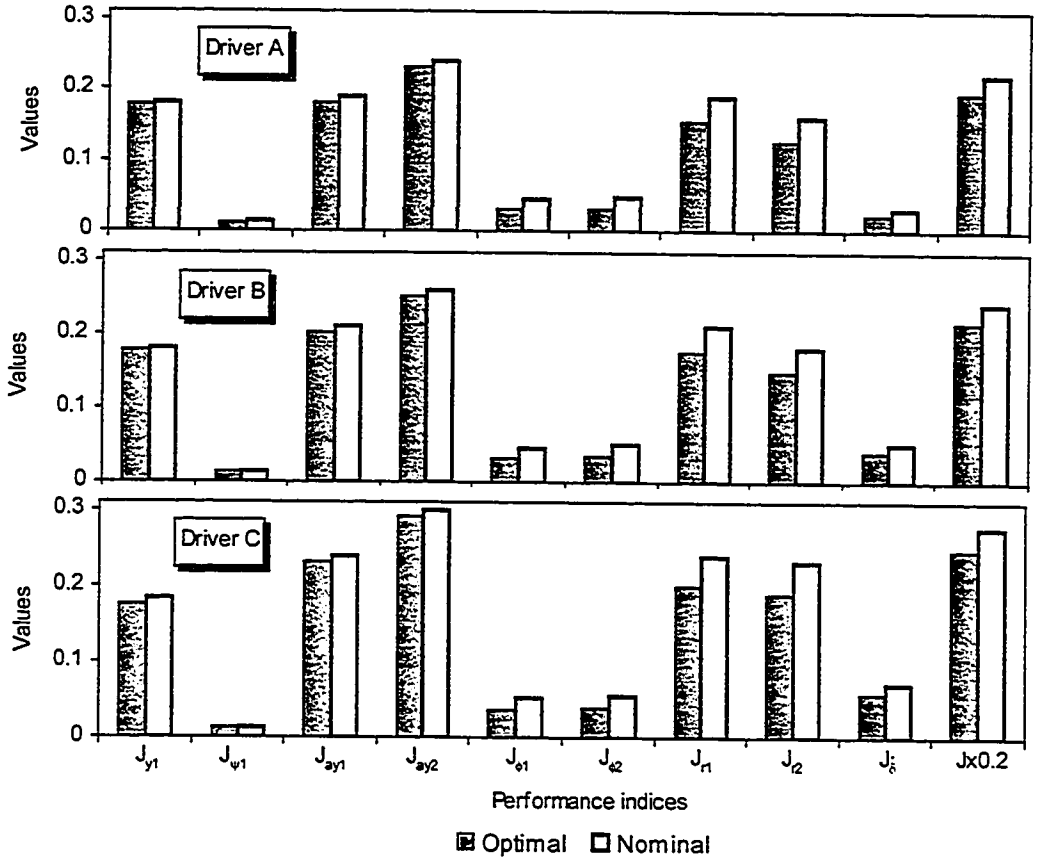

Figure 6.10: Comparison between the values of performance indices attained from the three drivers with optimal suspension parameters and those with nominal parameters.

Table 6.11: Performance improvement due to optimal suspension parameters using optimal geometric and inertial parameters.

Driver	Performance Indices Improvement (%)									
	J_{y1}	$J_{\psi 1}$	J_{ay1}	J_{ay2}	$J_{\phi 1}$	$J_{\phi 2}$	J_{r1}	J_{r2}	$J_{\dot{\delta}}$	J
A	1.72	6.08	4.74	3.75	33.33	34.69	18.42	20.63	26.67	11.84
B	2.27	6.82	4.29	3.08	29.79	30.2	17.14	18.33	19.2	10.81
C	4.37	7.61	4.17	3	26.92	28.57	16.67	17.39	15.71	10.76

6.4.4 Identification of Desirable Range of Tire Parameters

In addition to the geometrical, inertial and suspension parameters, the tire properties affect the lateral and roll dynamics of the vehicle, and thus the interactions between the driver and the vehicle. The tire properties are a complex function of the inflation pressure, vertical load, vehicle speed and the tire structure. Under a constant vehicle speed and small roll motions of the sprung mass, the variations in the vertical tire load may be considered small. The variation in the inflation pressure during operation over a period may also be considered as a constant. The lateral and roll dynamics of a vehicle are mostly affected by the cornering properties of the tire, which may be primarily attributed to the tire design factors. The analyses are thus performed to identify most desirable cornering stiffness and aligning moment due to tires on the tractor front axle ($C_{\alpha f}$ and C_{mf}), tractor rear axles ($C_{\alpha r}$ and C_{mr}), and semitrailer axles ($C_{\alpha s}$ and C_{ms}). The most desirable values of identified tire parameters are derived by minimizing the performance index, subject to limit constraints, summarized in Table 6.12, which represent possible variations in the selected tire parameters. It should be noted that the vehicle model is based upon optimal geometric, inertial and suspension parameters derived in the previous subsections. The resulting values of optimal tire parameters for the three different drivers are compared with the nominal values in Figure 6.11, where $C_{\alpha f}$, $C_{\alpha r}$ and $C_{\alpha s}$ are multiplied by 0.1, respectively, for clarity of illustration. The relative bias of the resulting tire parameters with respect to their nominal values are illustrated in Table 6.13.

The results show that the desirable values of cornering stiffness $C_{\alpha f}$ and the aligning moment coefficient C_{mf} due to front axle tires are considerably larger for the

skilled driver 'A' than those desired by drivers 'B' and 'C'. The driver 'A', however, adapts well to vehicle with lower cornering stiffness and aligning moment coefficient of tires on the tractor rear and semitrailer axles. It can be further seen that the cornering stiffness and aligning moment coefficients of the front axle tires tractor tend to decrease with decrease in the driver's driving ability, while those of the tractor rear axle and semitrailer axle tires tend to increase with decrease in the driver's driving ability. It should be noted that the cornering stiffness of front and rear axle tires of the tractor directly affect the steering characteristics of the tractor and the cornering stiffness of trailer tires directly affect the yaw stability of the articulated vehicle. Higher values of cornering stiffness of front axle tires or lower values of cornering stiffness of tractor rear axle tires can cause the steering characteristics of the vehicle to vary from understeer to oversteer. The results, therefore, suggest that the driver 'A' can adapt well to a relative oversteer vehicle, while a relative understeer vehicle is considered more suitable for drivers 'B' and 'C'. The optimal values obtained for the most skilled driver 'A' may further be considered to represent the limiting values of the vehicle tire parameters in view of the safety performance measures. These limiting values are summarized as: $C_{\alpha f}$<180000N/rad; $C_{\alpha r}$>136548N/rad; $C_{\alpha s}$>143219N/rad; C_{mf}<19765Nm/rad; C_{mr}>18543Nm/rad and C_{ms}>19871Nm/rad.

Table 6.12: Constraints of the range of tire parameters considered.

Name of parameters	Range (minimum, maximum)
$C_{\alpha f}$ (N/rad)	100000, 400000
C_{mf} (NM/rad)	10000, 40000
$C_{\alpha r}$ (N/rad)	100000, 400000
C_{mr} (NM/rad)	10000, 40000
$C_{\alpha s}$ (N/rad)	100000, 400000
C_{ms} (NM/rad)	10000, 40000

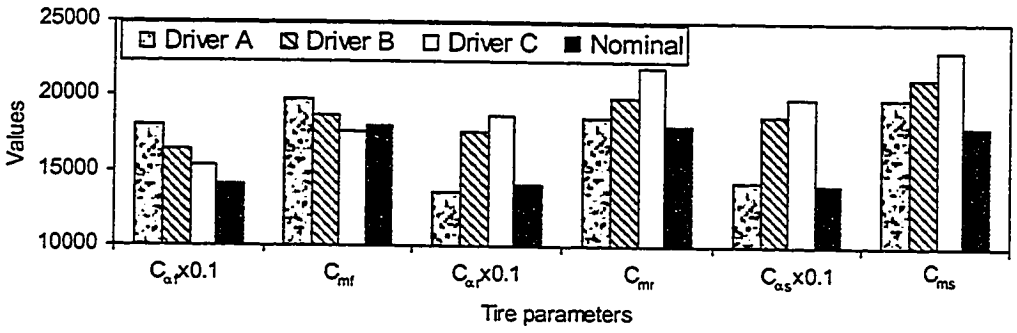

Figure 6.11: Comparison between optimal tire parameters for the three different drivers and the nominal parameters.

Table 6.13: Relative bias of resulting tire parameters relative to their nominal values.

Driver	Relative bias (%)					
	$C_{\alpha f}$	C_{mf}	$C_{\alpha r}$	C_{mr}	$C_{\alpha s}$	C_{ms}
A	27.5	9.54	-3.25	2.77	1.48	10.13
B	16.1	4	25.08	10.12	33	17.55
C	8.58	-2.2	32.93	21.18	40.8	28.08

The components of the performance index derived for the three drivers with optimal tire parameters are compared with those attained the analyses based upon nominal vehicle parameters, as shown in Figure 6.12. The performance improvement ratios are also illustrated in Table 6.14. The results clearly show that the dynamic performance of the vehicle and the steering effort demand posed on the driver can be improved considerably when optimal tire parameters are used. It should be noted that the performance improvement ratios, illustrated in Table 6.14, also include the contributions due to optimal geometrical, inertial and suspension parameters. The results show that optimal tire parameters together with the optimal geometrical, inertial and suspension parameters yield considerable improvements in the roll angle and yaw rate response of both units, and the driver's steering effort.

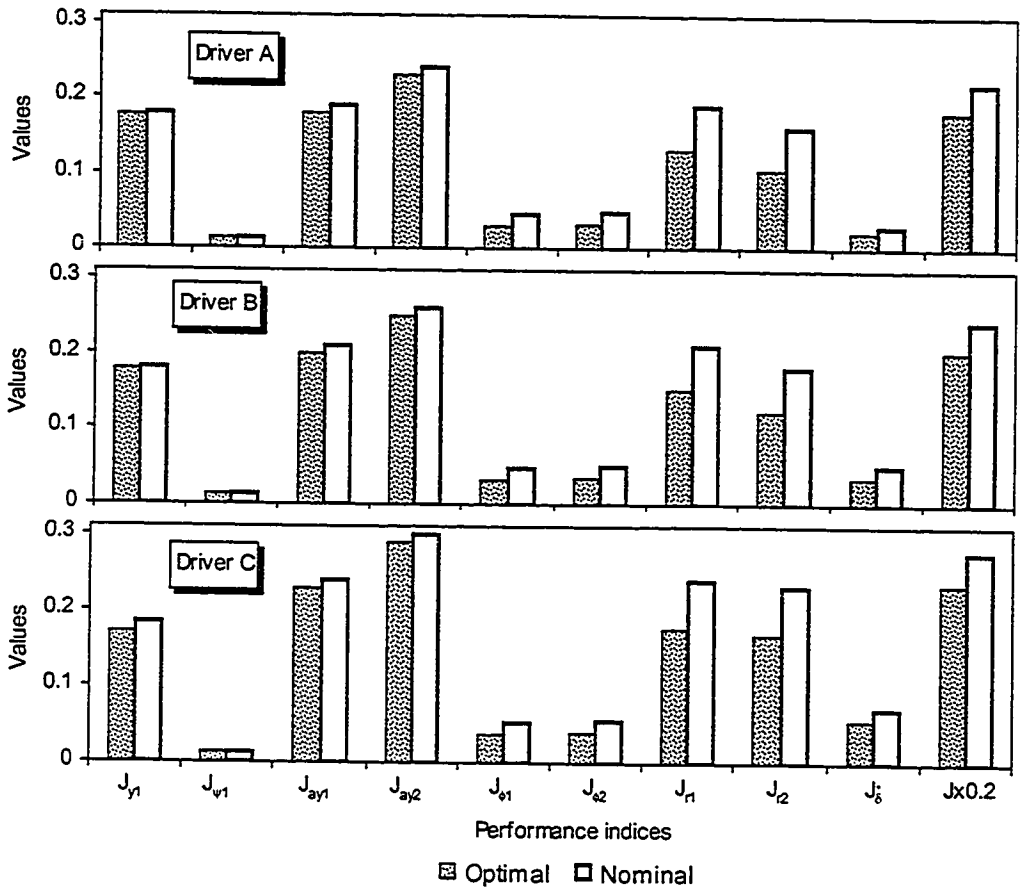

Figure 6.12: Comparison between the values of performance indices attained for the three drivers with optimal tire parameters and those with nominal parameters.

Table 6.14: Performance improvement due to optimal tire parameters using optimal geometric, inertial and suspension parameters.

Driver	Performance Indices Improvement (%)									
	J_{y1}	$J_{\psi 1}$	J_{ay1}	J_{ay2}	$J_{\phi 1}$	$J_{\phi 2}$	J_{r1}	J_{r2}	$J_{\dot{\delta}}$	J
A	1.83	6.15	5.26	4.17	35.56	36.73	31.58	34.38	30	16.6
B	2.43	7.58	4.76	3.85	31.91	32.35	28.57	32.22	28.6	15.74
C	6.01	7.84	4.58	3.33	28.85	30.36	27.08	27.39	22.86	15.1

6.4.5 Identification of Desirable Range of Fifth Wheel Parameters

From the results of the parametric sensitivity analysis presented in Chapter 3, it is evident that the articulation properties of an articulated vehicle affect the dynamic performance considerably. It is thus important to investigate the desirable fifth wheel parameters that can be ideally adapted to drivers with different skills and experience. The

vehicle model with optimal geometrical, inertial, suspension and tire parameters derived from previous subsections is further integrated with the driver model to minimize the performance index, J, in order to obtain the desirable range of the fifth wheel parameters corresponding to each driver. The fifth wheel parameters considered in the study include: (*i*) yaw damping coefficient, $C_{\psi h}$; (*ii*) roll stiffness associated with the tractor and trailer structure, k_{f1} and k_{f2}. The most desirable values of the identified fifth wheel parameters are derived by minimizing the performance index, subject to limit constraints, summarized in Table 6.15. The resulting values of optimal fifth wheel parameters for the three different drivers are compared with the nominal values in Figure 6.13, where k_{f1} and k_{f2} are multiplied by 0.5 respectively, for clarity of illustration. The relative bias of the resulting fifth wheel parameters with respect to their nominal values are illustrated in Table 6.16.

Table 6.15: Constraints of the range of inertial parameters considered.

Name of parameters	Range (minimum, maximum)
$C_{\psi h}$ (Nms/rad)	2000, 20000
k_{f1} (kNm/rad)	8000, 30000
k_{f2} (kNm/rad)	8000, 30000

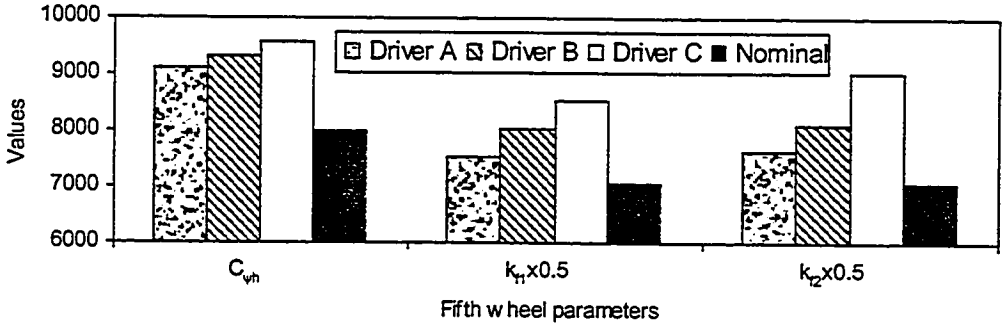

Figure 6.13: Comparison between optimal fifth wheel parameters for the three different drivers and the nominal parameters.

The results show that all the three drivers desire vehicle with relatively higher values of articulation yaw damping and roll stiffness. The driver 'A', however, tends to

adapt to lower values of damping and roll stiffness, when compared with those desired by drivers 'B' and 'C'. The optimal values obtained for the most skilled driver 'A' may further be considered to represent the limiting values of the fifth wheel parameters in view of the safety performance measures. These limiting values are summarized as: $C_{\psi h}$>9107Nms/rad; k_{f1}>15098kNm/rad; and k_{f2}> 15318kNm/rad.

Table 6.16: Relative bias of resulting fifth wheel parameters relative to their nominal values.

Driver	Relative bias (%)		
	$C_{\psi h}$	k_{f1}	k_{f2}
A	13.9	6.75	8.3
B	16.7	13.7	14.7
C	19.9	20.8	27.6

The components of the performance index computed for the three drivers with optimal fifth wheel parameters are compared with those attained from the analysis based upon nominal vehicle parameters, as shown in Figure 6.14. The performance improvement ratios are also illustrated in Table 6.17. The results clearly show that the roll angle and yaw rate response of both units can be improved considerably, when optimal fifth wheel parameters are used. It should be noted that the performance improvement ratios, illustrated in Table 6.17, also include the contributions due to optimal geometrical, inertial, suspension and tire parameters. The optimal fifth wheel parameters yield further reductions in the driver steering effort, and roll angle and yaw rate response of both units.

The results of the analyses clearly demonstrate that the safety dynamics performance of the coupled driver-vehicle system can be considerably enhanced using the sequential optimal strategy for the design of geometrical, inertial, suspension, tire and the fifth wheel parameters. It should be noted that the optimal vehicle parameters do not

yield considerable improvement in the lateral acceleration response of both units and the path tracking performance, while significant reductions in the magnitudes of roll angles and yaw rates of both the units are observed. It may be understood that the lateral position of the vehicle is directly governed by the lateral acceleration and a smaller lateral position error tracking, in general, yields larger lateral acceleration to perform the obstacle avoidance maneuver. Thus the lateral position tracking and lateral acceleration performance indices are mutually constrained during minimization of the performance index *J*. The results further suggest that an optimal vehicle design, considered suitable for a specific driver skill, can realize the adequate path tracking performance with lower driver effort, and reduced degrees of vehicle roll and yaw motions.

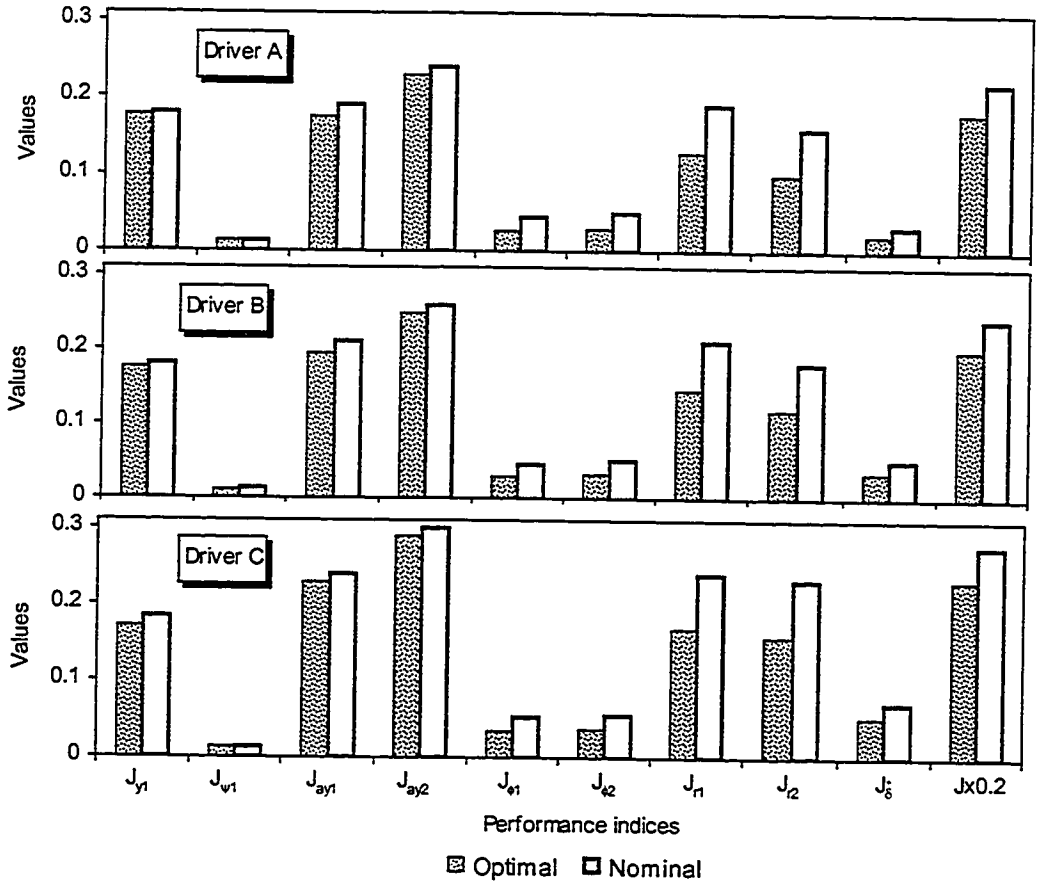

Figure 6.14: Comparison between the values of performance indices attained for the three drivers with optimal fifth wheel parameters and those with nominal parameters.

Table 6.17: Performance improvement due to optimal fifth wheel parameters using optimal geometric, inertial, suspension and tire parameters.

Driver	Performance Indices Improvement (%)									
	J_{y1}	$J_{\psi 1}$	J_{ay1}	J_{ay2}	$J_{\phi 1}$	$J_{\phi 2}$	J_{r1}	J_{r2}	$J_{\dot{\delta}}$	J
A	1.89	6.92	7.89	5	40	40.82	33.16	37.5	33.33	18.44
B	2.49	8.33	7.14	4.81	36.17	37.25	30.95	33.89	30	17.48
C	6.56	7.91	5	3.67	32.69	33.93	29.58	31.74	23.57	16.8

6.5 SUMMARY

The driver's control characteristics in terms of the compensatory gain, reaction time, preview distance and steering are briefly reviewed to identify a range of performance limits of the drivers. A concept of articulated vehicle design that can be adapted for varying driving skills is presented. The desirable ranges of the vehicle parameters including geometric, inertial, suspension, tire and the fifth wheel are derived using three drivers with different skill levels and the previously proposed multi-loop driver-vehicle model. The results of the study revealed the vehicles with large sizes, soft suspension and relative oversteer nature can be easily adapted by driver with superior skills. The adaptability of the vehicle can be considerably enhanced through variations in the weights and dimensions, suspension, tire and the fifth wheel properties. The results clearly show that the proposed concept of driver-adaptive vehicle offers considerable potential to enhance the safety dynamics of the vehicles.

CHAPTER 7 CONCLUSIONS AND RECOMMENDATIONS FOR FUTURE WORK

7.1 MAJOR HIGHLIGHTS OF THIS INVESTIGATION

In this thesis, the dynamic interactions between an articulated freight vehicle and its driver are investigated through systematic development and integration of driver and vehicle models. The coupled closed-loop driver-vehicle model is validated and analyzed to enhance an understanding of the complex interaction of the driver with the vehicle. The analyses are performed with following specific objectives:

- To identify the control performance limits of the driver in terms of preview, prediction and compensation abilities, and the significance of various motion cues on the directional performance of the coupled system.

- To gain an understanding of the control demands posed on the driver as functions of vehicle speed, nature of directional maneuver, and random steering disturbances.

- To identify design parameters of the articulated vehicle that can be ideally adapted by drivers with varying skill levels.

7.1.1 Development and Analysis of Open-loop Directional Dynamics Models of Heavy Vehicles

Linear and nonlinear yaw-plane and yaw-plane with roll-DOF models of an articulated vehicle are formulated to study its open-loop directional dynamic response. The nonlinear cornering properties of tires are modeled using proposed Magic Formula and neural network methods. Neural network method is also applied to derive an analytical model of the articulated vehicle. The effectiveness of the different models is evaluated by comparing their response characteristics with those derived from the widely accepted Yaw/Roll model and field measured data. It was concluded that linear and

nonlinear yaw-plane model with limited roll-DOF, developed in this study, yields reasonably accurate estimate of the vehicle response. Since the proposed model incorporates considerably fewer DOF and vehicle parameters, it can be conveniently integrated with the driver model. It should be emphasized that the vehicle models, reported in the literature, are either oversimplified, such as yaw-plane models, or quite complex, such as Yaw/Roll and Phase IV models. The simplified models cannot account for roll motion of the vehicle, which is known to be quite significant in such high c.g. vehicles. The complex models require extensive vehicle data, which poses unreasonable demands on the analyst. The selected model based upon yaw-plane and roll-DOF offers a good compromise between the simplified and complex models. Its validity is further demonstrated through reasonably good correlation with the field measured data.

7.1.2 Identification of Important Vehicle Parameters

A comprehensive parametric sensitivity analysis is performed to study the influence of various design and operating parameters and to identify vehicle parameters that influence on the directional response significantly. A performance index comprising various performance safety measures based upon lateral acceleration, yaw rates, roll angles and articulation angle, is formulated to study the contribution due to various parameters. Since identification of parameters associated with such large size vehicles poses many complexities, the results of the analysis are used to identify a set of most significant parameters. In view of high level of uncertainty associated with some of the parameters, system identification techniques are applied to obtain an estimate of these parameters. These parameters include yaw mass moments of inertia of different units, and

cornering properties of tires. The vehicle transfer function is identified from the response data of yaw-plane model. A parameter estimation algorithm is formulated to derive the uncertain vehicle parameters. The robustness of the proposed algorithm is further investigated using various levels of signal to noise ratio (SNR) and the data obtained from a more comprehensive Yaw/Roll model.

7.1.3 Study of Single and Multi-loop Driver Model Structures

The control characteristics of the driver in terms of path preview, prediction and compensation abilities related to path tracking performance are thoroughly investigated. It should be emphasized that the reported studies focus mostly on the light weight single unit vehicles, while only few studies have attempted to study the driver's control behaviour for multiple-unit vehicles. The data reported for two-axle vehicles, however, are examined to identify a range of various driver control parameters. Single- and multi-loop structures of driver models, incorporating different preview and prediction functions, and motion cues arising from the vehicle response are formulated. A performance index comprising different measures of driver control and effort, and vehicle response is formulated. The performance index is minimized to achieve specified path tracking performance using damped Gauss-Newton method, subject to limit constraints established from the reported data. The driver parameters corresponding to different single- and multi-loop based models, are identified. The results of the analysis are examined to identify the contributions due to various path prediction and correction strategies, and different motion cues. The resulting significant motion cues are further reviewed in view of their possible direct or indirect driver perception.

7.1.4 Development and Analysis of the Closed-loop Driver-Vehicle Model

The important and perceivable motion cues arising from the vehicle response, identified from the analyses, are integrated into a multi-loop structure to derive a comprehensive driver-vehicle model. The contributions due to gain and delays due to neuromuscular dynamics and proprioceptive elements associated with the limb motion and muscle tissues are modeled and integrated into the total model. The trailer roll motion, tractor lateral acceleration, and articulation rate of the vehicle are considered to form the essential motion cues. The previously defined performance index is minimized to identify various driver model parameters, including: preview time, path-follower coefficient, compensatory gain and time constant, proprioceptive gains and time constants, and gains and time delays associated with different motion cues.

The proposed driver-vehicle model is analyzed under a constant speed obstacle-avoidance maneuver. The analytical response is compared with the field measured data to demonstrate the validity of the analytical model. The validated model is further analyzed to study the control demands posed on the driver as functions of maneuver severity, vehicle speed and steering disturbances.

7.1.5 Development and Analysis of Driver-Adaptive Vehicle Concept

The control performance limits of the drivers are investigated in terms of reaction time, visibility and preview distance, compensatory gain, and frequency band of directional control. Three sets of control performance limits are established to represent varying skills and experience of different drivers. The proposed closed-loop driver-

vehicle model is analyzed in conjunction with the identified control limits of the driver to derive most desirable vehicle design parameters. The resulting design is then proposed as the ideal vehicle design that can be adapted to the driver skills. The adaptivity of the vehicle to the driver is analyzed in terms of the desirable vehicle geometrical and dynamics parameters adapted by different drivers with varying skill levels and experience, such that the safety performance of the driver-vehicle system maintains satisfied.

7.2 CONCLUSIONS

Based upon the studies carried out in this dissertation, the following major conclusions are drawn:

- From literature review, it can be concluded that almost all the driver models reported in the literature focus on the single unit vehicles and thus cannot utilize driver's perception of motion of the trailing unit. The directional control of articulated vehicles necessitates certain direct or indirect perception of the trailer motion to achieve effective path tracking and dynamic safety performance. The reported models thus cannot be used to study the contributions due to driver interactions with articulated vehicles.

- The cornering force and aligning moment properties of tires are known to be strongly nonlinear functions of normal load and side-slip angles. Such nonlinear characteristics can be effectively characterized using the Magic Formula and neural networks. The use of Magic Formula however involves identification of many coefficients, while the method based upon neural networks can provide an accurate estimation in an efficient manner.

- Comparison for various analytical vehicle models of varying complexities shows that a more sophisticated model does not necessarily yield more accurate response estimation than the relatively simpler models, due to cumulative effects of the errors in the measurements of a large number of input parameters. The comparison of response characteristics of various models with the measured data revealed that the contributions due to roll dynamics of such vehicles are significant and thus cannot be neglected. A

yaw-plane model with limited roll-DOF of the sprung mass can serve as an efficient tool for analysis of the directional behaviour of the vehicle. The response characteristics derived from the yaw-plane model with limited roll-DOF correlate reasonably well with the field measured data. The yaw-plane model, developed assuming negligible roll, yield poor correlation with the measured data.

- The analysis of vehicle response to a ramp-step steer input revealed that nonlinearities associated with vehicle suspension and cornering behaviour of tires yield higher gains of the lateral acceleration and yaw rate responses, when compared with those derived from linear models.

- Neural networks with tansig and linear activation functions, are applied to modeling the tire and vehicle dynamics, and the results show that an appropriate choice of network structure in terms of the number of layers and neurons and effective training based upon the target data can yield reasonably precise emulation of the tire and vehicle dynamics under a wide range of operating conditions.

- The open-loop directional dynamic response of the vehicle is most sensitive to the c.g. heights of the tractor and trailer units, which strongly affect the lateral, yaw and particularly roll response of the combination. While the least sensitive geometrical parameters are the horizontal distances between tractor front axle and its c.g. and between trailer axle and its c.g.

- In view of the group of dynamics parameters, the vehicle response is most sensitive to the sprung masses and roll and yaw mass moments of inertia of the units. The sprung mass and roll mass moment of inertia of the lead unit, and yaw moment of inertia of the trailing unit, however, affect the vehicle response more significantly. The vehicle response is also very sensitive to variations in the cornering stiffness and aligning moment coefficient of the tires. The roll dynamic response of the combination is more sensitive to the roll stiffness and roll damping coefficient of the trailer axle suspension. Furthermore, the roll stiffness of the fifth wheel coupling mostly influences the lateral acceleration of trailer, and the yaw rate and roll angle response of the tractor, while its yaw damping coefficient mostly affects the dynamic response of the tractor.

- The lateral dynamics of the vehicle and its parameters can be effectively identified using the system identification techniques based upon output error minimization model. The proposed methodology can yield an accurate estimation of lateral dynamic response, when the signal to noise ratio (SNR) is greater than or equal to 20dB, irrespective of the excitation signals selected. The lateral dynamics of the articulated vehicle could be optimally described by

a fourth order model and lowest estimation errors are obtained using a pseudo-random binary sequence (PRBS) input.

- Using the proposed methodology, the vehicle parameters can be estimated with reasonably high accuracy under different steering inputs and SNR superior to 20dB. The PRBS excitation signal yields peak estimation error well below 10%. Furthermore, the parameters, which are known to be uncertain and affect the system dynamics significantly, can be estimated with reasonable accuracy.

- A study of single-loop structure of the driver models reveals that the lateral position and orientation of the trailing unit as the feedback variables yield oscillatory vehicle response and pose unacceptable steering effort demands on the driver. The results also show that lateral position and orientation of the lead unit form the essential feedback variables to achieve stable path-tracking performance.

- A study of multi-loop structures of driver-vehicle system shows that the lateral position and orientation of the lead unit are the fundamental feedback variables forming the external loop in the multi-loop driver models, while the lateral acceleration of the lead unit, articulation rate and the roll angle of the trailing unit form the internal loop variables as the efficient motion feedback cues affecting the driver's directional control behaviour.

- A comparison of results obtained from single- and multi-loop structures shows that the multi-loop structures, irrespective of the motion feedback applied, yield significantly lower values of composite performance index than that derived from the single loop structures. It is thus concluded that the driver's directional control strategies are not only the function of path tracking but also the vehicle motion. The motion variables are thus considered as essential variables representing driver's perception that affects his/her control strategy.

- The proposed comprehensive driver-articulated vehicle model and the available experimental results exhibit very similar patterns, and a very good agreement can be observed between the measured data and the results obtained from the comprehensive models based upon both nonlinear and linear vehicle models. A linear yaw-plane model with limited roll-DOF can thus be considered appropriate for study of driver-vehicle interaction.

- The driver's parameters, thus the driver's directional control behaviour, are strongly affected by maneuver severity, vehicle forward speed, and external disturbance in a complex manner. Higher severity of maneuver and higher vehicle speed require faster prediction, and higher and rapid path correction abilities of the driver, and pose increasing demand on the muscle activity.

- The driver's preview time tends to decrease with increasing severity of the maneuver, decreasing vehicle forward speed and the noise frequency bandwidth until noise bandwidth approaches 10 Hz;

- A driver with superior driving skills can easily adapt a vehicle with relatively larger size and weight, softer suspension, lower coupling stiffness of the fifth wheel, and relatively over-steer characteristics. A driver with lower driving skills can adapt to a vehicle with smaller size, stiffer suspension, higher coupling stiffness of the fifth wheel, and relatively under-steer characteristics. The vehicle designs realized upon consideration of optimal geometric and dynamic parameters yield significantly enhanced directional performance for varying skills of drivers.

7.3 RECOMMENDATIONS FOR FUTURE WORK

The thesis research presents fundamental investigations involving characterization of driver's interaction with the vehicle and methodologies to derive design parameters of vehicles that can be ideally adapted by the drivers with varying skill levels. It is recommended to undertake the following future studies to further explore the performance potentials of the proposed concept and methodologies to facilitate its realization and implementations.

- The analytical yaw plane model with roll degree of freedom for articulated heavy vehicle needs to be validated through various field tests under different operating conditions.

- Field measured data sets need to be used to train the neural network vehicle dynamics model, while development of a database on different articulated vehicle configurations is recommended to train and to enhance the effectiveness of the neural network models.

- The field measured data sets should be further used to explore the proposed methodology of estimating the uncertain vehicle parameters. The proposed methodology may be further extended for identification of a wider matrix of parameters.

- More field or simulator based studies are extremely vital to identify reliable driver parameters and control performance limits under different driving conditions.

- Studies need to be undertaken in an attempt to quantify the motion perception abilities of the drivers.

- The proposed comprehensive driver/vehicle system model needs to be evaluated under different driver behaviours, driving conditions and vehicle configurations.

- Low cost on-board state monitors may be developed to provide indirect perception of important motion cues.

- The proposed concept of driver-adaptive heavy vehicle offers most significant potentials to minimize the highway safety risks posed by such vehicles. The concept should therefore be further explored to examine its feasibility.

REFERENCES

1. Segel, L., *The Mechanics of Heavy Duty Trucks and Truck Combinations*, Chapter 17, The International Association for Vehicle Design, Aston Clinton, UK, 1970.

2. Ervin, R. D., Guy, Y., *The Influence of Weights and Dimensions on the Stability and Control of Heavy-Duty Trucks in Canada*, UMTRI Report, No. 86-35, 1986.

3. Rakheja, S., Vallurupalli, R. K. and Woodrooffe, J., *Influence of Articulation Damping on the Yaw and Lateral Dynamic Response of the Vehicle*, Journal of Heavy Vehicle Systems 2(2), pp. 105-123, 1995.

4. Leucht, P. M., *The Directional Dynamics of the Commercial Tractor - Semi-trailer Vehicle during Braking*, SAE Paper No. 700371, 1970.

5. Mallikarjunarao, C. and Fancher, P., *Analysis of the Directional Response Characteristics of Double Tanker*, SAE Paper no 781064, 1978.

6. Crolla, D. A. and Hales, F. D., *The Lateral Stability of Tractor and Trailer Combinations*, Journal of Terramechanics, Vol. 16, No. 1, pp.1-22, 1979.

7. Fancher, P. S., *The Transient Directional Response of Full Trailers*, SAE Paper 821259, 1982.

8. Mayenburg , M. V., Rossow, G. and Patterson, C., *Truck Safety Technology for the 21st Century*, Truck Safety: Performances and Reality, University of Waterloo, Canada, 1996

9. Glasner, E. V., *Active Safety of Commercial Vehicles*, Proceedings of AVEC'94 Conference, Society of Automotive Engineers of Japan, Inc., pp.9-14, Oct., 1994.

10. Hancock, P. and Parasuraman, R., *Human Factors and Safety in the Design of Intelligent Vehicle-Highway Systems (IVHS)*. Journal of Safety Research, Vol.23, No.4, pp.181-198, 1992.

11. Heglund, R. E., *Truck Safety-An Agenda for the Future*, SAE Publication No. P181, pp.154, 1986.

12. Clarke, R. M., *Vehicle Factors in Accidents Involving Heavy Freight Vehicles*, Symposium sur le Rôle des Poids Lourds dans les Accidents de la Circulation, OCDE, Montreal, Quebec, 1987.

13. Mayenburg, M., et al., *Truck Safety Technology for 21st Century*, SAE paper 952260, 1995.

14. Leviso, W. H. and Junker, A. M., *A Model for the Pilot's Use of Motion Cues in Steady-State Roll-Axis Tracking Tasks*, Aerospace Medical Research Laboratory, AMRL-TR-77-40, pp.149-159, 1977.

15. Hess, R. A., *Model for Human Use of Motion Cues in Vehicular Control*, Journal of Guidance, Control and Dynamics, Vol. 13, No. 3, pp.476-482, 1990.

16. Yang, X., Zong, C., and Hu, Z., *Motion Sense Simulation Algorithm and its Evaluation on Vehicle Driving Simulator*, Journal of Automotive Engineering (In Chinese), No.6, 1994.

17. Yang, X., Zong, C., and Hu, Z., *Study on the Simulation Algorithm of Driver's Vestibular Cues*, Journal of Harbin University of Technology (In Chinese), No.4, 1993.

18. Yang, X., Gao, Y., *Mathematics Principle of Driver's Motion Perception Simulation*, Journal of Jilin University of Technology (In Chinese), No.3, Aug., 1991.

19. Kelley, C. R., *Manual and Automatic Control, A Theory of Manual Control and Its Application to Manual and to Automatic Systems*, John Wiley & Sons, Inc., pp.179-210, 1968.

20. Stapleford, R. L., McRuer, D. T. and Magdaleno, R. E., *Pilot Describing Function Measurements in a Multiloop Task*, IEEE Transactions on Human Factors in Electronics, Vol. HFE-8, No. 2, pp113-125, June, 1967.

21. McRuer, D. T. and Krendel, E. S., *Dynamic Response of the Human Operator*, Ohio: Wright-Patterson AFB, Wright Air Development Center Technical Report 56-524, AD 110693, 1957.

22. McRuer, D. T., Allen, R. W., Weir, D. H., and Klein, R. H., *New Results in Driver Steering Control Models*, Human Factors, Vol.19, No.4, pp.381-397, 1977.

23. Xia, X. and Law, E. H., *Nonlinear Analysis of Closed-Loop Driver/Automobile Performance with Four Wheel Steering Control*, SAE Transactions, Section 6, 920055, 1992.

24. Maeda, T., Irie, D. Hidaka, K. and Nishimura, H., *Performance of Driver-Vehicle System in Emergency Avoidance*, SAE Transactions, 770130, 1977.

25. McRuer, D. T., et al., *New Approaches to Human-Pilot/Vehicle Dynamic Analysis*, AFFDL-TR-67-150, Feb., 1968.

26. Sheridan, T. B. and Ferrell, W. R., *Man-Machine Systems: Information, Control, and Decision Models of Human Performance*, The MIT Press, pp.171-285, 1974.

27. Hess, R. A., *A Dual-Loop Model of the Human Controller*, Journal of Guidance, Control, Vol. 1, No. 2, pp.254-260, 1978.

28. McRuer, D. T. and Schmidt, D. K., *Pilot-Vehicle Analysis of Multiaxis Tasks*, Journal of Guidance, Control and Dynamics, Vol. 13, No. 2, pp.348-355, 1990.

29. MacAdam, C. C., *A Computer Simulation Study of the Closed-Loop Stability and Maneuverability of Articulated Coach/Driver Systems*, Proceedings of 8th IAVSD Symposium held in Massachusetts Institute of Technology Cambridge, MA, pp.331-347, August 15-19, 1983.

30. Yang, X. and Bourassa, P., *Analysis of Stability of Closed-loop Driver/Articulated Tractor-semitrailer System*, Paper Presented at CSME Forum in Hamilton, Canada, on the 6th to 9th, May, 1996.

31. Yang, X., Rakheja, S., Stiharu, I., *Study of Control Characteristics of An Articulated Vehicle Driver*, Heavy Vehicle Systems, International Journal of Vehicle Design, Vol. 4, Nos 2-4, pp.373-397, 1997.

32. Yang, X., Rakheja, S. and Stiharu, I., *Study of Directional Analysis of a Closed-Loop Driver/Tractor-Semitrailer Vehicle*, SAE 973262, Paper presented in the SAE International Truck & Bus Meeting & Exposition, Cleveland, Ohio, Nov. 17-19, 1997.

33. Weir, D. H. and McRuer, D. T., *Measurement and Interpretation of Driver/Vehicle System Dynamic Response*, Human Factors, Vol. 15, No. 4, 1973.

34. Ervin, R. D., *The Influence of Size and Weight Variables on the Roll Stability of Heavy Duty Trucks*, SAE Paper 831163, 1983.

35. Ranganathan, R., *Stability Analysis and Directional Response Characteristics of Heavy Vehicles Carrying Liquid Cargo*, PhD Thesis, Concordia University, Canada, 1990.

36. Sweatman, P. and Joubert, P. N., *Detection of Changes in Automobile Steering Sensitivity*, Human Factors, Vol. 16, No. 1, pp.29-36, 1974.

37. Billing, A. M., *Rollover Tests of Double Trailer Combinations*, Ontario Ministry of Transportation and Communications Report No. TVS-CV-82-114, 1982.

38. Allen, R. W., et al, *Test Methods and Computer Modeling for Analysis of Ground Vehicle Handling*, SAE Paper 860115, 1986.

39. Rakheja, S., Ranganathan, R. and Sankar, S., *Field Testing and Validation of Directional Dynamics Model of a Tank Trucks*, International Journal of Vehicle Design, 13(3), pp.251-275, 1992.

40. Wong, J. Y. and El-Gindy, M., *Computer Simulation of Heavy Vehicle Dynamic Behavior - User Guide to UMTRI Models*, No. 3, Road and Transport Association of Canada, 1985.

41. MacAdam, C. C., et al, *A Computerized Model for Simulating the Braking and Steering Dynamics of Trucks*, Tractor-Semitrailers, Doubles, and Triples Combinations, User's Manual, Phase 4, MVMA Project 1197, UM-HSRI-80-58, Sept., 1980.

42. Mathew, A., *Simple Models, User's Manual*, UMTRI, Feb., 1986.

43. Nelson, R. E. and Fitch, J. W., *Optimum Braking, Stability and Structural Integrity for Longer Truck Combinations*, SAE Paper 680547, 1968.

44. Pflug, H. C., *Lateral Dynamic Behaviour of Truck-Trailer Combinations due to the Influence of the Load*, Vehicle System Dynamics, Vol. 15, pp.155-175, 1986.

45. Mikulcik, E. C., *Stability Criteria for Automobile-Trailer Combinations*, Vehicle System Dynamics, Vol. 9, pp.281-289, 1980.

46. Uffelmann, F., *Automotive Stability and Handling Dynamics in Cornering and Braking Maneuvers*, Vehicle System Dynamics, Vol. 12, pp.203-223, 1983.

47. Vanderploeg, M. J. and Bernard, J. E., *Dynamics of Double Bottom Commercial Vehicles, International Journal of Vehicle Design*, Vol. 6, No. 2, pp.139-148, 1985.

48. Fancher, P., Matew, A., *A Vehicle Dynamics Handbook for Single-Unit and Articulated heavy Trucks*, DOT HS 807 185, Final Report, US Department of Transportation, May, 1987.

49. Fancher, P. S., *Directional Dynamics Considerations for Multi-Articulated, Multi-Axled Heavy Vehicles*, SAE Paper 892499, 1989.

50. Vlk, F., *A Linear Study of the Transient and Steady Turning Behavior of Articulated Buses*, International Journal of Vehicle Design, Vol. 5, No. 1-2, pp.171-196, 1984.

51. Sankar, S., Rakheja, S. and Piché, A., *Directional Dynamics of a Tractor-Semitrailer with Self- and Forced-Steering Axles*, SAE Paper 912686, 1991.

52. Kurtz, E. F. and Anderson, R. J., *Handling Characteristics of Car-Trailer Systems; A State-of-the-Art Survey*, Vehicle System Dynamics, Vol. 6, pp.217-243, 1977.

53. Liebermann, D. G., Ben-David, G., Schweitzer, N., and Parush, Y., *A Field Study on Braking Responses During Driving. I. Triggering and Modulation*, Ergonomics, Vol. 38, No. 9, pp.1894-1902, 1995.

54. Schweitzer, N., Apter, Y., Ben-David, G., Liebermann, D. G. and Parush, A., *A Field Study on Braking Responses During Driving. II. Minimum Driver Braking Times*, Ergonomics, Vol. 38, No. 9, pp.1903-1910, 1995.

55. An, P. E. and Harris, C. J., *An Intelligent Driver Warning System for Vehicle Collision Avoidance*, IEEE Transactions on Systems, Man, and Cybernetics-Part A: Systems and Humans, Vol. 26, No. 2, pp.254-261, Mar., 1996.

56. Susemihl, E.A. and Krauter, A. I., *Jackknifing of Tractor Semitrailer Trucks-Detection and Corrective Action*, Journal of Dynamic Systems, Measurement, and Control, Transaction ASME, pp.244-252, 1974.

57. Larocque, G. R., et al., *Feasibility Study of a System Safety Monitor for Hazardous Material Trucking*, SAE Paper 852357, 1985.

58. Troger, H. and Zeman, K., *A Nonlinear Analysis of the Generic Types of Loss of Stability of the Steady State Motion of a Tractor-Semitrailer*, Vehicle System Dynamics, Vol. 13, pp.161-172, 1984.

59. Verma, M.K. and Gillespie, T.D., *Roll Dynamics of Commercial Vehicles*, Vehicle System Dynamics, Vol. 9, pp.1-17, 1980.

60. Shapley, C. G., *The Rolling Motions of Road Vehicles*, Vehicle System Dynamics, Vol. 4, No. 1, 1975.

61. Fancher, P. S., *The Static Stability of Articulated Commercial Vehicles*, Vehicle System Dynamics, Vol. 14, pp.201-227, 1985.

62. MacAdam, C. C., *A Computer-Based Study of the Yaw/Roll Stability of Heavy Trucks Characterized by High Centers of Gravity*, SAE Paper 821260, 1982.

63. Bakker, E., Nyborg, L., and Pacejka, H.B., *Tire Modeling for Use in Vehicle Dynamics Studies*, SAE paper 870421, 1987.

64. Schuring, D. J. et al, *The BNPS Model-An Automated Implementation of the "Magic Formula" Concept*, SAE paper 931909, 1993.

65. Pacejka, H. B. and Bakker, E., *The Magic Formula Tire Model*, Proceedings of the 1st International Colloquium on Tire Models for Vehicle Dynamics Analysis held in Delft, the Netherlands, pp. 1-18, Oct. 2-22, 1991.

66. Hoffmann, E. et al, *The Incorporation of Tire Models into Vehicle Simulations*, Proceedings of the 1st International Colloquium on Tire Models for Vehicle Dynamics Analysis held in Delft, the Netherlands, pp. 49-57, Oct. 2-22, 1991.

67. Fancher, P. S. and Bareket, Z., *Including Roadway and Tread Factors in a Semi-empirical Model of Truck Tires*, Proceedings of the 1st International Colloquium on Tire Models for Vehicle Dynamics Analysis held in Delft, the Netherlands, pp. 92-101, Oct. 2-22, 1991.

68. Apetaur, M., *Modeling of Transient Nonlinear Tire Responses*, Proceedings of the 1st International Colloquium on Tire Models for Vehicle Dynamics Analysis held in Delft, the Netherlands, pp. 116-126, Oct. 2-22, 1991.

69. Sharp, R. S., *Tire Structure Mechanisms Influencing Shear Force Generation: Ideas from a Multi-Radial-Spoke Model*, Proceedings of the 1st International Colloquium on Tire Models for Vehicle Dynamics Analysis held in Delft, the Netherlands, pp. 145-155, Oct. 2-22, 1991.

70. Schieschke, R. and Hiemenz, R., *The Decisive Role the Quality of Tire Approximation Plays in Vehicle Dynamics Simulations*, Proceedings of the 1st International Colloquium on Tire Models for Vehicle Dynamics Analysis held in Delft, the Netherlands, pp. 156-166, Oct. 2-22, 1991.

71. Parsons, A. W. and Janssen, A. H. O., *Tire Vertical Force Description for Vehicle Handling Simulations*, Proceedings of the 1st International Colloquium on Tire Models for Vehicle Dynamics Analysis held in Delft, the Netherlands, pp. 175-177, Oct. 2-22, 1991.

72. Pacejka, H. B., and Sharp, R. S., *Shear Force Development by Pneumatic Tire in Steady State Conditions: A Review of Modeling Aspects*, Vehicle System Dynamics, Vol. 20, 1991.

73. Rakheja, S., Sankar, S. and Ranganathen, R., *Roll Plane Analysis of Articulated Tank Vehicles during Steady Turning*, Vehicle System Dynamics, No.17, pp.81-104, 1988.

74. Vlk, F., *Handling Performance of Truck-Trailer Vehicles: A State-of-the-Art Survey*, International Journal of Vehicle Design, Vol.6, No. 3, pp.323-361, 1985.

75. Vlk, F., *Lateral Dynamics of Commercial Vehicle Combinations-A Literature Survey*, Vehicle Systems Dynamics, Vol. 11, No. 6, pp.305-324, 1982.

76. Schmid, I., *Engineering Approach to Truck and Tractor Train Stability*, SAE Paper 670006, 1967.

77. Nalecz, A. G. and Genin, J., *Dynamic Stability of Heavy Articulated Vehicles*, International Journal of Vehicle Design, Vol. 5, No. 4, pp.417-426, 1984.

78. Vallurupalli, R. K., *Directional Dynamic Analysis of an Articulated Vehicle with Articulation Dampers and Forced-Steering*, Master Degree Thesis, Concordia University, Canada, 1993.

79. Laurien, F., *Untersuchung der Anhangerseitenschwingungen in Strassinzugen*, Dissertation, TH, Hannocer, 1955.

80. Paslay, P. R. and Slibar, A., *Uber Quersvhwingungen von Gelenkten Anhangern*, Ing.-Archiv, Vol. 26, No. 6, pp. 383-386, 1958.

81. Zakin, J. C., *Causes of the Origin of Trailer Oscillations*, (in Russian), Avtomob.promyshlennost, Vol. 26, No. 11, pp.9-12, 1959.

82. Zakin, J. C., *Lateral Stability of Trailer Movement*, (in Russian), Avtomob.promyshlennost, Vol. 27, No. 2, pp.27-31, 1960.

83. Morozov, B. I. Et al., *Research of the Full Trailer Oscillations*, (in Russian), Works NAMI, Moscow, No. 48, pp.29-39, 1962.

84. Meyer, J., *Zur Prage der Querschwingungen eine Zweiachsigen I.Kw.Anhangers*, Techn. Mitteilungen Krupp, Forsch.-Berichte, Vol. 21, No. 1, ,pp.34-36, 1963.

85. Jindra, F., *Off-tracking of Tractor-trailer Combinations*, Automobile Engineer, Vol. 53, No. 3, pp.96-101, 1963.

86. Gerlach, R., *Untersuchung der Querschwingungen von Lastzugen auf Analogrechnern, 8. Kraftfahrzeugtechnische Tagung*, Karl-Marx-Stadt, Vortrag A9, Kammer der Technik, Fachverband Fahrzeugbau und Verkehr IZV Automobilbau, 1968.

87. Nordstrom, O. and Strandberg, L., *The Dynamic Stability of Heavy Vehicle Combinations*, International Conference of Vehicle System Dynamics, Blacksburg, Virginia, 1975.

88. Isermann, H., *Overturning Limits of Articulated Vehicles with Solid and Liquid Loads*, Motor Industry Research Association, Translation No. 58/70, 1970.

89. Ranganathan, R., Rakheja, S., and Sankar, S., *Dynamics Analysis of a B-Train Carrying Liquid Cargo*, Advanced Automotive Technologies, The American Society of Mechanical Engineers, pp.1-30, 1989.

90. Liu, P, Rakheja, S., Ahmed, A.K.W., *Detection of Dynamic Roll Instability of Heavy Vehicles for Open-Loop RollOver Control*, Heavy vehicle and Highway Dynamics SAE SP-1308, pp.105-112, 1997.

91. Miller, D. W. G. and Barter, N. F., *Rollover of Articulated Vehicles, International Mechanical Engineering Conference on Vehicle Safety Legislation*, Paper No. C203/73, 1973.

92. Mallikarjunarao, C., et al., *Roll Response of Articulated Motor Trucks during Steady-Turning Maneuvers*, Computational Method in Ground Transportation Vehicles, ASME Winter Annual meeting, Nov., pp.133-152, 1982.

93. Gillespie, T. D. and Verma, M. K., *Analysis of the Rollover Dynamics of Double-Bottom Tankers*, SAE paper No. 781065, 1978.

94. Palkovics, L., El-Gindy, M., *Examination of Different Control Strategies of Heavy-Vehicle Performance*, Journal of Dynamic Systems, Measurement, and Control, Vol. 118, pp.489-498, 1996.

95. Gillespie, T.D., and MacAdam, C. C., *Constant Velocity Yaw/Roll Program, User's Manual*, UMTRI-82-39, Oct., 1982.

96. El-Gindy, M. and Wong, J. Y., *A Comparison of Various Computer Simulation Models for Predicting the Directional Responses of Articulated Vehicles*, Vehicle System Dynamics, 16, pp.249-268, 1987.

97. Yang, X., Rakheja, S., Stiharu, I., *Study of Driver Factors Affecting the Directional Response of an Articulated Vehicle Using Neural Network*, Transaction of the CSME, Vol. 22, No.3, pp. 291-306, 1998.

98. Senger, K. H. and Schwartz, W., *The Influence of A Four Wheel Steering System on the Stability Behaviour of A Vehicle-Driver System*, Proceedings of 10th IAVSD Symposium held in Prague, CSSR, August 24-28, pp.388-402, 1987.

99. Wierwille, W. W., Gagné, G. A. and Knight, J. R., *An Experimental Study of Human Operator Models and Closed-Loop Analysis Methods for High-Speed Automobile Driving*, IEEE Transactions on Human Factors in Electronics, Vol. HFE-8, No. 3, pp.187-201, 1967.

100. Apetaur, M. and Opicka, F., *Assessment of the Driver's Effort In Typical Driving Manoeuvers for Different Vehicle Configurations and Management*, Proceedings of 12th IAVSD Symposium held in Lyon, France, August 26-30, pp.42-56, 1991.

101. Good, M. C. and Joubert, P. N., *Driver-Vehicle Behaviour in Restricted-Path Turns*, Ergonomics, Vol. 20, No. 3, pp.217-248, 1977.

102. Baxter, J. and Harrison, J. Y., *A Nonlinear Model Describing Driver Behavior on Straight Roads*, Human Factors, Vol. 21, No. 1, pp87-97, 1979.

103. Good, M. C., *Effects of Free-Control Variables on Automobile Handling*, Vehicle System Dynamics, Vol. 8, pp253-285, 1979.

104. Smiley, A., Reid, L. and Fraser, M., *Changes in Driver Steering Control With Learning*, Human Factors, Vol. 22, No. 4, pp401-415, 1980.

105. Summala, H., Leino, M. and Vierimaa, J., *Driver's Steering Behavior When Meeting Another Car: The Case of Perceptual Tropism Revisited*, Human Factors, Vol. 23, No. 2, pp.185-189, 1981.

106. Reid, L. D., Solowka, E. N. and Billing, A. M., *A Systematic Study of Driver Steering Behaviour*, Ergonomics, Vol. 24, No. 6, pp.447-462, 1981.

107. Furukawa, Y. and Nakaya, H., *Effects of Steering Response Characteristics on Control Performance of the Driver-Vehicle System*, International Journal of Vehicle Design, Special Issue on Vehicle Safety, pp.262-278, 1986.

108. Godthelp, H., *Vehicle Control During Curve Driving*, Human Factors, Vol. 28, No. 2, pp.211-221, 1986.

109. Godthelp, H. and Käppler, W., *Effects of Vehicle Handling Characteristics on Driving Strategy*, Human Factors, Vol. 30, No. 2, pp.219-229, 1988.

110. MacAdam, C., C. and Fancher, P. S., *A Study of the Closed-Loop Directional Stability of Various Commercial Vehicle Configurations*, Proceedings of 9th IAVSD Symposium held in Linköping University, Linköping, Sweden, June 24-28, pp.367-382, 1985.

111. Harada, H., Iwasaki, T., *Stability Criteria and Objective Evaluation of a Driver-Vehicle System for Driving in Lane Change and Against Crosswind*, Proceedings of 13th IAVSD Symposium held in Chengdu, China, August 23-27, pp.197-208, 1993.

112. Cho, Y. H. and Kim, J., *Stability Analysis of the Human Controlled Vehicle Moving Along a Curved Path*, Vehicle System Dynamics, Vol. 25, pp.51-69, 1996.

113. Bekey, G. A., Burnham, G. O. and Seo, J., *Control Theoretic Models of Human Drivers in Car Following*, Human Factors, Vol. 19, No. 4, pp.399-413, 1977.

114. Guan, X., and Yang, X., *ARMAX Identification on the Parameters of Driver/Vehicle Closed-Loop Position Plus Orientation Preview Model*, Journal of Automotive Engineering (in Chinese), No.4, 1995.

115. Habib, M. S., *Vehicle Handling Quality Evaluation with 2WS and 4WS Based on Driver-Vehicle Dynamics*, Proceedings of CSME Forum, Hamilton, Canada, pp.357-363, May 7-9, 1996.

116. Godthelp, J., *Precognitive Control: Open-and Closed-Loop Steering in A Lane-Change Manoeuvre*, Ergonomics, Vol. 28, No. 10, pp.1419-1438, 1985.

117. Hess, R. A., *Theory for Aircraft Handling Qualities Based Upon A Structural Pilot Model*, Journal of Guidance, Control and Dynamics, Vol. 12, No. 4, pp792-797, 1989.

118. Tustin , A., *The Nature of the Operator's Response in Manual Control and Its Implications for Controller Design*, J. Inst. Elec. Engs. (London), Vol.94, pp.190-202, 1947.

119. Wierwille, W. W. and Casali, J. G., *Driver Steering Reaction Time to Abrupt-Onset Crosswinds, as Measured in a Moving-Based Driving Simulator*, Human Factors, Vol. 25, No. 1, pp.103-116, 1983.

120. Olson, P. L., *Driver Perception Response Time*, SAE Transactions, 890731, 1989.

121. McRuer, D. T., *Remarks on Some Neuromuscular Subsystem Dynamics*, IEEE Transactions on Human Factors in Electronics, Vol. HFE-7, No. 2, pp.129-130, 1966.

122. Magdaleno, R. E. and McRuer, D. T., *Experimental Validation and Analytical Elaboration for Models of the Pilot's Neuromuscular Subsystem in Tracking Tasks*, NASA Contractor Report, NASA CR-1757, Washington, D.C. April, 1971.

123. Iguchi, M., *A Study of Manual Control*, Journal of Mechanic Society of Japan, Vol.62, No.481, 1959.

124. Weir, D. H. and McRuer, D. T., *Dynamics of Driver Vehicle Steering Control*, Automatica, Vol. 6, pp.87-98, 1970.

125. Legouis, T., Laneville, A., Bourassa , P. A. and Payre , G., *Vehicle/Pilot System Analysis: A new Approach Using Optimal Control with Delay*, Vehicle System Dynamics, Vol. 16, pp.279-295, 1987.

126. Legouis, T., Bourassa, P. A., Laneville, A. and Gosselin, C., *On the Extension of the Gratzmuller Critical Velocity for Locked Steering Road Vehicle to the Case of Piloted Vehicle*, Proceedings of 9th IAVSD Symposium held in Linköping University, Linköping, Sweden, pp.307-319, June 24-28, 1985.

127. Legouis, T., Laneville, A, Bourassa, P. A. and Payre, G., *Characterization of Dynamic Vehicle Stability Using Two Models of the Human Pilot Behaviour*, Vehicle System Dynamics, Vol. 15, pp.1-18, 1986.

128. Hayashi, Y., *Optimum Control of A Driver/Four-Wheel-Steered-Vehicle System,* Proceedings of 10th IAVSD Symposium held in Prague, CSSR, pp.145-156, 1987.

129. Habib, M. S., *Driver-Vehicle Robust Steering Control*, Heavy Vehicle Systems, International Journal of Vehicle Design, No. 2-4, 1997.

130. Habib, M. S. and Bakr, E. M., *The Selection of Optimum Vehicle Parameters Based on the Pilot-Vehicle Directional Stability*, Proceedings of 13th IAVSD Symposium held in Chengdu, China, pp.182-196, August 23-27, 1993.

131. Habib, M. S., *Characterization of Driver-Vehicle Directional Control Using Three Models of Huamn Driver*, Proceedings of AVEC'94 Conference, Society of Automotive Engineers of Japan, Inc., pp.36-41, Oct. 1994.

132. McRuer, D. and Weir, D. H., *Theory of Manual Vehicular Control*, Ergonomics, Vol.12, No.4, pp.599-633, 1969.

133. Hess, R. A., *Structural Model of the Adaptive Human Pilot*, Journal of Guidance and Control, Vol. 3, No. 5, pp.416-423, Sept. 1980.

134. Sheridan, T. B., *Three Models of Preview Control*, IEEE Transactions on Human Factors in Electronics, June, Vol. HFE-7, No. 2, pp.91-102, 1966.

135. Modjtahedzadeh, A. and Hess, R. A., *A Model of Driver Steering Control Behavior for Use in Assessing Vehicle Handling Qualities*, Journal of Dynamic Systems, Measure and Control, Vol. 115, pp.456-464, 1993.

136. Yoshimoto, K., *Simulation of Driver/Vehicle System Including Preview Control*, Journal of Mechanics Society of Japan, Vol. 71, 1968.

137. MacAdam, C. C., *Application of an Optimal Preview Control for Simulation of Closed-Loop Automobile Driving*, IEEE Transactions on Systems, Man, and Cybernetics, Vol. SMC-11, No. 6, pp.393-399, 1981.

138. Gordon, D. A., *Experimental Isolation of Driver's Visual Input*, Public Roads, Vol.33, pp. 266-273, 1966.

139. Hoffmann, E. R. and Joubert, P. N., *The Effect of Changes in Some Vehicle Handling Variables on Driver Steering Performance*, Human Factors, Vol.8, pp. 245-263, 1966.

140. Kondo, M. et al., *Driver's Sight Point and Dynamics of Driver/Vehicle System Related to It*, SAE paper No. 680104, 1968.

141. Mourant, R. R., Rockwell, T. H., and Rackoff, N. J., *Drivers' Eye Movements and Visual Workload*, Highway Research Record, Vol. 292, 1970.

142. McLean, J. R. and Hoffmann, E. R., *The Effects of Restricted Preview on Driver Steering Control and Performance*, Human Factors, Vol. 15, No. 4, pp.421-430, 1973.

143. Kvalseth, T. O., *The Interaction of Driving Speed, Steering Difficulty and Lateral Tolerance: Some Comments*, Ergonomics, Vol. 27, No. 6, pp.701-703, 1984.

144. Perchonok, K. and Pollack, L., *Luminous Requirements for Traffic Signs*, Contract No. FHWA-RD-81-158. Federal Highway Administration, Washington, D.C Dec., 1981.

145. Sivak, M., Olson, P. L. and Green, P., *Human-Factors Methods in the Design of Vehicle Components*, International Journal of Vehicle Design, Special Issue on Vehicle Safety, pp. 331-337, 1986.

146. Plöchl, M. and Lugner, P., *Theoretical Investigations of Interaction Driver-Feedback-Controlled Automobile*, Proceedings of AVEC'94 Conference, Society of Automotive Engineers of Japan, Inc., pp.42-48, 1994.

147. Tomizuka, M. and Whitney, D. E., *The Human Operator in Manual Preview Tracking- An Experiment and Its Modeling Via Optimal Control*, Journal of Dynamic Systems, Measurement, and Control, Vol. 98, No. 4, pp.407-413, 1976.

148. Guo, K.H., *Vehicle Handling Dynamics*, Jilin Press of Science & Technology, 1991 (Chinese).

149. Guo, K, and Guan, X., *Modelling of Driver/Vehicle Directional Control System*, Vehicle System Dynamics, Vol. 22, pp.141-184, 1993.

150. Allen, R. W., Szostak, H. T., and Rosenthal, T. J., *Analysis and Computer Simulation of Driver/Vehicle Interaction*, SAE Transactions, 871086, 1987.

151. Nagai , M. and Mitschke , M., *An Adaptive Control Model of A Car-Driver and Computer Simulation of the Closed-Loop System*, Proceedings of 10th IAVSD Symposium held in Prague, CSSR, pp.275-286, 1987.

152. Mitschke, M., *Anticipatory Steering In A Driver-Vehicle Control Loop*, Proceedings of 11th IAVSD Symposium held in Kingston, Ont., pp.405-413, 1989.

153. Kageyama, I. and Pacejka, H. B., *On A New Driver Model with Fuzzy Control*, Proceedings of 12th IAVSD Symposium held in Lyon, France, pp.314-324, 1991.

154. Gu, X. and Yu, Q., *Driver-Vehicle-Environment Closed-Loop Simulation of Handling and Stability Using Fuzzy Control Theory*, Proceedings of 13th IAVSD Symposium held in Chengdu, China, pp.172-181, 1993.

155. Hayhoe, G. F., *A Driver Model Based on the Cerebellar Model Articulation Controller*, Vehicle System Dynamics, Vol. 8, pp.49-72, 1979.

156. Kramer, U. and Rohr, G., *A Model of Driver Behavior*, Ergonomics, Vol. 25, No. 10, pp.891-907, 1982.

157. Willumeit, H.P., Kramer, U. and Rohr, G., *Closed-Loop Simulation of the Driver-Vehicle-Road System*, Proceedings of 8th IAVSD Symposium held in Massachusetts Institute of Technology Cambridge, MA, pp.679-684, 1983.

158. Thakur, K. P. and White, D. M., *Development of Driver-Vehicle Model on 'Risk Time' Basis*, Heavy Vehicle Systems, International Journal of Vehicle Design, No. 2-4, 1997.

159. MacAdam, C. C. and Johnson, G. E., *Application of Elementary Neural Networks and Preview Sensors for Representing Driver Steering Control Behavior*, Vehicle System Dynamics, Vol. 25, pp.3-30, 1996.

160. Wong, J. Y., *Theory of Ground Vehicles*, Second Edition, A Wiley-Interscience Publication, John Wiley & Sons, Inc., 1993.

161. Ghazizadeh, A. and Fahim, A, El-Gindy, M., *Neural Networks Representation of a Vehicle Model: 'Neuro-Vehicle (NV)*, International Journal of Vehicle Design, Vol.17, No.1, pp.55-75, 1996.

162. Zadeh, A. Ghazi, Fahim, A. and El-Gindy, M., *Neural Network and Fuzzy Logic Applications to Vehicle Systems: Literature Survey*, International Journal of Vehicle Design, Vol. 18, No.2, pp.132-193, 1997.

163. Kraiss, K.F. and Kuettelwesch, H., *Teaching Neural Networks to Guide a Vehicle Through an Obstacle Course by Emulating a Human Teacher*, Proceedings, International Joint Conference on Neural Networks - IJCNN 90, 1990.

164. Kraiss, K.F. and Kuettelwesch, H., *Identification and Application of Neural Operator Models in a Car Driving Situation*, Proceedings, 5th IFAC/IFIP/IFORS/IEA Symposium on Analysis, Design and Evaluation of Man-Machine Systems, 1992.

165. Neusser, S., Hoefflinger, B. and Nijhuis, J., *A Case Study in Car Control by Neural Networks*. Proceedings, ISATA International Symposium, Florence, Italy, INRETS, 1991.

166. Neusser, S. et al., *Neurocontrol for Lateral Vehicle Guidance*, IEEE Micro, Vol.13, No.1, pp.57-66, 1993.

167. Fix, E., *Neural Network Based Human Performance Modeling*. Proceedings, IEEE National Aerospace and Electronics Conference - NAECON, 1990.

168. Pomerleau, D., *Efficient Training of Artificial Neural Networks for Autonomous Navigation*, Neural Computation, Vol.3, No.1, 1991.

169. Pomerleau, D., *Progress in Neural Network-Based Vision for Autonomous Robot Driving*, Proceedings, Intelligent Vehicles'92 Symposium, Detroit, IEEE Industrial Electronics Society, 1992.

170. Brown, M. and Harris, C.J., *Intelligent Control for Autonomous Vehicles Using Real-Time Adaptive Associative Memory Neural Networks*, Proceedings, 2nd International Conference on Artificial Neural Networks, 1991.

171. Luebbers, P.G. and Pandya, A.S., *Video-Image-Based Neural Network Guidance System With Adaptive View-Angles for Autonomous Vehicles*. Proceedings, Applications of Artificial Neural Networks II, 1991.

172. Fujioka, T. and Takubo, N., *Driver Model Obtained by Neural Network System*. JSAE Review, Vol.12, No.2, pp.82-85, 1991.

173. Kehtarnavaz, N. and Sohn, W., *Steering Control of Autonomous Vehicles by Neural Networks*, Proceedings, American Control Conference, 1991.

174. Kornhauser, A.L., *Neural Network Approaches for Lateral Control of Autonomous Highway Vehicles*, Proceedings, Vehicle Navigation & Information Systems, 1991.

175. Lubin, J.M. et al., *Analysis of A Neural Network Lateral Controller for an Autonomous Road Vehicle*, Proceedings, Future Transportation Technology Conference and Exposition, 1992.

176. Freeman, J. and Skapura, D., *Neural Networks, Algorithm, Applications, and Programming Techniques*, Addison-Wesley, 1991.

177. Karlin, A., Locatelli, A. and Zanardini, C., *On the Synthesis of Trajectory Insensitive Linear Systems*, Proceedings of the Third IFAC Symposium, Ischia, Italy, pp.183-189, June 18-23, 1973.

178. Lin, Y. and Kortum, W., *Identification of System Physical Parameters for Vehicle Systems with Nonlinear Components*, The Dynamics of Vehicles on Roads and Tracks, Proc. 12th IAVSD Symposium, Lyon, France, 1991.

179. Cao, K., *Measurements of Path and Other Parameters in Motor Vehicle Dynamics Tests and Their Errors*, Vehicle System Dynamics, Vol. 26, No.5, 1996.

180. Demic, M., *Identification of Vibration Parameters for Motor Vehicles*, Vehicle System Dynamics, Vol. 27, No. 2, pp. 65-88, 1997.

181. Eykhoff, P., *System Identification, Parameter and State Estimation*, John Wiley & Sons, 1977.

182. Ljung, L., *System Identification-Theory for the User*, Prentice Hall, Englewood Cliffs, N.J., 1987.

183. Letherwood, M. D. and Wehage, R. A., *Computer-based Analysis of the On- and Off-road Performance of High Mobility Trailers*, Heavy Vehicle Systems, International Journal of Vehicle Design, Vol. 1, No. 3, pp.240-257, 1994.

184. Kack, B. and Richard, M. J., *Effect of load-distributing devices on the Stability of Heavy Vehicles*, Heavy Vehicle Systems, International Journal of Vehicle Design, Vol. 4, No. 1, pp.29-48, 1997.

185. Hanselmann, H., *Implementation of Digital Controllers*, A Survey, Automatica, Vol. 23, pp.7-32, 1987.

186. Ljung, L., *System Identification Toolbox for Use with MATLAB*, The MATH Works Inc., 1995.

187. Kurka, U., and Braun, S.G., *System Identification and Order Determination via the Regularized Suboptimal Solution*, 14th International Modal Analysis Conference Proceedings, 1996.

188. Kuester, J. L. and Mize, J. H., *Optimization Techniques with FORTRAN*, McGRAW-Hill Book Company, 1973.

189. Jex, H. R., et al., *Roll Tracking Effects of G-Vector Tilt and Various Types of Motion Washout*, Proceedings of Fourteenth Annual Conference on Manual Control, University of Southern California, April 25-27, 1978.

190. Billing, J. R. and Mercer, W., Demonstration of Tractor-Trailer Performance: 7-Axle 48 ft Semi, CV-86-10, *Transportation Technology and Energy Branch, Ministry of Transportation and Communications*, Ontario, Canada, 1986.

191. Piche, A., *Detection of Onset of Instabilities for an early Warning Safety Monitor for Articulated Freight Vehicles*, Master Thesis, Concordia University, 1990.

192. Johansson, G. and Rumar, K., *Driver's Brake Reaction Times*, Human Factors, 1971, 13(1), pp.23-27.

193. Summala., H., *Driver/Vehicle Steering Response Latencies*, Human Factors, 1981, 23, 683-692.

194. Lin, R. C., Cebon, D. and Cole, D. J., *Optimal Roll Control of a Single-Unit Lorry*, Proc. Instn Mech. Engrs, Part D, Vol. 210, pp.45-55, 1996.